



Norwegian
University of
Life Sciences

Master's thesis 2025 60 ECTS

Faculty of Environmental Sciences and Natural Resource
Management

**A Novel Secondary Treatment Step for Tunnel
Wash Water: Impact on Retention and Toxicity
of Tire and Road Wear Particles, Tire Leachates,
and Metals**

Ole Holthusen

Environmental Science

Abstract

Urban expansion and increasing vehicular traffic have significantly intensified road related pollution in recent decades. Among the emerging contributors to environmental degradation are tire and road wear particles (TRWPs) and tire-derived chemicals (TDCs), which represent a growing source of microplastic and chemical contamination. These pollutants enter ecosystems through air deposition and surface runoff. A particularly concentrated source is tunnel wash water (TWW), generated during the maintenance of road tunnels. In Norway, this water is frequently discharged into adjacent rivers and fjords without adequate treatment. This study aimed to investigate the impacts a novel secondary treatment step for TWW may have on retention and toxicity of TRWPs, TDCs and metals taking into account the contaminant fluxes and seasonal variations by using the Ekeberg Tunnel as a case. A two-step treatment system, consisting of a 21-day sedimentation phase followed by filtration with Leca Filtralite HMR, was evaluated by testing the effectiveness of sedimentation alone and in combination with filtration for reducing key contaminants. Fieldwork was carried out during spring and autumn of 2024 to capture seasonal differences, with samples collected before and after each treatment stage. Metal samples were filtered through a 0.45 µm membrane to distinguish between particle bound and dissolved fractions. All samples were subsequently analyzed for metals, TRWPs, and TDCs using Agilent 8800 ICP-MS QQQ, Py-GC/MS, and UPLC-TOF-MS. A 14 day leaching test also evaluated metal release from particles retained before treatment. Acute toxicity was assessed using *Daphnia magna* at each TWW treatment stage, including detergent only exposures. Additional measurements included dissolved organic carbon, anions, and other water quality parameters. Results revealed that TWW contains a complex, seasonally variable contaminant mix. Higher concentrations of TRWP, TDCs and metals were observed in spring, due to winter accumulation. The treatment system effectively reduced particle bound metals (Al, Fe, Cu, Pb), TRWP and some TDCs like 6PPD and DPPD. However, dissolved metals (Zn, Mo, As) and water soluble TDCs such as HMMM, TMQ, and MTBT were not effectively removed, with some increasing post treatment. Biological assays showed that *D. magna* ingested particles in all treatments, but acute toxicity was observed only in untreated autumn samples at a 50% sample concentration. Microscopic analysis revealed that particles adhered to

appendages and exoskeletons, causing immobilization through physical obstruction. The leaching test confirmed that retained TWW particles also release metals such as iron (30.0 µg/L), zinc (9.32 µg/L), and copper (2.00 µg/L) over time. This study confirms that TWW from the Ekeberg Tunnel poses considerable environmental risks, particularly during the spring season. While the two step treatment system effectively reduced coarse, particle bound pollutants, it was less capable of removing some dissolved metals and water soluble TDCs. The combination of high concentrations of untreated TRWPs, TDCs, and metals along with evidence of particle ingestion, mechanical interference, and gradual metal leaching, raises concerns for aquatic life and water quality. These findings highlight the importance of effective treatment in reducing environmental risks, while also showing the need to improve the removal of finer particles and certain dissolved pollutants. Ongoing monitoring is essential to protect sensitive ecosystems like the Oslofjord.

Sammendrag

Byvekst og økende veitrafikk har i løpet av de siste tiårene betydelig forverret vegrelatert forurensning. Blant de fremvoksende bidragsyterne til miljøforringelse er dekk og veislitasjepartikler (TRWPs), samt tilsetningskemikaler i bildekk (TDCs) som utgjør en økende kilde til henholdsvis mikroplast og kjemisk forurensning. Disse forurensningene kommer inn i økosystemene via luftavsetning og overflateavrenning. En spesielt konsentrert kilde er vaskevann fra tunneler (TWW), som genereres under vasking av veitunneler. I Norge slippes dette vannet ofte ut i nærliggende elver og fjorder uten tilstrekkelig rensing. Denne studien hadde som mål å undersøke forekomst, sesongvariasjon og behandlingsmuligheter for TRWPs, TDCs og metaller i tunnel vaskevann fra Ekebergtunnelen. Et to-trinns behandlingssystem, bestående av en 21 dagers sedimenteringsfase etterfulgt av filtrering med Leca Filtralite HMR, ble evaluert ved å teste effektiviteten av sedimentering alene og i kombinasjon med filtrering for å redusere forurensninger. Feltarbeid ble gjennomført våren og høsten 2024 for å undersøke sesongmessige forskjeller, og prøver ble tatt før og etter hvert behandlingssteg. Metallprøver ble filtrert gjennom et 45 µm filter for å skille partikkelbundne og oppløste fraksjoner. Metaller, TRWPs og TDCs ble deretter analysert ved hjelp av Agilent 8800 ICP-MS QQQ, Py-GC/MS og UPLC-TOF-MS. En 14 dagers utlekkingsstest ble også gjennomført for å evaluere metallutslipp fra partikler beholdt før rense behandling. Akutt toksisitet ble vurdert ved bruk av *Daphnia magna* ved hvert behandlingssteg, inkludert eksponering for kun vaskemiddel. Tilleggsparametere inkluderte oppløst organisk karbon, anioner og andre vannkvalitetsparametere. Resultatene viste at TWW inneholder en kompleks og sesongavhengig blanding av forurensninger. Høyere konsentrasjoner av TRWP, TDCs og metaller ble observert om våren, som følge av akkumulering gjennom vinteren. Behandlingssystemet reduserte effektivt partikkelbundne metaller (Al, Fe, Cu, Pb), TRWP og enkelte TDCs som 6PPD og DPPD. Derimot ble ikke oppløste metaller (Zn, Mo, As) og vannløselige TDCs som HMMM, TMQ og MTBT effektivt fjernet, og noen økte etter behandling. Biologiske tester viste at *Daphnia magna* inntok partikler i alle prøver, men akutt toksisitet ble kun observert i ubehandlede høstprøver ved 50 % prøvekonsentrasjon. Mikroskopiske analyser viste at partikler festet seg til antenner og ytre skall, noe som førte til immobilisering gjennom fysisk blokkering. Utlekkings testen bekreftet også at partikler beholdt fra TWW gradvis slapp ut metaller som Fe, Zn og Cu over tid. Denne studien bekrefter at

tunnelvaskevann fra Ekebergtunnelen utgjør betydelige miljømessige risikoer, særlig i vårsesongen. Selv om det to-trinns behandlingssystemet effektivt reduserte større, partikkelbundne forurensninger, var det mindre effektivt for å fjerne enkelte oppløste metaller og vannløselige TDCs. Kombinasjonen av høye konsentrasjoner av ubehandlede TRWPs, TDCs og metaller, sammen med dokumentert partikkelinntak, mekaniske effekter og gradvis metallutlekking, vekker bekymring for vannkvalitet og akvatiske organismer. Disse funnene understreker viktigheten av effektiv behandling for å redusere miljøpåvirkning, samtidig som de viser behovet for å forbedre fjerningen av finere partikler og visse oppløste forurensninger. Kontinuerlig overvåking er avgjørende for å beskytte sårbare økosystemer som Oslofjorden.

Acknowledgments

With this thesis, I complete a Master degree in Environmental Science, specializing in Environmental Chemistry, Pollution, and Toxicology at the Norwegian University of Life Sciences (NMBU). This project was funded by the E134 Oslofjord connection from the Norwegian Public Roads Administration (NPRA) and by the Faculty of Environmental Sciences and Natural Resource Management (MINA) at NMBU. The thesis was carried out as part of the MikroRENS project, funded by the NPRA and NIVA. The analysis of tire and road wear particles (TRWP), tire derived chemicals (TDC), and the associated fieldwork were made possible through this project. First and foremost, I would like to thank Lene Sørli Heier for giving me the opportunity to collaborate with the NPRA and to pick an interesting topic. I am very grateful to my co-supervisor, Elisabeth Støhle Rødland, for her support throughout the project, especially during fieldwork. I would like to thank my supervisor, Ole Christian Lind, for overseeing this project and providing valuable guidance, helpful ideas and constructive feedback. Further I would like to thank co-supervisor Dag Anders Brede for his support in the laboratory, for sharing insights and motivation, and for being an inspiring teacher in ecotoxicology. My appreciation goes to the entire team at the Isotope Laboratory and soil building. Special thanks to Karl Andreas Jensen, Yetneberk Ayalew Kassaye, Marit Nandrup Pettersen, Magne Vrangén, Mona Mirgeloybayat and Hanae Hassani. I also want to thank Tânia Cristina Gomes from NIVA for providing the starter culture for the daphnids.

Lastly, I would like to thank myself for staying motivated and for staying committed to the process, even when it would have been tempting to just take off and travel. Also, daphnids are tough little creatures who withstood more than I expected! And for the record: water fleas don't scratch.



Ole Holthusen

Norwegian University of Life Sciences
Ås, May 15, 2025

Supervisors

Supervisor

Professor Ole Christian Lind

Centre for Environmental Radioactivity (CERAD) CoE

Faculty of Environmental Sciences and Natural Resource Management (MINA)

Environmental Chemistry Section

Norwegian University of Life Sciences (NMBU)

E-mail: ole-christian.lind@nmbu.no

Co-supervisor

Professor Dag Anders Brede

Centre for Environmental Radioactivity (CERAD) CoE

Faculty of Environmental Sciences and Natural Resource Management (MINA)

Environmental Chemistry Section

Norwegian University of Life Sciences (NMBU)

E-mail: dag.anders.brede@nmbu.no

Co-supervisor

Doctor Elisabeth Støhle Rødland

Norwegian Institute for Water Research | NIVA

Research Section: Urban Environments and Infrastructure

E-mail: elisabeth.rodland@niva.no

Co-supervisor

Doctor Lene Sørli Heier

Norwegian Public Roads Administration (NPRA)

Division for Construction

E-mail: lene.sorlie.heier@vegvesen.no

Abbreviations and Definitions

Abbreviations	Definitions
AADT	Annual Average Daily Traffic
BR	Butadiene Rubber
C0-C5	Exposure concentrations in dilution series
CRMs	Certified Reference Materials
DI	Deionized Water
DOC	Dissolved Organic Carbon
DO	Dissolved Oxygen
EC	Electrical Conductivity
EPA Water	Standardized synthetic water used in ecotoxicology
EQS	Environmental Quality Standards
HMR	High Metal Removal (as in Filtralite® HMR filter)
ICP-MS	Inductively Coupled Plasma Mass Spectrometry
LC ₁₀ / LC ₂₀ / LC ₅₀	Lethal Concentration for 10%, 20%, and 50% of organisms
LOD	Limit of Detection
LOQ	Limit of Quantification
M7	Standardization reconstituted freshwater medium for Daphnia
MPs	Microplastics
NOM	Natural Organic Matter
NOEC	No Observed Effect Concentration
PMB	Polymer-Modified Bitumen
PM	Particulate Matter
PS	Polystyrene
RAMP	Road-Associated Microplastic Particles
SBR	Styrene-Butadiene Rubber
SBS	Styrene-Butadiene-Styrene
TDCs	Tire Derived Chemicals
TDS	Total Dissolved Solids
TRWP	Tire and Road Wear Particles
TSS	Total Suspended Solids
TWP	Tire Wear Particles
TWW	Tunnel Wash Water
ζ (Zeta Potential)	Measure of surface charge on particles

List of Figures

Figure 1: Photos A and B show the washing procedure and advanced cleaning system used in the Ekeberg Tunnel. Images were taken during the autumn tunnel wash by Ole Holthusen.	8
Figure 2: The figure illustrates the sources of contamination observed in tunnel wash water. Illustration and photograph (Ekeberg tunnel) are done and taken by Ole Holthusen.	11
Figure 3: The figure illustrates the structural and material differences among winter and summer tire designs, along with the chemical composition of tire tread includes polymers, fillers, oil, vulcanizers, and additives used for tire preservation. The The figure is made by Ole Holthusen, with inspiration from (Johannessen et al., 2022; merityre, n.d).	14
Figure 4: Shows the surface conditions in the Ekeberg Tunnel showing features related to road wear and particle release. A: Corroded steel drainage outlet with dark streaks possibly indicating runoff containing oils or other organic residues. B: Worn thermoplastic road markings showing abrasion, a potential source of road associated microplastic particles. C: Exposed road aggregate (road skeleton) where the bitumen binder and finer particles have eroded, illustrating mineral-based road wear particle formation. All images take by Ole Holthusen in the Ekeberg tunnel	16
Figure 5: Scanning electron microscope (SEM) images of a tire and road wear particle (TRWPs). Image A shows elongated TRWP aggregates, while Image B provides a close up view highlighting the mineral inclusions embedded within the rubber matrix. These mineral incrustations, originating from the road surface, illustrate the composite nature of TRWPs formed through the interaction between tire material and road particles. Pictures is gathered from (Kreider et al., 2010)	18
Figure 6: The figure illustrates the regeneration process of an exhausted Filtralite HMR filter. During backwashing, retained cations and anions, along with accumulated filter residue, are flushed out and settled in a pre-treatment stage, such as the sedimentation pool in the Ekeberg tunnel. The illustration is taken from the brochure provided by the contractor, Containertech in Appendix A.	30
Figure 7: The figure illustrates a modified model of sedimented tire wear particles (TWP) from discharges on May 17 and 18 at Filipstadkaia and Myggbukta in Oslo. The color scale indicates the concentration of TWPs in the sediment, ranging from 1000 mg/m ² (orange) to 0.1 mg/m ² (dark blue) (Rødland & Lundgaard, 2023).The yellow box indicates where the effluent from the Ekeberg tunnel is.	31
Figure 8: The photo shows a 9-day old healthy <i>Daphnia magna</i> with the first set of offspring, which are incubated in a brood pouch located underneath the carapace to the back. Photo taken with the MDG41 Leica microsystem by Ole Holthusen with a descriptive anatomical structure.	32
Figure 9: Map showing the location of the Ekeberg Tunnel, the sampling area, and the outflow to the Alna River. The figure was created in QGIS by Ole Holthusen.	33
Figure 10: The figure shows the complete tunnel wash water treatment cycle is illustrated from step 1-5 for the Ekeberg tunnel from tunnel washing to outflow, through two treatment steps before being released into the Alna River and then further to the Oslofjord. The figure is made in Adobe illustrator by Ole Holthusen.	34
Figure 11: The figure illustrates the sampling points for untreated and treated tunnel wash water during two full tunnel washes conducted in spring and autumn 2024. Samples were collected from different stages of the treatment process. The figure is inspired by (Meland et al., 2023) and made in powerpoint.	36
Figure 12: Sampling setup at the Sedimentation Basin in the Ekeberg Tunnel. The electric pump (right) draws water from the basin (left) and passes it through a sequential filtration system (right) consisting of a 100 µm nylon net filter, a 5 µm filter, and 0,45 µm filter. Photos: Ole Holthusen.	38
Figure 13: Picture A shows the drain hole with the regulation chamber and the outflow to Alna River before flushing. Picture B shows the sampling setup during the flushing of the treated tunnel wash water. Photos: Ole Holthusen.	39
Figure 14: Image A and B shows the leaching experiment setup. Image (A) shows the particle pellets without the TWW. Further image (B) shows the samples on the roller board with 3 leaching samples and 1 blank.	45
Figure 15: The figure shows picture A from the timeline from day 0 with 50mL algae added from the previous batch and picture B after 10 days in the incubator chamber. Photos: Ole Holthusen	51

Figure 16: The figure shows the dilution setup in clean beakers for the different exposure concentrations for filtered tunnel wash water after the filtrate HMR from spring. Photo: Ole Holthusen	56
Figure 17: The figure shows the setup for the six well plates with concentration 1-5 plus the control group. The figure is made in Bio render by Ole Holthusen.	56
Figure 18: Illustrates the concentration gradient, with C1 representing the lowest concentration and C5 the highest from untreated TWW from the Spring wash water. Photos: Ole Holthusen	57
Figure 19: Illustrates the highest concentration of untreated autumn tunnel wash water in Petri dish, where particles are inhomogenously distributed. Photos: Ole Holthusen.....	57
Figure 20: The bar graphs show the concentrations of tire and road wear particles (TRWP) in tunnel wash water across different treatment depths and intervals for two particle size fractions: >5 µm (top panel) and 0.4–5 µm (bottom panel), measured during spring and autumn. The bars represent mean concentrations (mg/L) with error bars indicating standard deviation.	62
Figure 21: The boxplots shows the concentrations of rubber-associated microparticles (>5 µm) in tunnel wash water across different treatment stages (Untreated, Treatment 1, Treatment 2) and two seasonal conditions (spring and autumn). The compounds measured include SBR+BR (red), TRWP (blue), and TWP (yellow). Concentrations are shown on a logarithmic scale (mg/L).....	65
Figure 22: The bar graphs present the mean concentrations from 2 replicates of organic additives from tire wear particles (TWP) in untreated water at depths 1, 2, and 3, treated water from corresponding depths, and filtered water sampled from the outflow at 10-minute intervals. Additionally, the graphs indicate the sampling season and display concentrations in both total and centrifuged water samples in ng/L.	69
Figure 23: The bar graphs present the mean concentrations from 3 replicates of metals in untreated water at depths 1, 2, and 3, treated water from corresponding depths, and filtered water sampled from the outflow at 10-minute intervals. Additionally, the graphs indicate the sampling season and display concentrations in both total and 0.45 µm filtered water samples in µg/L.	76
Figure 24: Shows Dissolved Organic Carbon (DOC) concentrations (mg/L) across different treatment stages for spring and autumn samples in TWW. Treatments include untreated samples, Treatment 1, Treatment 2 samples combined with 0.45 µm filtration.	84
Figure 25: Shows the electrical conductivity (µS/cm) measurements across different treatment stages and seasons (spring and autumn). Conductivity levels are compared between untreated samples and those treated through Treatment 1 and Treatment 2.	85
Figure 26: Shows concentrations of selected anions (NO ₃ ⁻ , SO ₄ ²⁻ , Cl ⁻ , F ⁻) measured in untreated spring water. Chloride (Cl ⁻) was the dominant anion, with higher concentrations compared to nitrate (NO ₃ ⁻), sulfate (SO ₄ ²⁻), and fluoride (F ⁻).	86
Figure 27: Concentration-response curve showing survival probability of <i>Daphnia</i> exposed to TWW detergent at 48 hours. LC ₅₀ is indicated by the dotted line. The x-axis represents the dilution concentration, and the y-axis shows survival probability. The orange line is the median estimate, with the grey area indicating the 95% confidence interval.	89
Figure 28: <i>Daphnia magna</i> exposed to untreated TWW from spring, tested in EPA exposure media. The images show representative individual ingested particles visible in the intestine at all concentration (C1)-(C5), while (C0) have algae food and no particles from control (C0). Images are captured using darkfield (left) and brightfield (right) microscopy. All individuals are alive at the time of imaging. Images by Ole Holthusen. Scale bars: 500 µm.....	92
Figure 29: The images show a single <i>Daphnia</i> under darkfield microscopy, with a section highlighting the digestive tract. Several black particles are clearly visible and have been marked with yellow circles, indicating ingestion of particulate matter even at the lowest exposure level C1. Images by Ole Holthusen. Scale bars: 500 µm (left), 200 µm (right).	93
Figure 30: <i>Daphnia magna</i> exposed to Treatment 1 TWW from spring with M7 media. The images show individual <i>Daphnids</i> from control (C0) to increasing exposure concentrations (C1–C5), captured using darkfield (left) and brightfield (right) microscopy. All individuals were alive at the time of imaging. Images by Ole Holthusen. Scale bars: 500 µm.....	94
Figure 31: <i>Daphnia magna</i> exposed to the highest concentration of tunnel wash water from spring with M7 media in Treatment 1. A dense accumulation of ingested particles is visible along the entire digestive tract,	

marked by a yellow box, indicating particle uptake at this exposure level after treatment 1. The individual was alive at the time of imaging. Images by Ole Holthusen. Scale bars: 500 μ m.	95
Figure 32: <i>Daphnia magna</i> exposed to Treatment 2 tunnel wash water (TWW) from spring with M7 media. The images show individual <i>Daphnia</i> from control (C0) to increasing exposure concentrations (C1–C5), captured using darkfield (left) and brightfield (right) microscopy. All individuals were alive at the time of imaging. Images by Ole Holthusen. Scale bars: 500 μ m.	95
Figure 33: <i>Daphnia magna</i> exposed to the lowest concentration (C1) after Treatment 2 with no particle ingestion, from spring with M7 media. The images show one individual imaged under brightfield (left) and darkfield (right) microscopy. The individual was alive at the time of imaging. Images by Ole Holthusen. Scale bars: 500 μ m.	96
Figure 34: <i>Daphnia magna</i> exposed to the highest concentration (C5) after Treatment 2 with visible particle ingestion, from spring with M7 media. The images show a single <i>Daphnia</i> viewed under brightfield (left) and darkfield (right) microscopy. The individual was alive at the time of imaging. Images by Ole Holthusen. Scale bars: 500 μ m.	96
Figure 35: <i>Daphnia magna</i> exposed to the highest concentration (C5) after untreated TWW, from spring tested with EPA medium. The images show a single <i>Daphnia</i> viewed under brightfield (left) and darkfield (right) microscopy. A high level of particle ingestion is observed in the digestive tract (highlighted in yellow compared to the highest concentration). The individual was alive at the time of imaging. Images by Ole Holthusen. Scale bars: 500 μ m.	97
Figure 36: Concentration response curve showing estimated LC_{50} at 48 hours. The plot illustrates the survival probability of the test organisms as a function of concentration, with the orange line representing the modelled median response and the grey area indicating the 95% confidence interval. The dashed horizontal line marks the 50% survival probability threshold. The steepness of the curve and the width of the confidence band reflect uncertainty in the estimated response at higher concentrations.	99
Figure 37: Adsorbed particles from untreated TWW (Autumn, M7 media) on the swimming antenna of a live <i>D. magna</i> . The two photos were taken in brightfield and darkfield mode of the same individual by Ole Holthusen. Scale bars: 500 μ m.	100
Figure 38: Shows the adsorbed black particles and potential biofilm or decaying organic matter from untreated TWW Autumn with the M7 media on the dead <i>Daphnid</i> body, where the <i>Daphnid</i> has started to disintegrate. The two photos are taken in a brightfield and darkfield mode after 48 h on the same <i>Daphnid</i> by Ole Holthusen. Scale bars: 500 μ m.	101
Figure 39: Visualization of particle adsorption on <i>Daphnia magna</i> exposed to untreated (TWW) with M7. The images show three individual <i>Daphnia</i> , where specimen A is alive, and specimens B and C are dead. The photographs illustrate the accumulation of adsorbed particles and other associated matter on the exoskeleton. Each pair of images (left and right) represents the same individual image under darkfield (left) and brightfield (right) microscopy. All images were captured by Ole Holthusen. Scale bars: 500 μ m.	102
Figure 40: Microscopic images of a shed exoskeleton from <i>Daphnia magna</i> after exposure to untreated TWW from Autumn with M7. The images show a shed exoskeleton heavily covered with particles, visualized under darkfield (left) and brightfield (right) microscopy. Images by Ole Holthusen. Scale bar: 500 μ m.	103
Figure 41: Shows <i>Daphnia magna</i> exposed to untreated treated TWW from Autumn with EPA medium at C5, Petri dish experiment. The images show three live individuals (A–C) imaged under brightfield (left) and darkfield (right) microscopy. Images by Ole Holthusen. Scale bar: 500 μ m.	104
Figure 42: Shows the less lethal concentrations of adsorbed particles from untreated TWW autumn with the EPA media on the alive <i>Daphnids</i> swimming antenna. The two photos are taken in a brightfield and darkfield mode on the same <i>Daphnid</i> by Ole Holthusen. Scale bars: 500 μ m.	105
Figure 43: Metals above LOD with mean concentrations (μ g/L) in leachate from spring tunnel wash water particles after 12-day Milli-Q leaching under dark, agitated conditions.	109

List of Tables

Table 1: Overview of previous work on tunnel wash water, road associated microplastic and <i>Daphnia magna</i> in Norway	4
Table 2: Shows the minimum required tunnel cleaning frequencies based on average daily traffic per tunnel tube. Cleaning is divided into road surface, technical systems, and full tunnel cleaning, with frequency increasing with traffic volume. The table is taken from (Statens Vegvesen, 2024d) and modified.	9
Table 3: The table shows the given limit values in the discharge permit for the Ekeberg tunnel within 21 days. The threshold limits are given by the county governor of Oslo to the Norwegian Public Road Administration. ..	26
Table 4: Presents the sampling times for each depth during the study, with all compounds analyzed at each interval. Initially, due to system inefficiencies, the 0.45 µm filtration was performed at the end of the sampling process. This procedure was subsequently optimized in the following autumn wash to enhance efficiency.	39
Table 5: Presents the sampling depths and parameters taken on the field days during spring.	40
Table 6: Presents the sampling times for the autumn wash for each depth during the study, with all compounds analyzed at each interval.	41
Table 7: Presents the sampling depths and parameters taken on the field days during autumn.	42
Table 8: List of metals measured using ICP-MS, along with the detection limit (LOD) and quantification limit (LOQ) in µg/L based on 3×SD and 10×SD for the blank samples of the various metals.	43
Table 9: List of the tire-derived chemicals that were analyzed, along with their full names, molecular formulas, and CAS numbers.	47
Table 10: Calibration standards and detection limits used for dissolved organic carbon (DOC) analysis. Standard solutions included potassium hydrogen phthalate at concentrations of 1 mg/L (K1) and 5 mg/L (K5). The method included defined limits of detection (LOD) and quantification (LOQ) to ensure analytical accuracy.	49
Table 11: Gives an overview of the test duration, stressors, concentrations from start, volume of dilution, replicates and total number of daphnia used in tests.	58
Table 12: Presents the treatment efficiency (%) of rubber-associated microparticles for two size fractions (>5 µm and 0.4–5 µm), across spring and autumn. It includes total removal after Treatment 1 and Treatment 2, as well as the additional efficiency of Treatment 2 after Treatment 1. Color coding indicates total effect ranges	66
Table 13: Removal efficiencies (%) of selected tire-derived chemicals (TDCs) during Treatment 1 (sedimentation) and Treatment 2 (filtration) across spring and autumn sampling campaigns. Color coding indicates total removal efficiency: red (0–30%), orange (30–60%), yellow (60–85%), and green (85–100%).	72
Table 14: Removal efficiencies (%) of Metals during Treatment 1 (sedimentation) and Treatment 2 (filtration) across spring and autumn sampling campaigns. Color coding indicates total removal efficiency: red (0–30%), orange (30–60%), yellow (60–85%), and green (85–100%).	78
Table 15: The table shows the given limit values in the discharge permit for the Ekeberg tunnel within 21 days. The threshold limits are given by the county governor of Oslo to the Norwegian Public Road Administration ...	82
Table 16: Overview of the toxicity test results including titles of experiment, exposure media, test substance, immobilization % after 24 h and 48 h and the effect on <i>Daphnia magna</i>	88

Table of Contents

Abstract	ii
Sammendrag	iv
Acknowledgments	vi
Supervisors	vii
Abbreviations and Definitions	viii
List of Figures	ix
List of Tables	xii
1.0 Introduction	1
1.1 Aims of this study	2
1.2 Research Hypotheses	3
1.3 Research Objectives	3
1.4 Previous Research	4
1.5 Guidelines	5
1.6 Why is this study significant?	6
2.0 Background	7
2.1 Tunnels in Norway and Washing Procedures	7
2. 2 Contaminants in Tunnel Wash Water	10
2.2.1 Road-associated Microplastic Particles	11
2.2.2 Tire Derived Chemicals	19
2.2.3 Metals	21
2.2.4 Road Salt	22
2.2.5 Detergent	23
2.3 Laws and Regulation	25
2.4 Tunnel wash water Treatment Methods	26
2.4.1 Treatment Methods	26
2.4.2 Treatment 1 - Sedimentation Basin	28
2.4.3 Treatment 2 - Filtralite HMR	28
2.5 The Oslofjord	30
2.6 <i>Daphnia magna</i> (D.magna)	31
3.0 Materials and Method	33
3.1 Area description	33
3.2 Fieldwork	35
3.2.1 Spring wash	36
3.2.2 Autumn wash	40
3.3 Laboratory Work	42
3.3.1 Sample Pretreatment for ICP-MS Analysis	42
3.3.2 Leaching Experiment	44

3.3.3 Quantification of TWP and TRWP	46
3.3.4 Analysis of Tire Derived Chemicals	46
3.3.5 Uncertainty for TWP, TDCs and Metals	48
3.3.5 Dissolved Organic Carbon	49
3.3.6 Anion.....	50
3.4 Methods and Setup for The Acute Immobilization Test	50
3.4.1 Algae Cultivation and Diet: <i>Raphidocelis subcapitata</i>	50
3.4.2 Cultivation and Exposure water: M7 And EPA water	51
3.4.3 Study Species and Cultivation: <i>Daphnia magna</i>	52
3.4.4 Test Organism: <i>Daphnia magna</i> (<i>D.magna</i>).....	53
3.4.5 Experiment Setup	53
3.4.6 Observations and Analysis of Exposed Daphnids	58
3.4.7 Methodological Adjustments and Justifications	59
3.5 Data Processing and Statistical Analysis.....	60
3.6 Calculating Treatment Efficiency.....	60
3.7 Use of Artificial intelligence	61
4.0 Results and Discussion	61
4.1 Tire and Road Wear Particles.....	61
4.1.1 Seasonal Variation and Concentrations	61
4.1.2 Effect of Treatment 1 and 2.....	64
4.2 Tire Derived Chemicals	67
4.2.1 Seasonal Variation and Concentrations	67
4.2.2 Effect of Treatment 1 and 2.....	71
4.3 Metals	73
4.3.1 Seasonal Variation and Concentrations	73
4.3.1 Effect of Treatment 1 and 2.....	78
4.3.3 Threshold limit and EQS.....	82
4.4 Dissolved Organic Carbon / Anion	83
4.5 Toxicity Assessment.....	87
4.5.1 Detergent Toxicity Pre-Test.....	88
4.5.2 Toxicity of Untreated TWW - Spring	91
4.5.3 Toxicity of Treated TWW - Spring.....	93
4.5.4 Toxicity of Untreated TWW - Autumn	99
4.5.5 Leaching Experiment	108
5 Conclusion.....	111
6.0 References.....	112
7.0 Appendix	123

1.0 Introduction

With the global population and urban development increasingly growing, more vehicles and road structures are being built for people to navigate and commute efficiently (EEA, 2024; Rossbach, 2024). As a result, the release of pollutants is rising, thereby becoming a global environmental concern. Among these pollutants are tire and road wear particles (TRWPs), a complex mixture of tread rubber, encrusted mineral particles from road surfaces and other environmental sources like exhaust emissions and brake dust (Bouredji et al., 2023; Michael Kovochich et al., 2023). These particles are created through Tire wear particles (TWP) that are generated through friction with the road surface, causing the release of abraded tire tread fragments (Yu Wang et al., 2024). Car tire abrasion alone, give rise to emissions of 3.6 million tonne microplastic per year worldwide and it is proven that tires can contain up to 800 different chemicals (Miljødirektoratet, 2024). These particles, along with the tire derived chemicals (TDCs), have been identified as toxic to aquatic organisms and have gained significant attention as an emerging contaminant due to their wide detection, small size, mobility, and relatively high toxicity (Yu Wang et al., 2024). With the spread of tire and road wear particles, they accumulate in ecosystems through environmental pathways such as wind and water, eventually ending up in soil, water bodies and aquatic life (Brittney W. Parker et al., 2020; Stephan Wagner et al., 2022). Winter operations, such as snow plowing, snow dumping, and snow depot management, further contribute to the dissemination of microplastics (Samferdselsdepartementet, 2023-2024).

A recent study found Tire Wear Particles (TWPs) in rainwater in Svalbard, indicating that these particles can travel long distances through the air before settling via precipitation (Alling et al., 2023). Other research has also identified indoor climbing halls as potential hotspots for human exposure due to inhalation of airborne rubber particles, primarily from tire and road wear (Sherman et al., 2025). In short, TWPs are found nearly everywhere. Once deposited, the particles release additives and metals that leach out over time, posing a potential risk to the environment, additionally TRWP is assumed to feature slow weathering (Yu Wang et al., 2024). Studies have shown high levels of such additives like 6PPD and its secondary alteration product 6PPD-q exist in the Norwegian environment (Miljødirektoratet, 2024). Where 6PPD-quinone, in particular, has been identified as acutely toxic to some aquatic species (Markus

Brinkmann et al., 2022) . In Norway, the road sector is the largest contributor to microplastic pollution, primarily from tire wear, road markings, and asphalt degradation (Samferdselsdepartementet, 2023-2024). With Norway having one of the highest numbers of tunnels in Europe, these tunnels act as catchment area where the runoff are often referred to as a "cocktail" of pollutants (Meland, 2012). During tunnel washing, these accumulated pollutants are released into the surrounding ecosystem. With laws and regulation plans, like the Water Framework Directive, the Norwegian pollution law and the Norwegian transport plan, the Norwegian Public Roads Administration has initiated various treatment solutions in tunnels, that are imperative for preventing the discharge of these pollutants into the environment. One of these tunnels is the Ekeberg tunnel in Oslo, which discharges the tunnel wash water (TWW) into the Alna River, eventually flowing into the Oslo Fjord. The fjord already faces severe environmental challenges due to pollution and human activities and simultaneous measures across sectors are needed to improve its condition (Gunnar Omsted & Frigstad, 2025).

1.1 Aims of this study

The aim of this study is to evaluate the effectiveness of a new second-stage treatment step, as part of a two step solution for tunnel wash water from the Ekeberg Tunnel in Oslo. The research will assess the levels of road related pollutants, including tire wear particles, tire and road wear particles, metals, and tire derived chemicals, before treatment, after the first stage of treatment using a sedimentation pool for 21 days, and after the second stage of treatment with filtration using a Leca Filtralite Heavy Metal Removal (HMR) filter. The study aims to determine the effectiveness of each treatment stage in reducing the levels of these tire-related contaminants for a potential further use in the construction of new tunnels in Norway. The study will also investigate potential seasonal variations in pollutant concentrations between wash water collected in spring and autumn. Additionally, the study will compare treatment efficacy from previous studies and perform a risk assessment of the untreated wash water and the discharge of the treated wash water. To assess toxicity, an acute immobilization test will be performed using *Daphnia magna*, which will help determine the effects of residual chemicals and provide insight into the ecological safety and potential environmental risk of the treated discharge to the Oslo fjord.

1.2 Research Hypotheses

- **Hypothesis 1**

The concentration of TWP, TRWP, metals, and TDCs in tunnel wash water will be higher after spring washes compared to autumn washes due to seasonal accumulation and changes in tire usage.

- **Hypothesis 2**

The two-step treatment process will effectively reduce the concentration levels of TWP, TRWP, metals and TDCs in the tunnel wash water.

- **Hypothesis 3**

*Detergent residue in the tunnel wash water will not be the determining factor of lethality of *Daphnia magna*.*

- **Hypothesis 4**

*Both untreated and treated tunnel wash water from the Ekeberg Tunnel will cause toxic effects of *Daphnia magna*, with untreated water showing higher lethality.*

1.3 Research Objectives

To test the research hypotheses, three objectives have been defined.

- 1) Compare the levels of TWP, TRWP, metals, and TDCs in tunnel wash water collected during spring and autumn to identify potential seasonal differences in pollutant accumulation.
- 2) Quantify the reduction in TWP, TRWP, metals, and TDCs in the Ekeberg tunnel wash water after treatment through sedimentation and filtration using Leca Filtralite HMR, while also assessing the performance and efficiency of each individual treatment stage.
- 3) Conduct acute immobilization tests using *Daphnia magna* to evaluate the potential toxic effects of untreated and treated wash water, including the influence of residual detergent. If toxicity is observed, further identification of primary contributors to the toxicity in both untreated and treated samples should be done.

1.4 Previous Research

Table 1 presents previous work done on tunnel wash water, road associated microplastic, and *Daphnia magna* from the last 3 years in Norway. The research that is available has been important in shaping the framework of this study, offering foundational insights and methodologies.

Table 1: Overview of previous work on tunnel wash water, road associated microplastic and *Daphnia magna* in Norway

Author	Title	Where to find
Thea Oma	The effect of tunnel construction particles on <i>Daphnia magna</i>	Master Thesis: Norwegian University of Life Sciences https://nmbu.brage.unit.no/nmbu-xmlui/handle/11250/3038513
Gina Marie Granheim	Retention and treatment of tire wear particles, road wear particles, metals and organic additives in tires present in tunnel wash water from the Vålereng tunnel	Master Thesis Norwegian University of Life Sciences 2023-Masteroppgave-Granheim (3).pdf
Elisabeth Støhle Rødland	Microplastic particles from roads and traffic – occurrence and concentrations in the environment	Philosophiae Doctor (PhD) Thesis: Norwegian University of Life Sciences Brage NMBU: Microplastic particles from roads and traffic : occurrence and concentrations in the environment
Hanne Vistnes	Content and Treatment of Trace Elements and Organic Micropollutants in Tunnel Wash Water	Philosophiae Doctor (PhD) Thesis: Norwegian University of Science and Technology https://ntnuopen.ntnu.no/ntnu-xmlui/handle/11250/3166018
Sofie Eivik Karlsen	Evolution of tunnel wash water quality during sedimentation	Master thesis: Norwegian University of Science and Technology https://ntnuopen.ntnu.no/ntnu-xmlui/handle/11250/2788542

1.5 Guidelines

The methodology and toxicity tests for this thesis are based on established guidelines to ensure optimal conditions and reliable results. These guidelines provide standardized protocols that facilitate consistency, accuracy, and reproducibility in toxicity assessments.

Methods for Measuring the Acute Toxicity of Effluents and Receiving Waters to Freshwater and Marine Organisms Fifth Edition October 2002 (EPA, 2002).

The Methods for Measuring the Acute Toxicity of Effluents and Receiving Waters to Freshwater and Marine Organisms (Fifth Edition, 2002) is a key guideline published by the U.S. Environmental Protection Agency (EPA). It provides standardized methodologies for evaluating the acute toxicity of effluents and environmental waters using various test species, ensuring consistency and reliability in toxicity assessments.

OECD Guideline for Testing of Chemicals, *Daphnia* sp, Acute Immobilisation Test (OECD, 2004)

The OECD Guideline for Testing of Chemicals, *Daphnia* sp., Acute Immobilisation Test (OECD 202) is an internationally recognized method for assessing the short-term toxicity of chemicals on freshwater crustaceans, specifically *Daphnia* species. This test measures immobilization over a 48-hour period and determines the EC50 value, indicating the concentration at which 50% of the test organisms are immobilized. The OECD 202 guideline is crucial for chemical safety evaluations, as *Daphnia* are sensitive bioindicators of water quality, and their response to contaminants helps assess potential risks to aquatic life and ecosystems.

1.6 Why is this study significant?

This research is important for improving our understanding of TWP, TRWP, and TDCs, including their behavior within tunnel systems and their potential toxicity as environmental pollutants. By evaluating the new two-step water treatment process, it is also important to assess the retention of these pollutants in tunnel wash water from Norwegian tunnels and to determine how much is being released into the Oslofjord. Moreover, the findings provide valuable knowledge for the planning of treatment measures in future tunnel construction projects, such as the new Oslofjord Tunnel. Many road tunnels in Norway still lack advanced water treatment systems and instead rely mainly on basic infrastructure such as drainage channels connected to sand traps. These sand traps are designed to capture coarse debris and larger particles and coarse materials before discharge (AS, 2016). This highlights the importance of assessing the performance of the new two-step treatment method in comparison to existing methods. This study also addresses knowledge gaps by generating data to inform policies, particularly for road associated microplastic and tire derived chemicals, which currently lack discharge limits and effective mitigation measures to prevent their environmental impact. To evaluate ecological risks, the study uses *Daphnia magna* as a test organism to assess the potential toxicity of untreated and treated tunnel water. Using *D. Magna* for toxicity assessments is well established in ecotoxicology due to its sensitivity to pollutants, its ecological relevance in aquatic ecosystems, and its ability to provide insights into the broader impacts of pollutants on aquatic life (Ahmed, 2023). By identifying potential toxic effects and quantifying the reduction of harmful substances, this research contributes valuable knowledge for safeguarding water quality and informing future environmental remediation and mitigation strategies.

2.0 Background

2.1 Tunnels in Norway and Washing Procedures

Norway is well known for its fjords and mountains having a difficult topography related to road transport. With the difficult terrain and weather challenges, tunnels are imperative for safe travel. With that, Norway has close to 1300 road tunnels, spread over a distance that exceeds 1550 kilometers, being the second highest number of tunnel meters per capita in the world (Amund Bruland et al., 2024; Jære, 2024).

Tunnel washing is essential for maintaining road safety, visibility, and the durability of tunnel infrastructure. Unlike open roads, tunnels are enclosed environments with limited exposure to natural weather conditions, such as rain, snow and wind, which would otherwise help remove accumulated pollutants. Without this natural cleansing, dust, sand, exhaust particles, and other pollutants continuously build up on tunnel surfaces affecting air quality and lighting efficiency, ultimately leading to reduced visibility and increased accident risks posing risks to health, the environment, and traffic safety (NORVA24, 2017; Statens Vegvesen, 2024d). Washing the tunnel helps keep important signs clean while also removing oil and other substances that may reduce road friction. It further extends the tunnel's lifespan by preventing salt-induced corrosion of steel reinforcements, which can lead to concrete cracks (Meland & Torp, 2013; Statens Vegvesen, 2024d). Additionally, regular cleaning enhances air quality by reducing airborne particle levels inside the tunnel, but also keep pollution levels below threshold limits and reduce impact on the external environment (Byman, 2012; Meland & Torp, 2013; Statens Vegvesen, 2024d). It is recommended that particles are first removed from the roadway and shoulders in most tunnels to minimize pollution before the rest of the tunnel is washed, thereby reducing the load on drainage and treatment systems (Statens Vegvesen, 2023). In many tunnels, detergent is also used during the washing process to enhance cleaning effectiveness. Each tunnel must have a specific cleaning instruction to ensure consistent and effective maintenance; an example of the advanced cleaning method is illustrated in *Figure 1*. These instructions define the required cleaning methods for the specific tunnel, along with guidelines on cleaning frequency, as outlined in Handbook R610. The requirements apply to all tunnels, regardless of the construction method (Statens Vegvesen, 2024d).

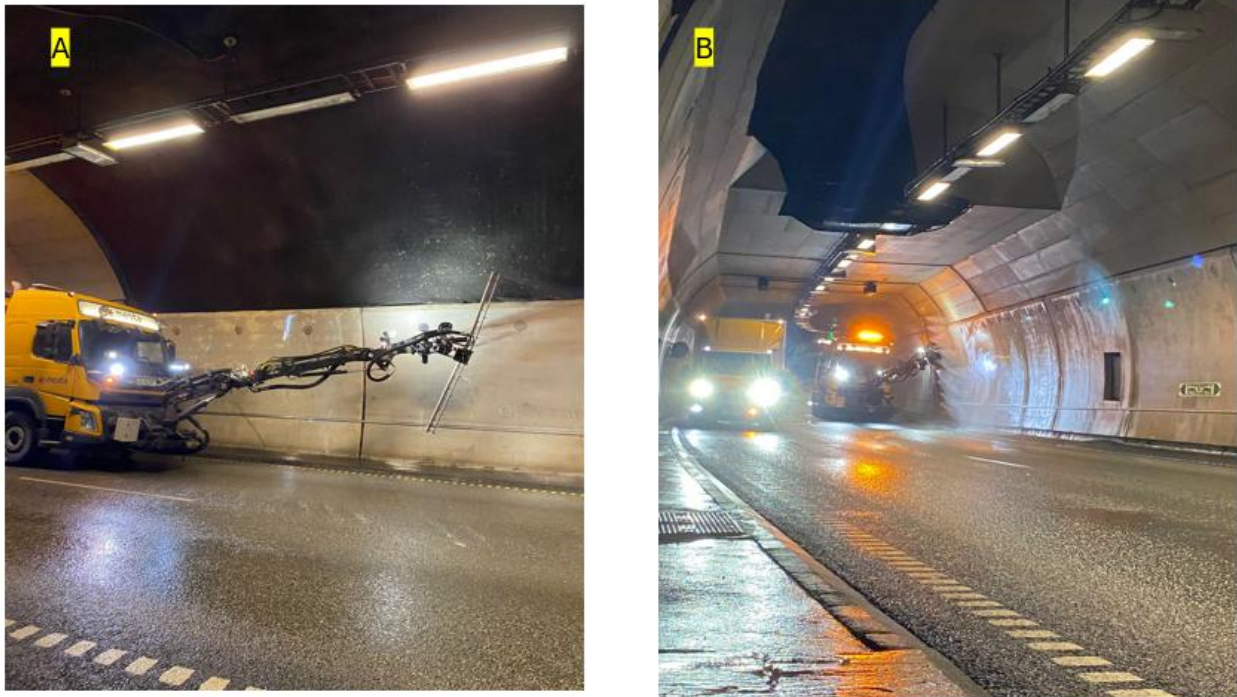


Figure 1: Photos **A** and **B** show the washing procedure and advanced cleaning system used in the Ekeberg Tunnel. Images were taken during the autumn tunnel wash by Ole Holthusen.

The frequency of tunnel cleaning is determined by the Average Annual Daily Traffic (AADT) per tunnel tube and is categorized into three types: road surface cleaning, technical cleaning, and full tunnel cleaning, as shown in *Table 2* (Statens Vegvesen, 2024d). For tunnels with an AADT exceeding 20,001 vehicles, a minimum of 8 technical cleanings, and 5 full tunnel cleanings are required per year. The Ekeberg Tunnel, with an AADT of approximately 90,000 vehicles, falls into this highest traffic category and thus requires frequent and comprehensive cleaning to ensure traffic safety and operational functionality. Full cleaning includes washing the road, shoulders, walls, ceiling, and technical equipment, and emptying sand traps while technical cleaning focuses on road surface and installations like signs, lighting, and emergency stations (Statens Vegvesen, 2024d). Cleaning must be evenly distributed throughout the year. However tunnel cleaning during cold periods can be challenging due to the risk of ice and slippery road surfaces. If temperatures are too low, cleaning is often postponed. Furthermore sand traps should be emptied before full cleaning, and surfaces left nearly dry ($\leq 200 \text{ g/m}^2$). If weather prevents full cleaning, technical cleaning may substitute. Lastly, wash water runoff must be managed, and salting applied if icing may occur (Statens Vegvesen, 2024d).

The final volume and quality of used tunnel wash water can vary depending on factors such as the cleaning method, tunnel dimensions, water usage, cleaning speed, equipment type, and the specific contractor performing the work.

Table 2: Shows the minimum required tunnel cleaning frequencies based on average daily traffic per tunnel tube. Cleaning is divided into road surface, technical systems, and full tunnel cleaning, with frequency increasing with traffic volume. The table is taken from (Statens Vegvesen, 2024d) and modified.

Traffic volume: Average annual daily traffic per tunnel tube	Cleaning: Road surface	Cleaning: Technical****	Cleaning: Complete
0 - 300	As determined locally	Every 5 years	Every 5 years
301 - 4000	As determined locally	1	1*
4001 - 8000	As determined locally	2	2**
8001 - 12000	As determined locally	4	2**
12001 - 15000	As determined locally	6	3***
15001 – 20000	As determined locally	8	4***
> 20001	As determined locally	8	5***

As outlined in *Table 2*, additional guidance is provided through the following notes:

- * Cleaning must be carried out after the winter season to remove accumulated salt and debris.
- ** Cleaning should be performed approximately every six months to ensure consistent maintenance.
- *** Ceiling cleaning can be reduced to twice per year based on local conditions. However, full tunnel cleaning should still be evenly spaced throughout the year, especially when pollution levels or cleaning needs are highest.
- **** Technical cleaning must also be evenly distributed and coordinated with full cleaning to maintain overall tunnel cleanliness and equipment function (Statens Vegvesen, 2024d).

2. 2 Contaminants in Tunnel Wash Water

Contaminants inside tunnels originate from various sources like vehicular traffic, road wear, tunnel infrastructure, winter operations along with combustion processes illustrated in *Figure 2*. As vehicles pass through, TWP, TRWP, metals, oil and petroleum residues settle on tunnel and road surfaces (Marinello et al., 2020; Meland et al., 2023). In winter, de-icing chemicals and road salts further contribute to the accumulation of pollutants, along with tunnel infrastructure and equipment, creating a mix of hazardous residues (Licbinsky et al., 2013; Piarc, 2022). These contaminants accumulate in the tunnel, where the level of contamination is influenced by factors as seasonal variation, traffic density (AADT), types of vehicles, tunnel volume, age of the tunnel, water usage during washing, the washing technique employed, and whether detergents are utilized or not (Vistnes et al., 2024). Further when the tunnels are washed, various traffic-related contaminants have been detected in the tunnel wash water, including trace elements, polycyclic aromatic hydrocarbons (PAHs), per- and polyfluoroalkyl substances (PFASs), benzothiazoles (BTHs), benzotriazoles (BTRs), bisphenols (BPs), and benzophenones (Meland et al., 2023; Vistnes et al., 2024).

Additionally, organic micropollutants from tire derived chemicals commonly used as processing aids in tire production such as, organophosphate compounds (OPC), benzothiazoles, hexa(methoxymethyl)melamine (HMMM) and N-1,3-dimethylbutyl-N 0-phenyl-p phenylenediamine-quinone (6-PPD-quinone) have been detected in both untreated and treated tunnel wash water (Rødland, 2022). Many of these substances can adversely affect aquatic life by acute and chronic toxicity, affecting aquatic ecosystems through bioaccumulation, endocrine disruption, and increased bioavailability of pollutants (Vistnes et al., 2024). Furthermore, several of these are classified as water soluble, mobile, and toxic (Yu Wang et al., 2024). There may also be numerous undetected compounds in tunnel wash water, contributing to mixture effects where, mixtures with more-than-additive effects have a higher overall toxicity than the sum of the individual pollutants (Gauthier et al., 2014; Vistnes et al., 2024). In contrast, many of the contaminants within tunnels are predominantly found in particulate forms, such as road dust, minerals, suspended solids, trace elements, tire and road wear particles, and particles from combustion sources. These particles often act as carriers for various pollutants, including metals, such as (zinc (Zn), copper (Cu), cadmium (Cd), nickel (Ni), Iron (Fe), aluminum (Al), and manganese (Mn) (Sossalla et al., 2025; Vistnes et al.,

2024). Research indicates that between 40 % and 90 % of major pollutants in tunnel wash water are particle-bound, highlighting the efficacy of sedimentation processes in removing these contaminants (Byman, 2012). However, sedimentation as a treatment step is less effective for many of the dissolved contaminants that remain in the tunnel wash water.

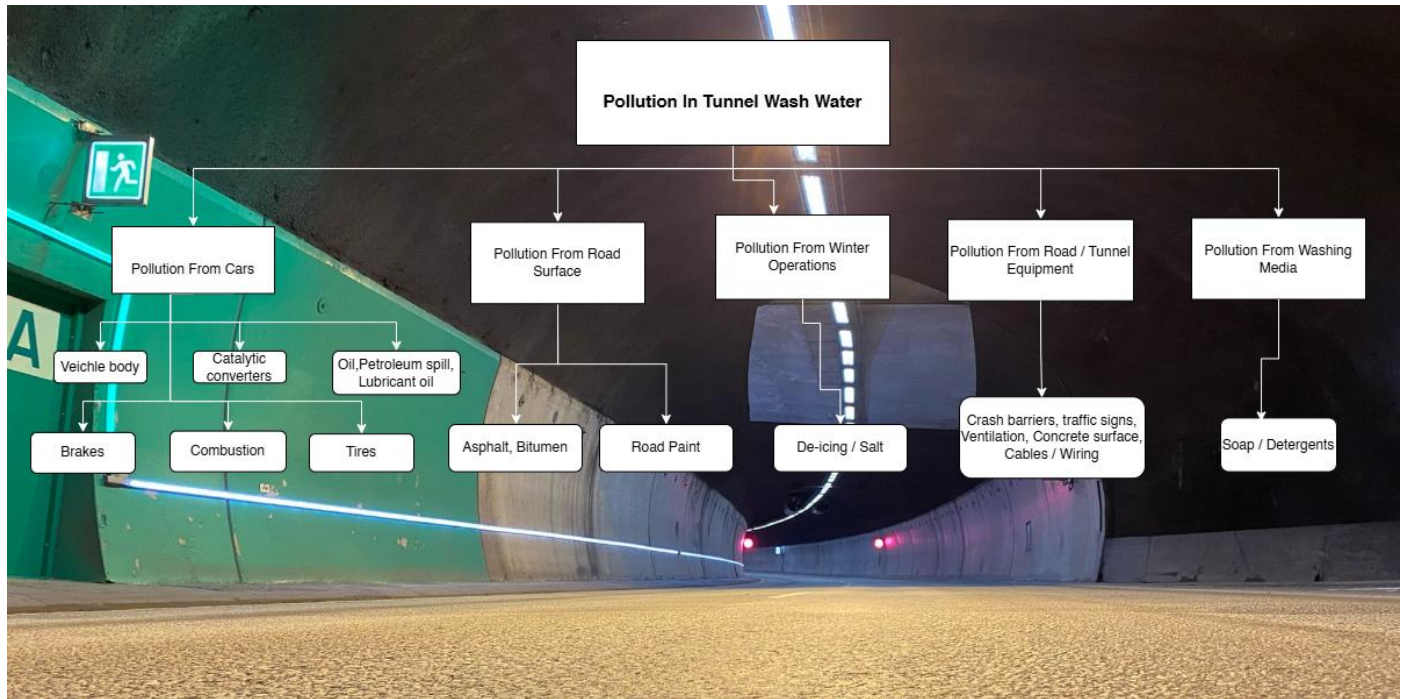


Figure 2: The figure illustrates the sources of contamination observed in tunnel wash water. Illustration and photograph (Ekeberg tunnel) are done and taken by Ole Holthusen.

2.2.1 Road-associated Microplastic Particles

Microplastics cause concerns for environment and health for many reasons due to their small size and the varying densities of different polymer materials, which facilitate their transport via atmospheric deposition and water currents. These particles can be ingested by a wide range of organisms across different trophic levels in marine, freshwater, and terrestrial ecosystems (Bank, 2022; Brittney W. Parker et al., 2020; Rødland, 2022; Stephan Wagner et al., 2022). Plastic debris in the environment exists along a continuum of sizes, typically classified as macroplastics (>25 mm), mesoplastics (5–25 mm), microplastics (1 µm to 5 mm), and nanoplastics (<1 µm) (Bank, 2022). These particles may pose significant toxicological risks due to their ability to infiltrate biological tissues, and penetrate cell membranes (Prata et al., 2020). Uptake of microplastics can furthermore cause harm to organisms.

This can occur, for example, in the form of physical blockage and abrasion (Wright et al., 2013). Smaller microplastics and nanoplastics also exhibit exaggerated surface areas and thus enhanced capacity for environmental interactions, including contaminant sorption (Bank, 2022; Wang et al., 2019). These nanoparticles, has possibly an even greater challenge for the environment and human health. Where nanoparticles can potential affect various human systems, including respiratory, cardiovascular, neurological, and immune systems (Xuan et al., 2023). Roads are estimated to be the largest single source of microplastic particles from land to the marine environment, with tire wear particles identified as the predominant contributors to microplastics entering aquatic systems (Rødland, 2022; Tamis et al., 2021). Plastics and rubbers are manufactured from synthetic or semi-synthetic organic materials, comprising either mixtures of different polymer components or single polymers. The most used synthetic rubber types include styrene-butadiene rubber (SBR), butadiene rubber (BR), styrene-butadiene-styrene (SBS), and acrylonitrile-butadiene-styrene (ABS). SBR and BR are primarily used in vehicle tires (Rødland, 2022; Wagner et al., 2018) while SBS is mainly applied in road surfaces, pavements, and roofing materials (Rødland, 2022). Synthetic rubbers are extensively used in vehicle tires and road surfaces, particularly in the form of polymer-modified bitumen (PMB) incorporated into asphalt or asphalt concrete (Rødland, 2022).

These materials are released into the environment through the friction generated between tires and the road surface, leading to the formation of tire wear particles (TWP) and road wear particles (RWP) containing polymer-modified bitumen (PMB) (Yu Wang et al., 2024). The amount and size of these wear particles are influenced by several factors, including average daily traffic (ADT), ambient temperature, the material composition of both tires and road surfaces, vehicle type, speed and driving behavior, as well as the type of interaction between the tire and the road whether it's acceleration, rolling, or braking (Alexandrova, 2007; Vogelsang et al., 2020). Wear on asphalt and road surfaces is particularly pronounced during winter, largely due to the use of studded tires, which accelerate surface degradation (Sundt et al., 2020). Additionally, road markings (RM) applied to road surfaces contain various synthetic polymers that degrade and release particles due to weathering and traffic load. Collectively, TWP, RWP, TRWP and RM are categorized as road-associated microplastic particles (RAMP), all originating from materials intentionally applied to vehicles or road infrastructure (Rødland, 2022; Vogelsang et al., 2020).

Tire Wear Particles

Tire wear particles are a significant source of non-exhaust particulate emissions in the environment. It has been estimated that between 5,000 to 11,000 tons of road particles, with at least 80% being TWP, are released into the environment each year in Norway (Alling et al., 2023). This estimate suggests that TWP could be the most substantial land-based source of microplastics in the Norwegian environment (Alling et al., 2023). Once generated, TWPs are either suspended in air or accumulate on road surfaces, from where they are transported to soils and aquatic systems via runoff and atmospheric deposition (Kole et al., 2017; Turner & Rice, 2010; Wik & Dave, 2009). Beyond their role as plastic pollutants, TWPs contribute to the dispersion of various metals and tire derived chemicals into air and soil environments (M. Zhang et al., 2023). Although they contribute 0.27–12.3% of $PM_{2.5}$ and 0.84–10% of PM_{10} , they are considered a significant diffuse pollution source (Grigoratos & Martini, 2014; Panko et al., 2019; Youn et al., 2021). The rise of electric vehicles (EVs), which are on average 24% heavier than conventional gasoline cars and also tend to accelerate faster, is predicted to further increase TWP emissions by 20% for PM_{10} and 30% for $PM_{2.5}$ (Timmers & Achten, 2016).

Tires are made from a complex blend of synthetic and natural materials optimized for performance, durability, and safety. The tire tread, in particular, is designed to withstand constant contact with the road, and consists of several major components by weight (Baensch et al., 2020; Sommer et al., 2018; Wagner et al., 2018). *Figure 3* shows the chemical composition of tire tread includes polymers, fillers, oil, vulcanizers, and additives used for tire preservation that consist of 40–50% polymers: including natural rubber (NR), styrene-butadiene rubber (SBR), and butadiene rubber (BR), which provide elasticity and tensile strength. 30–35% fillers: such as carbon black and silica, used to enhance mechanical strength and abrasion resistance. 15% softeners: including oils and resins, to improve processability and flexibility. 2–5% vulcanization agents: primarily sulfur and zinc oxide (ZnO), used for rubber cross-linking. 5–10% additives: such as antioxidants, plasticizers, and antiozonants. Specific compounds include 6PPD (*N*-(1,3-dimethylbutyl)-*N'*-phenyl-*p*-phenylenediamine) and HMMM (hexamethoxymethylmelamine), which contribute to the tire's performance, durability, and chemical stability (Johannessen et al., 2022; Sommer et al., 2018).

This blend, varying by manufacturer and tire type, creates a carbon-rich matrix with more than 70% of the tread consisting of carbonaceous materials, and organic carbon accounting for 75% of this (Park et al., 2016). Given the carbon content, tires are considered a notable source of particulate matter emissions (M. Zhang et al., 2023).

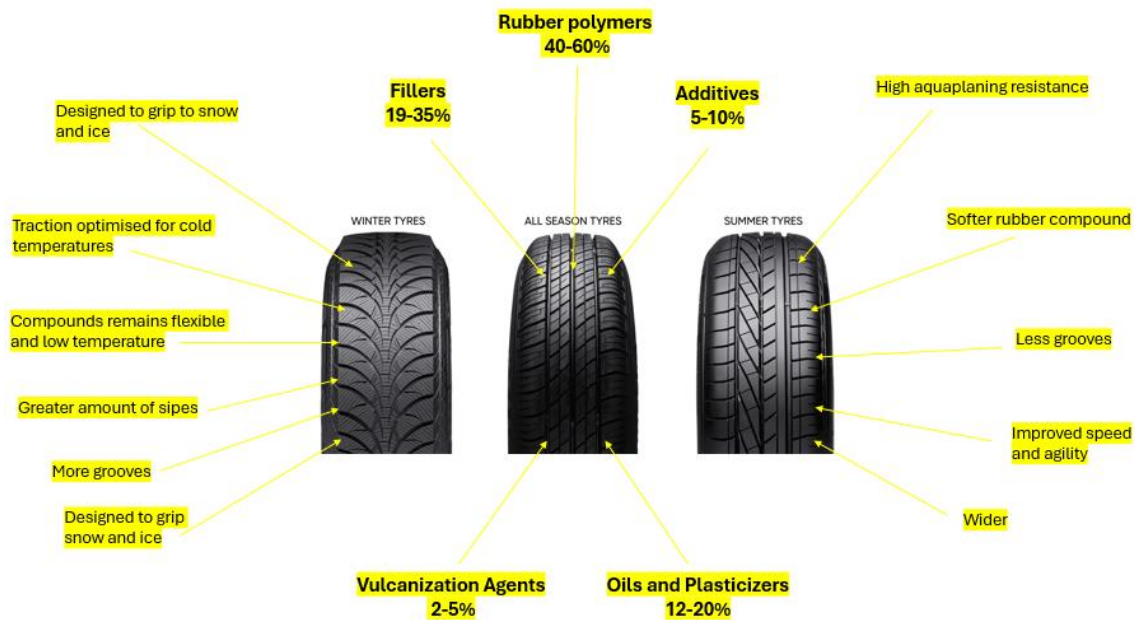


Figure 3: The figure illustrates the structural and material differences among winter and summer tire designs, along with the chemical composition of tire tread includes polymers, fillers, oil, vulcanizers, and additives used for tire preservation. The figure is made by Ole Holthusen, with inspiration from (Johannessen et al., 2022; merityre, n.d).

TWPs are heterogeneous in size, shape, and chemical composition, influenced by vehicle type, road surface, tire formulation, tire pressure and driving style (Alexandrova, 2007; Thorpe & Harrison, 2008). They typically range from 5.6 nm to 350 μm in size, with most particles falling within the 20–220 μm range (Foitzik et al., 2018; Kreider et al., 2010; Sommer et al., 2018). That said, it is suggested that the majority of tire wear particles (TWP) are smaller than 50 μm and are particularly dominant in road tunnel environments (Klöckner et al., 2021). TWPs commonly contain elements such as Al, Ba, C, Ca, Cl, Cr, Cu, Fe, K, Mg, Mn, Na, S, Ni, Ti, Zn, and Si, many of which derive from tire tread compounds and external road materials (Camatini et al., 2001; Zhang et al., 2020). Notably, Zn and S are especially associated with tires and are broadly distributed across different TWP size fractions (Gustafsson et al., 2008). The generation and physical properties of TWPs are influenced by road surface roughness, ambient temperature, humidity, and water presence.

Contact temperatures between tire and road can reach 30–50 °C, enhancing TWP production, especially on rough or humid surfaces (Chang et al., 2020). Humidity and water further act as lubricants and coolants, reducing wear intensity and resulting in smaller particle sizes (Chen et al., 2011; Tangudom et al., 2014). Tire type is also a major factor in TWP emissions. In Norway, studded tire use has declined significantly and now accounts for only about 29% of car trips nationally, with 64% using studless winter tires (Statens Vegvesen, 2024c). Still, regional differences are stark with over 72% of vehicles in northern Norway use studded tires in winter due to harsher conditions (Statens Vegvesen, 2024c). These generate significantly more particles compared to non-studded and summer tires up to 2–6.4 times more particles, and 60–100 times more PM₁₀ (Dahl et al., 2006; Gustafsson et al., 2008; Hussein et al., 2008; Kupiainen et al., 2003; Mathissen et al., 2011). The extent and type of treadwear also influence TWP morphology. Tires with low treadwear produce larger, strip-shaped, flocculent particles centered around 50–100 µm, whereas tires with higher wear create smaller, rounder particles and smoother wear surfaces (Lee et al., 2019; Woo et al., 2022).

Road Wear Particles

Road wear particles are typically similar in size and shape to tire wear particles (TWP) and tire and road wear particles (TRWP), although variations in morphology have been reported (Kreider et al., 2010; Sommer et al., 2018; Vogelsang et al., 2020). Although these particles are not analyzed in this thesis, it is important to distinguish them, as they represent a significant source of road related contamination and are likely to be present in tunnel wash water (TWW). RWPs primarily consist of mineral fragments such as quartz, feldspar, pyroxene, amphibole, and mica, which account for approximately 94–95% of their mass. These mineral components are typically held together by 5–6% bitumen derived from asphalt, while particles from road markings contributed less than 1%, and glass bead particles with the lowest detected fraction <0.1% (Järlskog et al., 2022; Sommer et al., 2018). Additional elemental constituents reported in RWPs include silicon (Si), aluminum (Al), calcium (Ca), sodium (Na), potassium (K), magnesium (Mg), iron (Fe), and sulfur (S) (Sommer et al., 2018). Bitumen wear particles (BiWP) are also commonly found in environmental samples. Bitumen, a crude oil derivative, contains elements such as sulfur, nitrogen, vanadium, nickel, and calcium in low concentrations (Holý & Remišová, 2019). It is used in both the wearing course and binder layers of pavements,

which typically contain high proportions of minerals. Due to its adhesive nature, bitumen can stick to mineral grains and form particle agglomerates (Järlskog et al., 2022). Road wear particles are dominated by the coarser size mode, but range from about 0.2–2000 μm (Järlskog et al., 2022). In *Figure 4 image C*, we can see the exposed road aggregate or so called "road skeleton," where the binder (bitumen) and finer wear particles have eroded away in the Ekeberg tunnel, leaving behind the coarse mineral structure. This illustrates the extent of physical degradation contributing to road wear particles (RWPs). Particles from road marking (RM) are also a source of microplastic and are expected to be in the size ranges 50–4000 μm (Vogelsang et al., 2020). RM differs from the other two RAMP particles by being more square like fragments formed by the breaking of road marking layers and are found both with and without glass beads present (Rødland, 2022). RM is expected to have lower densities ($>1.2 \text{ g/m}^3$) than both TWP/TRWP and PMB, depending on the amount of glass beads in each particle (Rødland, 2022). *Figure 4 image B* shows the road markings (thermoplastic paint) in the Ekeberg tunnel, showing partial abrasion of the paint. The image highlights the wear patterns of road marking materials. Kole et al. estimated that 5% of the total amount of road markings is released into the environment annually (Kole et al., 2017). The wear rate is notably higher in countries where road salting, winter maintenance, and studded tires are common practices (Järlskog et al., 2022).



Figure 4: Shows the surface conditions in the Ekeberg Tunnel showing features related to road wear and particle release.

- A:** Corroded steel drainage outlet with dark streaks possibly indicating runoff containing oils or other organic residues.
- B:** Worn thermoplastic road markings showing abrasion, a potential source of road associated microplastic particles.
- C:** Exposed road aggregate (road skeleton) where the bitumen binder and finer particles have eroded, illustrating mineral-based road wear particle formation. All images take by Ole Holthusen in the Ekeberg tunnel

In many modern road constructions, the bitumen used is polymer-modified bitumen (PMB), which contains 3–10% synthetic polymers or rubbers to improve asphalt performance by reducing temperature sensitivity and increasing resistance to cracking and rutting (Saba et al., 2012). The most commonly used polymer in PMB is styrene-butadiene-styrene (SBS), a thermoplastic elastomer (Rødland, 2022). In Norway, PMB asphalt makes up approximately 6% (3282 km) of the total state and county road network, however, it is used mainly in and around the largest cities and on roads where the traffic densities and speed is the highest (E. S. Rødland et al., 2022). PMB usually constitutes 5% of the total road asphalt and is only used in the top layer of the road surface. Several countries including Australia, China, Denmark, Norway, Russia, Sweden and the United Kingdom (EAPA, 2018), add PMB to their road surfaces to increase resistance to cracking and deformation of the road surface (Saba et al., 2012).

Tire Road Wear Particles

Tire wear debris is defined as particles produced by the rolling shear of the tire tread against the road surface (Rogge et al., 1993). However, as tires are subjected to prolonged use, the interaction with pavement alters the chemical and physical properties of the resulting particles. This transformation occurs through mechanisms such as frictional heat and the incorporation of road materials into the wear particles, leading to compositions that differ from the original tread (Adachi & Tainosho, 2004; Kreider et al., 2010; Williams & Cadle, 1978). During formation, tire wear particles often mix with road surface materials and brake wear residues, creating hybrid particles known as TRWPs, a blend of synthetic rubber, minerals, brake dust, paint, metals, and asphalt-based compounds (Adachi & Tainosho, 2004; Kreider et al., 2010; Panko et al., 2013; Sommer et al., 2018). These particles are not homogeneous; rather, they exhibit diverse shapes and densities due to their composite nature shown in *Figure 5*. Most TRWPs are characterized by elongated or irregular morphologies, formed by the aggregation of TWP rubber with road minerals and dust in the color of black (Sommer et al., 2018). As TRWPs roll along the road, they can accumulate additional material, including metals, quartz, and feldspar, which alters their surface chemistry and density (Sommer et al., 2018).

Previous studies have reported that the mineral content in TRWPs varies significantly, with literature estimating a range of 6–53% (Klößner et al., 2021; Kreider et al., 2010; Sommer et al., 2018). In some studies, estimates reach up to 50–60% mineral content (Kreider et al., 2010; Vogelsang et al., 2020), though there remains substantial uncertainty due to variability in sampling and analytical methods (Rauert et al., 2021). This mixed composition makes TRWPs more chemically and physically complex than pure TWPs, complicating their environmental behavior and potential toxicity (Knight, 2020). Size distributions for TRWPs are typically reported within the 50–350 μm range, with approximately 85% of particles falling within this window, where $<50\text{ }\mu\text{m}$ are around 15% of the particles (Kreider et al., 2010; Rødland, 2022). The density of TRWPs also varies due to their heterogeneous makeup. While the density of pure rubber TWP is around 1.2 g/cm^3 , environmental TRWPs can have densities ranging from 1.2 to over 2.1 g/cm^3 , depending on the degree of mineral integration (Degaffe & Turner, 2011; Jung & Choi, 2022; Kayhanian et al., 2012; Klößner et al., 2021; Rødland, 2022).

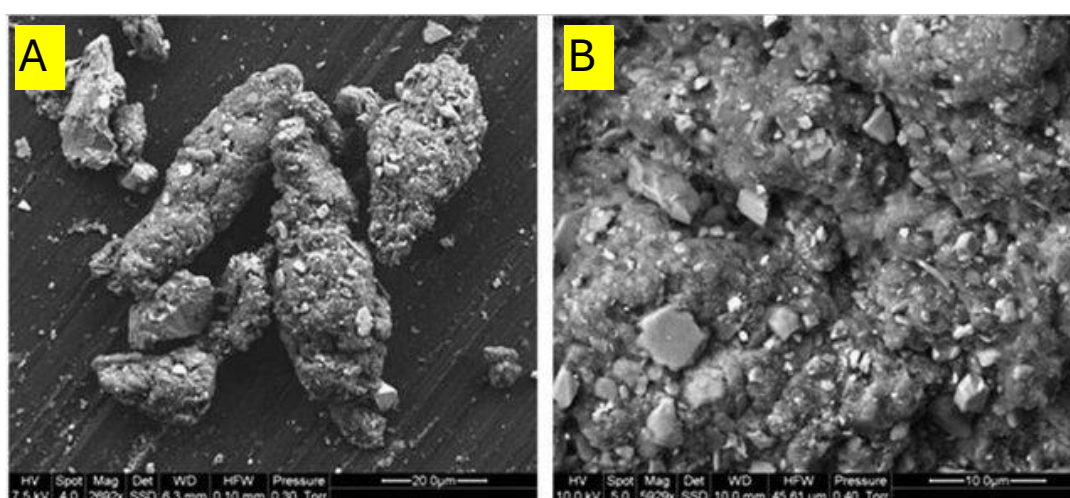


Figure 5: Scanning electron microscope (SEM) images of a tire and road wear particle (TRWPs). Image **A** shows elongated TRWP aggregates, while Image **B** provides a close up view highlighting the mineral inclusions embedded within the rubber matrix. These mineral incrustations, originating from the road surface, illustrate the composite nature of TRWPs formed through the interaction between tire material and road particles.

Pictures are gathered from (Kreider et al., 2010)

2.2.2 Tire Derived Chemicals

Tire derived chemicals (TDCs) are increasingly recognized as significant contributors to environmental pollution, as chemical additives present in tires can leach from tire and road wear particles (TRWPs) when exposed to water, thereby contributing substantially to environmental contamination (Müller et al., 2022). Tires are a chemically complex and heterogeneous mixture, consisting of different compounds and chemical additives (5–10% by mass) that are essential for their production, stability, and durability (Kole et al., 2017; Wagner et al., 2018). These tire derived chemicals, such as preservatives, antiozonants, antioxidants, desiccants, plasticizers, and processing aids, contribute to important characteristics like grip under different weather and road surface conditions, and external noise reduction (Meland et al., 2023). Variations in the composition and use of additives arise from differences between tire brands, types, and regional environmental factors such as temperature and UV exposure (Rødland, 2022). One recent study identified 214 organic compounds in tires, of which 145 of the compounds were classified as leachable substances, with nearly 60% considered mobile, suggesting a high potential for environmental transport (Müller et al., 2022).

Tires contain various chemicals, including metals such as zinc, which is essential for the vulcanization process, and organic compounds that provide protection against oxidative and ozone degradation (Alling et al., 2024). Vulcanizing agents are crucial for enhancing the physical and mechanical properties of rubber by accelerating the vulcanization reaction (Zhang et al., 2023). The most commonly used vulcanizing additives include thiazoles, thiurams, sulfenamides, and guanidines, such as 2-mercaptobenzothiazole (MBT), tetramethylthiuram disulfide (TMTD), N-cyclohexyl-2-benzothiazolesulfenamide (CBS), and 1,3-diphenylguanidine (DPG) (Rauert et al., 2022; Wik & Dave, 2009; Zhang et al., 2023). Protective antioxidants are also added to extend the storage and service life of rubber products by preventing oxidative degradation. Among these, p-phenylenediamine (PPD) antioxidants are the earliest developed group and are notable for their wide variety and protective effects (Zhang et al., 2023). However, the vast number of rubber products have resulted in an incredible release of PPDs and related degradation products into the environment. Various PPDs, such as *N*-(1,3-dimethylbutyl)-*N'*-phenyl-*p*-phenylenediamine (6PPD), *N,N'*-bis(1,4-dimethylpentyl)-*p*-phenylenediamine, *N*-phenyl-*N'*-cyclohexyl-*p*-phenylenediamine (CPPD), *N*-isopropyl-*N'*-phenyl-1,4-phenylenediamine (IPPD),

N,N'-di(*o*-tolyl)-*p*-phenylenediamine (DTPD), and *N,N'*-diphenyl-*p*-phenylenediamine (DPPD), have been detected in different environmental matrices, including airborne particles, water, and sediments (Cao et al., 2022; Rauert et al., 2022). Processing aids are further used to improve product quality and production efficiency. These additives include dispersants, homogenizers, plasticizers, and coupling agents, with common examples being dibutyl phthalate (DBP) and hexamethoxymethylmelamine (HMMM) (Rauert et al., 2022; Wik & Dave, 2009; Zhang et al., 2023). HMMM functions as a binding agent in tires, in addition to the tire industry, HMMM is also used as an additive in textiles, paints, and adhesives (Johannessen et al., 2021). DPG is used as a catalyst in the formation of rubber products, such as tires (Johannessen et al., 2022). Many of these additives in tires will further transform into new compounds during tire production, use, and once they enter the environment.

Experimental studies have identified 26 new chemicals as possible transformation products from the additive HMMM (Johannessen et al., 2021; Peter et al., 2018; Seiwert et al., 2020). These substances have demonstrated harmful effects on a wide range of organisms were one of the most critical additives is *N*-(1,3-dimethylbutyl)-*N'*-phenyl-*p*-phenylenediamine (6PPD), used as an antioxidant and antiozonant (Müller et al., 2022). Upon environmental exposure, 6PPD transforms into 6PPD-quinone (6PPD-Q), which has been linked to acute toxicity in aquatic species and sediment-dwelling organisms (Garrard et al., 2022; Hiki & Yamamoto, 2022; Tian et al., 2021). Furthermore, other antioxidants like TMQ (poly(1,2-dihydro-2,2,4-trimethylquinoline)) have also exhibited significant toxicity towards aquatic life (Wang et al., 2023). In addition, benzothiazoles are an important class of chemicals with various applications, particularly within the tire industry (Kloepfer et al., 2005). The largest amount of benzothiazoles has been used as vulcanization accelerators, such as 2-morpholiniothiobenzothiazole, in rubber production, where they are added at concentrations exceeding 1% (Kloepfer et al., 2005). In addition to improving the mechanical strength and abrasion resistance of rubber products, benzothiazoles are also incorporated as corrosion inhibitors, catalysts, and stabilizing agents (Schlabach et al., 2020). Environmental concerns arise as several benzothiazoles used in tire production are expected to leach from tire and road wear particles into aquatic environments (Reddy & Quinn, 1997). Among the benzothiazoles, benzothiazole (BT) and 2-(4-morpholinyl)benzothiazole (24MoBT) are particularly notable, as they can readily leach from rubber materials and asphalt surfaces into

the environment (Reddy & Quinn, 1997). Other leachable benzothiazole derivatives, such as benzothiazole-2-sulfonic acid (BTSA) and 2-hydroxybenzothiazole (OHBT), have also been detected at high concentrations in road runoff, highlighting their environmental relevance (Kloepfer et al., 2005). Given their widespread presence and transformation into harmful compounds, tire-derived pollutants pose a substantial threat to aquatic ecosystems and terrestrial organisms (Baensch et al., 2020; Johannessen et al., 2021).

2.2.3 Metals

Tunnel wash water is a complex and often highly contaminated matrix, in which metals represent a major environmental concern (Meland, 2010). These metals are often present at levels that exceed environmental quality standards. Some of them are classified as hazardous or particularly hazardous substances, which makes them subject to strict regulation and monitoring (I. Korytář et al., 2022). These contaminants primarily originate from road traffic and infrastructure, including wear and tear from vehicle components. In addition, particles and materials from asphalt, bitumen, and tunnel surfaces also contribute to the accumulation of metals in tunnel environments (Meland, 2010; Sossalla et al., 2025). Such metals come from different parts of the vehicles, such as tires (lead, zinc), exhaust gases (cobalt, nickel), brake linings (antimony, copper, iron, lead, zinc), batteries (zinc), and engine wear and welded metal plating (chrome, nickel) (Huber et al., 2016; Meland et al., 2010; Müller et al., 2020; Sossalla et al., 2025). In addition to vehicles, road components contribute to the release of pollutants. Road paints used for safety fences contain lead and zinc (Huber et al., 2016; Sossalla et al., 2025). Metals can also leach from solid particles into the water, especially under certain environmental conditions. For example, zinc (Zn) and copper (Cu) are known to leach from tunnel wash sediments, contributing to elevated dissolved metal concentrations (Posavec, 2018). The presence and behavior of these metals in water are highly dependent on their physico-chemical forms, or speciation. In contrast to many organic pollutants, metals cannot be broken down by biological or chemical degradation, as they are elemental and persist in the environment (Fairbrother et al., 2007). Instead, their mobility, bioavailability, and toxicity are governed by their speciation and defined by characteristics such as molecular mass, charge, oxidation state, and degree of complexation (Borgstrøm et al., 2010; Fairbrother et al., 2007; Meland, 2010). Further environmental conditions like pH, redox potential, water

temperature, ionic strength, and the presence of ligands such as carbonates and organic matter significantly influence metal speciation (Meland, 2010). Metals commonly associate with suspended particles in water, meaning that higher concentrations of suspended solids can lead to increased levels of particulate-bound metals. Consequently, reducing suspended solids often results in lower metal content. However, some metals exist in dissolved forms that do not readily attach to particles and are not easily removed through sedimentation (Sossalla et al., 2025). Additionally, changes in pH can influence metal behavior by causing them to desorb from particles or dissolve, making them more mobile in the water (Borgstrøm et al., 2010; Meland, 2010). The behavior of metals in aquatic environments is of particular concern due to their potential toxicity. Effects have been documented at multiple biological levels from molecular and cellular damage, such as protein denaturation and impaired osmoregulation, to reduced growth, behavioral changes, and even disruptions to population dynamics in aquatic organisms (Borgstrøm et al., 2010; Suryapratap Ray & Rahul Vashishth, 2024). Because of their persistence and potential for bioaccumulation, some heavy metals are also classified as environmental toxins. These substances can concentrate as they move up the food chain, eventually reaching levels that are harmful to both animals and humans (Suryapratap Ray & Rahul Vashishth, 2024).

2.2.4 Road Salt

Road salt is very commonly used substance in Norway to prevent or eliminate ice that has formed on road surfaces. The deicing work by lowering the freezing point of the ice that is present on the surface. It forms a brine which causes salt crystals, usually sodium chloride (NaCl), to pull water molecules out of the ice. This brine then dramatically speeds up the melting process as it continues to form over time. The sodium chloride in the applied salt is then dissolved into sodium and chloride ions and can significantly affect water chemistry and degrade water quality by altering the physical and chemical conditions of surface water (Mansberger, 2023). Each year, Norway uses around 250,000 tons of salt, however, salt is usually not applied inside tunnels, but it can still be deposited from the vehicles driving through (Bazilchuk, 2019; Meland, 2012). Salts not only mobilize heavy metals that are otherwise immobile or bound in particles but also transform them into more bioavailable forms such as free ions, soluble compounds, and weakly adsorbed species (Behbahani et al.,

2021; Matthew S Schuler & Relyea, 2018). This process typically occurs via ion exchange or complexation, increasing the proportion of free metal ions in the water that often are in more toxic forms. These are more readily absorbed by aquatic organisms and thus more likely to accumulate in the food web (Behbahani et al., 2021). Elevated chloride levels can also negatively affect aquatic organisms by disrupting osmoregulation, inhibiting growth and reproduction, altering food webs, and causing oxygen depletion in stratified water bodies (Mansberger, 2023). Road salt also contributes to car and infrastructure corrosion, deteriorating vegetation near the roads and the corrosion of asphalt (Szklairek et al., 2022). A recent study showed that high concentrations of 6PPD and 6PPD-quinone had lethal effects on rotifers. The presence of NaCl increased their sensitivity to 6PPD, amplifying toxic effects at lower concentrations. Conversely, 6PPD also intensified the toxicity of NaCl (Toni Klauschies & Jana Isanta-Navarro, 2022).

2.2.5 Detergent

Detergents are commonly used in tunnel wash water to remove dust, oils, rubber residue, and road salt, but they can also significantly influence the environmental impact of the wash water effluent (Roger Roseth & Søvik, 2006). A report investigated the chemical composition of detergents used for tunnel washing in Norway and found that they typically consist of three main components: surfactants, alkaline washing agents, and solvents (Roger Roseth & Søvik, 2006). Surfactants, depending on their electrical charge, can be classified into three categories: anionic (negatively charged), cationic (positively charged), and nonionic (uncharged) (Byman, 2012). These surfactants are surface-active substances that reduce water's surface tension, allowing for efficient removal of grease and dust. Their molecular structure, which includes both hydrophilic and hydrophobic ends, enables them to interact with both water and oil. However, because surfactants are organic compounds with long hydrocarbon chains, they can be toxic to aquatic organisms, not only due to their surface activity, but also due to the byproducts formed during biodegradation (Byman, 2012; Roger Roseth & Søvik, 2006). Studies have also shown that surfactants, along with sodium silicate, are among the primary contributors to the toxicity of detergents. This was confirmed in a toxicity study on Swedish detergents and softeners using *Daphnia magna* as a test organism (A Pettersson et al., 2000; Tomislav Ivanković & Hrenović, 2010). In practice, detergent use

during tunnel washing varies. Detergent consumption has previously been estimated at 0.2–0.5% of the total wash water volume, equating to roughly 500 liters per kilometer in a dual-tube, four-lane tunnel (Meland, 2012). However, detergent percentages are now substantially lower, with more recent data from the Ekeberg tunnel indicating lower detergent usage, with concentrations of approximately 0.03% in spring and 0.15% in autumn. Their use must comply with regulations regarding runoff to local water bodies or sewers and be tailored to the surface type and cleaning method. All detergents must be biodegradable according to OECD Test 301, meet Norwegian Product Regulations, be eco-labeled like the Nordic Swan or EU Ecolabel, and be approved for use on the specific equipment (Statens Vegvesen, 2023). Contractors are generally free to choose approved detergents, as cleaning contracts rarely specify exact products. However, detergents can contain substances harmful to the environment if discharged untreated. Therefore, regional rules and approved detergent types must be addressed in the cleaning contracts (Statens Vegvesen, 2023).

The degradation of the detergent is also important, where the standard tests of the product is often tested at room temperature (19–24 °C), which does not reflect the typically colder and darker conditions in tunnel sedimentation basins. As a result, detergent degradation in such environments may occur much more slowly (Sossalla et al., 2025). The use of detergents in tunnel washing can also interfere with the sedimentation process by dispersing particles, potentially reducing the effectiveness of sedimentation treatment (M. Hallberg et al., 2014). Detergents used in tunnel wash water have been shown to remobilize heavy metals from sediments, increasing their bioavailability and, consequently, their potential environmental impact (Bjotveit, 2020; Aasum, 2013). In parallel, research has found that detergents can also enhance the solubility of organic micropollutants, particularly individual benzothiazole (BTH) compounds during sedimentation processes, leading to elevated concentrations of these substances in the effluent (Meland et al., 2023). Beyond their direct chemical effects, detergents are believed to significantly influence the fate and behavior of tunnel-derived contaminants (TDCs) within treatment systems. This influence may be driven by multiple mechanisms, including enhanced desorption and solubilization of pollutants from particles, micelle formation that encapsulates contaminants, and changes in colloidal stability (Meland et al., 2023).

For instance, (Yan Xia et al., 2020) demonstrated that detergent can alter how microplastic particles adsorb ionic organic pollutants, further highlighting the complex ways in which detergents can impact contaminant dynamics in water treatment system (Meland et al., 2023; Yan Xia et al., 2020).

2.3 Laws and Regulation

The regulatory framework governing discharges of TWW is grounded in the Norwegian Pollution Control Act (Forurensningsloven), which in §1 aims to protect the external environment from pollution, reduce existing pollution, and promote better waste management (Lovdata, 2023). In Norway, tunnel wash water (TWW) discharges are regulated regionally through permits that define environmental criteria for various pollutants. However, it is important to note that out of approximately 1,200 tunnels in Norway, only about 50–60 are currently regulated with a discharge permit. Additionally, the scope of these permits varies significantly, many only include basic parameters such as pH, suspended solids (SS), and oil, leaving out a broader range of potentially harmful contaminants.

In this case the county governor of Oslo has given these thresholds limits. These permits typically set limits for parameters such as pH, suspended solids, trace elements including arsenic (As), lead (Pb), cadmium (Cd), chromium (Cr), copper (Cu), nickel (Ni), and zinc (Zn), as well as polycyclic aromatic hydrocarbons (PAHs), accounting for both their particle-associated and dissolved forms shown in *Table 3* for the Ekeberg tunnel. The regulatory framework is based on the European Union's environmental quality standards (EQS) for surface water, which aim to ensure the protection of aquatic environments and public health (Union, 2013; Vistnes et al., 2024). These EQS values are derived from the European Water Framework Directive (EU WFD), which requires that all water bodies achieve at least "good ecological status." In line with this directive, the Norwegian Environment Agency (Miljødirektoratet) has implemented a national classification system for water bodies (Miljødirektoratet, 2020b; Sossalla et al., 2025) and developed regional water management plans and action programmes aimed at meeting these environmental targets. The goal is to reach a minimum of Class II water quality, defined as "good," across all relevant water bodies in Norway (Sossalla et al., 2025; Vannportalen, 2022).

Table 3: The table shows the given limit values in the discharge permit for the Ekeberg tunnel within 21 days. The threshold limits are given by the county governor of Oslo to the Norwegian Public Road Administration.

Parameters	Threshold value
pH	6-8.5
Suspended solids	400 mg/L
Arsen	6 µg/L
Lead	13 µg/L
Cadmium	2 µg/L
Copper	50 µg/L
Chromium	10 µg/L
Nickel	40 µg/L
Zinc	110 µg/L
Oil	5 mg/l

2.4 Tunnel wash water Treatment Methods

2.4.1 Treatment Methods

The tunnel washing procedure generally follows a standardized process. Initially, dirt and larger particles are removed using a suction/sweeper truck. This is followed by washing the tunnel surface with water, and in some cases, detergent. To manage the resulting tunnel wash water (TWW), several treatment methods are currently in use or under evaluation. In many systems, sedimentation is supported by chemical precipitation (coagulation) to improve removal efficiency, especially when fine or colloidal particles are present. Coagulants like aluminum salts or sodium hydroxide help small particles form larger flocs that settle more easily (Byman, 2012). This method effectively removes dissolved and suspended pollutants, and by speeding up sedimentation, it reduces the required retention time allowing for smaller basin designs without reducing treatment performance (M. Hallberg et al., 2014). However, chemical precipitation is typically used for tunnel construction water during the building phase, and is not commonly applied for tunnel wash water in Norway. Biofiltration is another promising treatment method and has demonstrated significant removal efficiencies for both

low molecular mass (LMM) and particulate fractions of metals such as arsenic (As), chromium (Cr), copper (Cu), nickel (Ni), antimony (Sb), and zinc (Zn). According to recent results, significant decreases were observed in the particulate fraction of As, Cr, Cu, Sb, and Zn, and in the LMM fraction of As, Cu, Ni, Sb, and Zn by using biofiltration as a treatment method (Kjernsby, 2024). In addition a recent study from the Bjørnegård tunnel in Norway, several advanced technologies were tested to address trace elements, organic micropollutants, and biological effects in TWW with a secondary treatment step. As secondary treatment, the study tested bag filtration, ceramic microfiltration, and granular activated carbon (GAC) filtration. While membrane filtration reduced some particles and trace elements, it had little impact on dissolved micropollutants. In contrast, GAC filtration was highly effective at removing dissolved organic pollutants including persistent, mobile, and toxic (PMT) substances through adsorption (Vistnes, 2024). Previous studies on road runoff and stormwater have also shown that filter media such as calcite, zeolite, iron filings, and biochar-amended wood chips can effectively remove metals like cadmium (Cd), copper (Cu), lead (Pb), and zinc (Zn) (Krishna R. Reddy et al., 2014; Negin Ashoori et al., 2019; Sossalla et al., 2025). Additionally, constructed wetlands have demonstrated promising removal rates for trace metals and PAHs (Terzakis et al., 2008; Ventura et al., 2019). However, given the typically higher concentrations of pollutants in TWW compared to regular stormwater runoff, such systems may not only be insufficient but may also act as ecological traps accumulating contaminants and negatively affecting the biota that establish in these environments (Sossalla et al., 2025).

The Norwegian Public Roads Administration has previously considered various treatment options for tunnel wash water through earlier research and development projects (Garshol et al., 2015). These include stationary systems located at the tunnel site, conceptual mobile solutions for flexible deployment, and full scale integrated systems for space limited tunnels. However, mobile systems are not currently in active use. In practice, when wash water cannot be discharged to recipients, it is transported to approved disposal facilities. For new tunnel construction, the preferred approach is now the use of closed sedimentation basins, such as those implemented in the Ekeberg Tunnel.

2.4.2 Treatment 1 - Sedimentation Basin

Today, most constructed road tunnels in Norway are equipped with sedimentation basins as the primary treatment method for tunnel wash water (TWW). These basins allow particle-bound pollutants to settle by gravity before the water is released (Sossalla et al., 2025). This method is the predominant particle removal technique in urban areas, where TWW is stored in retention basins for days or weeks, typically ranging between 14 and 35 days, depending on the system design and pollution load (Sossalla et al., 2025). However, recent studies also show that TWW contains various dissolved contaminants such as PFASs, BTHs, BTRs, and low molecular weight PAHs, tire derived chemicals which may require additional treatment (Meland et al., 2023; Vistnes et al., 2024). According to the current guidelines, treatment of TWW should be done in enclosed treatment solutions where the TWW should remain in the sedimentation basin until pollutant levels and biodegradable detergents are reduced to environmentally safe concentrations (Statens Vegvesen, 2016). After each tunnel wash, accumulated sediment is removed from the basin using a suction truck to maintain capacity and efficiency.

2.4.3 Treatment 2 - Filtralite HMR

The following description of Filtralite HMR is based on information provided in the manufacturer's brochure, included in *Appendix A*. According to the brochure, Filtralite HMR is a high-quality filter media developed to efficiently remove heavy metals from various water sources including drinking water, industrial effluents, mining runoff, road and tunnel drainage as well as agricultural wastewater. The filter media is produced by thermally treating selected clay minerals, creating a highly porous structure with an extensive mineral surface area that enables a high sorption capacity for both cations and anions. The clay material consists of alumina silicates with exchangeable cations, enhancing its ability to bind metals through physico-chemical bonding and ion exchange mechanisms. The calcination process not only increases the surface area and microporosity of the material but also enhances its mechanical strength, ensuring that it functions as a durable and backwashable filtration material in water treatment plants. Filtralite HMR effectively captures dissolved metals such as nickel, copper, zinc, lead, and cadmium, as demonstrated in multiple laboratory studies, pilot-scale tests, and full-scale treatment operations. Research at the Norwegian University of Life Sciences has

shown high sorption capacity, with over 70% removal efficiency for key metals. Comparative studies with Granulated Activated Carbon (GAC) have demonstrated that Filtralite® HMR has a higher retention capacity for nickel and zinc while maintaining strong adsorption performance for lead and copper. Batch experiments and isotherm studies confirm that the material provides a large reactive surface, allowing for the rapid adsorption of contaminants. Filtralite HMR has also been shown to help stabilize pH toward neutral or slightly alkaline conditions, which may support metal sorption efficiency. Under standard laboratory conditions, studies have reported that up to 90% of metal removal can occur within the first 10 minutes of filtration, as shown in *Appendix A*. The lamellar interplanar structure of the clay is modified during production to optimize adsorption and ion exchange, while the material's large pore volume ensures effective hydraulic permeability, preventing clogging and maintaining consistent water flow. Unlike conventional modified clay materials, Filtralite HMR is designed for regeneration through backwashing, significantly extending its lifespan. During backwashing, weakly bound metal ions and filter dust are removed, restoring the adsorption capacity of the filter media shown in *Figure 6*. The mechanical erosion of the filter grains is limited to the outermost surface, ensuring that the material remains intact and effective for long-term use. Polluted backwash water can be recycled through sedimentation, separating the detached metal particles before disposal or further treatment. The backwashing process also improves water flow paths, ensuring that new micropores are exposed, enhancing continued metal removal over time.

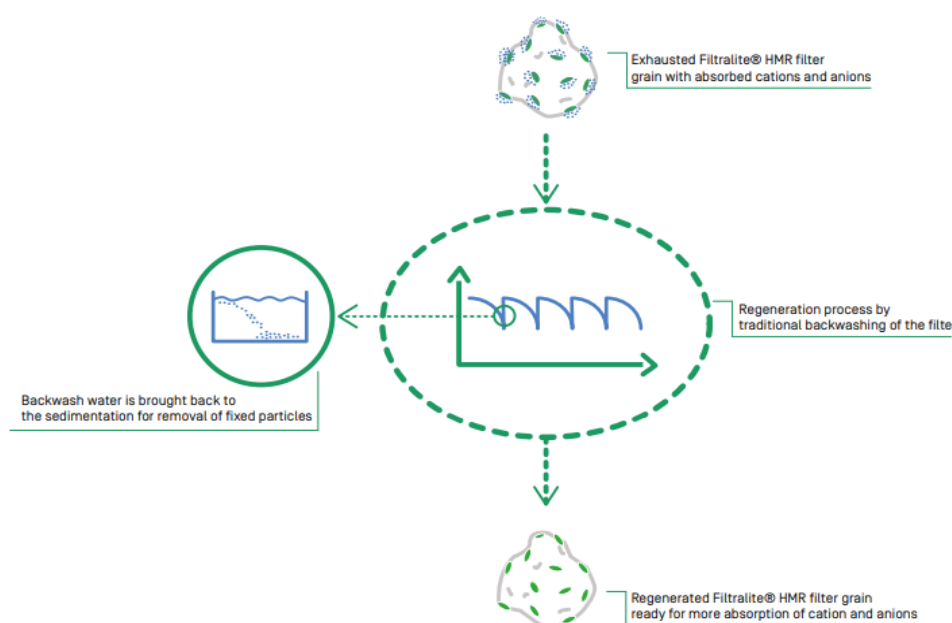


***Figure 6:** The figure illustrates the regeneration process of an exhausted Filtralite HMR filter. During backwashing, retained cations and anions, along with accumulated filter residue, are flushed out and settled in a pre-treatment stage, such as the sedimentation pool in the Ekeberg tunnel. The illustration is taken from the brochure provided by the contractor, Containertech in Appendix A.*

2.5 The Oslofjord

The Oslofjord is a biologically rich and historically significant fjord in Norway, that faces severe environmental challenges due to pollution and human activities. Over the years, the fjord has suffered from overfishing, nutrient runoff from agriculture, industrial discharges, and urban wastewater. These pollutants have led to the accumulation of toxic chemicals in the fjord and eutrophication, resulting in oxygen depletion and the decline of key species such as cod and eelgrass, which are essential for maintaining the ecological balance (Miljødirektoratet, 2023). The fjord's watershed encompasses 118 municipalities and supports a population of approximately 2.8 million people which is more than half of Norway's total population, placing significant pressure on the marine environment (Miljødirektoratet, 2023). The inner Oslofjord is especially affected, with its sediments acting as reservoirs for a range of hazardous substances, including PCBs, brominated flame retardants, siloxanes, metals, PFOS, and UV filters. Many of these compounds have been found to exceed environmental quality standards, raising concerns about their long-term impact on both aquatic organisms and the broader food chain (Merete Grung et al., 2021). In particular, tire wear particles (TWP) have been detected at high concentrations in the sediments of inner Oslofjord, especially near Akershuskaia and the area outside Bekkelaget wastewater treatment plant.

These particles likely settle quickly and accumulate nearshore due to their density, indicating a pattern of localized pollution from road runoff, tunnel wash water, stormwater pipes, and urban infrastructure (Alling et al., 2023). Low concentrations in surface water samples confirms the relevance of sinking and sedimentation for the distribution of TWP (Alling et al., 2023). The model in *Figure 7* demonstrates how tire wear particles and associated chemicals spread, dilute, and settle in the Oslofjord over time. The results highlight likely sedimentation zones, particularly near Myggbukta, which is the outflow from the Ekeberg Tunnel, as well as in shallow areas between Filipstadkaia, Hovedøya, and Bygdøy nearby. High concentrations are expected along Akershuskaia, aligning with previous findings of TWP in blue mussels

(Alling et al., 2023; Rødland & Lundgaard, 2023). The modeling has limitations due to uncertainty in input data, such as emission points, water volumes, and concentrations and may not reflect real-world variation environmental conditions (Rødland & Lundgaard, 2023).

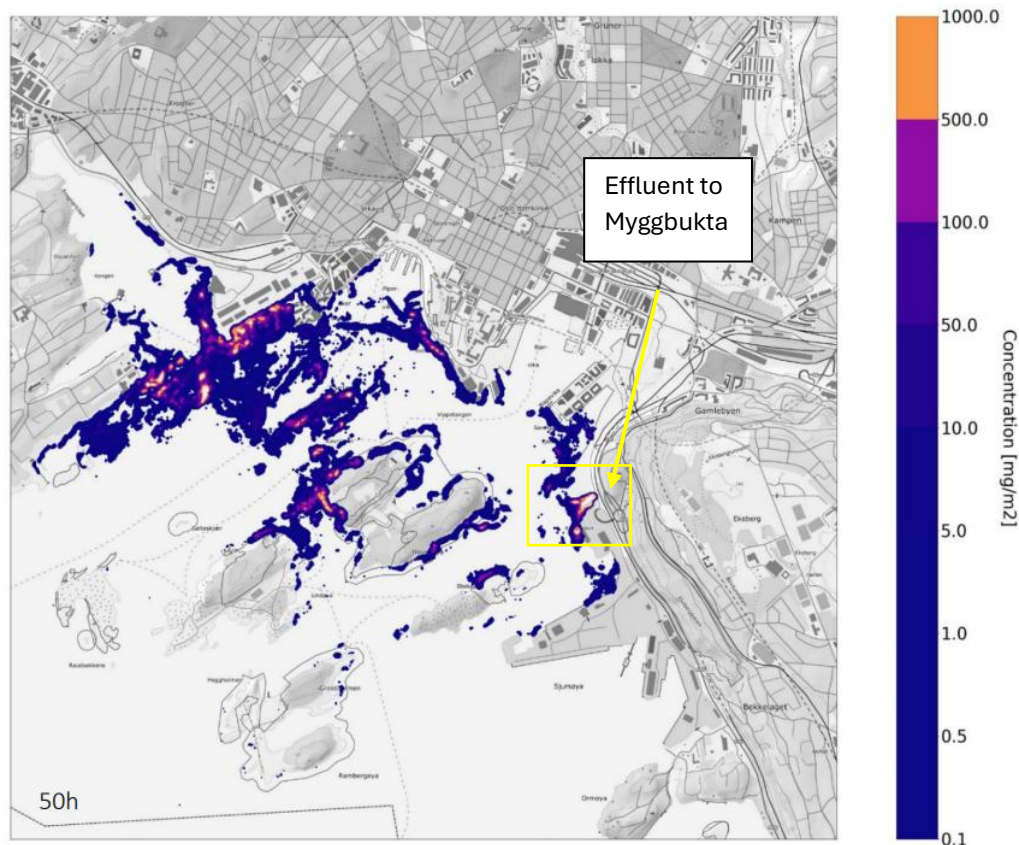


Figure 7: The figure illustrates a modified model of sedimented tire wear particles (TWP) from discharges on May 17 and 18 at Filipstadkaia and Myggbukta in Oslo. The color scale indicates the concentration of TWPs in the sediment, ranging from 1000 mg/m² (orange) to 0.1 mg/m² (dark blue) (Rødland & Lundgaard, 2023). The yellow box indicates where the effluent from the Ekeberg tunnel is.

2.6 *Daphnia magna* (D.magna)

Daphnia magna are planktonic crustaceans of the suborder Dafniidae (order Cladocera, class Branchiopoda), with a body length between 2 mm and 5 mm in length (Ebert, 2005; Elenbaas, 2013). The body is enclosed by a transparent shell structure, called a carapace. Due to this transparent carapace, the species tends to be the colour of what it is currently eating seen in Figure 8 (Elenbaas, 2013). The Daphnids have two sets of long, doubly branched antennae and six thoracic appendages that are held inside of the carapace.

Under stable environmental conditions, *Daphnia magna* reproduce through parthenogenesis, a form of asexual reproduction where females produce only female offspring (Seda & Petrusek, 2011). This process occurs regularly and predictably, allowing for rapid population growth. With a short generation time of approximately 7-10 days, large populations can be cultivated in a relatively short period, with offspring being exact genetic clones of their parents. *Daphnia magna* plays a significant role in maintaining water quality due to its ability to filter water while feeding. As planktonic filter feeders, *Daphnia magna* consumes suspended particles, including algae, microorganisms, and organic debris (Shiny et al., 2005). Their thoracic appendages create currents that draw water through their carapace, allowing them to filter out and ingest particles efficiently (Elenbaas, 2013). This natural filtration process not only helps to improve water clarity and quality but also regulates the growth of algae and microbial populations, preventing overgrowth and eutrophication in aquatic ecosystems (Ebert, 2005). In addition, *Daphnia magna* is highly valuable for ecotoxicological research.

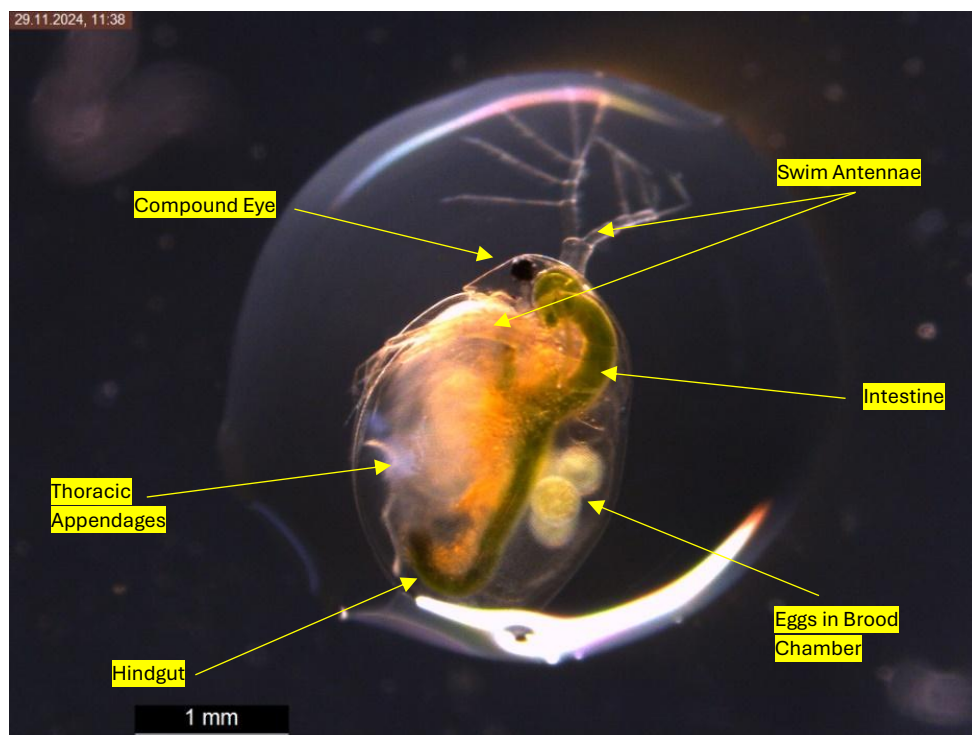


Figure 8: The photo shows a 9-day old healthy *Daphnia magna* with the first set of offspring, which are incubated in a brood pouch located underneath the carapace to the back. Photo taken with the MDG41 Leica microsystem by Ole Holthusen with a descriptive anatomical structure.

3.0 Materials and Method

3.1 Area description

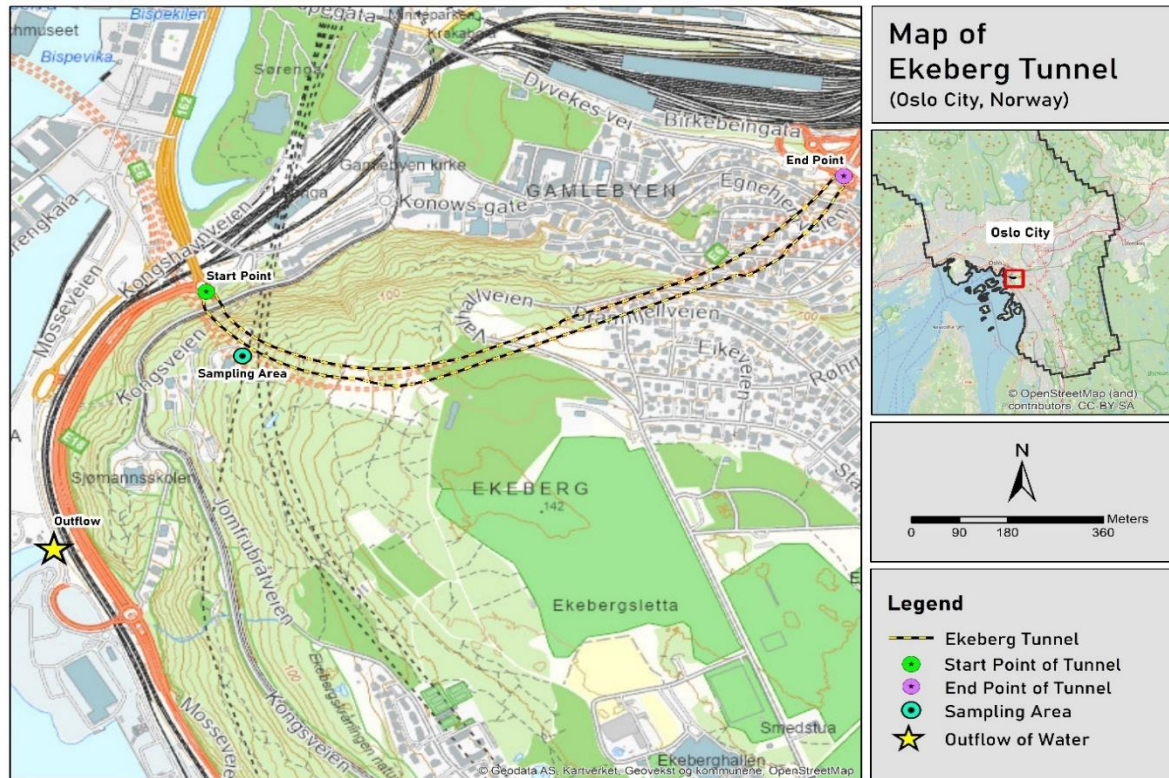


Figure 9: Map showing the location of the Ekeberg Tunnel, the sampling area, and the outflow to the Alna River. The figure was created in QGIS by Ole Holthusen.

The Ekeberg Tunnel (59°54'3"N 10°46'16"E) is an essential part of Oslo's Road infrastructure serving as a key segment of the European Route E18 and E6. It forms the second easternmost section of the Opera tunnel, a motorway system running beneath Ekebergåsen, which connects the Bjørvika tunnel to the west with the Svartdal tunnel to the east. Additionally, the Ekeberg tunnel provides a northern exit through Lodals bridges and Vålereng tunnel on the E6. Initially designated as Rv190, the tunnel was incorporated into the E6 network in 2010. The tunnel was officially opened in 1995 and has a total length of 1,580 meters, stretching from Sørenga to Lodalen (Wikipedia, 2009). The tunnel plays a crucial role in reducing traffic congestion in Oslo by diverting through-traffic away from the Oldtown. The structure consists of a 100 meter long concrete tunnel with two lanes in each direction, transitioning into twin rock tunnels with additional lanes at various ramps, and a driving speed limit of 70 km/h

(Wikipedia, 2009). The tunnel is part of a high-traffic road network, with an Annual Average Daily Traffic (AADT) around 79 000 vehicles recorded in 2024, with an average of 39 619 cars on the south lane and 39 024 on the north lane (Statens Vegvesen, 2024a, 2024b). In addition, the Bjørvika submerged tunnel project, completed in Oslo, connects the Festnings tunnel and Ekeberg tunnel into a longer city-center tunnel system, further increasing traffic efficiency and handling approximately 90,000 vehicles per day upon opening (Statens Vegvesen, 2010). Due to its high traffic volume, the Ekeberg Tunnel undergoes regular maintenance and rehabilitation, included upgrading technical equipment, resurfacing the roadway and washing where most of this work is carried out at night to minimize traffic disruptions, with only one tunnel bore being closed at a time (Skanska, n.d). As part of routine maintenance, the Ekeberg Tunnel undergoes approximately a minimum of 8 technical cleanings, and 5 full tunnel cleanings per year. The complete wash water treatment cycle is illustrated in *Figure 10* detailing five key stages.

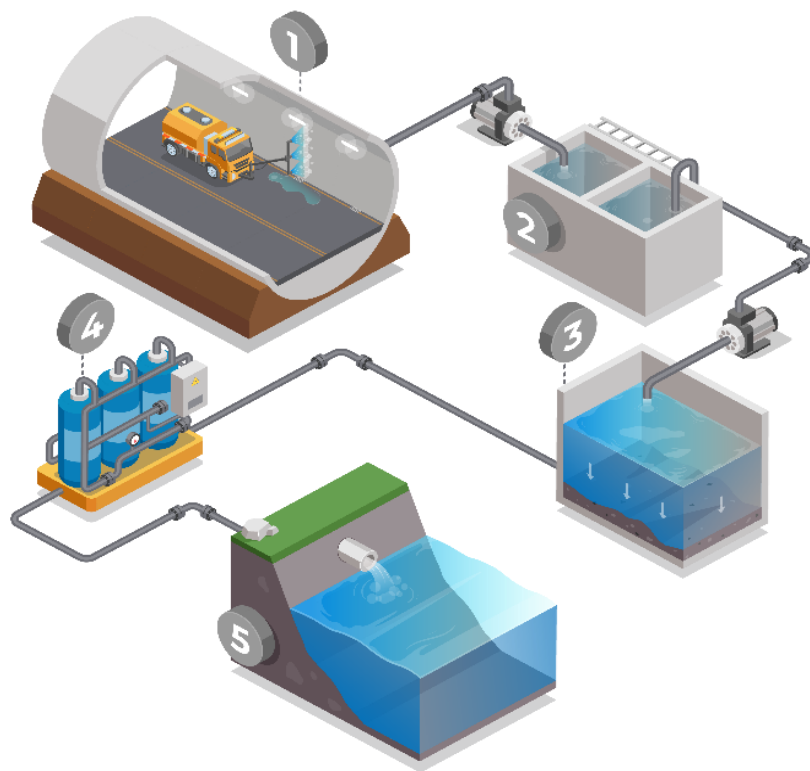


Figure 10: The figure shows the complete tunnel wash water treatment cycle is illustrated from step 1-5 for the Ekeberg tunnel from tunnel washing to outflow, through two treatment steps before being released into the Alna River and then further to the Oslofjord. The figure is made in Adobe illustrator by Ole Holthusen.

In Stage 1, tunnel wash water is generated and collected before being directed to a pump station (Stage 2). At this stage, the water passes through an oil separator and is then pumped into a sedimentation basin (Stage 3), where it remains for 21 days to allow particulate matter to settle. The sedimentation basins for both the northbound and southbound lanes have a volume of approximately 590 m³ each. In Stage 4, the wash water undergoes secondary treatment using the newly implemented Filtralite HMR filtration system. Finally, in Stage 5, the treated water is discharged into the Alna River, which ultimately flows into the Oslo Fjord. In general, tunnel wash water and infiltration or surface water are managed through separate systems. Infiltration and runoff water are typically diverted away from treatment facilities, as they do not require the same level of treatment as wash water. Although specific details for the Ekeberg Tunnel were not confirmed, it is common practice in Norway to direct infiltration water to a separate collection basin, which may ultimately discharge through the same outlet as treated wash water. Treated tunnel wash water (TWW) is typically discharged into nearby water bodies or municipal wastewater systems, where it must comply with industrial wastewater standards (Sossalla et al., 2025). The tunnel wash water (TWW) will also further be diluted once released into a recipient, such as the Alna River. Although the exact dilution factor for the Alna is unknown, a conservative estimate of at least 1:10 is commonly used for road runoff entering small natural water bodies. From there, the water undergoes further dilution upon entering the Oslo Fjord.

3.2 Fieldwork

The fieldwork and tunnel wash sampling were conducted across two seasons: a spring wash and an autumn wash. A total of four site visits to the Ekeberg Tunnel were carried out for the sample collection shown in *Figure 11*. Access to the tunnel required an escort vehicle associated with the Norwegian Road Administration to guide the entry. A mandatory light beacon was also installed on the transportation vehicle for safety. During the washing procedure, the tunnel was temporarily closed to ensure safe and efficient operations during the night.

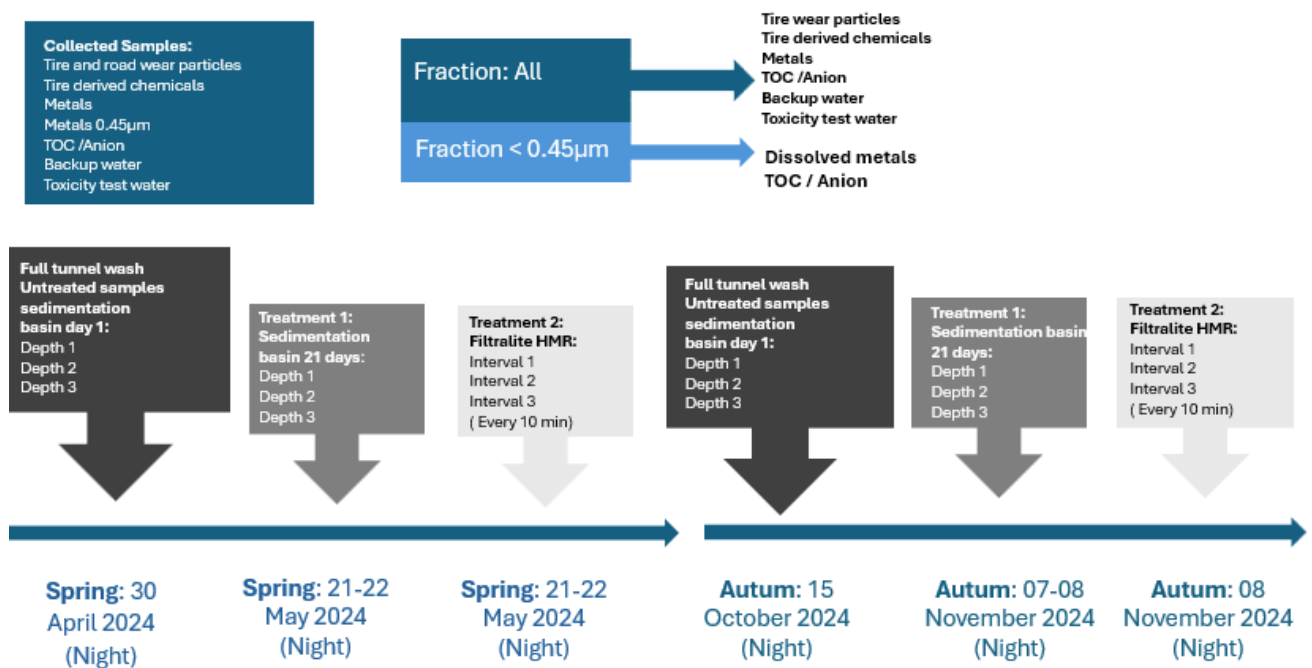


Figure 11: The figure illustrates the sampling points for untreated and treated tunnel wash water during two full tunnel washes conducted in spring and autumn 2024. Samples were collected from different stages of the treatment process. The figure is inspired by (Meland et al., 2023) and made in powerpoint.

3.2.1 Spring wash

Influent Sampling Procedure and Observations - Day 1

The first sampling of untreated wash water was conducted in spring, on April 30, 2024, between 03:00 and 05:30 a.m., at the corner of the sedimentation basin shown in *Figure 12*. The contractors performed a full wash of the tunnel, with wash water collected from one lane on the eastbound at the Ekeberg tunnel. The other lane was washed on 02-03.05.2024. During the spring wash, a total of 255 m³ of water and 75 liters of detergent were used for the east tunnel lane and 256 m³ for the west tunnel lane with same amount of detergent. The detergent used was Mac 213 Bio (UFI: P7QG-CWSC-78CC-QA1Q) pre-diluted at a 1:10 ratio before being added to the washing truck, and then further diluted 1:10 when applied in the tunnel. The water depth in the basin at the time was recorded at 1.34 meters according to the depth sensors. Sampling began around 04:30, but issues with the electronic pump required adjustments beforehand. The pump was initially installed incorrectly and did not draw water as expected. To address this, we had to reinstall the tube and secure it with climbing gear to facilitate easier access to the water surface. Due to these limitations and short time before

the tunnel was set to open, we were only able to collect samples from one depth at 15 cm below the water surface. Both 500 mL and 250 mL high-density polyethylene bottles were rinsed twice with tunnel wash water before filling to minimize cross-contamination that could impact measurements, while the 50 mL and 15 mL bottles were filled directly. Rinsing the smaller tubes for the ICP-MS was avoided due to risk of contamination or cause particles to adhere to the container walls. Filtered samples were also collected using a pre-made filter setup that was done at the lab, as shown in *Figure 12*. The filter setup included a sequential filter system consisting of a 100 μm nylon net filter, a high-capacity in-line groundwater sampling capsule 5 μm filter, and a high capacity in-line groundwater sampling capsule 0.45 μm filter. Before collecting each sample, tunnel wash water was run through the filter for 30 seconds to remove any initial contaminants and stabilize the filtration process, ensuring more accurate results. A total of 9 samples of 500 mL bottles were collected for tire and road wear particles (TRWP) and 6 samples of 250 mL bottles for tire additives (TA). Additionally, 9 samples of 15 mL unfiltered water were taken for mass spectrometry (ICP-MS), along with 9 filtered 15 mL samples for dissolved ions for ICP-MS. Nine 500 mL backup samples were also collected for total suspended solids (TSS) and particle size distribution (PSD). Finally, 3 unfiltered and 3 filtered 50 mL samples were collected for total organic content (TOC) and filtered anions (FA). All samples for tire derived chemicals and samples for toxicity test were frozen down at -21°C at first opportunity to avoid breakdown of organic contaminants.

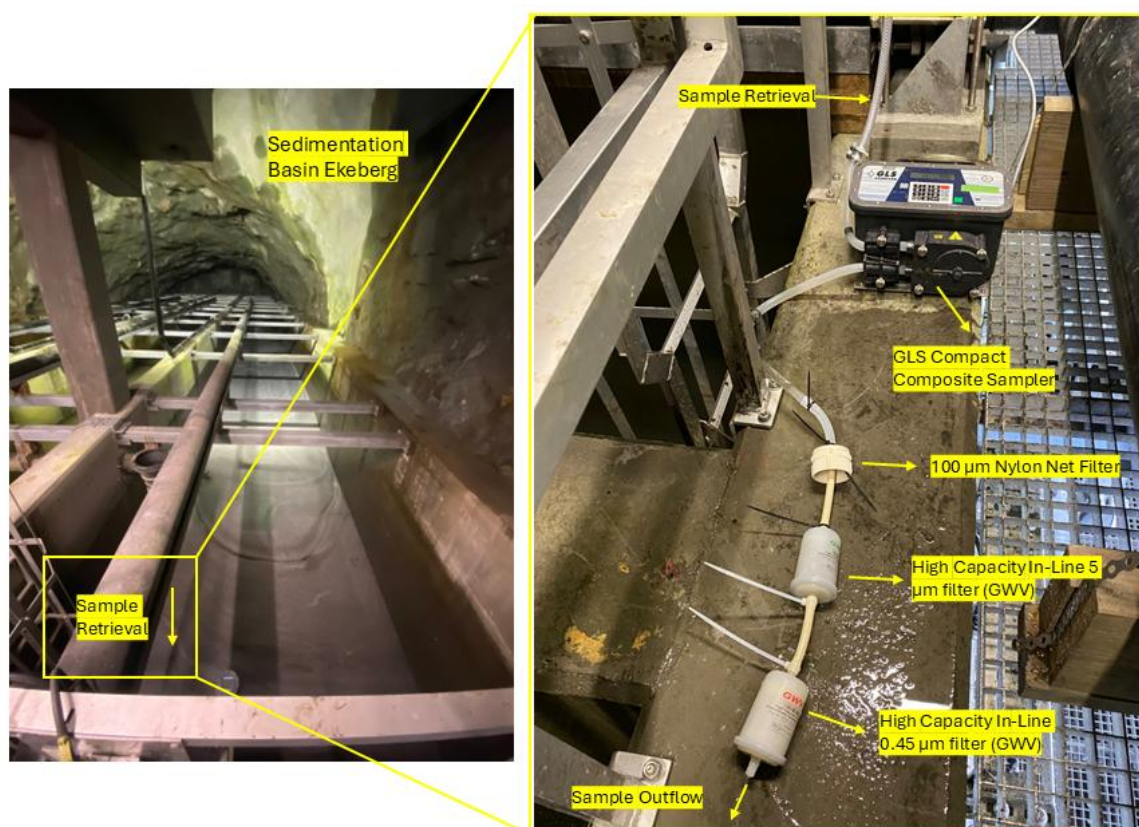


Figure 12: Sampling setup at the Sedimentation Basin in the Ekeberg Tunnel. The electric pump (right) draws water from the basin (left) and passes it through a sequential filtration system (right) consisting of a 100 μm nylon net filter, a 5 μm filter, and 0,45 μm filter. Photos: Ole Holthussen.

Effluent Sampling Procedure and Observations - Day 21

After 21 days, on May 21, 2024, we returned to the Ekeberg tunnel site to conduct a second round of sampling starting at 23:00 pm - 02:30 am. The samples were taken from the same corner of the sedimentation basin as during the first sampling session, but this time we were able to follow the planned procedure by collecting samples from three different depths, as shown in *Table 4*. These depths included measurements at the surface, middle, and bottom of the basin, enabling a comprehensive analysis of pollutant distribution. The sedimentation pool had been partially discharged earlier in the day, but we managed to halt the outflow before the pool was emptied, ensuring a stable sample environment. The sampling procedure was done as on day 1. Shortly after sampling from the basin, the treated water was pumped from the basin to treatment stage 2. Further, additional samples were collected from the drain hole and effluent from the second water treatment stage to capture representative samples. A plastic bucket was rinsed 3 times prior to sampling to remove any residual particles that might affect the results, and then placed under the regulation chamber with an outflow on 1.5 L/s.

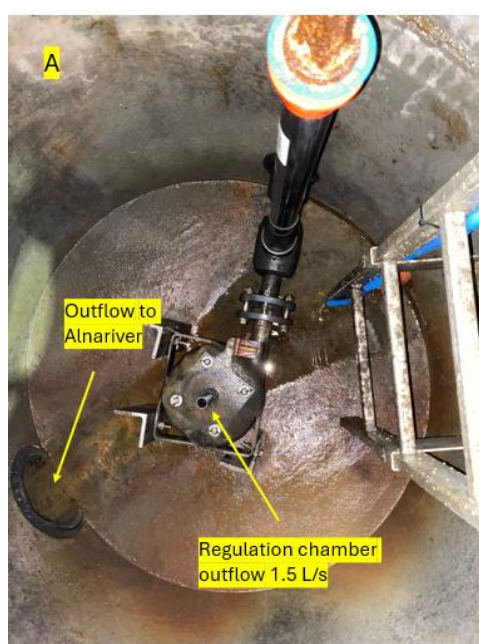


Figure 13: Picture **A** shows the drain hole with the regulation chamber and the outflow to Alna River before flushing. Picture **B** shows the sampling setup during the flushing of the treated tunnel wash water. Photos: Ole Holthusen.

The bucket was put under the regulation chamber so that it could capture the treated water directly and at the same time continuously add new treated water to keep it circulating. The bucket was also placed under the chamber regulator to avoid particles and turbulence directly from the drain hole. From this setup shown in *Figure 13*, samples were collected in three rounds, with a 10-minute interval between each sample to account for any potential fluctuations in water quality or contaminant distribution. The same filter system as used previously was used for the metals samples in the drain hole. The 100 μm nylon net filter was changed, and outflow treated water was run through the filter for 30 seconds before taking samples.

Table 4: Presents the sampling times for each depth during the study, with all compounds analyzed at each interval. Initially, due to system inefficiencies, the 0.45 μm filtration was performed at the end of the sampling process. This procedure was subsequently optimized in the following autumn wash to enhance efficiency.

Spring wash	Untreated	Treatment 1		Treatment 2	
Date	30.04.2024	22-23.05.2024		23.05.2024	
Sample nr:	Sample time am:	Sample nr:	Sample time pm/am:	Sample nr:	Sample time am:
Untreated depth - 1	04:05-04:17	Treated depth - 1	23:20-23:40	Filtered timeline - 1	01:25-01:35
Untreated depth - 1	04:17-04:29	Treated depth - 2	23:45-23:49	Filtered timeline - 1 0,45 μm	01:36-01:38
Untreated depth - 1	04:29-04:42	Treated depth - 3	23:52-23:57	Filtered timeline - 2	01:48-01:53
Untreated depth - 1 0,45 μm	04:46-04:48	Treated depth -3 0,45 μm	00:02-00:07	Filtered timeline - 2 0,45 μm	01:54-01:56
Untreated depth - 1 0,45 μm	04:48-04:50	Treated depth - 2 0,45 μm	00:10-00:13	Filtered timeline - 3	02:06-02:09
Untreated depth - 1 0,45 μm	04:50-04:52	Treated depth - 1 0,45 μm	00:15-00:20	Filtered timeline - 3 0,45 μm	02:10-02:11

Table 5: Presents the sampling depths and parameters taken on the field days during spring.

Sedimentation pool depth		Spring wash		Parameters	Untreated	Treatment 1	Treatment 2
Date	30.04.2024		22.05.2024		30.04.2024	22.05.2024	22.05.2024
Total water level	1.34 m		1.79 m	Temperature	9.0 °C	9.6 °C	9.3 °C
Sampling Day	Day 1		Day 2	Conductivity	3460 µS/cm	3440 µS/cm	3710 µS/cm
Depth 1-Surface	15 cm below the surface		5 cm below the surface	pH	7.403	7.522	7.367
Depth 2-Middle layer	15 cm below the surface		46 cm below the surface				
Depth 3-Bottom layer	15 cm below the surface		95 cm below the surface				

3.2.2 Autumn wash

Influent Sampling Procedure and Observations - Day 1

For the second round of fieldwork conducted in autumn, sampling was carried out during the night of October 14, 2024, extending into the morning of October 15, 2024. Due to lower water levels in the sedimentation basin, sampling depths were adjusted accordingly, as shown in *Table 7*. All sample containers were rinsed twice with wash water before sampling to prevent contamination. Following coordination with the contractor, a detergent-mixed wash water sample was collected by the contractor from the tank, before tunnel wall application and provided to us. This was further frozen down and used for toxicity testing. During the tunnel wash on October 15, 2024, 252 liters of water and 400 liters of detergent were used, with the detergent pre-diluted at a 1:10 ratio before being loaded into the vehicle and further diluted at a 1:10 ratio upon application in the tunnel. The following day, on October 16, 2024, 175 liters of water and 250 liters of detergent were used (Mac 213 Bio detergent (UFI: P7QG-CWSC-78CC-QA1Q), following the same dilution process. Despite the lower water levels in the basin, all procedures were followed successfully, and sampling was completed within the scheduled timeframe.

Effluent Sampling Procedure and Observations - Day 21

The second day of sampling occurred on the night of Thursday, November 7, 2024, continuing into Friday morning, November 8, starting around 22:30 pm - 01:00 am. Samples were collected from three different depths in the sedimentation basin, following the same procedure as in the spring round. During this session, the filter used for the total water samples became partially clogged toward the end, resulting in reduced water pressure. However, it still allowed flow, and the final samples were successfully collected without compromising the sampling process. All other procedures were carried out as planned, ensuring a comprehensive sample collection for analysis.

Table 6: Presents the sampling times for the autumn wash for each depth during the study, with all compounds analyzed at each interval.

Spring wash	Untreated	Treatment 1		Treatment 2	
Date	15.10.2024	07.11.2024		07-08.11.2024	
Sample nr:	Sample time am:	Sample nr:	Sample time pm/am:	Sample nr:	Sample time am:
Untreated depth - 1	02:55-03:00	Treated depth - 1	22:52-22:56	Filtered timeline - 1	23:57-00:00
Untreated depth - 1 0,45µm	03:03-03:05	Treated depth - 1 0,45µm	22:58-23:01	Filtered timeline - 1 0,45µm	00:01-00:04
Untreated depth - 2	03:08-03:11	Treated depth - 2	23:04-23:08	Filtered timeline - 2	00:14-00:19
Untreated depth - 2 0,45µm	03:14-03:18	Treated depth - 2 0,45µm	23:11-23:14	Filtered timeline - 2 0,45µm	00:20-00:23
Untreated depth - 3	03:22-03:26	Treated depth - 3	23:19-23:23	Filtered timeline - 3	00:33-00:37
Untreated depth - 3 0,45µm	03:28-03:31	Treated depth - 3 0,45µm	23:26-23:30	Filtered timeline - 3 0,45µm	00:38-00:41

Table 7: Presents the sampling depths and parameters taken on the field days during autumn.

Sedimentation pool depth	Autum wash		Parameters	Untreated	Treatment 1	Treatment 2
Date	15.10.2024	07.11.2024		15.10.2024	07.11.2024	07.11.2024
Total water level	0.82 m	2.57 m	Temperature	10.4 °C	9.7°C	9.8 °C
Sampling Day	Day 1	Day 2	Conductivity	1042 $\mu\text{S}/\text{cm}$	1129 $\mu\text{S}/\text{cm}$	918 $\mu\text{S}/\text{cm}$
Depth 1-Surface	15 cm below the surface	5 cm below the surface	pH	7.735	7.527	7.682
Depth 2-Middle layer	21 cm below the surface	46 cm below the surface				-
Depth 3-Bottom layer	70 cm below the surface	95 cm below the surface				

3.3 Laboratory Work

3.3.1 Sample Pretreatment for ICP-MS Analysis

Samples collected from the untreated TWW, treatment 1 and treatment 2, along with 0.45 μm filtered samples, were analyzed using Inductively Coupled Plasma Mass Spectrometry (ICP-MS) to determine the total metal concentration. The specific metals analyzed are listed in *Table 8*. To prepare the tunnel wash water samples for ICP-MS analysis, an acid digestion procedure was conducted to ensure the complete dissolution of metal-containing particles. Initially, the collected samples were pre-acidified with 2% Ultra-Pure (UP) nitric acid (HNO_3) and allowed to stand for 24 hours before further processing. The samples were then thoroughly mixed, and 15 mL was transferred into clean 17 mL Teflon UltraClave tubes. These subsequently evaporated to dryness at 90°C in an oven (VENTI-Line 56 Prime) over the weekend. Certified Reference Materials (CRMs) for water (NIST 1643f) and soils (NCS ZC 73007, NCS DC 73325, and NCS DC 73324a) were prepared using the same procedure. Specifically, 1.5 mL of CRM water and 10 mg of soil CRMs were transferred to Teflon tubes, mixed with 8.5–10 mL of MilliQ water, and evaporated under identical conditions. Additionally, three blank samples ($n=3$) were included in the process, where 10 mL of MilliQ water was evaporated alongside the test samples and CRMs.

The blanks were prepared following the same procedure as the tunnel wash water samples, including filtration through a 0.45 µm membrane filter with MilliQ water. Once the samples were dry, 1.5 mL of UP HNO₃ was added to all samples, blanks, and CRMs, and digestion was performed using an UltraClave system at 260°C for 30 minutes. However, during the first round of UltraClave digestion, technical issues arose, causing the samples to be removed mid-process. To complete the digestion, the procedure was resumed using the UltraWAVE system (Milestone, Italy), but due to its capacity limitations, fewer samples were processed per run. Additional challenges occurred because the wider and shorter Teflon tubes, originally designed for the UltraClave, were incompatible with the UltraWAVE system. As a result, some Teflon tube lids detached when the tubes were removed from the instrument. Following digestion, the samples were transferred back to their original 15 mL tubes and diluted to a final volume of 15 mL using MilliQ water. All samples were weighed before evaporation, after evaporation, and after digestion to ensure precise tracking of mass loss during preparation.

For the second round of digestion, a revised approach was followed in which the collected samples were not pre-acidified before being transferred to the Teflon tubes. Additionally, a different type of Teflon tube was used that were longer and thinner tubes, which proved easier to handle. These tubes were placed into a vacuum chamber to facilitate sample evaporation by air removal. However, after a week in the vacuum chamber, the method proved ineffective. Consequently, the samples were transferred to an oven and evaporated at 90°C over the weekend, following the same evaporation procedure as in the first round. The digestion was then performed in the UltraWAVE system using the same protocol as the first round. Once digestion was complete, the prepared samples were analyzed using an Agilent 8800 ICP-MS QQQ. To ensure accuracy, external calibration was conducted using internal standards, and the limits of detection (LOD) and limits of quantification (LOQ) were established, as shown in *Table 8*.

Table 8: List of metals measured using ICP-MS, along with the detection limit (LOD) and quantification limit (LOQ) in µg/L based on 3×SD and 10×SD for the blank samples of the various metals.

Metals Spring	LOD µg/L	LOQ µg/L	Metals Autumn	LOD µg/L	LOQ µg/L
Al (Aluminum)	6	21	Al (Aluminum)	30	93
V (Vanadium)	0.01	0.042	V (Vanadium)	0.9	0.31

Cr (Chromium)	4	15	Cr (Chromium)	3	11
Mn (Manganese)	1	3.6	Mn (Manganese)	0.4	1.3
Fe (Iron)	30	110	Fe (Iron)	20	77
Co (Cobalt)	0.1	0.37	Co (Cobalt)	1	4,4
Ni (Nickel)	9	31	Ni (Nickel)	8	26
Cu (Copper)	1	3.3	Cu (Copper)	2	5.4
Zn (Zink)	5	15	Zn (Zink)	5	18
As (Arsenic)	0.0007	0.0024	As (Arsenic)	0.1	0.4
Mo (Molybdenum)	2	5.7	Mo (Molybdenum)	1	3.7
Cd (Cadmium)	0.04	0.15	Cd (Cadmium)	0.009	0.32
Sn (Tin)	0.02	0.052	Sn (Tin)	0.5	1.5
Sb (Antimony)	0.05	0.17	Sb (Antimony)	0.1	0.36
W (Tungsten)	0.2	0.63	W (Tungsten)	0.08	0.28
Pb (Lead)	0.07	0.24	Pb (Lead)	0.1	0.46

3.3.2 Leaching Experiment

To better understand the potential leaching of substances from particles present in TWW, excluding the influence of detergent, an additional leaching experiment was performed. Particles were collected from untreated tunnel wash water and separated by filtration prior to testing, focusing on the release of metals and other potentially leachable compounds. 3 L of samples from the inflow from the 30 of April were used. To concentrate the particles from the tunnel wash water, sediment and particles were collected from the bottom layer of 500 mL bottles containing wash water, as this lower layer contained the highest concentration of wear particles. A pipetboy was used to transfer the water out of the bottles, further the leftover water and particles were transferred to 50 mL centrifuge tubes. This process was repeated for each sample, resulting in a total of four samples: three regular samples and one blank control (without particles). The samples collected were centrifuged at 5000 rpm for 2,5 minutes and with a slow down cycle of 15 minutes, which concentrated the particles and sediments into a pellet at the bottom of each centrifuge tube. After centrifugation, approximately all the original tunnel wash water was carefully removed from each tube without disturbing the pellet. This ensured that the pellet contained the concentrated particles required for the leaching study. The wet weight of the particle pellets was recorded for each sample: Sample 1 contained 0.5592 g, Sample 2 had 0.7673 g, and Sample 3 had

0.7437 g of particles. Based on a recent leaching study by (Cheong et al., 2023) which used tire wear particles (TWP) at a concentration of 40 g/L, this experiment aimed to replicate a similar ratio at a smaller scale. Due to the limited availability of material, an adjusted target concentration of approximately 1 gram of particles per 25 mL of water was used, in line with the approach applied in the referenced study. However, unlike Cheong et al., who used pure TWP, the current experiment measured total particle mass, which likely included a mix of tunnel-derived materials such as mineral dust, TWP, and other road related debris. To maintain the correct particle-to-water ratio, the formula $C_1V_1 = C_2V_2$ was applied to determine the appropriate volume of Milli-Q water for each sample. The calculated volumes added were as follows: 13.98 mL to Sample 1, 19.18 mL to Sample 2, and 18.59 mL to Sample 3. Milli-Q water was used to replace the original tunnel wash water in order to remove any residual cleaning agents that might interfere with the leaching process. The samples were further incubated in darkness for 14 days, allowing time for additives to leach from the particles into the water. To ensure consistent distribution of particles and additives, samples were gently stirred continuously during the incubation period on a roller board shown in *Figure 14*.

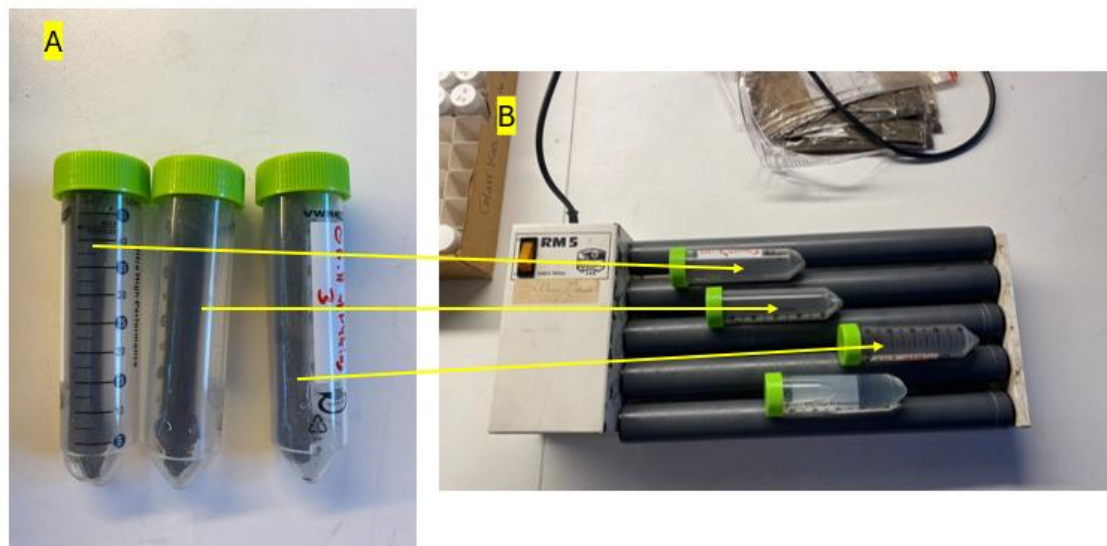


Figure 14: Image A and B shows the leaching experiment setup. Image (A) shows the particle pellets without the TWW. Further image (B) shows the samples on the roller board with 3 leaching samples and 1 blank.

After the incubation period, samples were frozen for preservation. However, after freezing, several samples developed cracks despite using freeze-tolerant tubes and leaving headspace. Consequently, samples were defrosted and transferred to new tubes, and re-centrifuged

following the original procedure to obtain a clear supernatant. From each sample, 10 mL of supernatant was taken for toxicity evaluation, 0.5 mL was allocated for ICP-MS analysis, and the remaining supernatant was reserved for further analysis of TDCs.

3.3.3 Quantification of TWP and TRWP

The quantification of TWP and TRWP was performed at the Norwegian Institute for Water Research (NIVA) using pyrolysis gas chromatography-mass spectrometry (Py-GC/MS), following the methodology outlined by (E. S. Rødland et al., 2022) in *A novel method for the quantification of tire and polymer-modified bitumen particles in environmental samples by pyrolysis gas chromatography-mass spectrometry*. This technique enables the identification and quantification of TRWP by analyzing the pyrolysis products of styrene-butadiene rubber (SBR) and butadiene rubber (BR), both of which are commonly found in tire tread. Pyrolysis was performed at 700°C for 12 seconds in a single-shot mode, and the resulting pyrolysis products were separated and detected using gas chromatography coupled with mass spectrometry (GC/MS). Quantification was based on key marker compounds, including benzene (mz 78), α -methylstyrene (mz 118), ethylstyrene (mz 117) and butadiene trimer (mz 91), which serve as reliable indicators of TWP content in the samples. In addition, three other pyrolysis products were monitored to add additional quality control of the quantification (4-Vinylcyclohexene (mz 54), SB dimer (mz 104) and SBB trimer (mz 91)). Additionally, the mass of tire wear particles was estimated using site-specific traffic data and a Monte Carlo simulation model assess TWP contributions across different treatment stages of tunnel wash water. Finally, the concentration of TWP was converted to TRWP using an assumed average of 50% mixture of minerals and other particles to the tire wear particles, following previous literature (Klöckner et al., 2021).

3.3.4 Analysis of Tire Derived Chemicals

The analysis of tire-derived chemicals (TDCs) was conducted by the Norwegian Institute for Water Research (NIVA), following the methodology described in *Screening of Tire-Derived Chemicals and Tire Wear Particles in a Road Tunnel Wash Water Treatment Basin* by (Meland et al., 2023). The analysis was performed using ultra-performance liquid chromatography coupled with time-of-flight mass spectrometry (UPLC-TOF-MS).

The analysed chemicals are shown in *Table 9*. Separation was achieved on an Acquity BEH C8 column (100 × 2.1 mm, 1.7 µm) with a gradient of water and acetonitrile (both containing 0.1% formic acid), ranging from 10% to 99% acetonitrile over 10 minutes at 0.5 mL/min. Detection was carried out on a Xevo G2-S Q-ToF (Waters) in positive electrospray ionization (ESI) mode, scanning m/z 100–1100. Key parameters included a capillary voltage of 0.7 kV, desolvation temperature of 450 °C, source temperature of 100 °C, and nitrogen gas flow of 900 L/h. Analytes were identified using extracted ion chromatograms (mass tolerance: 0.03 u), and semi-quantification was based on a six-point calibration curve (0.1–50 ng/mL). Selected TDCs were then quantified using UPLC coupled with triple quadrupole mass spectrometry (UPLC-MS/MS) on a Xevo TQ-S instrument. The same column was used with a mobile phase of acetonitrile–methanol (75:25) and water containing 5 mM ammonium formate and 0.1% formic acid. A gradient from 5% to 100% organic phase was applied over 10 minutes at 0.5 mL/min. Detection was in both positive and negative ESI modes, and external calibration used a six-point curve (0.1–200 ng/mL). Method recovery was assessed by spiking 100 ng of mixed standards onto 200 mg Oasis HLB cartridges with 10 mL of tap water, performed in triplicate before and twice during the sample run to ensure quality control.

Table 9: List of the tire-derived chemicals that were analyzed, along with their full names, molecular formulas, and CAS numbers.

Abbreviation	Name	Molecular Formula	CAS
6PPD	N-(1,3-Dimethylbutyl)-N'-phenyl-p-phenylenediamine	C ₁₈ H ₂₄ N ₂	793-24-8
6PPD-quinone	N-(1,3-Dimethylbutyl)-N'-phenyl-p-phenylenediamine-quinone	C ₁₈ H ₂₂ N ₂ O ₂	2754428-18-5
DPPD	N1,N4-Diphenylbenzene-1,4-diamine	C ₁₈ H ₁₆ N ₂	74-31-7
IPPD	N-Isopropyl-N'-phenyl-1,4-phenylenediamine	C ₁₅ H ₁₈ N ₂	101-72-4
CPPD	N1-Cyclohexyl-N4-phenylbenzene-1,4-diamine	C ₁₈ H ₂₂ N ₂	101-87-1
7PPD	N-(1,4-Dimethylpentyl)-N'-phenyl-1,4-benzenediamine	C ₁₉ H ₂₆ N ₂	3081-01-04
HMMM	Hexa(methoxymethyl)melamine	C ₁₅ H ₃₀ N ₆ O ₆	3089-11-0
DPG	1,3-Diphenylguanidine	C ₁₃ H ₁₃ N ₃	102-06-7
TMQ	2,2,4-Trimethyl-1,2-dihydroquinoline	C ₁₂ H ₁₅ N	26780-96-1
PhBT	2-Phenylbenzothiazole	C ₁₃ H ₉ NS	883-93-2

3.3.5 Uncertainty for TWP, TDCs and Metals

For the analysis of tire wear particles, pyrolysis GC/MS was applied using four chemical markers (benzene, α -methylstyrene, ethylstyrene and butadiene trimer) instead of relying on a single compound. This multi-marker approach has been demonstrated to give a more reliable result for samples with a mixture of tires present (Rødland et al., 2022). As different tires contain a large variation of different types of SBR and BR rubbers, with various concentrations of these rubber along with different molecular structures, this can influence the pyrolysis markers used for identification and quantification of TWP. Using a multi-marker approach can compensate for the variations in single markers, as well as using the expected levels in different types of tires used in a local area. For the Norwegian environment, NIVA has established a car tire database with more than 40 tires and relevant tires, such as summer tires, studded winter tires, studless winter tires are used according to local information and adjusted for the expected presence in the samples. These data, along with the measured data from the tunnel samples were used in a Monte Carlo simulation model (100,000 iterations) to estimate the total concentration of TWP in the sample based on the measured SBR and BR rubbers. The Monte Carlo simulations were also used to account for variability in the output, and generated a mean predicted TWP concentration, alongside the median, standard deviation and percentiles. In key input parameters, such as rubber composition across vehicle types. While these steps reduced overall uncertainty, some uncertainty remains as we do not know the exact composition of tires in the tunnel wash water and are therefore not able to adjust the analytical method to the exact blend of tires present. In the absence of site-specific data from the Ekeberg Tunnel, a conservative assumption of 50% rubber content by mass was applied to estimate total TRWP levels.

Further the behavior of tire-derived chemicals after entering the water phase is not fully understood. These compounds may degrade or transform into by-products during storage. To limit such changes, all water samples were frozen immediately after collection and defrosted only prior to analysis. However, repeated freeze thaw cycles and thawing at room temperature may have caused degradation or chemical transformation, potentially affecting the measured concentrations. This introduces uncertainty in the representativeness of the analytical results for in-situ environmental conditions.

Lastly metals were analyzed using inductively coupled plasma mass spectrometry (ICP-MS) with an Agilent 8800 Triple Quadrupole ICP-MS (ICP-QQQ), a widely accepted and sensitive method with low instrumental uncertainty. Nevertheless, minor errors could have been introduced during sample collection, transport, or preparation, including potential contamination. Additional uncertainty arose during sample pre-treatment. Due to technical issues, the acid digestion process had to be shifted from the UltraClave to the UltraWAVE system. Although certified reference materials and blanks were included, these factors could have contributed to variability in final metal concentration results.

3.3.5 Dissolved Organic Carbon

Dissolved Organic Carbon (DOC) were analyzed using a SHIMADZU TOC-VCPH/CPN Organic Carbon Analyzer (Shimadzu Corporation, Kyoto, Japan) by the technician at NMBU. The Non-Purgeable Organic Carbon (NPOC) method was employed, with a detection range of 1-10 ppm. High-purity air from a cylinder was used as the carrier gas, maintained at a pressure of approximately 300-600 kPa. Measurement uncertainty varied depending on concentration levels: $\pm 25\%$ for TOC below 1 mg/L, $\pm 10\%$ for TOC below 10 mg/L, and $\pm 5\%$ for TOC above 10 mg/L. The instrument complies with EMC Directive 89/336/EEC and Low Voltage Directive 73/23/EEC standards. The LOD and LOQ can be shown in *table 10*. Due to a misunderstanding for the analysis, the results for untreated spring samples were not reliable and have therefore been excluded from the dataset.

Table 10: Calibration standards and detection limits used for dissolved organic carbon (DOC) analysis. Standard solutions included potassium hydrogen phthalate at concentrations of 1 mg/L (K1) and 5 mg/L (K5). The method included defined limits of detection (LOD) and quantification (LOQ) to ensure analytical accuracy.

DOC (mg/L)	
LOD	LOQ
0,06788	0,22625

3.3.6 Anion

Anion concentrations were analyzed using a Dionex ICS-6000 ion chromatograph by the technician at NMBU. The analysis included the quantification of fluoride (F^-), chloride (Cl^-), sulfate (SO_4^{2-}), nitrate (NO_3^-), and phosphate (PO_4^{3-}) in mg/L. Due to the high expected concentrations and the complex matrix of tunnel wash water, all samples were diluted 100 times prior to measurement to ensure accurate analysis and protect the instrument's column. The instrument setup followed standard ion chromatography procedures to ensure reliable detection and quantification of anions in the water samples. However, as the instrument was not functioning after the first sampling period, further measurements for the spring and autumn samples could not be performed, with the exception of the untreated spring sample.

3.4 Methods and Setup for The Acute Immobilization Test

3.4.1 Algae Cultivation and Diet: *Raphidocelis subcapitata*

The starter concentration of green algae was obtained from the refrigerator at 4°C at the Isotope Laboratory at the Norwegian University of Life Sciences (NMBU). The batch, originally sourced from the Norwegian Institute for Water Research (NIVA) on February 3, 2024, was stored in a 5 L glass flask containing 100% Z8 cultivation medium under sterile conditions. This culture served as the foundation for the first round of algae cultivation. Over the course of two months, a 5 L flask was filled with 4 L of deionized (DI) water, and Z8 medium was prepared using stock solutions Z-1, Z-2, and Z-3 along with trace metals that had to be made with the recipe in *Appendix E*. A 50 mL sub-sample of algae was added to the 5 L flask containing the Z8 medium. The flask was then placed in an incubator chamber set at 20°C ($\pm 2^\circ C$) under a 16:8 h light/dark cycle shown in *Figure 15* and aerated with an air pump for 10 days to promote growth. After 10 days, the algae culture was transferred to a fridge at 4°C to allow sedimentation. The glass flask was covered with a parafilm to avoid any contaminants. 10 days later, the supernatant (clear liquid) was carefully decanted from the 5 L glass flask ensuring the algae was not disturbed or re-mixed into the medium. The remaining concentrated algae were transferred into 250 mL special centrifuge plastic holders and centrifuged (name of centrifuge) at 2500 RPM for 3 minutes at 18°C with DEC 9 and ACC 3

settings, followed by a 10-minute breakdown cycle. After centrifugation, the supernatant was decanted, and the algae pellets were transferred into 50 mL sterile tubes for further centrifugation until all clear liquid was removed, leaving only concentrated algae pellets. This harvesting process was repeated until the 5 L flask was emptied, and a 50 mL sterile tube was filled with concentrated algae that was stored in the fridge. The procedure was repeated approximately every 10 days after sedimentation until the end of the experiment. For *Daphnia* feeding, 1-2 mL of concentrated algae was added to each beaker on Mondays, Wednesdays, and Fridays, ensuring a slight green coloration of the water to maintain adequate nutrition, with no feeding on Saturdays and Sundays.

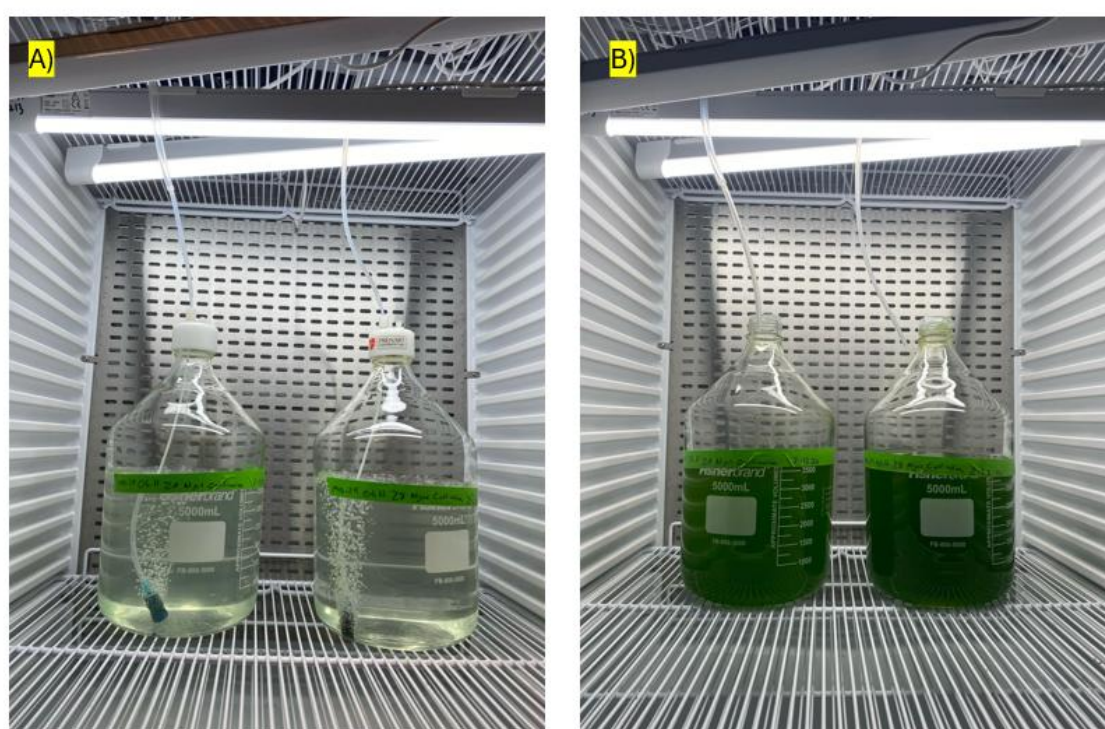


Figure 15: The figure shows picture **A** from the timeline from day 0 with 50mL algae added from the previous batch and picture **B** after 10 days in the incubator chamber. Photos: Ole Holthusen

3.4.2 Cultivation and Exposure water: M7 And EPA water

All non-disposable sample containers and tanks were cleaned thoroughly following procedures adapted from *Methods for Measuring the Acute Toxicity of Effluents and Receiving Waters to Freshwater and Marine Organisms* (EPA, 2002). The cleaning process included detergent soaking, machine washing, sequential rinses with tap water, 10% nitric acid, deionized water, and isopropanol, followed by a final deionized water rinse.

Equipment was then soaked in DI water over the weekend to ensure complete removal of contaminants. Following this process, the M7 medium was prepared following a standardized recipe shown in *Appendix C*, where a 10 L jug was filled with Milli-Q water, and stock solutions 1 and 2 were added along with essential chemicals and vitamins. The jug was shaken and subjected to continuous aeration for one week before use to ensure oxygenation and proper homogenization. The initial pH of the M7 medium was measured at 7.9, and the solution was stored at room temperature (20°C) under regular aeration using an aquatic pump. Before use, the dissolved oxygen (DO) level was measured and recorded at 8.6 mg/L, which met the OECD recommendation of maintaining levels above 3 mg/L. Similarly, EPA medium (standardized synthetic, moderately hard water) was prepared using a separate recipe in *Appendix D*, where Milli-Q water and the required chemicals were added to a 10 L jug, placed next to the M7 medium with clear labeling, and aerated under the same conditions. The pH was adjusted to 6.7 using HCl and NaOH for the EPA water.

3.4.3 Study Species and Cultivation: *Daphnia magna*

A batch of approximately 60 neonates was collected from the Norwegian Institute for Water Research (NIVA) in Oslo and carefully transported by car to the incubation facility at the Isotope Laboratory at the Norwegian University of Life Sciences (NMBU). Upon arrival, 50 neonates were distributed into two 1 L beakers, each containing 800 mL of M7 cultivation medium that was prepared a week before arrival with aeration, with 25 neonates per beaker. They were further fed with concentrated algae (*Raphidocelis subcapitata*) and placed in an incubator set at 20°C (±2°C) under a 16:8 h light/dark cycle. To maintain optimal water quality, the M7 medium was replaced three times per week in the beakers (Monday, Wednesday, and Friday). During each water change, an additional beaker containing deionized (DI) water was prepared to prevent potential contamination from soap residues on new beakers. *Daphnia* and their cultivation water were first transferred into the empty temporary DI water beaker. The old cultivation beaker was rinsed three times with DI water, and residual algae and debris were carefully removed using a lint-free paper towel before another three rinses. Finally, the beaker was refilled with 800 mL of fresh M7 medium. A 1.5 mL pipette with a cut-off tip was used to carefully transfer the *Daphnia* back into their original beaker, ensuring they were released below the water surface to prevent air bubble formation, which could lead to stress

and flotation issues. During each M7 medium replacement, *Daphnia* were sorted by life stage, with neonates removed and adults retained to sustain the culture, while algae and debris were excluded. The number of *Daphnia* in each beaker was recorded at every water change to monitor the culture's status.

3.4.4 Test Organism: *Daphnia magna* (*D.magna*)

For the toxicity test to be valid, it was essential to ensure a healthy generation of daphnids. According to OECD/OCDE 202 guidelines, it is recommended that neonates (<24 hours old) are not taken from the first brood in order to minimize variability and ensure a more stable and consistent test population. Therefore, third-generation neonates were used, ensuring they were derived from a healthy stock, free from stress indicators such as high mortality, presence of males and ehippia, delayed brood production, or discoloration. All organisms used in the Acute Immobilization Test originated from cultures established from the same stock of *Daphnia*, maintained under consistent culture conditions (light, temperature, and medium) identical to those used in the test. To further ensure test validity, neonates under 24 hours old were used to reduce variability, ensuring all *Daphnia* were at the same developmental stage. This helped minimize differences in size, metabolism, and sensitivity to environmental factors, preventing age-related variations from affecting the results.

3.4.5 Experiment Setup

The acute immobilization test was conducted following standardized guidelines to evaluate the toxic effects of tunnel wash water, including detergent containing wash water, wash water from different treatment steps, and a leaching experiment from particles in tunnel wash water, on *D. magna*. Test organisms were exposed to five different concentrations of test solutions, including a control group, to assess dose-dependent immobilization effects over a 48-hour period. Prior to the experiment, frozen toxicity samples were placed in a water bath at room temperature to ensure a controlled and stable defrosting process. The temperature of the samples was verified to be at room temperature before use to prevent any thermal shock that could affect the daphnids. Additionally, all frozen test solutions were fully melted to ensure a homogeneous sample composition before dilution.

Once fully defrosted, the samples were diluted in clean beakers that had been rinsed three times with deionized (DI) water to minimize contamination. The incubation conditions were maintained according to standardized guidelines to ensure test validity. The temperature was kept between 18°C and 22°C, with minimal fluctuations of $\pm 1^\circ\text{C}$ per test. A 16-hour light and 8-hour dark cycle was used and the daphnids were not fed during the exposure period. The test vessels were not aerated, and no pH adjustments were made after test solutions were prepared. To ensure appropriate exposure conditions, several water quality parameters were measured before the test. The pH of the test solution was required to be within the range of 6 to 9, as recommended by OECD guidelines with pH measurements taken before the test using a Multi 340i meter with a SenTix® pH probe. Conductivity ($\mu\text{S}/\text{cm}$) was measured at the beginning of the test using a Multi 340i meter with a WTW TetraCon® 325 probe. Dissolved oxygen concentrations were also measured before the test to ensure compliance with the OECD guideline requirement of at least 3 mg/L in control and test vessels.

Toxicity Testing of Tunnel Wash Detergent

To assess the potential toxicity of the detergent used in tunnel washing, a toxicity test was conducted to evaluate whether the detergent alone could contribute to lethal effects on *D. magna*. Information on the detergent's chemical composition can be found in *Appendix L*. This test was important to ensure that detergent was not a confounding factor in subsequent toxicity tests involving tunnel wash water. During the spring wash, a total of 255 m³ of water and 75 liters of detergent were used. The detergent was pre-diluted at a 1:10 ratio before further dilution in the tunnel system. The overall dilution ratio in the tunnel was calculated as:

$$\text{Total dilution} = \frac{\text{Total water (L)}}{\text{Detergent volume (L)}} = \frac{255,000}{75} = 3,400$$

Accounting for the initial 1:10 pre-dilution, the final estimated detergent concentration in the tunnel was approximately 1:34,000. For simplicity in experimental design, this was rounded to 1:30,000 for toxicity testing. A stepwise dilution method was used to prepare test solutions. First, a 1:100 dilution was created by mixing 1 mL of the 1:10 detergent solution with 99 mL of M7 media. To achieve the target 1:30,000 dilution, 3.33 mL of the 1:100 solution was

further diluted with 96.67 mL of M7. This stock concentration was then used to prepare a dilution series of 1:60,000, 1:120,000, 1:240,000, and 1:480,000 by sequential dilutions in M7 media. The control group consisted of 10 mL of M7 media without any detergent.

Toxicity Testing of Tunnel Wash Water

The acute immobilization test (OECD, 2004) followed a five-concentration dilution series, with 50% tunnel wash water (C1) as the highest concentration due to water chemistry considerations. In total 6 tests were carried out with M7 as exposure media, and 4 tests with EPA media. Each subsequent concentration was prepared by diluting the previous concentration 1:2 with exposure media, ensuring a consistent stepwise reduction in exposure levels. The test solutions included C1 (50%), C2 (25%), C3 (12.5%), C4 (6.25%), C5 (3.125%) illustrated in *Figure 16*, and a blank control (exposure media only) shown in *Figure 17*. To prepare the dilution series, 25 mL of tunnel wash water was mixed with 25 mL of exposure media to create 50 mL of C1 (50%). For each subsequent dilution, 25 mL of the previous concentration was combined with 25 mL of dilution media, resulting in C2 (25%), C3 (12.5%), C4 (6.25%), and C5 (3.125%), with the blank consisting of exposure media only. During the test setup, key water quality parameters were measured for each concentration, including conductivity, pH, and dissolved oxygen (DO), ensuring that the exposure conditions remained within an appropriate range for *Daphnia magna*. The prepared solutions were used to expose the test organisms over a 48-hour period, following the standardized procedure used in previous toxicity assessments.



Figure 16: The figure shows the dilution setup in clean beakers for the different exposure concentrations for filtered tunnel wash water after the filtrate HMR from spring. Photo: Ole Holthusen

Before distributing the exposure media, a pipette was used to stir the solution in each beaker, ensuring a homogeneous sample when transferring 10 mL of exposure water into each well. The exposure setup consisted of six wells (VWR Tissue Culture Plate, Sterilized) shown in Figure 17. Each replicate consisted of one blank control and five test concentrations (C1–C5). In each well, five daphnids were carefully introduced using a disposable 3 mL pipette with a cut-off tip, ensuring no cross-contamination between test solutions. The experimental design included four replicates per test solution, resulting in 30 daphnids per concentration and a total of 120 daphnids per test experiment.

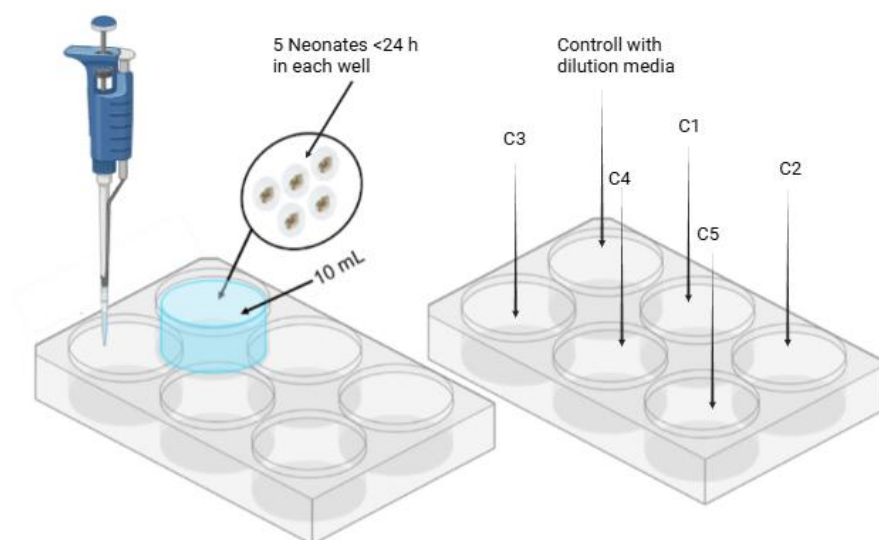


Figure 17: The figure shows the setup for the six well plates with concentration 1-5 plus the control group. The figure is made in Bio render by Ole Holthusen.

Once all daphnids were added to their respective wells, starting with the control group, a cover was placed over the wells to prevent airborne contamination and minimize water evaporation. The wells were then transferred to the incubation chamber for a 48-hour exposure period with the start time documented.

For the final test with untreated autumn tunnel wash water, using EPA water as the exposure medium, a slight modification in the exposure setup was necessary due to a shortage of six-well plates. As a result, sterilized Petri dishes (60 x 15 mm Style polystyrene) were used instead. The same experimental procedure was followed, ensuring consistency in dilution preparation, daphnid exposure, and incubation conditions. However, instead of six-well plates, each daphnid group was placed in individual Petri dishes, maintaining the same exposure volumes. Additionally, the pH of the EPA water was adjusted a week before to 6.67 to examine whether a slightly more acidic environment would influence metal toxicity, particularly in relation to metal bioavailability. *Figure 18* illustrates the difference in particle distribution between the highest concentration of untreated spring tunnel wash water in a six-well plate and *Figure 19* the highest concentration of untreated autumn tunnel wash water in Petri dishes. The difference in particle distribution may be considered when interpreting toxicity outcomes between these tests.



Figure 18: Illustrates the concentration gradient, with C1 representing the lowest concentration and C5 the highest from untreated TWW from the Spring wash water. Photos: Ole Holthusen



Figure 19: Illustrates the highest concentration of untreated autumn tunnel wash water in Petri dish, where particles are inhomogenously distributed. Photos: Ole Holthusen.

Toxicity Testing of Leachate from the Experiment

For the toxicity test for the leaching experiment the same procedure was followed as the tunnel wash water tests. Due to little supernatant only 3 replicates were made, and M7 was used as exposure media. *Table 11*, gives a overview of all tests conducted.

Table 11: Gives an overview of the test duration, stressors, concentrations from start, volume of dilution, replicates and total number of daphnia used in tests.

Test duration	Stressor	Concentration (Start of the test)	Volume Of M7 / EPA media added	Replicates	Total Daphnids (< 24 h neonates)
48 – hour test	Diluted detergent	C5 - 1:30,000	0.0 mL	4 replicates with 5 daphnids in each well	n=120
		C4 - 1:60,000	5.0 mL		
		C3 - 1:120,000	7.5 mL		
		C2 - 1:240,000	8.75 mL		
		C1 – 1:480,000	9.375 mL		
48 – hour test	Tunnel wash water from spring and autumn from different treatment steps	C5 - 50%	5 mL	4 replicates with 5 daphnids in each well	n=1200
		C4 - 25%	7.5 mL		
		C3 - 12.5%	8.75 mL		
		C2 - 6.25%	9.375 mL		
		C1 - 3.125%	9.6875 mL		
48 – hour test	Supernatant leachate originating from particles in tunnel wash water	C5 - 50%	5 mL	3 replicates with 5 daphnids in each well	n=90
		C4 - 25%	7.5 mL		
		C3 - 12.5%	8.75 mL		
		C2 - 6.25%	9.375 mL		
		C1 - 3.125%	9.6875 mL		

3.4.6 Observations and Analysis of Exposed Daphnids

After 24 and 48 hours, the six-well plates were removed from the incubation chamber and examined for immobilized daphnids. In addition to immobilization, abnormal behavior and changes in appearance were recorded. At the end of the 48-hour exposure period, the daphnids were examined more closely using magnifying glass to further assess immobilization, abnormal behavior, and overall physical condition. According to the OECD (2004) guideline, immobilization is defined as: "Those animals that are not able to swim within 15 seconds after gentle agitation of the test vessel are considered to be immobilized (even if they can still move their antennae). Gentle agitation was achieved either by carefully disturbing the water in the vessel or by using a pipette to stir the solution slightly. While immobilization does not

necessarily indicate mortality, it is the primary endpoint for assessing toxicity effects in this study. To obtain detailed observations, daphnids from each replicate were further examined under a microscope (MDG41 Leica Microsystems) to assess the Daphnids and photographs were taken for documentation. Following microscopic analysis, all daphnids from each concentration were collected from the six wells using a pipette and transferred into Eppendorf tubes. Excess water in the tubes was carefully removed using a 200 µm pipette, leaving the daphnids in the tubes without liquid. The collected daphnids were then frozen at -21°C for potential further analysis.

3.4.7 Methodological Adjustments and Justifications

Several deviations from the OECD guideline for chemical testing were made during the study, primarily due to practical constraints and methodological considerations. One key deviation involved the use of M7 medium, despite the OECD recommendation to avoid media containing chelating agents when testing substances with metals, as they may interfere with metal bioavailability. To confirm that the use of M7 medium did not affect the results, an additional four tests were conducted using EPA water, which is free of chelating agents. However, it is important to note that M7 does not interfere with organic chemicals, meaning that the test results for organic contaminants remain valid regardless of the medium used. Furthermore, in the first three tests conducted during the spring wash toxicity assessment, water quality parameters were not measured for each concentration, which could be a methodological limitation. However, since later tests showed consistent water chemistry, it is likely that conditions remained stable, minimizing the impact of the missing data on the results. Additionally, post-exposure parameter measurements in the wells were not conducted for most tests, as a preliminary measurement indicated only minimal changes in water quality parameters after exposure. Given time constraints, it was determined that further post-exposure measurements were unnecessary. Also, in the leaching experiment, only three replicates were used, and no water parameters were measured due to the limited volume of available liquid. Another procedural adjustment occurred during the final test with untreated autumn tunnel wash water, where Petri dishes were used instead of standard six-well plates due to equipment shortages. Although this was a deviation from the original setup, the exposure conditions and test procedure remained consistent.

3.5 Data Processing and Statistical Analysis

Statistical analysis was conducted in RStudio (version 2024.12.1+563) using R. The R packages ggplot2, dplyr, and tidyr were employed for data cleaning, manipulation, and visualization, using bar plots and boxplots to represent group-level trends. For each compound, data were filtered based on relevant conditions such as treatment or season, and non-numeric or missing values were excluded. Descriptive statistics, including mean and standard deviation, were calculated for each group. The Shapiro Wilk test was used to assess normality (for sample sizes between 3 and 5000). When normality was confirmed ($p > 0.05$), two-sample t-tests were used to compare groups. In cases where the data were not normally distributed, the Mann Whitney U test (Wilcoxon rank-sum test) was applied as a non-parametric alternative.

Lethal concentrations for the detergent and autumn TWW toxicity tests were calculated using the online platform Mosaic (Modeling and Statistical tools for ecotoxicology), available at <https://mosaic.univ-lyon1.fr>. The platform was also used to generate dose response curves and graphical visualizations of the results.

3.6 Calculating Treatment Efficiency

For the total treatment effectivity (%) for treatment 1 and treatment 2 the formula (1) and (2) below was used. This was calculated according to the initial concentrations from untreated tunnel wash water and the concentrations after the sedimentation for 21 days and for after treatment 2 with Filtralite HMR. Further the efficiency effect of treatment 2 was calculated using the same formula (3), but the concentrations from treatment 1 was used as the initial concentration.

1) Removal efficiency treatment 1

$$\text{Removal effectivity treatment 1} = ((C_{init} - C_{Sed}) / C_{init}) * 100\%$$

2) Removal total efficiency treatment 1 + treatment 2

$$\text{Total removal efficiency (treatment 1 + 2)} = ((C_{init} - C_{Filter}) / C_{init}) * 100\%$$

3) Removal efficiency treatment 2

$$\text{Removal efficiency treatment 2} = ((C_{Sed} - C_{Filter}) / C_{Sed}) * 100\%$$

3.7 Use of Artificial intelligence

Artificial intelligence (AI) has been used as a supportive tool throughout the work on this master thesis. The websites used are NMBUs Sikt KI-chat and ChatGPT. AI has provided assistance with statistical scripting in R, including guidance on appropriate types of analysis, data sorting, and general use of RStudio. It has also been helpful in navigating tasks in Word, QGIS and Excel and obtaining general technical information for the program. Furthermore, AI has contributed to improving the written content of the thesis by identifying and correcting language errors, as well as suggesting more precise and scientific phrasing. AI tools were also used to efficiently locate relevant scientific literature, particularly through the use of the thorough research function, which helped save time during the literature search process.

4.0 Results and Discussion

4.1 Tire and Road Wear Particles

4.1.1 Seasonal Variation and Concentrations

Concentrations of TRWP in the two size fractions greater than 5 micrometres and between 0.4 and 5 micrometres in tunnel wash water samples varied considerably with treatment type, sampling depth, time interval, season, and particle size. The results for Treatment 1 using a sedimentation basin and Treatment 2 using Filtralite HMR are presented in *Figure 20* and detailed further in *Appendix F*. For TRWP particles $>5\ \mu\text{m}$ (top panel), untreated concentrations were highest in spring with mean values (54.79 mg/L) and lower in autumn (33.71 mg/L). The difference was statistically significant, with a t-test confirming that spring concentrations were significantly higher than those in autumn (SD = 10.07 and 11.68, respectively; $p = 0.001$). Treatment 1 reduced levels to 6.67 mg/L in spring and 2.00 mg/L in autumn. After Treatment 2, concentrations dropped further to 3.34 mg/L in spring and 0.72 mg/L in autumn.

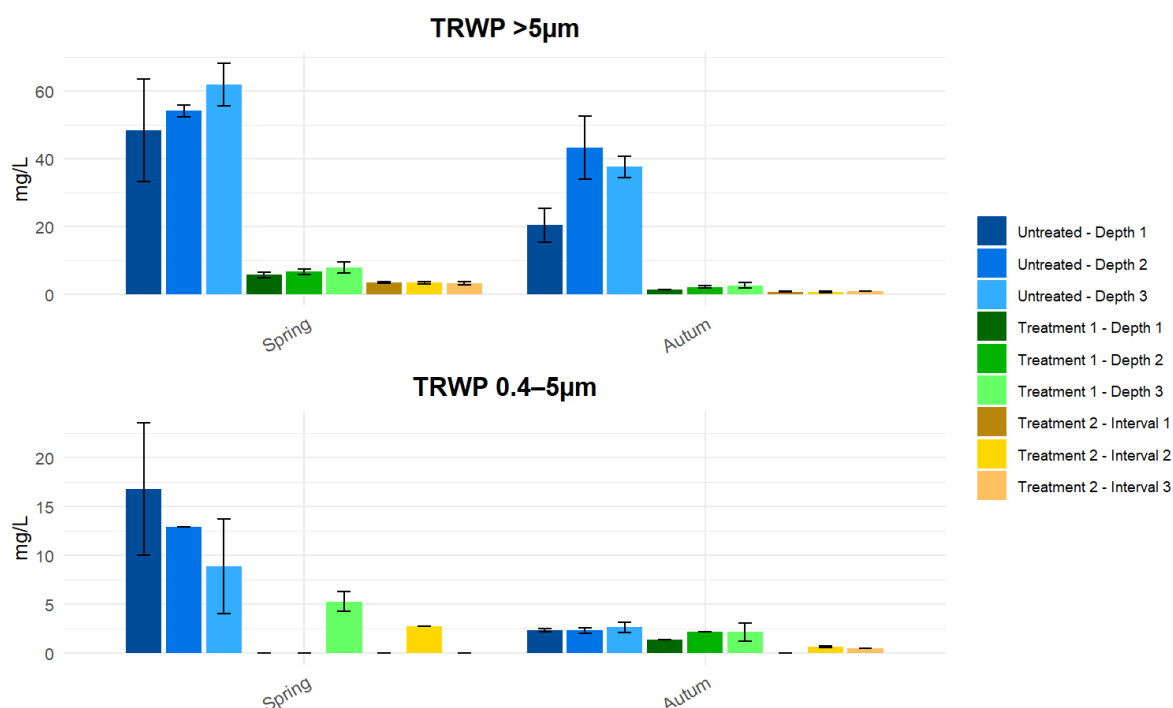


Figure 20: The bar graphs show the concentrations of tire and road wear particles (TRWP) in tunnel wash water across different treatment depths and intervals for two particle size fractions: $>5\ \mu\text{m}$ (top panel) and $0.4\text{--}5\ \mu\text{m}$ (bottom panel), measured during spring and autumn. The bars represent mean concentrations (mg/L) with error bars indicating standard deviation.

For the $0.4\text{--}5\ \mu\text{m}$ fraction (bottom panel), untreated samples also showed elevated mean levels, particularly in spring with 12.84 mg/L compared to autumn with 2.41 mg/L. Treatment 1 lowered concentrations to 5.25 mg/L in spring and 1.90 mg/L in autumn. Following Treatment 2, levels declined to 2.75 mg/L in spring and 0.56 mg/L in autumn. Final concentrations after treatment 2 were minimal across both seasons, confirming effective removal of fine TRWPs through the treatment process. The seasonal reduction in particle concentrations was more pronounced in the $0.4\text{--}5\ \mu\text{m}$ fraction, which decreased by approximately 81% from spring to autumn. In comparison, the $>5\ \mu\text{m}$ fraction decreased by around 39%. This suggests that finer particles show stronger seasonal variation, potentially due to differences in road abrasion from winter tires. The measured TRWP concentrations in TWW from the Ekeberg tunnel during spring ranged from 48–62 mg/L and 20–43 mg/L in autumn ($>5\ \mu\text{m}$ fraction). However, when both fractions measured in this study are included ($>5\ \mu\text{m}$ and $0.4\text{--}5\ \mu\text{m}$), total TRWP concentrations reached average values of approximately 67.6 mg/L in spring and 36.1 mg/L in autumn ($>0.4\ \mu\text{m}$), aligning well with those reported in other Nordic studies, that used a particle size of $>1.6\ \mu\text{m}$. In the study by (Rødland et al., 2022)

TRWP and TWP levels were assessed in the Smestad tunnel (Oslo, Norway) using samples collected before and after tunnel wash water treatment in April–May. The average TRWP concentration in untreated TWW was 48.6 ± 13.3 mg/L, with a range of 20.9 to 69.2 mg/L, while TWP alone averaged 33.6 ± 9.2 mg/L (Rødland et al., 2022). These findings are consistent with the TRWP levels observed in Ekeberg tunnel during spring with a mean 67,63 mg/L, underscoring the accumulation potential of TRWP in tunnels even with moderate traffic volumes (AADT ~22,000 vehicles per tube). Similarly, Meland et al. reported peak TWP concentrations of 134 ± 39.7 mg/L in the Vålereng tunnel (Meland et al., 2023), with a mean and median of 71.8 and 67.5 mg/L, respectively, based on wash water samples collected in November and December. The elevated concentrations in Vålereng were linked to its significantly higher traffic volume with an ADT of 66,400 vehicles compared to 44,000 in Smestad for two lanes. Given that the Ekeberg tunnel recorded an even higher AADT of approximately 79,000 vehicles in 2024, higher concentrations of TWP in Ekeberg were expected. One possible explanation for the less TWP levels observed in this study can be traffic-related factors such as increased braking and acceleration. However, these alone may not fully explain the differences in road surface wear.

Another contributing factor could be the use of different cleaning agents, which may vary in how effectively they mobilize TWP and polymer-modified bitumen (PMB) from tunnel surfaces (Granheim, 2023). Additionally, particle retention in tunnel infrastructure such as gully traps or pump basins before water reaches the sedimentation basin could reduce or alter measured concentrations, depending on how much material is intercepted or resuspended during cleaning. Other possible explanations include tunnel specific characteristics such as gradient, ventilation induced airflow patterns, and road surface texture, all of which can influence how particles are transported, accumulate over time, and are ultimately released during tunnel washing. Overall, the TRWP and TWP concentrations observed in this study fall within expected ranges for Norwegian tunnel wash waters. Seasonal patterns also play a key role with higher levels in spring are a result of Nordic-specific conditions. Laboratory and field studies show that switching to studded tires can increase road-dust emissions by factors of 10–100 (Gehrke et al., 2023). In fact, studded tires are one of the largest sources of PM and the main cause of road abrasion in Northern Europe (Gehrke et al., 2023). Throughout winter, TRWP and TWP build up inside tunnels due to constant wear and minimal runoff.

These particles remain until spring cleaning operations trigger a first flush, releasing months of accumulated particles and resulting in elevated TSS, TWP and TRWP concentrations. In contrast, autumn samples reflect only the lighter wear of summer conditions, with less accumulation from seasonal factors and studded tire abrasion. The higher concentrations in spring further confirms Hypothesis 1.

4.1.2 Effect of Treatment 1 and 2

The results from both the boxplot in *Figure 21* and the treatment efficiency *Table 12* clearly show that the applied treatment system consisting of Treatment 1 and Treatment 2 is effective at reducing road associated microplastic particles larger than 5 µm in tunnel wash water. The compounds analyzed include styrene-butadiene rubber and butadiene rubber (SBR + BR), tire and road wear particles (TRWP), and tire wear particles (TWP). The concentrations were studied across two seasons, spring and autumn, through three stages: untreated, after Treatment 1, and after Treatment 2. In spring, TRWP removal for particles >5 µm reached 88% after Treatment 1, increasing to 94% following Treatment 2, indicating an additional 50% efficiency gain in the second stage. TWP (>5 µm) followed a similar trend, improving from 88% to 94% across the two treatment steps. Statistically, TRWP concentrations for the >5 µm fraction decreased significantly in both seasons. In autumn, mean levels dropped from 1.85 mg/L to 0.70 mg/L (t-test, $p = 0.006$), while in spring, concentrations declined from 6.67 mg/L to 3.34 mg/L (Mann–Whitney U, $p = 0.001$), confirming the treatment's effectiveness. This pattern is also evident in the boxplot, where spring concentrations of TRWP and TWP dropped sharply after the first treatment stage and continued to decline following the second stage, though the second step provided a smaller absolute reduction. In autumn, removal efficiencies improved further. TRWP and TWP (>5 µm) reached 94% after Treatment 1 and 98% after Treatment 2, gaining 65% in the second stage. The graph confirms these findings, showing lower starting concentrations than in spring and a consistent downward trend through the treatment stages. This suggests that initial particle loads are lower in autumn, leading to overall more efficient removal.

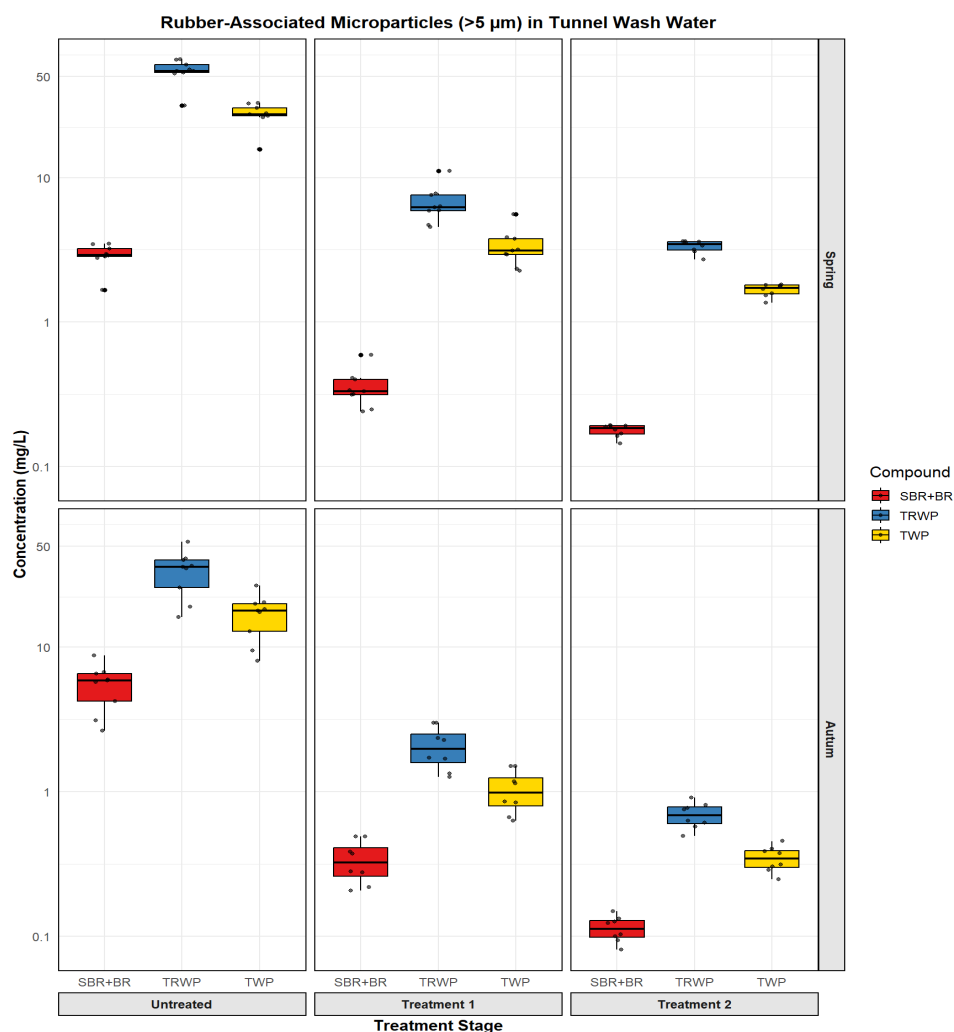


Figure 21: The boxplots shows the concentrations of rubber-associated microparticles (>5 µm) in tunnel wash water across different treatment stages (Untreated, Treatment 1, Treatment 2) and two seasonal conditions (spring and autumn). The compounds measured include SBR+BR (red), TRWP (blue), and TWP (yellow). Concentrations are shown on a logarithmic scale (mg/L).

When comparing particle sizes, the treatment process was less effective for the 0.4–5 µm fraction. In spring, TRWP and TWP (0.4–5 µm) removal was only 59% after Treatment 1, increasing to 79% after Treatment 2, with a 48% gain. These values, although improved in the second step, indicate the difficulty of removing smaller, more suspended road associated microplastics using sedimentation. This is reflected in the color coded table in *Table 12*, where the smaller fraction in spring remained in the yellow orange zone, suggesting moderate efficiency. Autumn treatment results for the 0.4–5 µm fraction were more effective. TRWP and TWP (0.4–5 µm) started much lower, at 21%, but increased significantly to 77% after

Treatment 2, with a 70% polishing effect. However, this exact result should be viewed with caution, as it is based on a single value from the available replicates compared to the other results. As such, the percentage may not reliably represent typical treatment performance and could be influenced by analytical uncertainty.

Table 12: Presents the treatment efficiency (%) of rubber-associated microparticles for two size fractions ($>5\ \mu\text{m}$ and $0.4\text{--}5\ \mu\text{m}$), across spring and autumn. It includes total removal after Treatment 1 and Treatment 2, as well as the additional efficiency of Treatment 2 after Treatment 1. Color coding indicates total effect ranges.

Tire Road Wear Particles	Spring	Spring	Spring	Autumn	Autumn	Autumn	Legend
	Total Treatment	Total Treatment	Efficiency of Treatment 2 after treatment 1	Total Treatment	Total Treatment	Efficiency of Treatment 2 after treatment 1	
	Treatment 1	Treatment 2	Treatment 2	Treatment 1	Treatment 2	Treatment 2	Total Effect%
SBR+BR $>5\mu\text{m}$	87.8%	93.9%	49.9%	93.8%	97.8%	65.6%	0-30%
SBR+BR $0.4\text{--}5\mu\text{m}$	41.6%	69.3%	47.5%	63.0%	90.8%	75.2%	30-60%
TRWP $>5\mu\text{m}$	87.8%	93.9%	49.9%	93.8%	97.8%	65.6%	60-85%
TRWP $0.4\text{--}5\mu\text{m}$	59,1%	78,5%	47.5%	21,2%	76,6%	70,3%	85-100%
TWP $>5\mu\text{m}$	87,8%	93,9%	49,9%	93,8%	97,8%	65.6%	
TWP $0.4\text{--}5\mu\text{m}$	59,1%	78,5%	47,5%	21,2%	76,6%	70,3%	

These findings align well with (Rødland et al., 2022), who reported a 63% TRWP removal efficiency in the Smestad tunnel after 21 days of sedimentation, with TWP showing similar results. Moreover, the study observed limited differences in particle size distribution before and after treatment, with over 83% of particles remaining $<30\ \mu\text{m}$ in both phases, further underscoring the challenge of capturing smaller TRWP fractions through sedimentation alone. This supports the observations from this study that smaller particles ($0.4\text{--}5\ \mu\text{m}$) were less effectively removed. In contrast, larger particles ($>5\ \mu\text{m}$) in this study reached 87–94% removal in spring and up to 98% in autumn, aligning more closely with (Meland et al., 2023) who observed 98% TWP removal in the Vålerenga tunnel. The boxplot and table together reveal that particles larger than $5\ \mu\text{m}$ (TRWP, TWP) are consistently removed more efficiently than smaller ones, with Treatment 1 already achieving high reductions, especially in autumn.

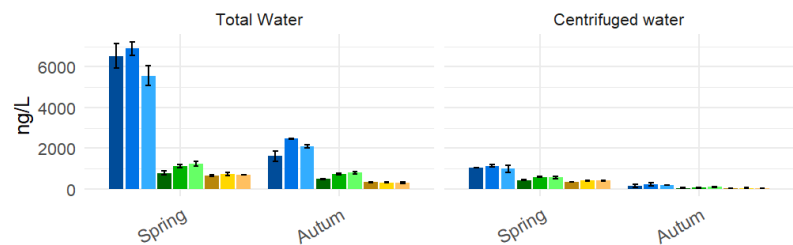
Smaller particles (0.4–5 μm) are more difficult to remove, particularly in spring, likely because they remain more suspended in the water column, making them less responsive to sedimentation in Treatment 1. The limited effectiveness of the sedimentation basin for these finer particles highlights the importance of Treatment 2, which acts as a critical polishing step. While Treatment 2 highly improves removal, it still has limitations for complete retention of these smaller road associated microplastic particles. However, these results further confirm hypothesis 2.

4.2 Tire Derived Chemicals

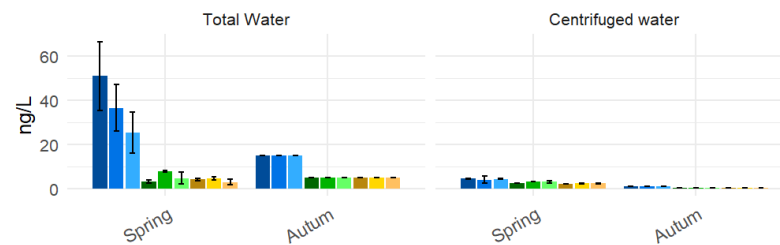
4.2.1 Seasonal Variation and Concentrations

The tire-derived chemicals were measured in the tunnel wash water to assess their concentrations across treatment stages, sampling depths, and seasons. The compounds analyzed include 6PPD, 6PPD-Q, 7PPD, CPPD, DPPD, IPPD, PhBT, TMQ, HMMM, DPG, and MTBT. Samples were analyzed as either total water, representing the full, unprocessed sample, or centrifuged water, where samples were spun at 2800 RPM for 5 minutes to remove particulate matter. This approach helped distinguish how the chemicals are distributed between dissolved and particle-bound phases. Concentrations were measured in both spring and autumn, where values in *Figure 22* represent the mean of two replicate samples. Further details are provided in *Appendix G*. Among the eleven tire-associated compounds analyzed, clear seasonal trends and compound-specific treatment responses were observed. All tested tire derived additives showed statistically significant seasonal differences in TWW concentration between spring and autumn ($p < 0.05$). Specifically, 6PPD ($p = 0.005$), 6PPD-Q ($p < 0.001$), DPPD ($p = 0.005$), IPPD ($p < 0.001$), CPPD ($p = 0.003$), 7PPD ($p = 0.003$), HMMM ($p = 0.005$), DPG ($p = 0.005$), TMQ ($p = 0.005$), and PhBT ($p = 0.003$) mostly all had significantly higher concentrations in spring, suggesting a strong seasonal pattern and confirming hypothesis 1. In contrast, MTBT ($p = 0.005$) was the only additive that showed significantly higher concentrations in autumn, indicating a distinct seasonal behavior compared to the others.

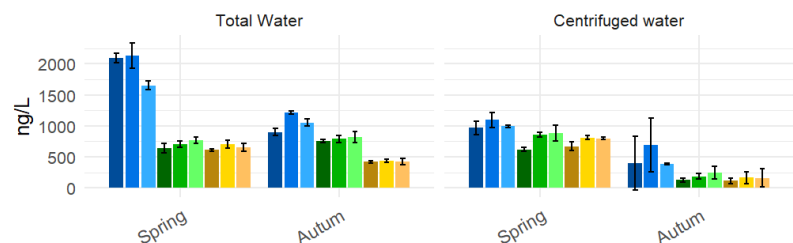
6PPD



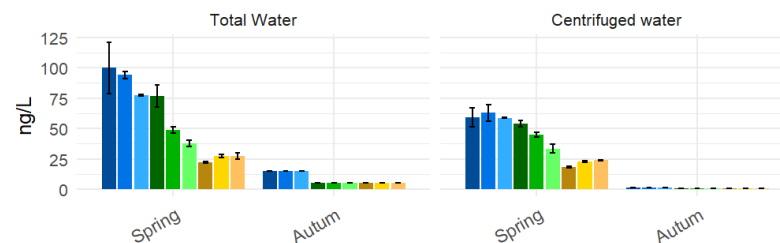
CPPD



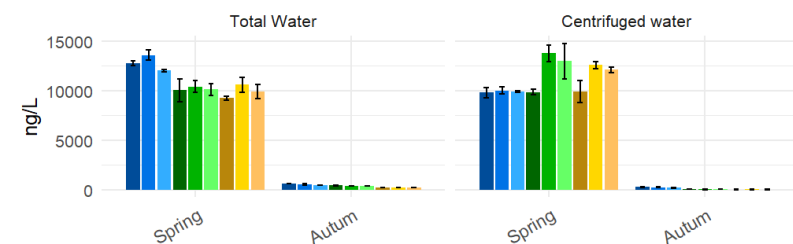
6PPD Q



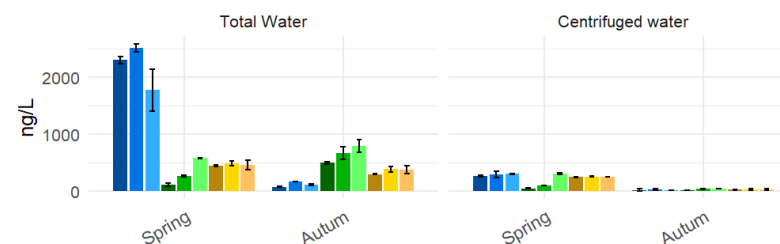
7PPD



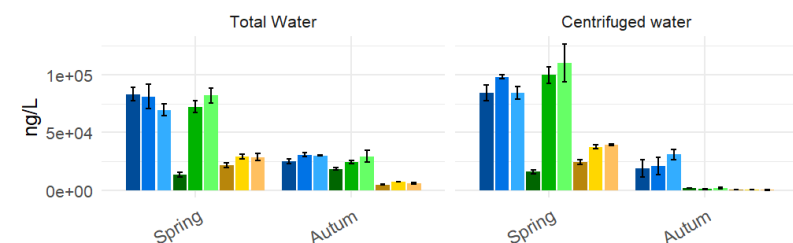
HMMM



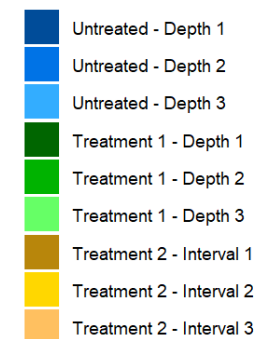
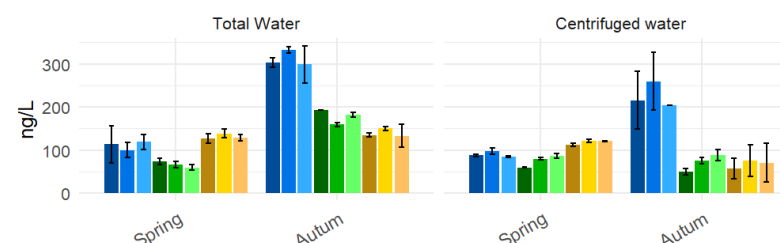
TMQ



DPG



MTBT



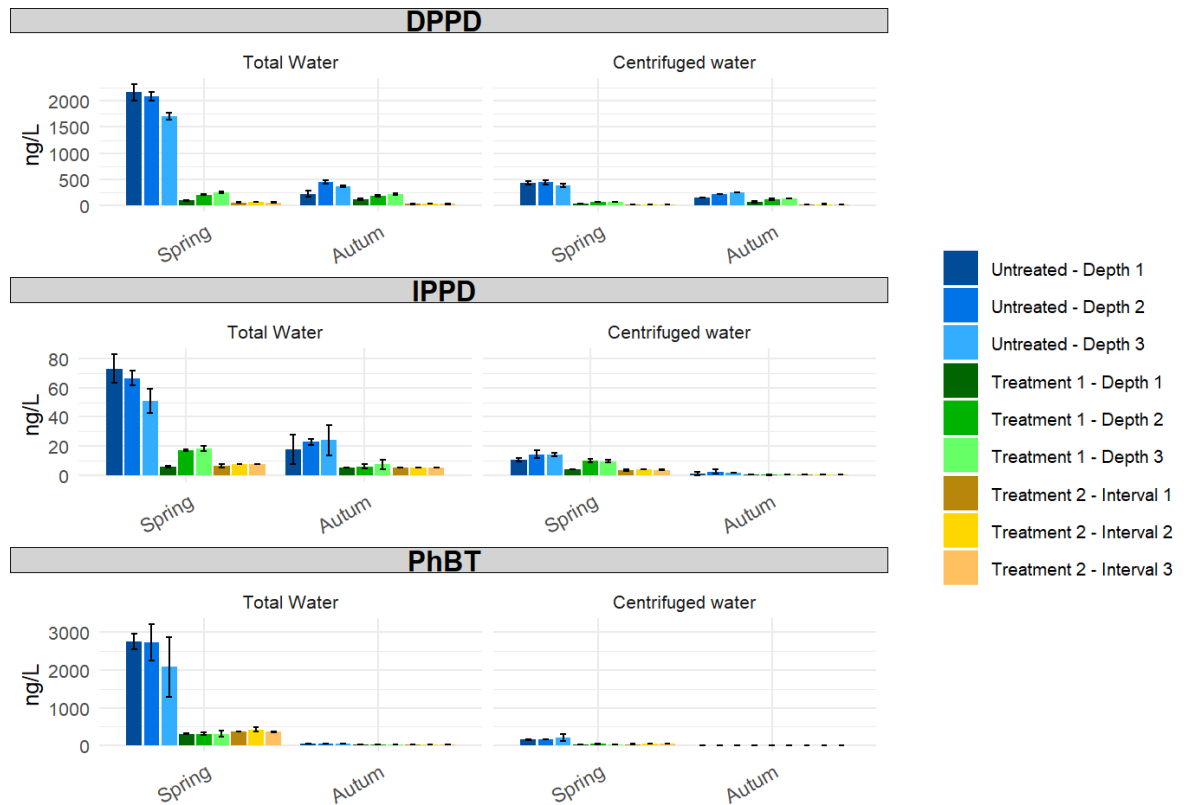


Figure 22: The bar graphs present the mean concentrations from 2 replicates of organic additives from tire wear particles (TWP) in untreated water at depths 1, 2, and 3, treated water from corresponding depths, and filtered water sampled from the outflow at 10-minute intervals. Additionally, the graphs indicate the sampling season and display concentrations in both total and centrifuged water samples in ng/L.

A comparison of untreated and discharge concentrations between this study and (Meland et al., 2023) reveals both consistent trends and notable differences for tire-associated compounds. While these authors collected samples from a sedimentation basin equivalent to Treatment 1, the present study includes an additional treatment step beyond sedimentation. Hence, our comparisons should be interpreted as an indication of differences rather than exact differences. For 6PPD, untreated concentrations in this study ranged from 5563 to 6895 ng/L in spring, substantially lower than the 50,000- 91,200 ng/L peaks, reported by (Meland et al., 2023). Similarly, 6PPD-Q levels were also lower in this study (1652–2135 ng/L) compared to Meland’s 3000–3300 ng/L. These differences may reflect site-specific factors such as traffic intensity, tunnel design, or sampling timing. At the discharge stage, however, this study had lower final concentrations for both compounds: 660–740 ng/L for 6PPD and 609–768 ng/L for 6PPD-Q, compared to 8 000-15,000ng/L and around 2000–2300 ng/L in Meland’s findings.

For HMMM, both studies showed comparable untreated concentrations, with this study reporting 12,048–13,588 ng/L in spring and (Meland et al., 2023) measuring 11,000–13,000 ng/L. Discharge values were also similar (9,266–10,592 ng/L vs. 8800–14600 ng/L), indicating a little to no removal performance across both systems. In contrast, DPG showed the highest concentrations in this study in spring, with slightly higher untreated levels (69,500–83,250 ng/L) versus Meland’s approximately 55,000–64,000 ng/L. Final concentrations after Treatment 2 were also slightly lower in this study (21,690–28,975 ng/L) compared to Meland’s 38 000–40 000 ng/L, reinforcing DPG’s persistence.

MTBT exhibited a reversed trend compared to other compounds. In spring, untreated concentrations in this study were considerably lower (99.7–118 ng/L) than those reported by (Meland et al., 2023) with 750–1,000 ng/L. Notably, discharge concentrations in this study increased after treatment 2, reaching 127–138 ng/L, which may indicate leaching from TRWP/TWP after the treatment process. In contrast, Meland observed a decrease in MTBT levels at discharge, to approximately 200–500 ng/L. Additionally, MTBT was the only additive in this study to show substantially higher concentrations in autumn, suggesting a seasonal behavior that differs from the trends observed for other tire-associated compounds.

For PhBT, untreated spring concentrations in this study ranged from 2,079 to 2,749 ng/L, which is substantially higher than the approximate 340 ng/L reported by Meland. This may suggest a seasonal difference, as autumn concentrations in this study were much lower, around 50 ng/L. Despite the higher initial values, discharge concentrations in spring were 376–427 ng/L, compared to Meland’s lower range of approximately 200–240 ng/L, indicating strong removal but also some residual presence. Lastly in the case of TMQ, untreated spring concentrations in this study ranged from 1769 to 2511 ng/L, considerably lower than Meland’s, who reported values around 10,000–12,500 ng/L. Interestingly, while TMQ discharge levels in this study remained relatively low (442–489 ng/L) there was an increase in concentrations after treatment 2 in spring, (Meland et al., 2023) also observed an increase in TMQ concentrations after sedimentation, with discharge values reaching approximately 7,500 ng/L. This suggests that TMQ may leach out during sedimentation but also after Treatment 2 in this study, showing that Treatment 2 has no effect on the compound shown in *Table 13*, reinforcing its classification as a moderately water soluble compound. Notably, 6PPD-Q remained relatively stable in centrifuged samples, suggesting it is less particle-

associated than 6PPD and likely persists in the dissolved phase. Similar patterns were observed for DPG, HMMM, and MTBT, all showing limited reduction through centrifugation, indicating they are primarily dissolved and less effectively removed by sedimentation from Treatment 1. Overall, the concentrations of tire derived compounds (TDCs) measured in this study are largely comparable to those reported in the Vålerenga tunnel. However, it should be noted that the (Meland et al., 2023) data were interpreted from figure graphics rather than extracted from raw tables, and thus should be viewed as approximations. Nonetheless, the findings from both studies reinforce the conclusion that road tunnels serve as key accumulation and release points for TDCs into the aquatic environment.

4.2.2 Effect of Treatment 1 and 2

Further statistical analysis was conducted to assess differences in additive concentrations in tunnel wash water between Treatment 1 and Treatment 2. Normality was evaluated using the Shapiro-Wilk test. An independent samples t-test was applied to compounds with normally distributed data ($p > 0.05$), while the Mann-Whitney U test was used for non-normally distributed data ($p < 0.05$). Statistically significant differences between treatments were observed for several additives, including 6PPD, 6PPD-Q, DPPD, and DPG ($p < 0.05$), with concentrations consistently higher in Treatment 1, indicating potential removal by Treatment 2. In contrast, no significant differences were found for IPPD, CPPD, 7PPD, HMMM, TMQ, MTBT, and PhBT ($p \geq 0.05$), suggesting limited or variable treatment efficiency for these compounds. It is important to note that Hypothesis 2 involved comparing concentrations between treatment groups regardless of season. Treatment efficiencies for both Treatment 1 and Treatment 2 across spring and autumn are presented in *Table 13* for the analyzed tire-derived chemicals.

Table 13: Removal efficiencies (%) of selected tire-derived chemicals (TDCs) during Treatment 1 (sedimentation) and Treatment 2 (filtration) across spring and autumn sampling campaigns. Color coding indicates total removal efficiency: red (0–30%), orange (30–60%), yellow (60–85%), and green (85–100%).

Season:	Spring	Spring	Spring	Autumn	Autumn	Autumn	Legend
	Total Treatment		Efficiency of Treatment 2 after treatment 1	Total Treatment		Efficiency of Treatment 2 after treatment 1	
Tire-derived chemicals	Treatment 1	Treatment 2	Treatment 2	Treatment 1	Treatment 2	Treatment 2	Total Effect%
6PPD	83.3%	88.9%	33.8%	67.3%	84.3%	52.2%	0-30%
6PPD Q	63.9%	66.4%	6.87%	25.4%	59.6%	45.8%	30-60%
DPPD	90.6%	96.8%	66.2%	49.2%	90.5%	81.4%	60-85%
IPPD	78.2%	88.5%	47.4%	71.4%	76.8%	18.9%	85-100%
CPPD	86.0%	89.7%	26.5%	66.6%	66.6%	0%	
7PPD	39.9%	71.8%	53.0%	66.6%	66.6%	0%	
HMMM	20.3%	22.4%	2.75%	27.1%	57.3%	41.4%	
DPG	28.1%	66.0%	52.7%	15.7%	78.8%	74.8%	
TMQ	85.6%	78.9%	-46.3%	-462.0%	-204.2%	45.8%	
MTBT	40.2%	-18.7%	-98.5%	42.7%	55.3%	21.9%	
PhBT	87.5%	84.5%	-24.2%	60%	60%	0%	

When comparing the discharge percentages of tire derived chemicals in this study with those reported by Meland et al. (2023), clear differences in treatment effectiveness are shown. In this study, Treatment 2 during the spring season achieved high removal efficiencies for compounds such as DPPD (96.8%), 6PPD (88.9%), and IPPD (88.5%), CPPD (89,7%) indicating strong responsiveness to the treatment process. Treatment of PhBT also showed high performance at 84.5%, while 6PPD-Q, DPG, and 7PPD demonstrated moderate to good results, generally ranging between 60–78%, with some seasonal variation, for instance, DPG improved from 66% in spring to 78.8% in autumn. In contrast, Meland et al. reported generally lower discharge percentages for many of the same compounds. Although 6PPD showed 84% ,DPG appeared at 8% , IPPD 38 % , PhBT 44% discharge, showing less consistent removal compared to the trends seen in this study. These discrepancies likely reflect differences in treatment conditions, methodologies, or environmental factors. In particular, water samples in the Ekeberg study were separated and centrifuged in the lab, while in the Vålereng study, attempts were made to process samples directly onto HLB columns in the field.

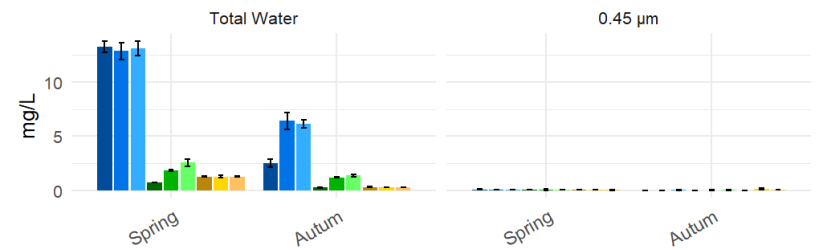
Despite this, both studies highlight challenges with more persistent compounds. In this study, HMMM showed limited removal (22.4–57.3%), while MTBT had poor performance, including a negative efficiency of -18.7% in spring and only moderate improvement in autumn (55.3%). TMQ showed the most concerning result, with a strongly negative efficiency of -204.2% in autumn, suggesting possible re-release into the environment post-treatment. Similarly, Meland et al. reported discharge values of -65% for HMMM, and -2% for TMQ, reinforcing concerns over their resistance to treatment and potential mobility. Overall, the findings show that Treatment 2 is effective for a range of antioxidants and moderately successful for others, but a group of more persistent compounds remains resistant to removal, with seasonal variation playing a key role. These substances, particularly those with low or negative treatment performance, continue to leak after the TWW treatment. Therefore, the results provide partial support for Hypothesis 2.

4.3 Metals

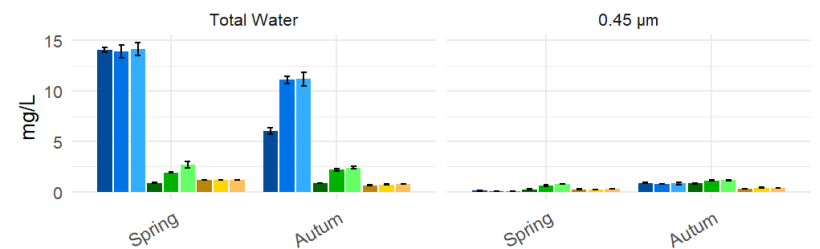
4.3.1 Seasonal Variation and Concentrations

Metals were measured in tunnel wash water to assess concentrations across treatment stages, depths, and seasons. Analyzed elements included Al, Fe, V, Cr, Mn, Co, Ni, Cu, Zn, As, Mo, Cd, W, Pb, Sn, and Sb. Samples were taken as total (unfiltered) and 0.45 µm filtered water to distinguish between particulate-bound and dissolved metals. *Figure 23* shows seasonal concentrations for both sample types, based on the mean of three replicates that can be found in *Appendix H*. Further statistical analysis revealed significant seasonal differences for most metals in untreated TWW. Normality was assessed using the Shapiro-Wilk test; when data were non-normally distributed ($p < 0.05$), the Mann-Whitney U test was applied for Al, V, Fe, Co, Ni, Cu, Zn, As, Mo, Cd, W, and Pb. For metals with normally distributed data (Cr, Mn, Sn, and Sb), an independent samples t-test was used. Significant differences between spring and autumn were observed for most metals ($p < 0.001$), including Al, V, Cr, Fe, Co, Ni, Cu, Zn, As, Mo, Cd, Sb, and Pb. In contrast, Mn, Sn, and W showed no statistically significant seasonal variation ($p > 0.05$). While most metals exhibited higher concentrations in spring, Mo, Sn, and Sb were higher in autumn, indicating that seasonal patterns varied among individual elements. These results provide limited support for Hypothesis 2.

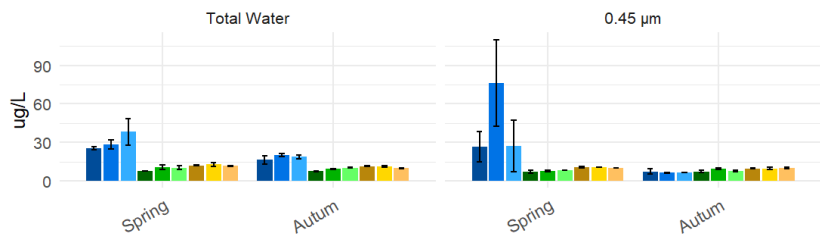
Al



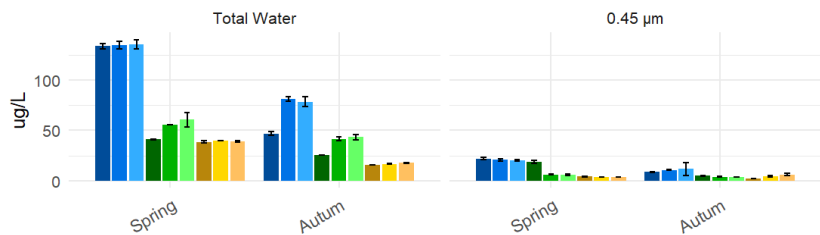
Fe



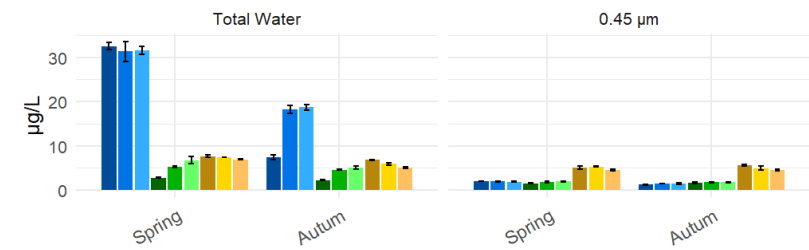
Ni ug/L



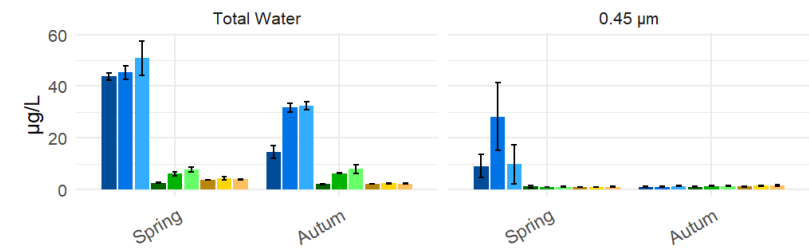
Cu ug/L



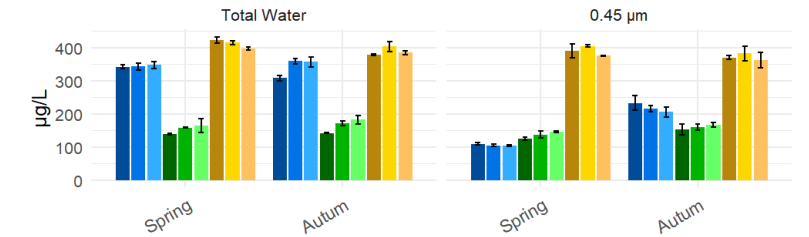
V



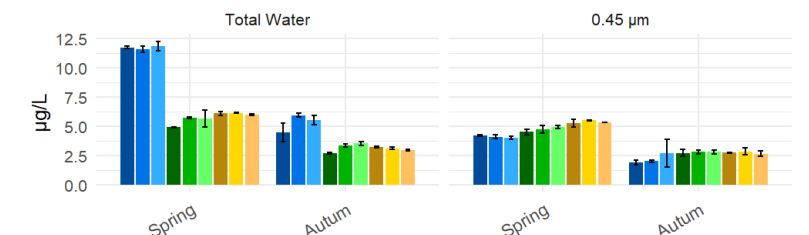
Cr



Mn

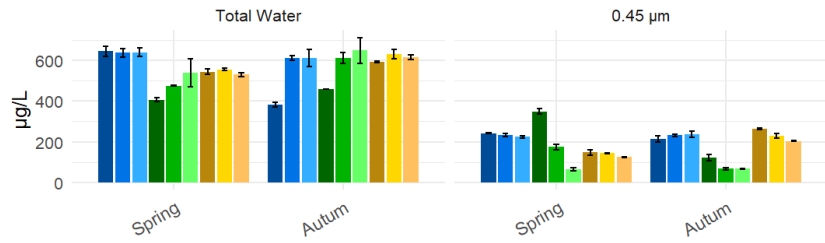


Co

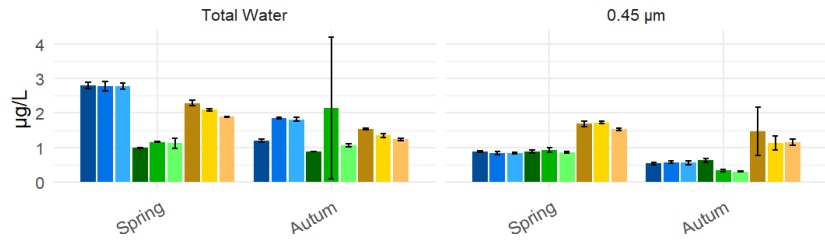


- Untreated - Depth 1
- Untreated - Depth 2
- Untreated - Depth 3
- Treatment 1 - Depth 1
- Treatment 1 - Depth 2
- Treatment 1 - Depth 3
- Treatment 2 - Interval 1
- Treatment 2 - Interval 2
- Treatment 2 - Interval 3

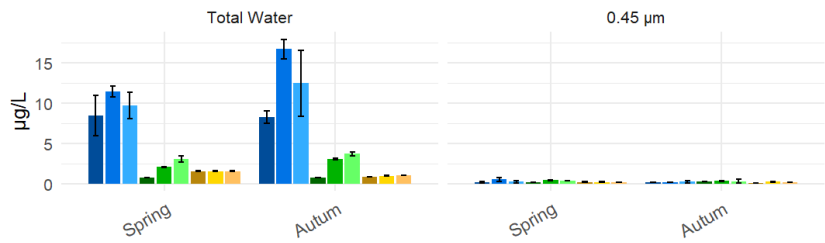
Zn ug/L



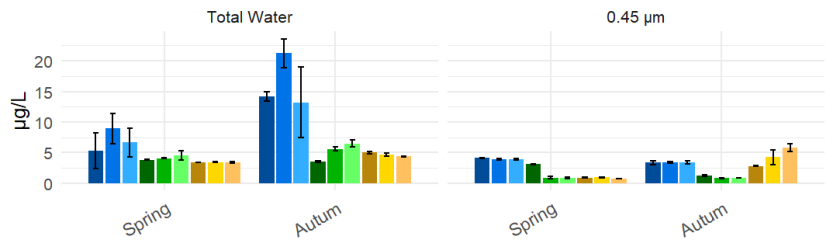
As ug/L



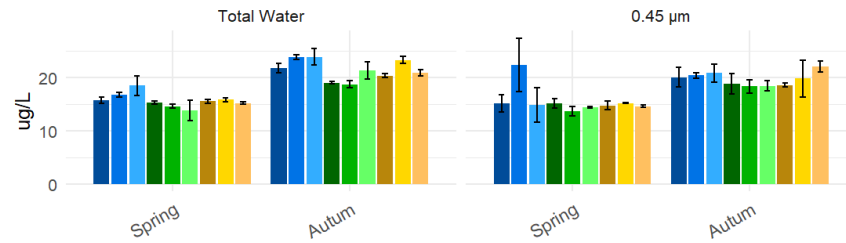
Sn ug/L



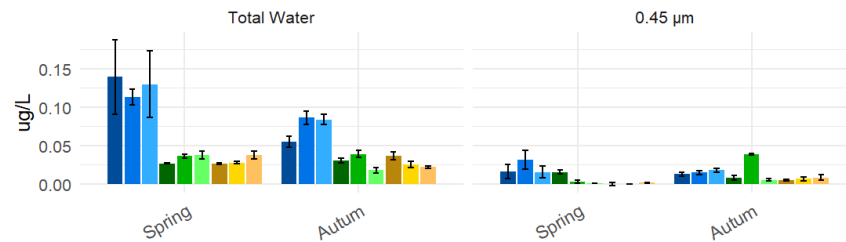
Sb ug/L



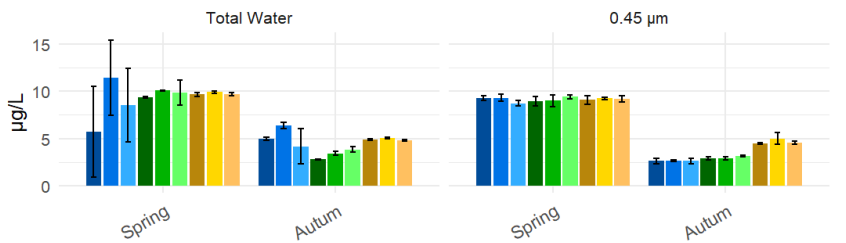
Mo ug/L



Cd ug/L



W ug/L



Pb ug/L

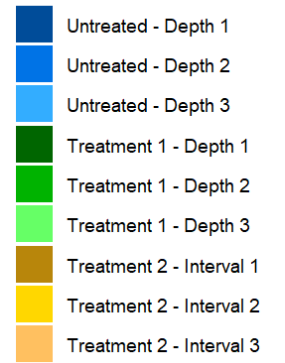
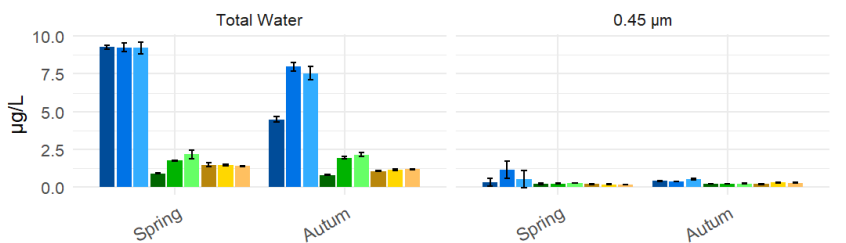


Figure 23: The bar graphs present the mean concentrations from 3 replicates of metals in untreated water at depths 1, 2, and 3, treated water from corresponding depths, and filtered water sampled from the outflow at 10-minute intervals. Additionally, the graphs indicate the sampling season and display concentrations in both total and 0,45 µm filtered water samples in µg/L.

Among the metals studied, Aluminium (Al) and Iron (Fe) stood out due to their high concentrations in untreated tunnel wash water (TWW), with Al at 13.1 mg/L and Fe at 14.1 mg/L. After treatment, both dropped substantially in total water to 0.75 mg/L (Al) and 0.88 mg/L (Fe), and were even lower in 0.45 µm filtered samples, confirming they are primarily particle bound and effectively removed by standard treatment. Similarly, Lead (Pb) peaked at 9.3 µg/L in untreated spring samples and dropped to <2.2 µg/L after treatment, indicating strong particle association and high removal efficiency. In contrast, Zinc (Zn) showed little seasonal variation and limited removal through treatment. In spring, total Zn started at 640 µg/L, dropped to 473 µg/L after Treatment 1, but then increased again to 543 µg/L after Treatment 2. A similar trend was seen in autumn. Although Zn is partly particle-bound, 0.45 µm filtered samples still showed around 200 µg/L in most treatment stages in spring, confirming a substantial dissolved fraction. This indicates that Zn continues to leak from TWW particles, as further demonstrated in the leaching experiment. Copper (Cu) also appeared at relatively high concentrations, peaking at 135.5 µg/L and decreasing to 30–55 µg/L after Treatment 2. Manganese (Mn) reached 423 µg/L in untreated samples and remained above 300 µg/L after treatment, with concentrations up to 400 µg/L after treatment 2, confirming it is mostly dissolved and poorly removed. Tungsten (W) showed higher concentrations in spring than in autumn in both total and 0,45 filtered water, with levels around 9–10 µg/L across all treatment stages, indicating that W is largely present in spring and in dissolved form and not affected by treatment.

Overall, metal concentrations in tunnel wash water from this study exhibited clear seasonal trends, with the highest levels typically observed in spring, following winter conditions. This aligns with findings from several Nordic studies showing that winter traffic significantly elevates metal loads due to increased mechanical wear, use of studded tires, and the accumulation of road-associated pollutants. In this study, metals such as aluminium (Al), iron (Fe), zinc (Zn), copper (Cu), and manganese (Mn) peaked during the first spring wash. These results support previous observations that winter traffic contributes disproportionately to annual metal emissions (Gavrić et al., 2021; Sossalla et al., 2025). A key contributor to this seasonal spike is the use of studded winter tires, which are widely used in Nordic regions.

These tires contain tungsten carbide pins (with cobalt binders), and their abrasion against pavement introduces tungsten (W) and other metals along with minerals into the environment (Furberg et al., 2019). In this study, W concentrations were slightly higher in spring (mean 8.5 µg/L) than in autumn (mean 5.1 µg/L), although the difference was not statistically significant. While W is a recognized tracer of studded tire wear, a variety of factors such as wash timing, tunnel cleaning, or background levels may dampen the expected seasonal contrast. In addition to W, metals like Al and Fe were found at the highest concentrations in our study and are consistent with values reported in Norwegian tunnel studies. In one such study, total Al and total Fe showed the highest mean concentrations (18,349 µg/L and 11,147 µg/L, respectively), followed by Zn (533 µg/L) and Mn (365 µg/L) (Sossalla et al., 2025). The elevated Al levels observed in both this study and (Sossalla et al., 2025) study may also reflect the increasing use of aluminum in newer vehicles, combined with a growing number of newly registered vehicles in the studied areas (Sossalla et al., 2025).

Various vehicle components contribute distinct metal signatures to tunnel wash water, which are clearly reflected in the measured concentrations. For example, brake pads are a well-documented source of copper (Cu), particularly in older formulations (Straffellini et al., 2015). Similarly, tire rubber is a major source of zinc (Zn) due to the use of zinc oxide in tire vulcanization (Alling et al., 2024). In this study, Cu peaked at 135.5 µg/L and Zn reached 640 µg/L in untreated tunnel wash water, highlighting the continued contribution of brake and tire wear particles. The chemical form of metals whether particle bound or dissolved also critically influences their transport, treatment efficiency, and environmental risk. Most metals in this study, such as Al and Fe, were found predominantly in the particle bound phase. This was confirmed by the sharp concentration drops after filtration (0.45 µm). A similar study showed that these metals exist mainly as precipitated hydroxides or bound to suspended solids (Sossalla et al., 2025). Sossalla and co-workers further confirmed that Al and Fe dominated the particulate fraction in tunnel wash water (Sossalla et al., 2025). Copper (Cu) and zinc (Zn) exhibited intermediate behavior while largely particle-bound, a significant dissolved fraction remained even after 0.45 µm filtration. Similarly (Sossalla et al., 2025) found that dissolved Zn and Mn were some of the metals that occurred at the highest concentrations among dissolved metals in TWW, aligning well with the results in this study.

4.3.1 Effect of Treatment 1 and 2

Statistically significant differences between treatments were observed for several metals, including V, Cr, Mn, Ni, Cu, Zn, As, Cd, and Pb ($p < 0.05$). Concentrations of Zn, V, Mn, Ni, and As were significantly higher after Treatment 2, while Cr, Cu, Cd, and Pb were significantly lower after Treatment 2, suggesting selective removal or transformation processes occurring during treatment. In contrast, no significant differences were found for Al, Fe, Co, Mo, Sn, Sb, and W ($p \geq 0.05$), indicating a good treatment effect from treatment 1 for these elements. These comparisons were made across all data irrespective of seasonal variations, slightly aligning with Hypothesis 2 that the two step treatment process will effectively reduce all contaminants such as metals.

Table 14: Removal efficiencies (%) of Metals during Treatment 1 (sedimentation) and Treatment 2 (filtration) across spring and autumn sampling campaigns. Color coding indicates total removal efficiency: red (0–30%), orange (30–60%), yellow (60–85%), and green (85–100%).

Season:	Spring	Spring	Spring	Autumn	Autumn	Autumn	Legend
	Total Treatment	Total Treatment	Efficiency of Treatment 2 after treatment 1	Total Treatment	Total Treatment	Efficiency of Treatment 2 after treatment 1	
Metals	Treatment 1	Treatment 2	Treatment 2	Treatment 1	Treatment 2	Treatment 2	Total Effect%
Al	86.90%	90.21%	25.27%	81.01%	93.87%	67.76%	0-30%
V	84.58%	77.02%	-49.04%	73.34%	60.09%	-49.73%	30-60%
Cr	88.36%	91.40%	26.13%	79.46%	91.54%	58.83%	60-85%
Mn	55.26%	-19.74%	-167.6%	51.52%	-13.78%	-134.7%	85-100%
Fe	86.94%	91.54%	35.27%	80.51%	92.21%	60.05%	
Co	53.64%	48.24%	-11.64%	39.87%	41.76%	3.156%	
Ni	69.24%	60.59%	-28.12%	50.77%	41.38%	-19.07%	
Cu	61.13%	70.86%	25.02%	46.23%	75.62%	54.66%	
Zn	26.05%	15.20%	-14.66%	-7.327%	-14.75%	-6.922%	
As	60.83%	24.77%	-92.07%	15.95%	15.34%	-0.732%	
Mo	14.18%	8.604%	-6.105%	15.05%	7.166%	-9.280%	
Cd	73.51%	75.72%	8.363%	61.05%	62.57%	3.892%	
Sn	80.04%	84.12%	20.45%	79.83%	92.27%	61.71%	
Sb	40.44%	50.71%	17.25%	67.84%	71.09%	10.12%	
W	-14.01%	-13.91%	0.084%	35.17%	4.781%	-46.88%	
Pb	82.91%	84.70%	10.47%	75.77%	83.48%	31.81%	

The final removal efficiencies of metals after Treatment 2 reveal clear differences in treatment performance across elements and seasons shown in *Table 14*. Metals such as chromium (Cr), iron (Fe), and tin (Sn) showed the highest treatment efficiency, with removal rates consistently above 85% in both spring and autumn, indicating their strong particle-bound nature and responsiveness to sedimentation and filtration. This is generally consistent with (Sossalla et al., 2025) findings for Cr (81%), Fe (83%), and Al (81%) with a similar treatment step as treatment 1. While (Sossalla et al., 2025) reported a high 93% removal of particulate Mn, this study showed poor or even negative efficiency for Mn in both seasons, suggesting a dominant dissolved fraction or possible remobilization during treatment. Aluminium (Al), copper (Cu), cadmium (Cd), lead (Pb), and antimony (Sb) also demonstrated high to moderate efficiency (60–85%), suggesting effective removal through the two treatment steps, though with some seasonal variation. In contrast, vanadium (V), nickel (Ni), and cobalt (Co) exhibited only moderate removal, while zinc (Zn), arsenic (As), molybdenum (Mo), and tungsten (W) showed low or even negative treatment effects, particularly in spring. This suggests a substantial dissolved fraction, remobilization or potential leaching from particles during and after the treatment process. Manganese (Mn) and tungsten (W) stood out with inconsistent or negative efficiencies across both seasons in this study. (Sossalla et al., 2025) also reported negative removal in the dissolved phase, particularly for Cd, Fe, Mn, Ni, and Pb.

Zinc (Zn) and arsenic (As) showed no removal in both seasons after treatment 2 in this study, where concentration after $\leq 0.45 \mu\text{m}$ filter show that they occur in still high concentrations in dissolved form. (Sossalla et al., 2025) found Zn removal of 42% in particulates and 46% in dissolved form, while this study recorded even lower total efficiencies and negative values in both seasons after treatment 2, suggesting persistent leaching, possible remobilization or dissolved phase dominance. (Sossalla et al., 2025) further showed that Arsenic had a less treatment effect with 16%. The treatment steps in this study showed limited effectiveness in removing certain dissolved metals. While the sedimentation basin (Treatment 1) more effectively removed larger particles and their associated metals, the Filtralite HMR filter (Treatment 2) had little to no impact on some dissolved metal fractions, particularly for elements such as zinc (Zn), manganese (Mn), arsenic (As), molybdenum (Mo), and tungsten (W).

This limited performance can likely be explained by the fact that the test was conducted on a full-scale pilot system that was still under development, which may have influenced the treatment efficiency. Additionally, the chemical characteristics of tunnel wash water (TWW) and other interfering factors could have contributed to the reduced performance. One plausible explanation is the presence of surfactants (detergents), particularly in autumn, when detergent use was substantially higher. Surfactant molecules are known to form stable metal ligand complexes or micelles that keep metal ions dissolved in solution. For example, anionic surfactants can form micelles that electrostatically bind divalent metal cations such as Zn^{2+} and Mn^{2+} at their surface, keeping these metals in the dissolved phase and thereby limiting their removal by conventional filtration or adsorption media (Peng et al., 2020). In some cases, insoluble surfactant metal complexes can even form at sub micellar concentrations, further preventing adsorption by physical or chemical means (Jiménez-Castañeda & Medina, 2017). Additionally, surfactants themselves can adsorb onto the surface of expanded clay materials like for example Filtralite HMR through ion exchange or hydrophobic interactions, potentially forming a coating that blocks or reduces access to active binding sites (Jiménez-Castañeda & Medina, 2017).

Furthermore, the exceptionally high salinity as evident by the measured conductivity $\sim 3460 \mu\text{S}/\text{cm}$, may have negatively impacted the performance of Filtralite HMR. In a different study, (Kagalkar et al., 2025) demonstrated that increased ionic strength can reduce adsorption efficiency in ZnO-MXene nanocomposites by compressing the electrical double layer and weakening electrostatic interactions between the adsorbent and metal ions. While their findings apply to a different, more advanced system, the same principle could be a potential theory here where high concentrations of background ions such as Na^+ and Ca^{2+} can compete with heavy metals for available adsorption sites on the surface of clay-based media like for example Filtralite HMR. (Acosta et al., 2011) also showed that added salts like NaCl, CaCl_2 effectively mobilize Zn^{2+} and Pb^{2+} by displacing them from sorption sites and by forming soluble chloro-complexes. Further Cl^- can coordinate with metal ions, both of which keep metals in solution rather than fixed to the filter. Together, these salt-mediated processes could have potentially reduce the filter's ability to remove dissolved Zn and Mn under tunnel wash water conditions.

Another theory for the poor removal of arsenic (As), molybdenum (Mo), and tungsten (W) is that Filtralite HMR might not effectively bind oxyanions. In oxygenated, neutral-pH waters, arsenic primarily exists as arsenate (AsO_4^{3-}) which is a stable oxyanion. Effective removal of arsenate typically requires anion exchange resins or iron-based media (Dupont, n.d). Molybdenum commonly occurs as molybdate (MoO_4^{2-}) at most pH values. Adsorption of molybdate is highly pH-dependent and tends to decline with increasing pH (Kurmysheva et al., 2023). Similarly, tungsten exists mainly as tungstate (WO_4^{2-}), and its mobility increases under alkaline conditions due to growing repulsive forces between the negatively charged tungstate ions and similarly negative mineral surfaces (Iwai & Hashimoto, 2017). As a result, tungstate adsorption decreases as pH rises. Research by (Iwai & Hashimoto, 2017) demonstrated that tungstate binds effectively only under acidic conditions, with removal efficiency dropping significantly at neutral to alkaline pH levels. While Filtralite HMR has a high surface area and can adsorb both cations and some anions, its surface chemistry might not be optimized to attract and retain soluble, stable oxyanions like arsenate, molybdate, and tungstate.

However Filtralite HMR normally shows strong metal removal, especially for Zn by cation exchange. For example, in clean stormwater tests Filtralite HMR removed >90% of dissolved Zn (Lundgren, 2021). Also research from NMBU has shown that Filtralite® HMR achieves over 70% removal of key heavy metals, outperforming GAC in retaining nickel and zinc, and effectively adsorbing lead and copper due to its large reactive surface area shown in *Appendix A*. The Filtralite HMR brochure does also not specifically address its capacity to retain fine particles based on size. Instead, it emphasizes the material's high sorption capacity for dissolved metals, suggesting that the product is primarily designed to remove contaminants in dissolved form, rather than to physically filter out very fine or colloidal particles. This interpretation is supported by results from the current study, where tire and road wear particles (TRWP and TWP) were still detected after Treatment 2. These residual particles may act as secondary sources, potentially leaching additional metals and contributing to unexpectedly elevated metal concentrations in the treated effluent.

It is also important to mention that while some metals showed negative removal efficiencies after Treatment 2, this should not automatically be interpreted as poor treatment performance. In many cases, small concentration differences and measurement variability can lead to large percentage changes. Potential contamination during sampling or pretreatment

may also affect accuracy at low concentrations. Despite this, the Filtralite HMR system remains promising due to its high surface reactivity, modular design, and suitability for container based setups. However future studies should investigate how for example surfactants and salt levels in tunnel wash water affect metal speciation and adsorption efficiency on Filtralite HMR.

4.3.3 Threshold limit and EQS

Based on the data presented in *Table 15*, the mean concentrations of most monitored parameters after Treatment 2 such as pH, arsenic (As), lead (Pb), cadmium (Cd), copper (Cu), chromium (Cr), and nickel (Ni) remain within the regulatory threshold limits set by the county governor of Oslo in accordance with the Norwegian Pollution Control Act. This indicates the removal of these substances through the treatment process and compliance with environmental discharge requirements. However, zinc (Zn) levels substantially exceeded the permitted limit of 110 µg/L in both spring (542.7 µg/L) and autumn (612.7 µg/L), suggesting a persistent issue with Zn retention or source control.

Table 15: The table shows the given limit values in the discharge permit for the Ekeberg tunnel within 21 days
The threshold limits are given by the county governor of Oslo to the Norwegian Public Road Administration

Parameters	Threshold value	Mean Concentration after Treatment 2 Spring	Mean Concentration after Treatment 2 Autumn
pH	6-8.5	7.367	7,682
Suspended solids	400 mg/L	*	*
Arsen	6 µg/L	2,091	1,372
Lead	13 µg/L	1,416	1,100
Cadmium	2 µg/L	0,030	0,028
Copper	50 µg/L	39,19	16,72
Chromium	10 µg/L	4,005	2,218
Nickel	40 µg/L	12,08	10,74
Zinc	110 µg/L	542,7	612,7
Oil	5 mg/l	*	*

An assessment of the treated tunnel wash water against Norwegian EQS thresholds (Miljødirektoratet, 2020a) indicates that while several metals meet acceptable environmental standards, others remain concerning. Cadmium concentrations (0.030 µg/L in spring, 0.028 µg/L in autumn) fall at the boundary of Class I–II, reflecting very good to good water quality. However, it is important to note that cadmium threshold values are dependent on water hardness, and exact classification may vary based on local water chemistry. Lead (1.42 µg/L in spring, 1.10 µg/L in autumn) ranges from Class III (moderate) to Class II (good), indicating some seasonal variation. In contrast, arsenic and nickel exceeded Class II thresholds, placing them in Class III (moderate). Notably, copper (39.2 µg/L in spring, 16.7 µg/L in autumn) and zinc (542.7 µg/L and 612.7 µg/L) far exceeded their respective Class V thresholds (5.2 µg/L for copper, 60 µg/L for zinc), indicating very poor water quality. These results suggest that while the treatment system effectively reduces several metal concentrations, zinc and copper remain priority pollutants requiring further mitigation due to their elevated ecotoxicological risk.

4.4 Dissolved Organic Carbon / Anion

Figure 24 presents the measured concentrations of Dissolved Organic Carbon (DOC) across various treatment stages for both spring and autumn tunnel wash water (TWW) samples. In both seasons, DOC levels were highest in the samples that underwent 0.45 µm filtration indicating a high concentration of truly dissolved organic matter. In comparison, the unfiltered samples for both spring and autumn showed lower DOC values. This is likely due to the presence of larger particles in the unfiltered samples, which may have been retained within the sampling apparatus or settled prior to analysis, resulting in an underestimation of total organic carbon. Despite the application of sample dilution to minimize measurement error, the filtered samples provide a more accurate representation of the dissolved organic fraction, as they exclude particulate bound carbon and focus solely on the dissolved phase.

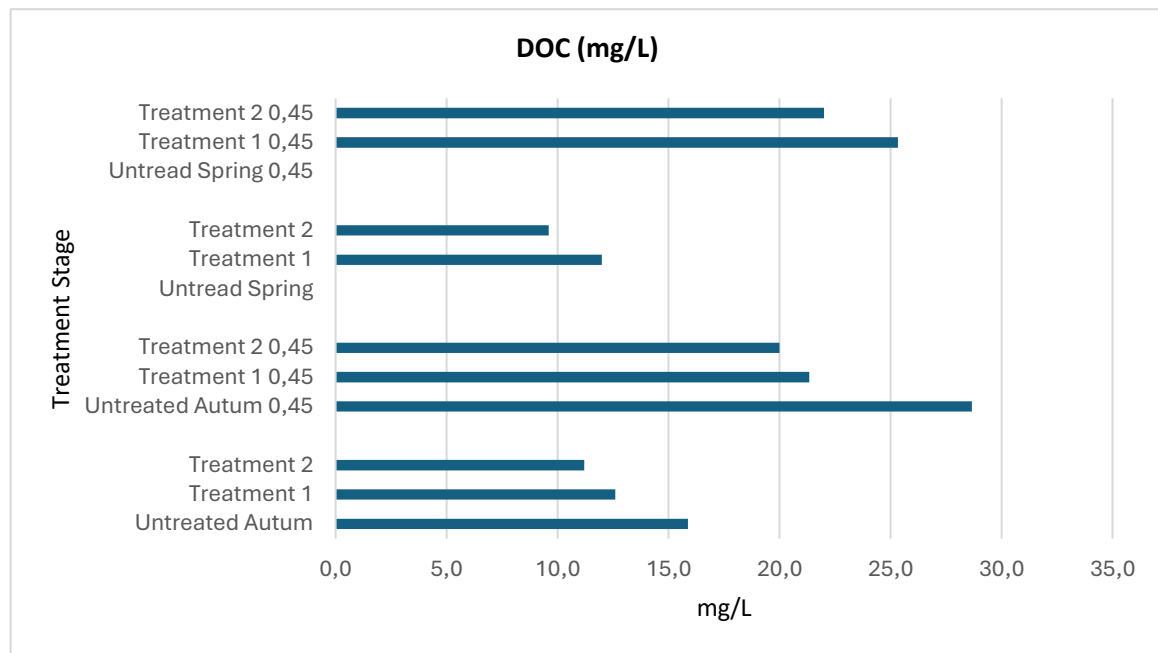


Figure 24: Shows Dissolved Organic Carbon (DOC) concentrations (mg/L) across different treatment stages for spring and autumn samples in TWW. Treatments include untreated, Treatment 1, Treatment 2 samples combined with 0.45 μ m filtration.

Tunnel wash water generally contains high levels of dissolved organic carbon (DOC), often ranging between 10 and 50 mg/L. A survey of 34 Norwegian tunnels reported an average DOC concentration of 49 ± 44 mg/L (Meland & Rødland, 2018), while Swedish studies observed DOC levels ranging from 15 to 47 mg/L (Byman, 2012). In another study, conducted in the Bjørnegård Tunnel in Oslo, Norway, DOC concentrations in untreated tunnel wash water (TWW) were found to be around 26 ± 3 mg/L. The primary source of DOC was identified as the detergent used during tunnel cleaning, which itself had a DOC concentration of 1.7 ± 0.1 g/L. The first treatment step, consisting of 35 days of sedimentation, resulted in a modest reduction of approximately 25%, lowering the DOC to an average of 19 ± 2 mg/L. However, this process achieved less than 60% removal efficiency, indicating limited effectiveness in reducing detergent-related DOC. The second treatment step, using granular activated carbon (GAC), was the only method that significantly further reduced DOC concentrations, achieving a final value of 7.9 ± 2.4 mg/L (Vistnes et al., 2024). Similarly, in the Ekeberg Tunnel, a consistent decrease in DOC concentrations was observed across treatment steps during both spring and autumn sampling campaigns. In the spring, DOC was reduced from 12.0 mg/L in the treatment 1 sample to 9.6 mg/L after Treatment 2. For the filtered samples, DOC dropped from 25.3 mg/L to 22.0 mg/L following the same treatment steps. In the autumn samples,

untreated DOC concentrations were 15.9 mg/L, decreasing to 11.2 mg/L after Treatment 2. For the 0.45 μm filtered autumn samples, DOC was reduced from 28.7 mg/L to 20.0 mg/L through the full treatment train. These results show that both Treatment 1 and Treatment 2 contribute to DOC removal. It is important to note that these ranges are typical estimates, but actual DOC concentrations can vary significantly depending on local conditions such as traffic volume, tunnel design, and pollutant accumulation over time (Sossalla et al., 2025).

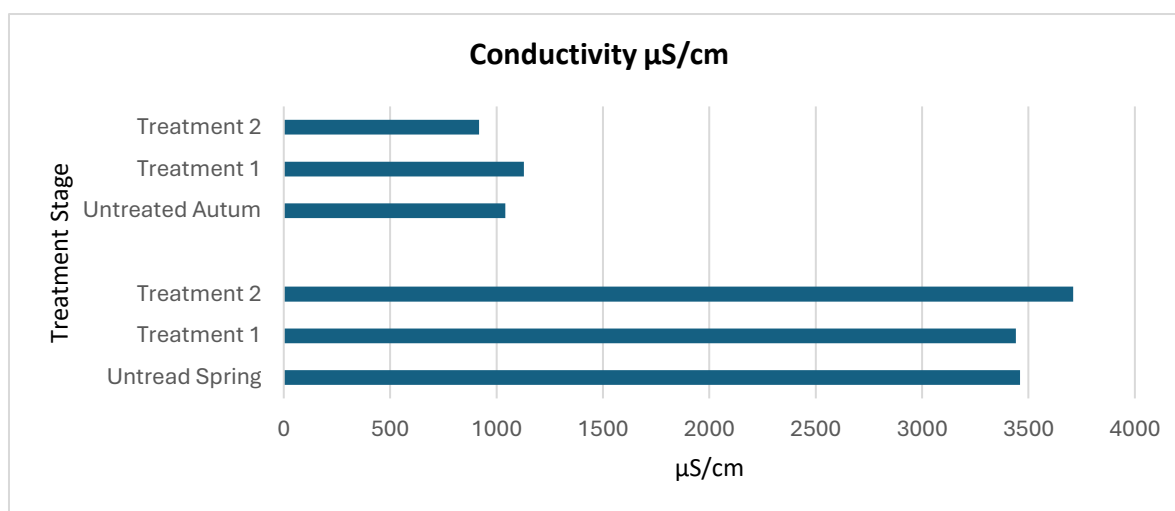


Figure 25: Shows the electrical conductivity ($\mu\text{S/cm}$) measurements across different treatment stages and seasons. Conductivity levels are compared between untreated, Treatment 1 and Treatment 2.

Electrical conductivity measurements revealed distinct differences between seasons from spring and autumn shown in *Figure 25*. In the spring samples, untreated conductivity levels were very high at around 3460 $\mu\text{S/cm}$. Even after Treatment 1 and Treatment 2, conductivity remained high, only slightly increasing to around 3600 $\mu\text{S/cm}$ after Treatment 2. In contrast, autumn samples exhibited lower conductivity values, starting at approximately 1040 $\mu\text{S/cm}$ in untreated conditions. Treatment further reduced conductivity modestly, reaching values below 1000 $\mu\text{S/cm}$ after Treatment 2.

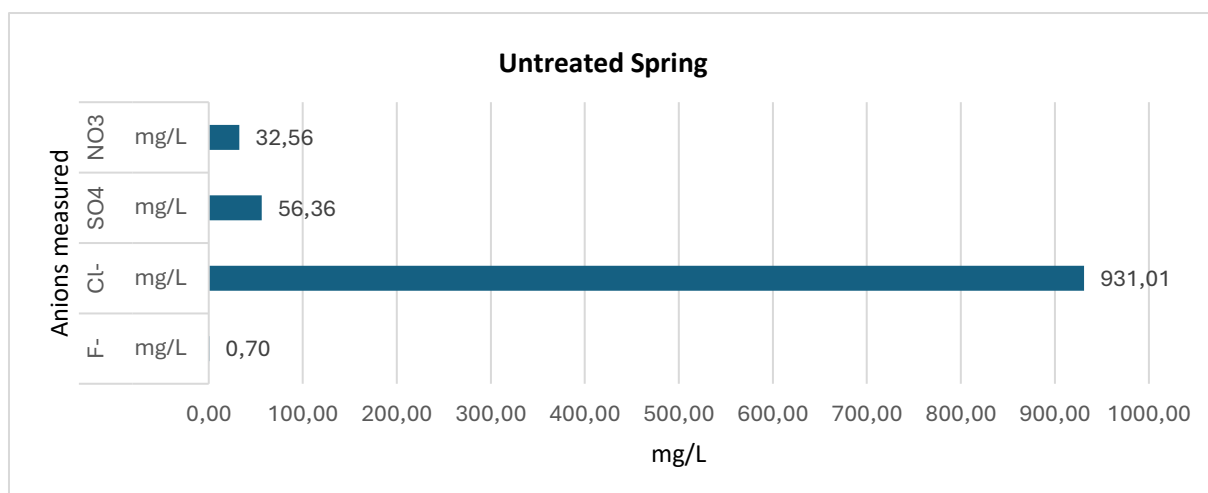


Figure 26: Shows concentrations of selected anions (NO_3^- , SO_4^{2-} , Cl^- , F^-) measured in untreated spring water.

In the untreated spring water, chloride (Cl^-) was by far the dominant anion, measured at a concentration of 931.01 mg/L Figure 26. This concentration was substantially higher than that of sulfate (SO_4^{2-}) at 56.36 mg/L, nitrate (NO_3^-) at 32.56 mg/L, and fluoride (F^-) at 0.70 mg/L. The exceptionally high chloride concentration strongly suggests contamination from an external source, most likely road de-icing salts. This interpretation is further supported by the very high electrical conductivity observed in the untreated spring samples, which ranged from approximately 3400 $\mu\text{S}/\text{cm}$ to 3600 $\mu\text{S}/\text{cm}$ after treatment. Conductivity increases proportionally with ionic content, particularly with dominant ions like chloride, confirming the correlation between road salt contamination and high elevated conductivity (Vistnes et al., 2024). High conductivity values are often directly associated with elevated concentrations of road salt constituents. For example, a study reported particularly high conductivity and chloride concentrations during a wash conducted in March, corresponding with peak road salting activity (Vistnes et al., 2024). In contrast, autumn samples from Ekeberg exhibited much lower conductivity values, starting at approximately 1200 $\mu\text{S}/\text{cm}$ under untreated conditions, indicating the absence of road salting during summer periods.

The conductivity values observed in the untreated spring samples in this study are also comparable to previous findings by (Meland & Rødland, 2018) who reported mean EC levels of $2453 \pm 2474 \mu\text{S}/\text{cm}$ in tunnel wash water (TWW). On average, TWW conductivity has been reported at $1150 \pm 230 \mu\text{S}/\text{cm}$, which is approximately 50 times higher than that of tap water (40 $\mu\text{S}/\text{cm}$)(Vistnes et al., 2024). Notably, electrical conductivity did not change much during

either Treatment 1 or Treatment 2. This outcome was expected for Treatment 1 which is primarily designed to remove suspended solids and particle-bound ions, not dissolved salts. In Treatment 2, which involved filtration using Filtralite HMR, a similar pattern was observed. Filtralite HMR is specifically developed to remove heavy metals such as copper, zinc, nickel, and lead via adsorption and ion exchange, but it does not target chloride ions specifically. Since conductivity is largely governed by dissolved ions like chloride, only minor changes were observed after filtration. A similar trend was observed in another study, where conductivity remained largely unchanged across both primary and secondary treatment processes, including sedimentation, bag filtration, ceramic microfiltration, and GAC (Vistnes et al., 2024). These findings highlight a serious environmental concern. The continuous release of high salt concentrations into the environment alters the natural chemical properties of soil, water, and sediments, leading to ecological risks (Szklairek et al., 2022). In particular, when untreated TWW is discharged directly into freshwater systems, the accumulation of chloride can severely impact aquatic ecosystems, influencing species composition, increasing water density, and reducing oxygen solubility (Mansberger, 2023; Vistnes et al., 2024).

4.5 Toxicity Assessment

To evaluate the potential acute toxicity of tunnel wash water a series of immobilization tests were carried out using *Daphnia magna*. A maximum concentration of 50% TWW was selected to prevent lethal conditions like high pollutant load, low pH, elevated salinity from causing nonspecific stress or immediate mortality as perviously described. Dilution with either EPA or M7 exposure media helped maintain water chemistry parameters such as pH, hardness, and dissolved oxygen within the optimal ranges for *Daphnia*, consistent with OECD Test Guideline 202 (OECD, 2004). Additionally, a separate detergent toxicity test was conducted to determine whether the cleaning agent used in tunnel maintenance could itself be a contributing factor to any observed toxicity. This control ensured that any immobilization observed in subsequent TWW exposures could be distinguished from effects caused solely by the detergent. *Table 16* below summarizes the test setups, immobilization observed at 24 and 48 hours, and qualitative observations of *Daphnia magna* responses.

Table 16: Overview of the toxicity test results including titles of experiment, exposure media, test substance, immobilization % after 24 h and 48 h and the effect on *Daphnia magna*.

Title of Experiment	Exposure media	Test substance	Immobilization % after 24 h	Immobilization % after 48	Impact on <i>Daphnia magna</i>
TWW Detergent experiment	M7 water	Diluted detergent	C0=0% C1=0% C2=0% C3=5% C4=40% C5=75%	C0=0% C1=0% C2=0% C3=5% C4=50% C5=90%	Lethality
Inflow Spring	M7 water	Tunnel wash water	No immobilization	No immobilization	High particle ingestion
Sedimentation Spring	M7 water	Tunnel wash water	No immobilization	No immobilization	Moderate particle ingestion
Filter Spring	M7 water	Tunnel wash water	No immobilization	No immobilization	Low particle ingestion
Inflow Autumn	M7 water	Tunnel wash water	C0=0% C1=0% C2=0% C3=0% C4=0% C5=35%	C0=0% C1=0% C2=0% C3=0% C4=0% C5=45%	C5 Lethality Particles adsorbed to antenna and body. Little ingestion of particles on those affected.
Sedimentation Autumn	M7 water	Tunnel wash water	No immobilization	No immobilization	Moderate particle ingestion
Filter Autumn	M7 water	Tunnel wash water	No immobilization	No immobilization	Low particle ingestion
Leachate Exposure	M7 water	Leachate from TWW particles	No immobilization	No immobilization	No effect
Inflow Spring	EPA water	Tunnel wash water	No immobilization	No immobilization	High particle ingestion
Sedimentation Spring	EPA water	Tunnel wash water	No immobilization	No immobilization	Moderate particle ingestion
Filter Spring	EPA water	Tunnel wash water	No immobilization	No immobilization	Low particle ingestion
Inflow Autumn	EPA water	Tunnel wash water	No immobilization	No immobilization	Particles adsorbed to antenna and body. Little ingestion of particles on those affected.

4.5.1 Detergent Toxicity Pre-Test

A concentration-response analysis was conducted to evaluate the toxicity of diluted Mac 213 Bio on *Daphnia magna*. Additional details are provided in *Appendix K*. The exposure was carried out over 48 hours using M7 water as the exposure medium. The concentration-response curve in *Figure 27* shows a steep decline in survival probability with increasing detergent concentration, indicating onset of acute toxicity.

The toxicity results from the immobilization tests in *Table 16* confirm the modeled outcomes, with no immobilization observed in the control and low-concentration treatments (C0–C3), while moderate to complete immobilization occurred at higher concentrations (C4–C5). Notably, 10 out of 20 *Daphnia* were immobilized at C4 after 48 hours, which aligns closely with the modeled LC₅₀ of 1.63×10^{-5} (95% credible interval: 1.33×10^{-5} to 2.05×10^{-5}). This corresponds to a dilution of approximately 1:60,000, or 0.00167% v/v Mac 213 Bio in the exposure medium. This means that for every 60,000 parts of the solution, 1 part is detergent. For comparison, tunnel wash operations resulted in estimated final dilutions of 1:340,000 in spring (0.00029% v/v) and 1:66,000 in autumn (0.00152% v/v), based on reported water and detergent volumes, further matching the concentration of the C4 treatment and supporting the validity of the modelled toxicity thresholds.

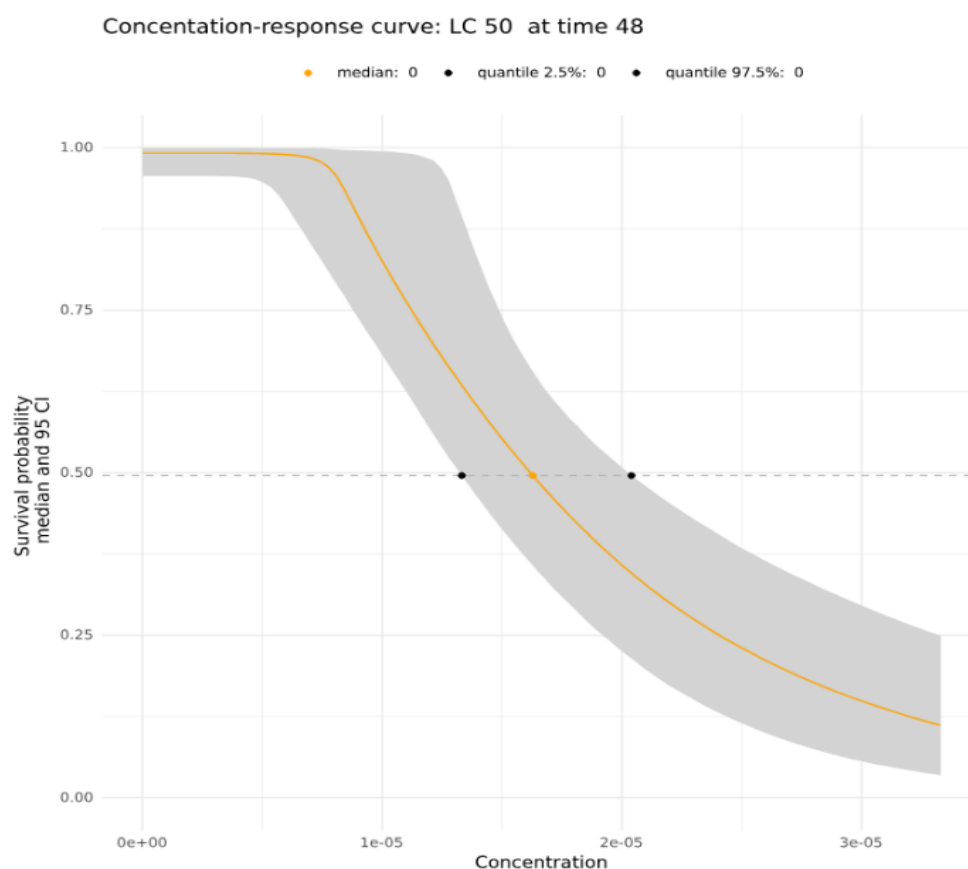


Figure 27: Concentration-response curve showing survival probability of *Daphnia* exposed to TWW detergent at 48 hours. LC₅₀ is indicated by the dotted line. The x-axis represents the dilution concentration, and the y-axis shows survival probability. The orange line is the median estimate, with the grey area indicating the 95% confidence interval.

Conversely, the most concentrated treatment, 1:30,000, is above the estimated LC_{50} and resulted in 18 out of 20 *Daphnia* being immobilized, further confirming the steep dose-response relationship observed in the model. Physicochemical conditions during the test remained stable across all treatments, with conductivity ranging from 641 to 710 $\mu S/cm$, pH between 8.67 and 8.80, temperature near 20–21.5 °C, and dissolved oxygen between 7.95 and 8.42 mg/L. These values confirm that the observed effects were not due to water quality fluctuations. Detailed parameter values can be found in *Appendix J*. For the experimental setup, dilution calculations were based on spring wash data, where 255 m³ of water and 75 L of detergent were used. According to the contractor, the detergent was initially pre-diluted at a 1:10 ratio before being loaded into the washing truck. It was first assumed that this pre-diluted mixture was applied directly in the tunnel, resulting in an estimated final dilution ratio of 1:34,000. However, later clarification revealed that the pre-diluted detergent was further diluted by an additional factor of 1:10 during tunnel application. This means the actual final dilution was closer to 1:340,000 substantially lower than originally estimated.

It is also important to note the seasonal variation in detergent usage during tunnel washing operations. In spring, a total of 511 m³ of water and 150 L of detergent were used across both tunnel lanes, resulting in a base dilution of approximately 1:3,400. In autumn, 427 m³ of water and 650 L of detergent were used, yielding a much lower base dilution of about 1:660. Applying the same pre-dilution (1:10) and in-tunnel dilution (1:10) factors, the final estimated dilution ratios become approximately 1:340,000 in spring and 1:66,000 in autumn. This suggests that autumn wash water likely contained substantially higher concentrations of detergent, which could have greater environmental implications.

Although the estimated detergent dilution in the autumn tunnel wash water was approximately 1:66,000, close to the modeled LC_{50} concentration of 1:60,000 determined in the spring toxicity test. The non-lethal detergent concentration in autumn may be ascribed to several important other factors. Firstly, the spring test was conducted using only detergent diluted in M7 medium, a clean and controlled environment that may not reflect the complex interactive effects of real tunnel wash water. In contrast, the autumn test used actual tunnel wash water, which contains a variety of suspended solids, dissolved ions, metals, TRWP, road dust, and other organic/inorganic components that may influence the toxicity profile.

Secondly, pH differences might have played a role. In the M7 media used for the detergent test, the pH was around 8.6–8.8, while the pH in the TWW from autumn remained closer to neutral to around pH 7.2–7.6. Thirdly, no lethal effects on *Daphnia magna* were observed in the spring samples of untreated TWW, Treatment 1, or Treatment 2. Similarly, in the autumn samples, no lethality was observed in Treatment 1, Treatment 2, or in the lower concentrations (C1–C4) of untreated TWW. This confirms the non-lethality of the detergent at low concentrations, further supporting Hypothesis 3. While C5 showed lethality in untreated TWW during autumn due to particle adhesion, this effect was not due to toxicity, as clarified in the following results. These results highlight that detergent residues present in both spring and autumn TWW were not toxic to *Daphnia magna* at the tested conditions. This could indicate that the detergent had already begun to break down or that its concentrations were significantly more diluted than initially estimated. Nonetheless, visible detergent residues were observed in samples collected after Treatment 2 during both spring and autumn. These residues likely persisted due to reduced sunlight and lower microbial activity in the tunnel environment. This observation suggests that, even in the absence of acute toxicity, residual detergents may still be released into the Oslofjord, raising concerns about their potential environmental impact.

4.5.2 Toxicity of Untreated TWW - Spring

Exposure of *Daphnia magna* to untreated tunnel wash water from the spring season resulted in a clear, concentration dependent ingestion of suspended particles, as revealed by the microscopy pictures. *Figure 28* presents representative individuals that were alive from each exposure group: control (C0) and five increasing concentrations of TWWC1 (3.125%), C2 (6.25%), C3 (12.5%), C4 (25%), and C5 (50%) after 48 hours of exposure. All individuals survived the immobilization test and were alive and exhibited normal mobility at the time of imaging. In the control group (C0), no visible particles were observed in the digestive tract, confirming the absence of background particulate ingestion from the exposure medium.



Figure 28: *Daphnia magna* exposed to untreated TWW from spring , tested in EPA exposure media. The images show representative individual ingested particles visible in the intestine at all concentration (C1)-(C5), while (C0) have algae food and no particles from control (C0). Images are captured using darkfield (left) and brightfield (right) microscopy. All individuals are alive at the time of imaging. Images by Ole Holthusen. Scale bars: 500 µm.

Starting at the lowest exposure concentration (C1), particles became visible in the gut, as shown in Figure 29, although at relatively low density. The dark coloration and compact form of these ingested particles suggest that they may be road associated particles and potentially TRWP. Their presence at this low exposure level indicates that *D. magna* efficiently filter and ingest suspended contaminants from the surrounding water. Particle accumulation increased progressively with concentration C2 and C3 exhibited moderate ingestion, while C4 and particularly C5 (the highest concentration) showed extensive gut filling with dark, dense material consistent with particulate matter. Under brightfield illumination, these particles were clearly distinguishable and appeared to occupy much of the digestive tract in C5 individuals. The observed gradient in particle ingestion across treatments provides visual evidence of dose dependent uptake. The internal accumulation seen in C5 suggests a high burden of ingested particles, likely including rubber and road-associated debris present in the TWW. Despite this, no mortality or immobilization was recorded in any of the 4 replicates after 48 hours.

The visible ingestion, however, implies that sublethal or physiological effects may be occurring and warrants further investigation through biochemical or chronic exposure and chemical analysis to assess the extent of systemic uptake of contaminants.

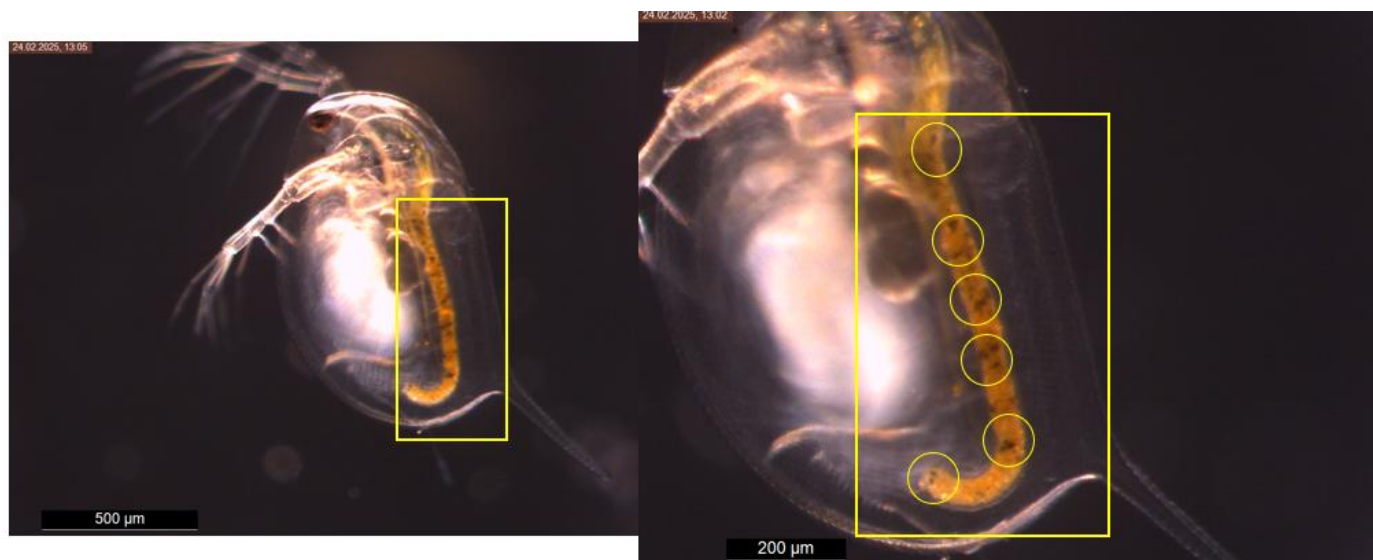


Figure 29: The images show a single *Daphnia* under darkfield microscopy, with a section highlighting the digestive tract. Several black particles are clearly visible and have been marked with yellow circles, indicating ingestion of particulate matter even at the lowest exposure level C1. Images by Ole Holthusen. Scale bars: 500 μm (left), 200 μm (right).

4.5.3 Toxicity of Treated TWW - Spring

Treatment 1

Exposure of *Daphnia magna* to TWW from the spring season (Treatment 1) also resulted in a concentration dependent ingestion of suspended particles, though to a lesser extent than the untreated TWW observed. *Figure 30* presents individuals from the control group (C0) through increasing TWW concentrations (C1–C5) after 48 hours of exposure. All daphnids survived and exhibited normal mobility. No visible particles were observed in the control group except algae, while low amounts of ingested particles were seen at C1. A gradual increase in gut particle content was noted in C2 and C3, with more pronounced but still moderate accumulation observed in C4 and C5, where *Figure 31* depicts a closer look at the ingestion at the highest concentration (C5).



Figure 30: *Daphnia magna* exposed to Treatment 1 TWW from spring with M7 media. The images show individual *Daphnids* from control (C0) to increasing exposure concentrations (C1–C5), captured using darkfield (left) and brightfield (right) microscopy. All individuals were alive at the time of imaging. Images by Ole Holthusen. Scale bars: 500 µm.

This trend indicates dose dependent uptake, although overall particle ingestion appeared slightly reduced compared to earlier exposures with untreated TWW from the same season. The results indicate that Treatment 1 effectively promotes particle sedimentation, as evidenced by the slightly reduced ingestion of particles by *Daphnia magna*.



Figure 31: *Daphnia magna* exposed to the highest concentration of tunnel wash water from spring with M7 media in Treatment 1. A dense accumulation of ingested particles is visible along the entire digestive tract, marked by a yellow box, indicating particle uptake at this exposure level after treatment 1. The individual was alive at the time of imaging. Images by Ole Holthusen. Scale bars: 500 μm .

Treatment 2

Exposure of *Daphnia magna* to tunnel wash water (TWW) from the spring season (Treatment 2) resulted in a concentration-dependent ingestion of suspended particles, though particle accumulation was notably lower than in both the untreated TWW and Treatment 1. *Figure 32* presents individuals from the control group (C0) through increasing concentrations (C1–C5) after 48 hours of exposure. All daphnids survived and displayed normal mobility. No visible particles were observed in the control group, and only algal residues were present in the gut at C1. Comparing C1 in *Figure 33* to *Figure 29* in untreated TWW from spring show clear differences, especially regarding the smaller black particles that were ingested in the untreated TWW. Up to concentration C3, the gut content primarily consisted of algal material, with limited evidence of non-algal particles.



Figure 32: *Daphnia magna* exposed to Treatment 2 tunnel wash water (TWW) from spring with M7 media. The images show individual *Daphnia* from control (C0) to increasing exposure concentrations (C1–C5), captured using darkfield (left) and brightfield (right) microscopy. All individuals were alive at the time of imaging. Images by Ole Holthusen. Scale bars: 500 μm .

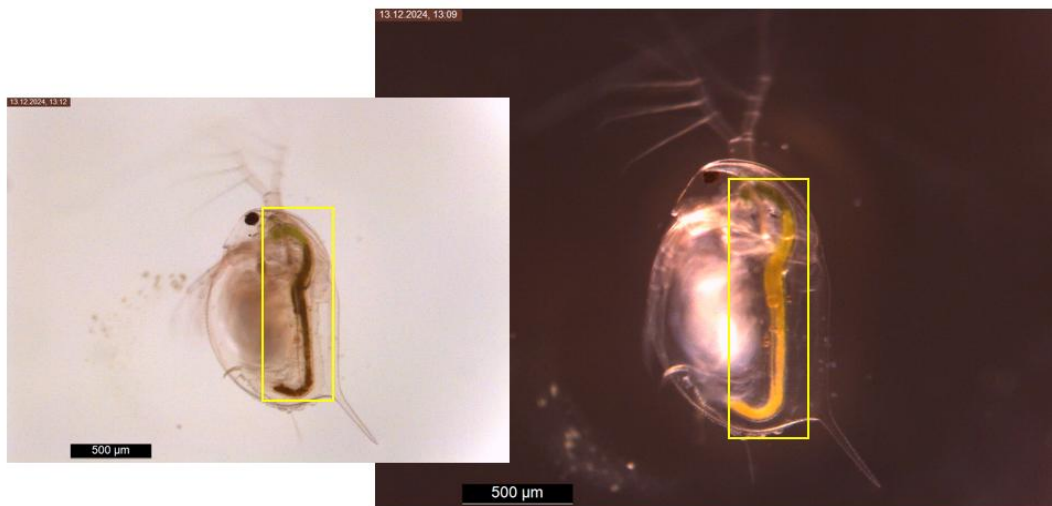


Figure 33: *Daphnia magna* exposed to the lowest concentration (C1) after Treatment 2 with no particle ingestion, from spring with M7 media. The images show one individual imaged under brightfield (left) and darkfield (right) microscopy. The individual was alive at the time of imaging. Images by Ole Holthusen. Scale bars: 500 µm.

A slight increase in non-algal particle ingestion became noticeable at C4 and C5, although the overall particle load remained low. Compared to earlier treatments, the reduced gut accumulation in C5 shown in Figure 34, further suggests that Treatment 2 further improved particle removal. To highlight the overall difference from untreated TWW to Treatment 2, Figure 35 from untreated TWW spring is shown under the *Daphnia magna* exposed to concentration (C5) after Treatment 2.



Figure 34: *Daphnia magna* exposed to the highest concentration (C5) after Treatment 2 with visible particle ingestion, from spring with M7 media. The individual was alive at the time of imaging. Images by Ole Holthusen. Scale bars: 500 µm.



Figure 35: *Daphnia magna* exposed to the highest concentration (C5) after untreated TWW, from spring tested with EPA medium. The images show a single *Daphnia* viewed under brightfield (left) and darkfield (right) microscopy. A high level of particle ingestion is observed in the digestive tract (highlighted in yellow compared to the highest concentration). The individual was alive at the time of imaging. Images by Ole Holthusen. Scale bars: 500 µm.

All 48-hour exposure experiments showed that *Daphnia magna* readily ingested particles from untreated tunnel wash water, as well as from samples at different treatment stages, across both seasons. Visible gut accumulation increased with particle concentration. This is for example consistent with prior findings that *D. magna* ingests tire wear particles, and that uptake increases with concentration (Schell et al., 2022). Likewise, (Rist et al., 2017) found that both micro (2 µm) and nano-sized (100 nm) plastic particles were readily ingested by *Daphnia magna*, with the larger particles resulting in five times higher ingested mass. Although complete egestion was not observed within 24 hours, more of the 2 µm particles were expelled compared to the nanosized ones. Notably, feeding rates decreased by 21% in the presence of 100 nm particles, suggesting a greater physiological impact (Rist et al., 2017). For the spring TWW, no immobilization or lethality was observed even at the highest concentration (50% TWW), suggesting that acute toxicity thresholds were not reached. This aligns with findings from (Schell et al., 2022) who reported “no significant effects on mobility, survival, or reproductive output” in *Daphnia magna* following both acute and chronic exposure to car tire particles. However, polyester fibers had a more pronounced effect, impairing reproduction and survival due to entanglement and restricted mobility during chronic exposure, with a reported no-observed-effect concentration (NOEC) of 0.15 mg/L.

Car tire particles also impacted reproduction (NOEC: 1.5 mg/L) and survival (NOEC: 0.15 mg/L) after long-term exposure (Schell et al., 2022). In contrast, (Liu et al., 2023) reported a 48-hour LC₅₀ of approximately 57 mg/L for tire wear particles (TWP) in *D. magna*, indicating that considerably higher concentrations are necessary to induce acute lethality. Although survival was unaffected in the spring TWW experiments, ingestion of particles can induce subtle physiological stress. (Liu et al., 2023) showed that physical damage to the gut was identified as a potential mechanism of particle-induced toxicity, while compounds leached from TWP were responsible for the acute toxicity of the leachate. The observed visible gut lesions in *D. magna* exposed to TWP, suggesting injury to digestive tissue (Liu et al., 2023). Even if not lethal, these impairments could reduce feeding efficiency and energy acquisition.

In this study, decreased motility or feeding was not quantified during the 48-hour acute immobilization experiments with TWW, but the visible presence of particles in the gut suggests a potential burden and obstruction. The visible accumulation of particles in the gut suggest a risk of obstruction, which may in turn impair nutrient uptake or clearance if sustained over time (Liu et al., 2023). The study further reported that particles generally exhibited greater toxicity than their leachate, and exposure resulted in significant inhibition of swimming speed, acceleration, filtration, and ingestion rates, along with reduced thoracic limb activity (Liu et al., 2023). Additionally, heart rate increased significantly in daphnids exposed to 200 mg/L of particles, indicating both physical and physiological stress responses (Liu et al., 2023). At the biochemical level, TWP and similar particles can trigger stress responses. (Liu et al., 2023) observed reduced superoxide dismutase (SOD) activity and total antioxidant capacity in *D. magna*, along with elevated acetylcholinesterase (AChE) activity, indicating oxidative stress and neurotoxic effects (Liu et al., 2023).

While the 48-hour trial cannot capture long term effects. However, prolonged or repeated exposure to particles may result in bioaccumulation and delayed adverse. (Schell et al., 2022) found that after 21 days of continuous exposure to tire particles, *D. magna* guts contained 20–60 times more particles than after 48 hours. (Trotter et al., 2021) also reported significant reductions in body length and offspring number following chronic exposure to polystyrene microplastics. Analysis of protein activity further showed that several digestive enzymes were significantly reduced in *Daphnia magna* exposed to polystyrene (PS) microplastics. This likely impaired their ability to absorb nutrients, which may explain the changes observed in their

body shape and life cycle (Trotter et al., 2021). These findings suggest that even in the absence of acute lethality, long-term exposure to road associated microplastics commonly found in the environment could negatively impact the overall health and fitness of *Daphnia*. This may, in turn, affect the broader food web, as many organisms rely on *Daphnia* as a key food source

4.5.4 Toxicity of Untreated TWW - Autumn

Another concentration response analysis was conducted to evaluate the acute toxicity of untreated tunnel wash water from autumn on *Daphnia magna*. Additional details are provided in *Appendix K*. The exposure was carried out over 48 hours using M7 media as exposure media. As outlined in *Figure 36*, the test followed a five-step dilution series, with C5 (50% TWW) as the highest concentration and each subsequent treatment diluted by a factor of two down to C1 (3.125%).

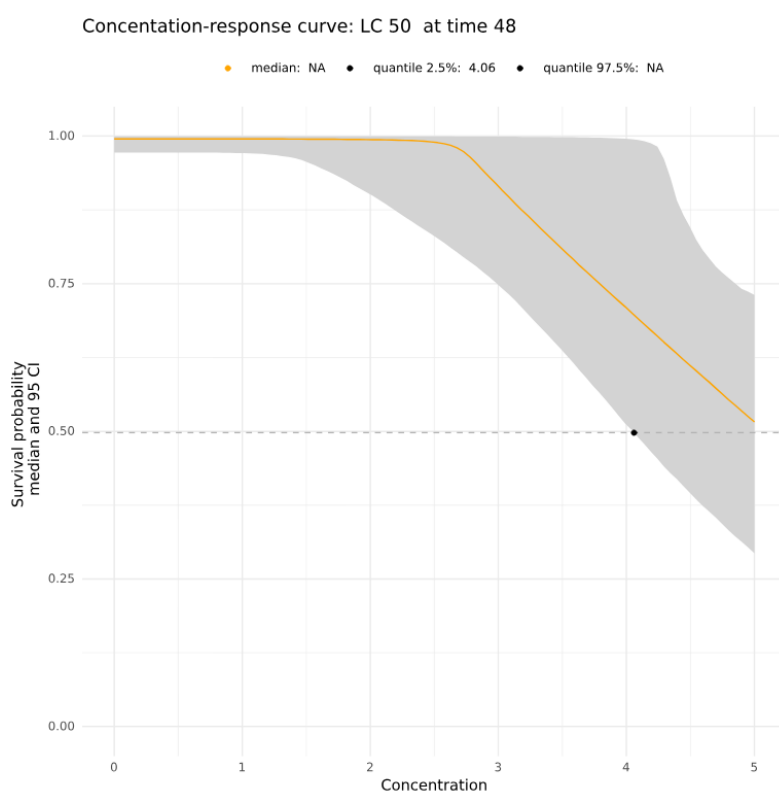


Figure 36: Concentration response curve showing estimated LC_{50} at 48 hours.

The plot illustrates the survival probability of the test organisms as a function of concentration, with the orange line representing the modelled median response and the grey area indicating the 95% confidence interval. The dashed horizontal line marks the 50% survival probability threshold. The steepness of the curve and the width of the confidence band reflect uncertainty in the estimated response at higher concentrations.

The estimated LC_{10} was 3.10 mg/L [2.05–4.42 mg/L], and LC_{20} was 3.57 mg/L [2.73–4.66 mg/L]. These values fall between concentrations represented by C4 (25% TWW) and C5 (50% TWW), placing C5 above the estimated thresholds for observable toxicity. Consistently, acute immobilization was only observed at C5, where 9 out of 20 *Daphnia* were affected, while no immobilization occurred at lower concentrations (C0–C4). Due to uncertainty in the upper range of the data, the LC_{50} median and upper credible interval could not be determined, and only the lower bound (4.06 mg/L) is shown on the curve. Physicochemical conditions during the test remained stable across all treatments. Conductivity ranged from 650 to 769 $\mu\text{S}/\text{cm}$, dissolved oxygen levels were between 8.40 and 8.68 mg/L, temperature remained consistent at approximately 21.0–21.3 °C, and pH values ranged from 7.27 to 7.74. These stable conditions indicate that observed effects were not the result of fluctuations in water quality. Detailed parameter values are presented in *Appendix J*. Furthermore, visual assessment suggests that the observed immobilization at C5 was not primarily due to chemical toxicity, but rather to physical interference caused by particle adhesion. As shown in *Figure 37*, microscopy revealed small black particles, adhered to the antennae and body surfaces of *Daphnia magna*. At the 24-hour observation point, the particles appeared to adsorb primarily to the antennae of the *Daphnia*, suggesting these structures may be particularly prone to initial particle attachment, possibly due to their movement or surface properties. By 48 hours, particle accumulation had visibly increased, with aggregates clustering not only around the antennae but also across larger areas of the body surface on nearly all individuals in the C5 concentration.

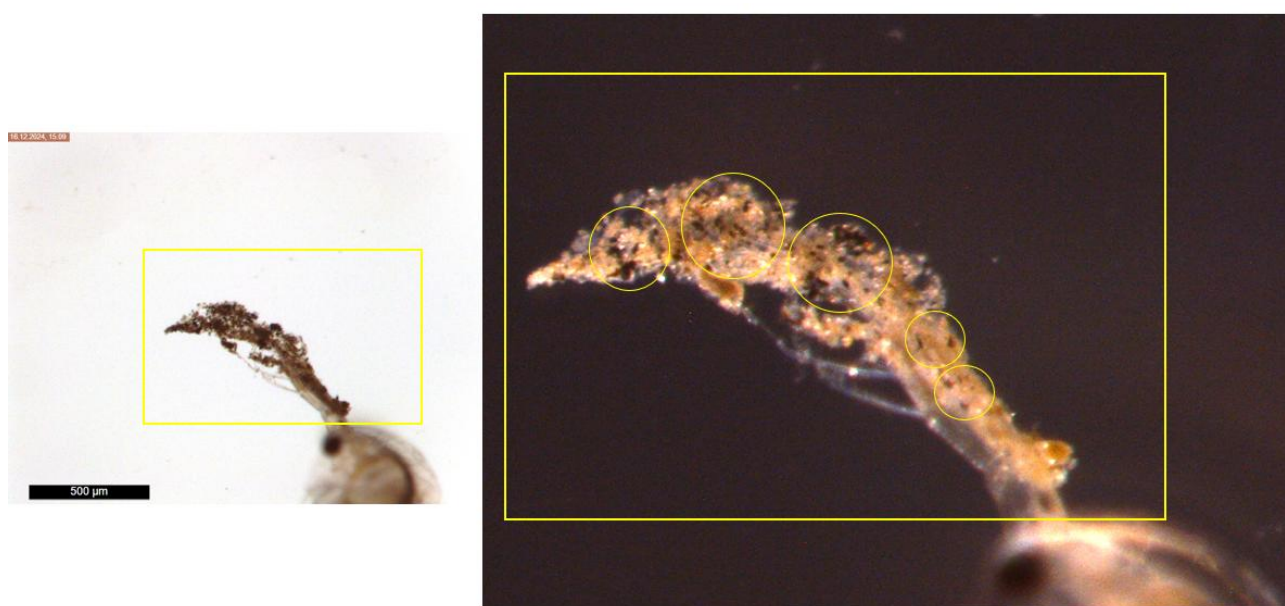


Figure 37: Adsorbed particles from untreated TWW (Autumn, M7 media) on the swimming antenna of a live *D. magna*. The two photos were taken in brightfield and darkfield mode of the same individual by Ole Holthusen. Scale bars: 500 μm .

Figure 37 illustrates this phenomenon, where the left panel shows an alive *Daphnia* specimen under low magnification with a dense aggregation of particulate matter on its antenna. The right panel provides a close-up view of the same *Daphnia*, with several distinct clusters of particles circled, highlighting how these materials densely cover sensory and anatomical structures. Such adhesion likely impairs swimming and feeding behavior by mechanically obstructing the movement of the antennae and filtering appendages leading to reduced mobility and feeding efficiency. Since the acute immobilization test is designed to detect chemical toxicity within a 48-hour window, these findings suggest that the observed immobilization at C5 may not accurately reflect toxicological effects. Rather, the mechanical stress imposed by particle coverage may be the primary cause of impaired movement. Moreover, this kind of physical interference would be expected to worsen with longer exposure durations, beyond the standard test timeframe. As a result, interpreting these effects as acute toxicity would be misleading and may overestimate the actual chemical hazard of the tunnel wash water. However, we know that these particles can leach toxic chemicals, which may further contribute to acute toxicity in *Daphnia*.

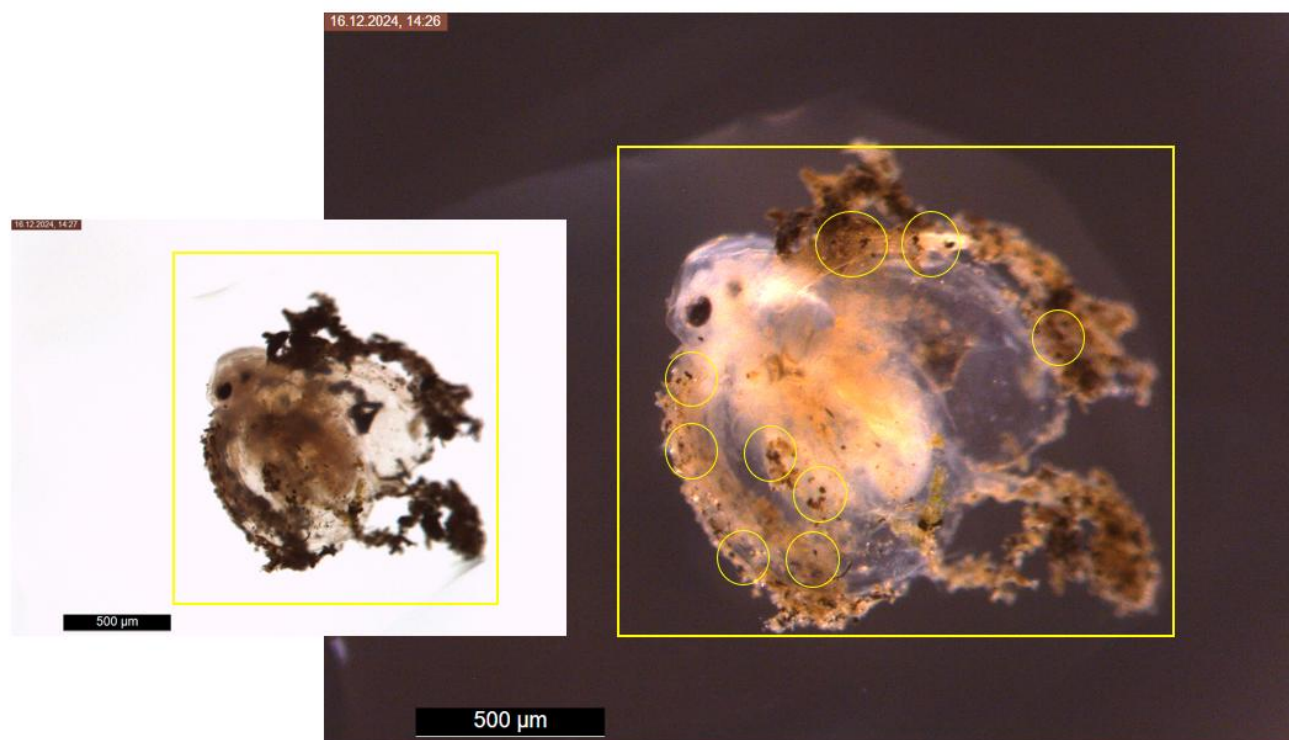


Figure 38: Shows the adsorbed black particles and potential biofilm or decaying organic matter from untreated TWW Autum with the M7 media on the dead *Daphnid* body, where the *Daphnid* has started to disintegrate. The two photos are taken in a brightfield and darkfield mode after 48 h on the same *Daphnid* by Ole Holthusen. Scale bars: 500 µm.

In addition these particles that were adsorbed to the anatomical structure visually, could potentially resemble tire and road wear particles in *Figure 37* and *Figure 38*. These particles, characterized by their dark coloration, irregular or fibrous morphology, and relatively low density, show strong similarities to TRWPs previously described in the literature (Jung & Choi, 2022; Sommer et al., 2018). This indicates the possibility that TRWPs may have interacted physically with the organisms during the test, shown in *Figure 38*. The figure displays a *Daphnia* individual in a state of advanced decomposition, with clear structural degradation and tissue collapse, indicating that the organism is no longer viable. Numerous black particles are visible across the body surface, particularly around the appendages and body margins, strongly suggesting particle adsorption. These particles could resemble TRWPs in color, size and morphology. Additionally, diffuse, irregular material surrounding the organism may represent biofilm, decaying organic matter, or microbial colonization. The loss of transparency and tissue definition, along with particle aggregation, supports the interpretation of physical interaction and possible stress or damage caused during the exposure period. However, it is important to note that no further chemical or structural analyses were performed to confirm the identity of these particles. As such, there remains uncertainty regarding whether the particles observed are definitively TRWPs or another type of black polymeric or carbonaceous material from the tunnel wash water.

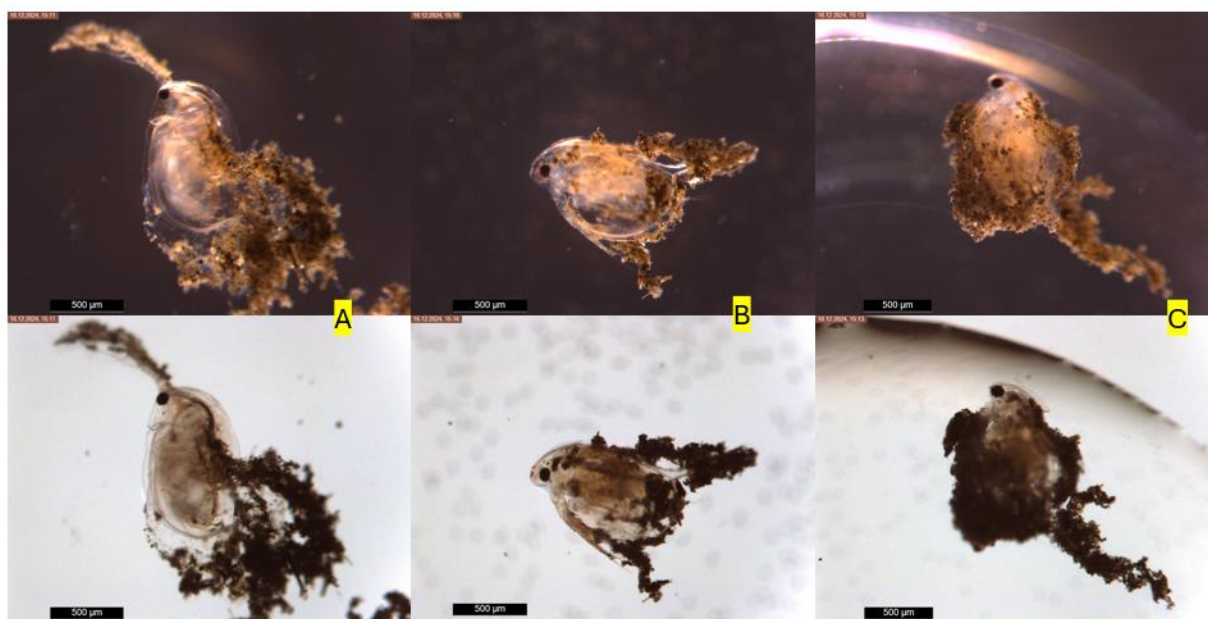


Figure 39: Visualization of particle adsorption on *Daphnia magna* exposed to untreated (TWW) with M7. The images show three individual *Daphnia*, where specimen **A** is alive, and specimens **B** and **C** are dead. The photographs illustrate the accumulation of adsorbed particles and other associated matter on the exoskeleton. All images were captured by Ole Holthusen. Scale bars: 500 µm.

Figure 39 gives further an visualization of particle adsorption on *Daphnia magna* exposed to untreated tunnel wash water in autumn. The figure displays three individual *Daphnia*, with specimen A representing an alive individual, and specimens B and C representing dead individuals. In specimens B and C, there is a noticeable increase in particle accumulation, with extensive clustering along the entire body surface, particularly in the posterior region. This suggests a progressive interaction between particles and the organism, possibly increased post mortem. Another interesting observation was that particles are clearly adhered to the shed exoskeleton shown in Figure 40. Since *Daphnia* regularly molt as part of their growth cycle, it is likely that adsorbed particles are removed along with the exoskeleton during this process.

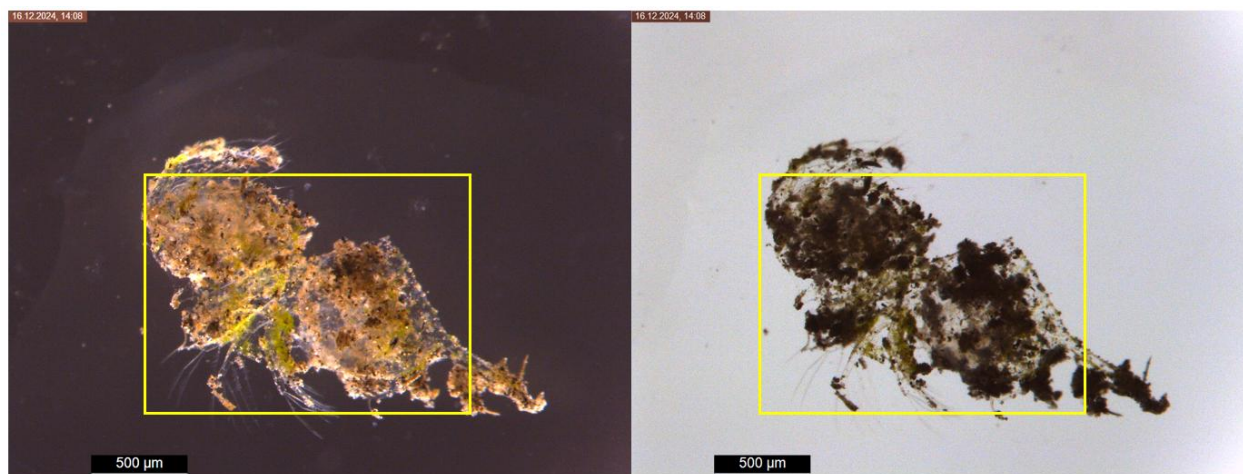


Figure 40: Microscopic images of a shed exoskeleton from *Daphnia magna* after exposure to untreated TWW from Autum with M7. The images show a shed exoskeleton heavily covered with particles, visualized under darkfield (left) and brightfield (right) microscopy. Images by Ole Holthusen. Scale bar: 500 μm .

Multiple studies confirm this and show that micro and nanoparticles adhere to the *Daphnia magna* carapace, which is later shed as part of the molting process. In a study, Dabrunz et al. used electron microscopy to visualize nanosized titanium dioxide (nTiO_2) agglomerates coating the surface of *D. magna*, particularly on the spines and body (Dabrunz et al., 2011). These particles formed visible "biological surface coatings" within hours of exposure during which the first molting was successfully managed by 100% of the exposed organisms. Continued exposure up to 96 h led to a renewed formation of the surface coating and significantly reduced the molting rate to 10%, resulting in 90% mortality (Dabrunz et al., 2011).

In another study (Masseroni et al., 2024) observed that polyvinyl chloride nanoplastics (PVC-NPs) adhered to the negatively charged body surface of *Daphnia magna*, potentially stimulating increased molting frequency as an adaptive response to physical surface stress. Their findings indicated also that exposure to PVC-NPs induced higher body dimensions and increased molting behavior. It was hypothesized that ingestion of PVC-NPs may impair reduce molting frequency, with increased molting events potentially representing an adaptive response to the adverse effects of PVC-NP adhesion to the organism's body surface (Masseroni et al., 2024).

Untreated Autumn TWW

To investigate the potential influence of water chemistry on particle behavior and toxicity, a comparative exposure experiment was conducted using untreated autumn tunnel wash water (TWW) prepared with EPA-standard water instead of M7 medium. Additionally, the pH was adjusted to assess whether changes in metal bioavailability would affect *Daphnia magna* responses. Due to logistical constraints and a miscommunication regarding the availability of six well plates, standard Petri dishes were used for the exposure setup. All *Daphnia magna* individuals survived the exposure period, and no or only minimal visible ingestion of particles into the gut was observed at the highest concentration (C5) shown in *Figure 41* with an almost empty gut.



Figure 41: Shows *Daphnia magna* exposed to untreated treated TWW from Autumn with EPA medium at C5, Petri dish experiment. The images show three live individuals (A–C) imaged under brightfield (left) and darkfield (right) microscopy. Images by Ole Holthusen. Scale bar: 500 µm.

This again strongly suggests that adhesion likely impairs feeding behavior by mechanically obstructing the filtering appendages leading to reduced mobility and feeding efficiency. However, as in the M7-based exposures, particles were clearly adsorbed to the body surface of the organisms, particularly on the antennae and appendages shown in *Figure 42*. This consistency in particle adhesion across both media types suggests that the choice of exposure medium (EPA vs. M7) had little effect on surface adsorption of particles. Interestingly, the extent of particle adherence appeared to be lower in the EPA water petri dish setup compared to the M7-based exposures conducted in well plates. One possible explanation is that the use of Petri dishes being larger and shallower may have altered particle distribution and exposure dynamics. During transfer of the dishes to the incubator, water movement, caused particles to settle more centrally in the dish, as shown in *Figure 19* in the method part. This likely resulted in reduced overall contact between the daphnids and suspended particles, compared to the more confined environment of a well plate where particles may remain more uniformly suspended. The larger surface area of the Petri dishes may have contributed to reduced particle adsorption. Regarding the physicochemical conditions during the test, all parameters were consistent across all treatments. Conductivity ranged from 930 to 948 $\mu\text{S}/\text{cm}$, pH values ranged from 6.83 to 6.98, temperature remained stable at approximately 20.6–21.5 °C, and dissolved oxygen levels were between 8.21 and 8.61 mg/L. These stable parameters suggest that any observed effects were not due to fluctuations in water quality. Detailed parameter values are provided in *Appendix J*.

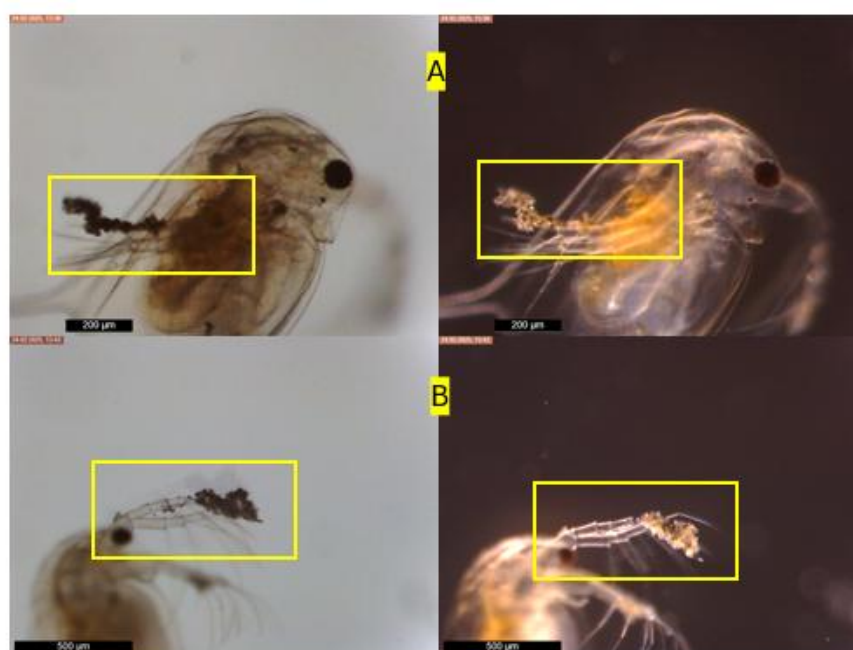


Figure 42: Shows the less lethal concentrations of adsorbed particles from untreated TWW autumn with the EPA media on the alive *Daphnids* swimming antenna. The two photos are taken in a brightfield and darkfield mode on the same *Daphnid* by Ole Holthusen. Scale bars: 500 μm .

Interestingly, there were clear seasonal differences in the results. While particle ingestion remained relatively consistent, particle adherence occurred only with the untreated autumn TWW and not with the spring TWW. This pattern was observed across both M7 and EPA media. The seasonal difference in particle adsorption to *Daphnia magna* likely reflects the contrasting of many factors like water chemistry, and other particle properties between the spring and autumn samples. In spring, the tunnel wash water had very high ionic strength with conductivity of 3460 $\mu\text{S}/\text{cm}$ and Cl^- 931 mg/L, whereas in autumn conductivity was much lower at 1040 $\mu\text{S}/\text{cm}$. High electrolyte concentrations compress the electrical double layers around colloidal particles, effectively masking or neutralizing their surface charges.

This reduction in electrostatic repulsion lowers the energy barrier between particles and can promote aggregation (Rai et al., 2022). These findings highlight that lower ionic strength favors smaller, more stable particles that remain suspended. Therefore, under spring conditions TWW particles likely formed larger aggregates, reducing the number of discrete particles available to adhere to the *Daphnia*'s body, in contrast to autumn where particles were potentially more suspended. (Seitz et al., 2015) demonstrated that ionic strength and natural organic matter (NOM) significantly influence how TiO_2 nanoparticles interact with *Daphnia magna*. In high-ionic-strength media, such as ASTM, nanoparticles rapidly aggregated into large clusters that settled out of the water column, reducing contact with daphnids and limiting surface coating on the daphnids outer shell. In contrast, nanoparticulate TiO_2 remained dispersed under low ionic strength conditions, which preserved their small size and potential toxicity, with adhesion to the *Daphnia* carapace being more likely, when particles are small and natural organic matter (NOM) is absent (Seitz et al., 2015).

Another explanation could be that the electrostatic and surface-charge effects also play a key role. The *D. magna* carapace carries a net negative charge $\zeta \approx -14.5$ mV in standard medium (Gajda-Meissner et al., 2020). The negative charge of the carapace can interact with charged particles leading to increased adsorption to *D. magna* for positively charged particles or vice versa negatively charged particles (Gajda-Meissner et al., 2020). In the latter study it was also

proposed that some physicochemical properties of particles in media, including zeta potential and agglomerate diameter, can lead to higher adsorption but do not necessarily affect toxicity (Gajda-Meissner et al., 2020). This aligns well with the experiments from TWW from autumn where no toxicity was observed, but rather adsorption that led to immobilization and stress to the *Daphnia*. However, in both these 2 studies, the findings were based on nanoparticle exposures and may not fully apply to microparticles, which behave differently in terms of surface interaction and biological uptake. The consistent observation of more particle adhesion under these low-salt conditions further supports the conclusion that ionic strength and specifically chloride rich environments strongly modulates the particle *Daphnia* binding dynamics through a combination of electrostatic screening and colloidal aggregation.

However, it is important to consider that multiple factors may influence the water chemistry and the extent of particle adsorption onto *Daphnia magna*. One clear example is the difference in detergent concentrations between the two sampling seasons, which could affect particle dispersion and surface interactions. Another possible explanation involves seasonal differences in tire composition. Spring samples are likely dominated by particles from winter tires, which are made from softer rubber compounds designed to remain flexible in cold conditions. In contrast, autumn samples likely contain more wear particles from summer tires, which are made with harder rubber formulations optimized for warmer temperatures. These differences in rubber chemistry may affect the surface properties and environmental behavior of the particles. As a result, road associated micro plastic and tire and road wear particles from summer tires may have a greater tendency to adsorb onto biological surfaces, such as the negatively charged carapace of *Daphnia magna*. Galloway et al. highlight that hydrophobic microplastics with little to no surface charge readily attract and retain a wide range of substances, including nutrients, pollutants, organic matter, and microbes. This is largely due to the formation of surface-bound biological and chemical coatings, which enhance particle surface interactions (Galloway et al., 2017). Different studies also highlight that hydrophobic polymers found in micro plastic, readily adsorb dissolved organic matter (DOM) and adhere to biological surfaces via van der Waals forces and other nonpolar interactions, promoting surface level binding (Liu et al., 2023; Yan et al., 2023).

These findings further suggest that road-associated microplastics may also adhere to *Daphnia magna* under suitable environmental conditions. In warmer seasons, particles in natural waters are also more likely to be colonized by microbial biofilms which can alter their surface properties (Schmitt-Jansen et al., 2022). Although it is difficult to determine a single dominant factor responsible for the adsorption of particles to *Daphnia*, due to the complex interplay of physical, chemical, and biological variables, the results clearly show that adsorption did occur. This indicates that even in the absence of complete mechanistic understanding, such interactions can have biological consequences. These findings underscore the importance of further studies aimed at exploring the conditions under which adsorption becomes harmful, including variations in particle type, concentration, and water chemistry. Moreover, long-term exposure experiments are needed to assess whether chronic along with seasonal accumulation could exacerbate the effects observed in this 48 h experiment. Thus, a more comprehensive understanding of both acute and prolonged exposure scenarios is crucial for evaluating ecological risk and informing environmental policy and regulation. To conclude,

Hypothesis 4: Both untreated and treated tunnel wash water from the Ekeberg Tunnel will cause toxic effects on Daphnia magna, with untreated water showing higher lethality is therefore partially rejected for the 48-hour acute toxicity test. While untreated and treated water did not show short-term toxicity, this does not rule out potential effects from longer term exposure, which was not assessed in this study.

4.5.5 Leaching Experiment

Figure 43 shows the concentrations of metals leached into the supernatant from tunnel wash water (TWW) particles after 12 days of incubation in the dark at room temperature. Although detection limits were met for most of the metals, several important metals were quantified. Iron (Fe) had the highest concentration at 30.0 µg/L, followed by zinc (Zn) at 9.32 µg/L and manganese (Mn) at 3.53 µg/L. Copper (Cu) and molybdenum (Mo) were both measured at 2.00 µg/L, while tungsten (W) and antimony (Sb) were detected at lower concentrations of 0.35 µg/L and 0.42 µg/L. Trace levels of arsenic (As) and cadmium (Cd) were also detected, at 0.02 µg/L and 0.01 µg/L. These values reflect average concentrations from replicate leaching tests and indicate that Fe and Zn are the most mobile metals released from TWW particles under the test conditions.

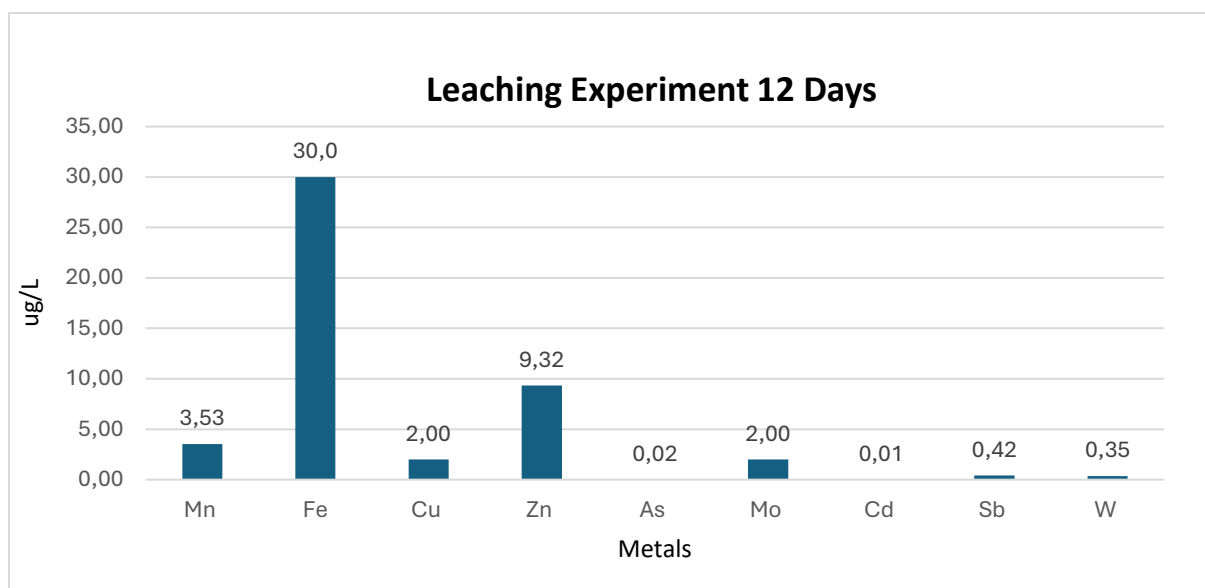


Figure 43: Metals above LOD with mean concentrations (µg/L) in leachate from spring tunnel wash water particles after 12-day Milli-Q leaching under dark, agitated conditions.

An acute immobilization toxicity test was also performed using the supernatant from the leachate of the tunnel wash water particles. However, no lethal or observable immobilization effects were recorded in any of the test organisms during the exposure period. The leaching experiment further demonstrated that tunnel wash water particles release concentrations of metals into water after prolonged contact. It should also be noted that the particles used in this study were not fresh or pristine but had already undergone environmental exposure. Despite this, they continued to leach considerable amounts of metals over the 12-day period, indicating ongoing release potential. These concentrations are consistent with findings from other tunnel-related studies. For instance, reported elevated levels of Zn, Cu, and Fe in tunnel wash water, attributing these metals to sources such as brake wear, corrosion of vehicle and tunnel infrastructure, and tire abrasion (Meland, 2010). Other studies also confirm that zinc and copper are among the most readily leached metals due to their high mobility and solubility (Posavec, 2018). Despite the presence of various metals in the leachate, no acute immobilization effect on *Daphnia magna* was observed after 48 hours of exposure. Although the total concentrations of metals in the leachate were generally low, copper (2,0 µg/L) and zinc (9,32 µg/L) nearly approached environmental thresholds relevant for chronic toxicity to sensitive species such as *Daphnia magna*.

The European Chemicals Agency (ECHA) has established a Predicted No-Effect Concentration (PNEC) for copper in freshwater at 7.8 µg/L, intended to protect 90% of aquatic species. The measured copper concentration falls below this threshold, suggesting a low potential for long-term toxic effects on freshwater invertebrates (ECI, 2008). For Zn, the UK Technical Advisory Group under the EU Water Framework Directive defines Environmental Quality Standards (EQS) for bioavailable Zn ranging from 8 to 125 µg/L, depending on water hardness. The measured Zn concentration of 9,32 µg/L falls near the lower end of this range, indicating that it does not exceed regulatory thresholds for most freshwater conditions (Maycock et al., 2012). However, this result should be interpreted with caution due to the use of the M7 medium as exposure , which contains EDTA, a strong chelating agent known to reduce the bioavailability of free metal ions such as Cu^{2+} and Zn^{2+} (OECD, 2004). EDTA forms stable complexes with dissolved metals, thereby decreasing their toxicity during bioassays. For this reason, the OECD advises against using media with chelators when testing substances that contain metals, as they may mask potential toxic effects (OECD, 2004). However, the cultivation media was due to a mistake used as exposure media. Regarding the particle load and leaching potential, it is important to note that the amount of particles used in the experiment was minimal compared to the total particulate matter present in the sedimentation basin. The extended sedimentation period of 21 days likely enhanced leaching by allowing prolonged contact between particles and water, facilitating the continuous release of metals and organic additives. This proves that if these TWW particles including tire and road wear particles (TRWP), are discharged into the Oslofjord, they could continue to leach contaminants over time and be harmful to the environment. Further analysis is also needed to assess whether organic compounds were also leached during this time.

5 Conclusion

This study confirms that tunnel wash water (TWW) from the Ekeberg Tunnel contains elevated levels of TRWP, TDCs, and metals, particularly after spring washes, supporting Hypothesis 1 on seasonal accumulation and winter abrasion from studded tires. The two-step treatment system effectively reduced many pollutants, especially TRWP ($>5\ \mu\text{m}$) and particle-associated metals like Fe and Al, supporting Hypothesis 2. However, finer particles ($0.4\text{--}5\ \mu\text{m}$), dissolved metals (Zn, Mn), and several water-soluble TDCs such as MTBT, HMMM, and TMQ were less efficiently removed, thus partially contradicting Hypothesis 2. These mixed results indicate that while the system is effective for certain contaminant classes, it has limitations with respect to the removal of finer and more water-soluble contaminants. Thus, Hypothesis 2 is only partially supported in that respect. However, elevated concentrations of detergent and ions from road salt may have interfered with Treatment 2 by limiting adsorption and altering compound behavior. This highlights the need for improved treatment technologies targeting mobile and chemically stable compounds under varying environmental conditions. Detergent alone was acutely toxic to *Daphnia magna*, but no immobilization occurred in actual TWW exposures from untreated TWW, Treatment 1, or Treatment 2 in spring, as well as from Treatment 1 and 2 in autumn confirming Hypothesis 3 and rejecting Hypothesis 4. The observed effect at high autumn TWW concentrations appeared to be caused by particle adhesion rather than chemical toxicity, thereby partially rejecting Hypothesis 4. Seasonal differences in conductivity and tire use may have affected *Daphnia* exposure, with lower ionic strength in autumn likely keeping particles suspended and more susceptible to adhesion, while higher salt levels in spring promoted aggregation and reduced adhesion. While no acute effects were seen post-treatment, visible ingestion and particle adhesion indicate the potential for sublethal and long-term impacts. Lastly, the leaching experiment demonstrated that TWW particles can slowly release metals over time, reinforcing the risk associated with the discharge of these particles. Together, the findings highlight the seasonal variability and complexity of tunnel runoff pollution, and the importance of targeting fine particles and dissolved contaminants in future treatment and risk assessment efforts.

6.0 References

- A Pettersson, Marie Adamsson, & G Dave. (2000). Toxicity and detoxification of Swedish detergents and softener products. *Chemosphere*, 41. [https://doi.org/http://dx.doi.org/10.1016/S0045-6535\(00\)00035-7](https://doi.org/http://dx.doi.org/10.1016/S0045-6535(00)00035-7)
- Acosta, J. A., Jansen, B., Kalbitz, K., Faz, A., & Martínez-Martínez, S. (2011). Salinity increases mobility of heavy metals in soils. *Chemosphere*, 85(8). <https://doi.org/10.1016/j.chemosphere.2011.07.046>
- Adachi, K., & Tainosho, Y. (2004). Characterization of heavy metal particles embedded in tire dust. *Environment International*, 30(8), 1009–1017. <https://doi.org/10.1016/j.envint.2004.04.004>
- Ahmed, S. (2023). Applications of *Daphnia magna* in Ecotoxicological Studies: A Review. . *Journal of Advanced Laboratory Research in Biology*, 6. https://www.researchgate.net/publication/376750470_Applications_of_Daphnia_magna_in_Eco_toxicological_Studies_A_Review
- Alexandrova, O., Kaloush, K. E., & Allen, J. O. . (2007). Impact of Asphalt Rubber Friction Course Overlays on Tire Wear Emissions and Air Quality Models for Phoenix, Arizona, Airshed. *Transportation Research Record*, 2011, 98-106. <https://doi.org/https://doi.org/10.3141/2011-11>
- Alling, V., Lund, E., Lusher, A., Knight, J., Hjelset, S., Singdahl-Larsen, C., Martinez-Frances, E., Røddland, E., Pakhomova, S., Kloster Snekkevik, V., Consolaro, C., van Bavel, B., Schmidt, N., & Herzke, D. (2024). Monitoring of microplastics in the Norwegian environment (MIKRONOR) 2023. 49. <https://www.miljodirektoratet.no/publikasjoner/2024/desember-2024/monitoring-of-microplastics-in-the-norwegian-environment-mikronor-2023/> (NIVA)
- Alling, V., Lund, E., Lusher, A., van Bavel, B., Kloster Snekkevik, V., Hjelset, S., Singdahl-Larsen, C., Consolaro, C., Jefroy, M., Martinez-Frances, E., Røddland, E., Pakhomova, S., Knight, J., Schmidt, N., & Herzke, D. (2023). *Monitoring of microplastics in the Norwegian environment (MIKRONOR) / Overvåking av mikroplast i det norske miljø (MIKRONOR)* (7922-2023). <https://www.miljodirektoratet.no/publikasjoner/2024/januar-2024/monitoring-of-microplastics-in-the-norwegian-environment-mikronor/>
- Amund Bruland, Reidar Hugstved, & Nordahl, R. S. (2024). *tunnel*. <https://snl.no/tunnel>
- AS, E. P. (2016). *Rensing av vaskevann fra veitunneler*. <https://vaforum.no/vaforum-artikler/rensing-av-vaskevann-fra-veitunneler/>
- Baensch, B., Beate , Kocher, B., Stock, F., & Reifferscheid, G. (2020). Tyre and road wear particles (TRWP) - A review of generation, properties, emissions, human health risk, ecotoxicity, and fate in the environment, . *Science of The Total Environment*, 733(137823,). <https://doi.org/https://doi.org/10.1016/j.scitotenv.2020.137823>.
- Bank, M. S. (2022). *Microplastic in the Environment: Pattern and Process* (M. S. Bank, Ed. Environmental Contamination Remediation and Management ed.). <https://doi.org/https://doi.org/10.1007/978-3-030-78627-4>
- Bazilchuk, N. (2019, 29.04.2019). *Vi salter veiene for mye*. Forskning.no. <https://www.forskning.no/miljo-ntnu-partner/vi-salter-veiene-for-mye/1259629>
- Behbahani, A., Ryan, R. J., & McKenzie, E. R. (2021). Impacts of salinity on the dynamics of fine particles and their associated metals during stormwater management, . *Science of The Total Environment*, 777. <https://doi.org/https://doi.org/10.1016/j.scitotenv.2021.146135>.
- Bjotveit, Å. (2020). *Investigation of Particle and Heavy Metal Removal and Detergent Degradation in Sedimented Tunnel Wash Water* NTNU]. ntnu.no. <https://ntnuopen.ntnu.no/ntnu-xmlui/handle/11250/2779433>
- Borgstrøm, R., Meland, S., Heier, L. S., Rosseland, B. O., Lindholm, O., & Salbu, B. (2010). Chemical and ecological effects of contaminated tunnel wash water runoff to a small Norwegian stream, .

- Science of The Total Environment*, 408(19), Pages 4107-4117,.
<https://doi.org/https://doi.org/10.1016/j.scitotenv.2010.05.034>.
- Bouredji, A., Pourchez, J., & Forest, V. (2023). Biological effects of Tire and Road Wear Particles (TRWP) assessed by in vitro and in vivo studies – A systematic review. *Science of The Total Environment*, 894. <https://www.sciencedirect.com/science/article/pii/S0048969723036124>
- Brittney W. Parker, Barbara A. Beckingham, Brianna C. Ingram, Joseph C. Ballenger, John E. Weinstein, & Sancho, G. (2020). Microplastic and tire wear particle occurrence in fishes from an urban estuary: Influence of feeding characteristics on exposure risk. *Marine Pollution Bulletin*, 160, Article 111539. <https://www.sciencedirect.com/science/article/pii/S0025326X20306573>
- Byman, L. (2012). *TREATMENT OF WASH WATER FROM ROAD TUNNELS* Royal Institute of Technology (KTH)]. [diva-portal.org. https://www.diva-portal.org/smash/get/diva2%3A844623/FULLTEXT01.pdf](https://www.diva-portal.org/smash/get/diva2%3A844623/FULLTEXT01.pdf)
- Camatini, M., Crosta, G. F., Dolukhanyan, T., Sung, C., Giuliani, G., Corbetta, G. M., Cencetti, S., & Regazzoni, C. (2001). Microcharacterization and identification of tire debris in heterogeneous laboratory and environmental specimens, . *Materials Characterization*, 46(4), 271-283. [https://doi.org/https://doi.org/10.1016/S1044-5803\(00\)00098-X](https://doi.org/https://doi.org/10.1016/S1044-5803(00)00098-X).
- Cao, G., Wang, W., Zhang, J., Wu, P., Zhao, X., Yang, Z., Hu, D., & Cai, Z. (2022). New Evidence of Rubber-Derived Quinones in Water, Air, and Soil. *Environmental Science & Technology Letters*, 56(7), 4142–4150. <https://doi.org/https://doi.org/10.1021/acs.est.1c07376>
- Chang, X.-d., Huang, H.-b., Jiao, R.-n., & Liu, J.-p. (2020). Experimental investigation on the characteristics of tire wear particles under different non-vehicle operating parameters, . *Tribology International*, 150. <https://doi.org/https://doi.org/10.1016/j.triboint.2020.106354>.
- Chen, B., Wang, J., & Yan, F. (2011). Friction and Wear Behaviors of Several Polymers Sliding Against GCr15 and 316 Steel Under the Lubrication of Sea Water. *Tribology Letters*, 42, 17-25. <https://doi.org/DOI: 10.1007/s11249-010-9743-9>
- Cheong, R. S., Roubeau Dumont, E., Thomson, P. E., Castañeda-Cortés, D. C., Hernandez, L. M., Gao, X., Zheng, J., Baesu, A., Macairan, J. R., Smith, A. J., Bui, H. N. N., Larsson, H. C. E., Ghoshal, S., Bayen, S., Langlois, V. S., Robinson, S. A., & Tufenkji, N. (2023). Nanoparticle-specific and chemical-specific effects of tire wear particle leachate on amphibian early life stages. *Journal of Hazardous Materials Advances*, 12. <https://doi.org/https://doi.org/10.1016/j.hazadv.2023.100357>
- Dabrunz, A., Duester, L., Prasse, C., Seitz, F., Rosenfeldt, R., Schilde, C., Schaumann, G. E., & Schulz, R. (2011). Biological Surface Coating and Molting Inhibition as Mechanisms of TiO₂ Nanoparticle Toxicity in *Daphnia magna*. *PLOS ONE*, 6(5). <https://doi.org/https://doi.org/10.1371/journal.pone.0020112>
- Dahl, A., Gharibi, A., Swietlicki, E., Gudmundsson, A., Bohgard, M., Ljungman, A., Blomqvist, G., & Gustafsson, M. (2006). Traffic-generated emissions of ultrafine particles from pavement–tire interface, . *Atmospheric Environment*, 40(7), Pages 1314-1323,. <https://doi.org/https://doi.org/10.1016/j.atmosenv.2005.10.029>.
- Degaffe, F. S., & Turner, A. (2011). Leaching of zinc from tire wear particles under simulated estuarine conditions. *Chemosphere*, 855(5), 738–743. <https://doi.org/10.1016/j.chemosphere.2011.06.047>
- Dupont. (n.d). *Separation of Arsenic from Liquid Media*. Dupont water solutions. <https://www.dupont.com/water/periodic-table/arsenic.html>
- EAPA, E. A. P. A. (2018). *HEAVY DUTY SURFACES*
- THE ARGUMENTS FOR SMA. https://www.sma16jena.pl/wp-content/uploads/2021/08/EAPA_Heavy_Duty_Surfaces_The_Arguments_for_SMA.pdf
- Ebert, D. (2005). *Introduction to Daphnia Biology*. National library of medicine. <https://www.ncbi.nlm.nih.gov/books/NBK2042/>
- ECI, E. C. I. (2008). *Voluntary Risk Assessment Report on Copper and its Compounds: Copper(II)sulfate pentahydrate, Copper(I)oxide, Copper(II)oxide, Dicopper chloride trihydroxide*. (European Union Risk Assessment Report., Issue. E. C. Institute. <https://echa.europa.eu/registration-dossier/-/registered-dossier/1322/6/2/1>
- EEA. (2024). Transport in Europe: Some signs of progress but difficult journey ahead to sustainability. <https://www.eea.europa.eu/en/newsroom/news/transport-in-europe>
- Elenbaas, M. (2013). *Daphnia magna*. University of Michigan. https://animaldiversity.org/accounts/Daphnia_magna/

- EPA, U. S. E. P. A. (2002). Methods for measuring the acute toxicity of effluents and receiving waters to freshwater and marine organisms. In (Vol. EPA-821-R-02-012). Washington, D.C.: Office of Water
- Fairbrother, A., Wenstel, R., Sappington, K., & Wood, W. (2007). Framework for Metals Risk Assessment, . *Ecotoxicology and Environmental Safety*, 68(2), Pages 145-227,.
<https://doi.org/https://doi.org/10.1016/j.ecoenv.2007.03.015>.
- Foitzik, M.-J., Unrau, H.-J., Gauterin, F., Dörnhöfer, J., & Koch, T. (2018). Investigation of ultra fine particulate matter emission of rubber tires. *Wear*, 394-395, Pages 87-95,.
<https://doi.org/https://doi.org/10.1016/j.wear.2017.09.023>.
- Furberg, A., Arvidsson, R., & Molander, S. (2019). Dissipation of tungsten and environmental release of nanoparticles from tire studs: A Swedish case study. *Journal of Cleaner Production*, 207.
<https://doi.org/https://doi.org/10.1016/j.jclepro.2018.10.004>
- Gajda-Meissner, Z., Matyja, K., Brown, D., Hartl, M. G. J., & Fernandes, T. F. (2020). Importance of Surface Coating to Accumulation Dynamics and Acute Toxicity of Copper Nanomaterials and Dissolved Copper in *Daphnia magna* *Environmental Toxicology and Chemistry* 39(2).
<https://doi.org/10.1002/etc.4617>
- Galloway, T. S., Cole, M., & Lewis, C. (2017). Interactions of microplastic debris throughout the marine ecosystem. *Nature Ecology & Evolution* 1. <https://doi.org/10.1038/s41559-017-0116>
- Garrard, S. L., Spicer, J. I., & Thompson, R. C. (2022). Tyre particle exposure affects the health of two key estuarine invertebrates. *Environmental Pollution*, 314.
<https://doi.org/https://doi.org/10.1016/j.envpol.2022.120244>
- Garshol, F. K., Estevez, M. M. R., Dadkhah, M. E., Prosjektnummer, Stang, P., Subhash S. Rathnaweera, Eilen Arctander Vik, & Sahu, A. (2015). *Laboratory tests - treatment of tunnel wash water from the Nordby tunnel*. S. Vegvesen. <https://vegvesen.brage.unit.no/vegvesen-xmlui/bitstream/handle/11250/2671290/Rapport%20521%20Laboratorietester%20-%20rensing%20av%20vaskevann%20fra%20Nordbytunnelen.pdf?sequence=1&isAllowed=y>
- Gauthier, P. T., Norwood, W. P., Prepas, E. E., & Pyle, G. G. (2014). Metal-PAH mixtures in the aquatic environment: A review of co-toxic mechanisms leading to more-than-additive outcomes. *Aquatic Toxicology*, 154, Pages 253-269. <https://doi.org/https://doi.org/10.1016/j.aquatox.2014.05.026>
- Gavrić, S., Leonhardt, G., Österlund, H., Marsalek, J., & Viklander, M. (2021). Metal enrichment of soils in three urban drainage grass swales used for seasonal snow storage. *Sci Total Environ.*, 760.
<https://doi.org/https://doi.org/10.1016/j.scitotenv.2020.144136>
- Gehrke, I., Schläfle, S., Bertling, R., Öz, M., & Gregory, K. (2023). Review: Mitigation measures to reduce tire and road wear particles. *Science of The Total Environment*, 904.
<https://doi.org/https://doi.org/10.1016/j.scitotenv.2023.166537>
- Granheim, G. M. (2023). *Retention and treatment of tire wear particles, road wear particles, metals and organic additives in tires present in tunnel wash water from the Vålereng tunnel* NMBU].
- Grigoratos, T., & Martini, G. (2014). Non-exhaust traffic related emissions – Brake and tyre wear PM. <https://doi.org/https://dx.doi.org/10.2790/22000> (Publications Office of the European Union)
- Gunnar Omsted, & Frigstad, H. (2025). Oslofjorden: Alvorlige funn i ny tilstandsrapport. <https://www.niva.no/nyheter/oslofjorden-alvorlige-funn-i-ny-tilstandsrapport>
- Gustafsson, M., Blomqvist, G., Gudmundsson, A., Dahl, A., Swietlicki, E., Bohgard, M., Lindbom, J., & Ljungman, A. (2008). Properties and toxicological effects of particles from the interaction between tyres, road pavement and winter traction material, . *Science of The Total Environment*, 393(2-3), Pages 226-240,. <https://doi.org/https://doi.org/10.1016/j.scitotenv.2007.12.030>.
- Hiki, K., & Yamamoto, H. (2022). The Tire-Derived Chemical 6PPD-quinone Is Lethally Toxic to the White-Spotted Char *Salvelinus leucomaenis pluvius* but Not to Two Other Salmonid Species. *Environmental Science & Technology Letters*, 9(12), 1050-1055.
<https://doi.org/https://doi.org/10.1021/acs.estlett.2c00683>
- Holý, M., & Remišová, E. (2019). Analysis of influence of bitumen composition on the properties represented by empirical and viscosity test. *Transportation Research Procedia*, 40, 34-41.
<https://doi.org/https://doi.org/10.1016/j.trpro.2019.07.007>

- Huber, M., Welker, A., & Helmreich, B. (2016). Critical review of heavy metal pollution of traffic area runoff: Occurrence, influencing factors, and partitioning, . *Science of The Total Environment*, 541, Pages 895-919,. <https://doi.org/https://doi.org/10.1016/j.scitotenv.2015.09.033>.
- Hussein, T., Johansson, C., Karlsson, H., & Hansson, H.-C. (2008). Factors affecting non-tailpipe aerosol particle emissions from paved roads: On-road measurements in Stockholm, Sweden, . *Atmospheric Environment*, 42(4), Pages 688-702,. <https://doi.org/https://doi.org/10.1016/j.atmosenv.2007.09.064>.
- I. Korytář, L. Mravcová, J. Raček, K. Velikovská, & P. Hlavínek. (2022). Treatment of tunnel wash water: case study from Brno, . *Desalination and Water Treatment*, 271, Pages 27-37,. <https://doi.org/https://doi.org/10.5004/dwt.2022.28791>.
- Iwai, T., & Hashimoto, Y. (2017). Adsorption of tungstate (WO₄) on birnessite, ferrihydrite, gibbsite, goethite and montmorillonite as affected by pH and competitive phosphate (PO₄) and molybdate (MoO₄) oxyanions. *Applied Clay Science*, 143. <https://doi.org/https://doi.org/10.1016/j.clay.2017.04.009>
- Jiménez-Castañeda, M. E., & Medina, D. I. (2017). Use of Surfactant-Modified Zeolites and Clays for the Removal of Heavy Metals from Water. *Water*, 9(4). <https://doi.org/10.3390/w9040235>
- Johannessen, C., Helm, P., & Metcalfe, C. D. (2021). Detection of selected tire wear compounds in urban receiving waters. *environment pollution*, 287. <https://doi.org/https://doi.org/10.1016/j.envpol.2021.117659>
- Johannessen, C., Liggio, J., Zhang, X., Saini, A., & Harner, T. (2022). Composition and transformation chemistry of tire-wear derived organic chemicals and implications for air pollution, . *Atmospheric Pollution Research*, 13(9). <https://doi.org/https://doi.org/10.1016/j.apr.2022.101533>.
- Jung, U., & Choi, S.-S. (2022). Classification and Characterization of Tire-Road Wear Particles in Road Dust by Density. *polymers*, 14(5), 1005. <https://doi.org/https://doi.org/10.3390/polym14051005>
- Jære, L. (2024). Norge rundt med Tunnelstudiet. <https://www.viderebloggen.no/norge-rundt-med-tunnelstudiet/>
- Järnskog, I., Jaramillo-Vogel, D., Rausch, J., Perseguers, S., Gustafsson, M., Strömvall, A.-M., & Andersson-Sköld, Y. (2022). Differentiating and Quantifying Carbonaceous (Tire, Bitumen, and Road Marking Wear) and Non-carbonaceous (Metals, Minerals, and Glass Beads) Non-exhaust Particles in Road Dust Samples from a Traffic Environment. *Water, Air, & Soil Pollution*, 233. <https://link.springer.com/article/10.1007/s11270-022-05847-8> (10.1007/s11270-022-05847-8)
- Kagalkar, A., Dharaskar, S., Chaudhari, N., Vakharia, V., & Karri, R. R. (2025). Enhanced metal ion adsorption using ZnO-MXene nanocomposites with machine learning-based performance prediction. *Scientific Reports*. <https://doi.org/https://doi.org/10.1038/s41598-025-21659-3>
- Kayhanian, M., McKenzie, E. R., Leatherbarrow, J. E., & Young, T. M. (2012). Characteristics of road sediment fractionated particles captured from paved surfaces, surface run-off and detention basins. *Sci Total Environ.*, 439, 172–186. <https://doi.org/10.1016/j.scitotenv.2012.08.077>
- Kjærnsby, H. M. (2024). *Using a chipwood-biofilter for removal of dissolved metals and metalloids from tunnel wash water* NMBU]. nmbu.brage.unit.no. <https://nmbu.brage.unit.no/nmbu-xmlui/bitstream/handle/11250/3148315/no.nmbu%3awiseflow%3a7110070%3a59109774.pdf?sequence=1&isAllowed=y>
- Kloepfer, A., Jekel, M., & Reemtsma, T. (2005). Occurrence, Sources, and Fate of Benzothiazoles in Municipal Wastewater Treatment Plants. *Environmental Science & Technology Letters*, 39(10). <https://doi.org/https://doi.org/10.1021/es048141e>
- Klöckner, P., Seiwert B, Weyrauch S, Escher BI, Reemtsma T, & S., W. (2021). Comprehensive characterization of tire and road wear particles in highway tunnel road dust by use of size and density fractionation. *chemosphere*, 279. <https://doi.org/10.1016/j.chemosphere.2021.130530>
- Knight, L. J. P.-J., F. N. F.; Al-Sid-Cheikh, M.; Thompson, R. C. (2020). Tyre wear particles: an abundant yet widely unreported microplastic? *Environmental Science and Pollution Research International*, 27(15), 18345–18354. <https://doi.org/10.1007/s11356-020-08187-4>
- Kole, P., Löhr AJ, Van Belleghem FG AJ, & AMJ., R. (2017). Wear and Tear of Tyres: A Stealthy Source of Microplastics in the Environment. . *Lnt J Environ Res Public Health*. <https://doi.org/doi:10.3390/ijerph14101265>.

- Kreider, M., Panko JM, McAtee BL, Sweet LI, & BL., F. (2010). Physical and chemical characterization of tire-related particles: comparison of particles generated using different methodologies. . *Sci Total Environ.*, 408(4), 652-659. <https://doi.org/10.1016/j.scitotenv.2009.10.016>
- Krishna R. Reddy, Tao Xie, & Sara Dastgheibi. (2014). Removal of heavy metals from urban stormwater runoff using different filter materials, . *Journal of Environmental Chemical Engineering*,, Volume 2, Issue 1,, Pages 282-292,. <https://doi.org/https://doi.org/10.1016/j.jece.2013.12.020>.
- Kupiainen, K., Tervahattu, H., & Räisänen, M. (2003). Experimental studies about the impact of traction sand on urban road dust composition, . *Science of The Total Environment*,, 308(1-3), Pages 175-184,. [https://doi.org/https://doi.org/10.1016/S0048-9697\(02\)00674-5](https://doi.org/https://doi.org/10.1016/S0048-9697(02)00674-5).
- Kurmysheva, A. Y., Vedenyapina, M. D., Kulaishin, S. A., Podrabinnik, P., Pinargote, N. W. S., Smirnov, A., Metel, A. S., Bartolomé, J. F., & Grigoriev, S. N. (2023). Adsorption Removal of Mo(VI) from an Aqueous Solution by Alumina with the Subsequent Regeneration of the Adsorbent. *International Journal of Molecular Sciences*, 24(10). <https://doi.org/10.3390/ijms24108700>
- Lee, S., Lee, S., Kim, Y., & Woo, S. H. (2019). Effect of Tire Treadwear Rate on the Physical Characterization of Tire Wear Particles in Laboratory Measurements. *Journal of Korean Society for Atmospheric Environment*, 35(6), 741-756. <https://doi.org/10.5572/KOSAE.2019.35.6.741>
- Licbinsky, R., Huzlík, J., Frýbort, A., & Kreislova, K. (2013). Specific Air Pollution in Road Tunnels *Transactions on Transport Sciences* 6(3). https://doi.org/https://tots.upol.cz/artkey/tot-201303-0001_specific-air-pollution-in-road-tunnels.php
- Liu, J., Feng, Q., Yang, H., Fan, X., Jiang, Y., & Wu, T. (2023). Acute toxicity of tire wear particles and leachate to *Daphnia magna*. *Comparative Biochemistry and Physiology Part C: Toxicology & Pharmacology*, 272. <https://doi.org/10.1016/j.cbpc.2023.109713>
- Lovdata. (2023). Lov om vern mot forurensninger og om avfall (forurensningsloven). In. Lovdata.no: Lovdata.
- Lundgren, L. (2021). *Metal Removal Efficiency of Five Filter Media Intended for Use in Road Stormwater Treatment Facilities* KTH Royal Institute of Technology]. Sweden. <https://www.diva-portal.org/smash/get/diva2:1539703/FULLTEXT01.pdf#:~:text=The%20influent%20of%20total%20Zn,89%25%20and>
- M. Hallberg, G. Renman, L. Byman, G. Svenstam, & Norling, M. (2014). Treatment of tunnel wash water and implications for its disposal *Water Science and Technology*, 69(10). <https://doi.org/https://doi.org/10.2166/wst.2014.113>
- Mansberger, J. (2023, October 27, 2023). *Environmental Hazards of Road Salt*. PennState Extension. <https://extension.psu.edu/environmental-hazards-of-road-salt>
- Marinello, S., Lolli, F., & Gamberini, R. (2020). Roadway tunnels: A critical review of air pollutant concentrations and vehicular emissions. *Transportation Research Part D: Transport and Environment*, 86. <https://doi.org/https://www.sciencedirect.com/science/article/pii/S1361920920306659?via%3Dihub>
- Markus Brinkmann, David Montgomery, Summer Selinger, Justin G. P. Miller, Eric Stock, Alper James Alcaraz, Jonathan K. Challis, Lynn Weber, David Janz, Markus Hecker, & Wiseman, S. (2022). Acute Toxicity of the Tire Rubber-Derived Chemical 6PPD-quinone to Four Fishes of Commercial, Cultural, and Ecological Importance. 9(3). <https://pubs.acs.org/doi/10.1021/acs.estlett.2c00050>
- Masseroni, A., Federico, L., & Villa, S. (2024). Ecological fitness impairments induced by chronic exposure to polyvinyl chloride nanospheres in *Daphniamagna*. *Heliyon*, 10(23). <https://doi.org/10.1016/j.heliyon.2024.e40065>
- Mathissen, M., Scheer, V., Vogt, R., & Benter, T. (2011). Investigation on the potential generation of ultrafine particles from the tire-road interface, . *Atmospheric Environment*,, 45(34), Pages 6172-6179,. <https://doi.org/https://doi.org/10.1016/j.atmosenv.2011.08.032>.
- Matthew S Schuler, & Relyea, R. A. (2018). A Review of the Combined Threats of Road Salts and Heavy Metals to Freshwater Systems. *BioScience*, 68(5), 327-335. <https://doi.org/https://doi.org/10.1093/biosci/biy018>
- Maycock, D., Peters, A., Merrington, G., & Crane, M. (2012). *Proposed EQS for Water Framework Directive Annex VIII substances: zinc (For*

- consultation). https://www.wfduk.org/sites/default/files/Media/Zinc%20-%20UKTAG.pdf#:~:text=values%20ranging%20between%208%20and,the%20PNECadd%2Cfres hwater _lt%20based%20on%20an
- Meland, S. (2010). *Ecotoxicological Effects of Highway and Tunnel Wash Water Runoff* (Publication Number Thesis number 2010:25) NMBU]. nmbu.brage.no. https://nmbu.brage.unit.no/nmbu-xmlui/bitstream/handle/11250/2431910/2010-25_Sondre%20Meland_%28IMV%29.pdf?sequence=1&isAllowed=y
- Meland, S. (2012). Tunnelvaskevann –
- En kilde til vannforurensning. <https://www.vegvesen.no/globalassets/fag/fokusomrader/forskning-innovasjon-og-utvikling/norwat/tunnelvaskevann-en-kilde-til-vannforurensning-vannno22012.pdf>
- Meland, S., Granheim, G. M., Rundberget, J. T., & Rødland, E. (2023). Screening of Tire-Derived Chemicals and Tire Wear Particles in a Road Tunnel Wash Water Treatment Basin. *Environmental Science & Technology Letters*, 11(1). <https://doi.org/https://pubs.acs.org/doi/10.1021/acs.estlett.3c00811>
- Meland, S., Heier, L. S., Salbu, B., Tollefsen, K. E., Farmen, E., & Rosseland, B. O. (2010). Exposure of brown trout (*Salmo trutta* L.) to tunnel wash water runoff — Chemical characterisation and biological impact, . *Science of The Total Environment*, 408(13), Pages 2646-2656,. <https://doi.org/https://doi.org/10.1016/j.scitotenv.2010.03.025>.
- Meland, S., & Rødland, E. S. (2018). Forurensning i tunnelvaskevann –
- en studie av 34 veitunneler i Norge <https://nmbu.brage.unit.no/nmbu-xmlui/handle/11250/2833191>
- Meland, S., & Torp, M. (2013). Estimering av forurensning i tunnel og tunnelvaskevann. In. vegvesen.brage.unit.no: Statens vegvesen.
- Merete Grung, Morten Jartun, Kine Bæk, Anders Ruus, Thomas Rundberget, Ian Allan, Bjørnar Beylich, Christian Vogelsang, Martin Schlabach, Linda Hanssen, Katrine Borgå, & Helberg, M. (2021). *Environmental Contaminants in an Urban Fjord, 2020* (7674-2021). Miljødirektoratet. <https://www.miljodirektoratet.no/publikasjoner/2022/januar/environmental-contaminants--in-an-urban-fjord-2020/>
- merityre. (n.d). *SUMMER TYRES*. <https://www.merityre.co.uk/tyres/seasonal-tyres/summer-tyres>
- Michael Kovichich, Su Cheun Oh, Jessica P. Lee, Jillian A. Parker, Tim Barber, & Unice, K. (2023). Characterization of tire and road wear particles in urban river samples. *Environmental Advances*, 12, Article 100385. <https://www.sciencedirect.com/science/article/pii/S2666765723000455#bbib0025>
- Miljødirektoratet. (2020a). Grenseverdier for klassifisering av vann, sediment og biota – revidert 30.10.2020 / Quality Standards for Water, Sediment and Biota – revised 2020.10.30. In (pp. 13). Norway: Miljødirektoratet (Norwegian Environment Agency).
- Miljødirektoratet. (2020b). Grenseverdier for klassifisering
- av vann, sediment og biota –
- revidert 30.10.2020. In (Vol. 608, pp. 13). Miljødirektoratet.no: Miljødirektoratet.
- Miljødirektoratet. (2023). Gjennomføring av helhetlig tiltaksplan for Oslofjorden. Rapport fra året 2022–2023. In (pp. 32). Miljødirektoratet.no: Miljødirektoratet.
- Miljødirektoratet. (2024). Mikroplast frå bildekk forureinar Arktis. <https://www.miljodirektoratet.no/aktuelt/nyheter/2024/desember-2024/mikroplast-fra-bildekk-forureinar-arktis/> (Miljødirektoratet.no)
- Müller, A., Österlund, H., Marsalek, J., & Viklander, M. (2020). The pollution conveyed by urban runoff: A review of sources, . *Science of The Total Environment*, 709(136125,). <https://doi.org/https://doi.org/10.1016/j.scitotenv.2019.136125>.
- Müller, K., Hübner, D., Huppertsberg, S., Knepper, T. P., & Zahn, D. (2022). Probing the chemical complexity of tires: Identification of potential tire-borne water contaminants with high-resolution mass spectrometry
- Sci Total Environ.*, 802. <https://doi.org/https://doi.org/10.1016/j.scitotenv.2021.149799>
- Negin Ashoori, Marc Teixido, Stephanie Spahr, Gregory H. LeFevre, David L. Sedlak, & Richard G. Luthy. (2019). Evaluation of pilot-scale biochar-amended woodchip bioreactors to remove nitrate, metals, and trace organic contaminants from urban stormwater runoff,

- Water Research, . Volume 154, 1-11. <https://doi.org/https://doi.org/10.1016/j.watres.2019.01.040>.
- NORVA24. (2017). *Tunnel cleaning*. Norva24. <https://norva24.no/en/tjeneste/vask-av-tunnel/#:~:text=The%20purpose%20of%20tunnel%20cleaning,of%20equipment%20placed%20inside%20tunnels>
- OECD, O. f. E. C.-o. a. D. (2004). OECD guidelines for the testing of chemicals: Daphnia sp., acute immobilisation test. In *OECD Test Guidelines*. Paris: OECD Publishing.
- Panko, J., Hitchcock, K., Fuller, G. W., & Green, D. (2019). Evaluation of Tire Wear Contribution to PM2.5 in Urban Environments. *Atmosphere*, 10(99). <https://doi.org/10.3390/atmos10020099>
- Panko, J. M., Chu, J., Kreider, M. L., & Unice, K. M. (2013). Measurement of airborne concentrations of tire and road wear particles in urban and rural areas of France, Japan, and the United States *Atmospheric Environment*, 72, 192-199. <https://doi.org/10.1016/j.atmosenv.2013.01.040>
- Park, I., Lee, J., & Lee, S. (2016). Laboratory study of the generation of nanoparticles from tire tread. *Aerosol Science and Technology*, 51, 188–197. <https://doi.org/https://doi.org/10.1080/02786826.2016.1248757>
- Peng, Z., Chen, H., Li, Y., Feng, K., Wang, C., Liao, F., Deng, H., & Huang, Y. (2020). Chelating surfactant for the removal of heavy metals from wastewater and surfactant recovery. *Desalination and Water Treatment*, 206. <https://doi.org/10.5004/dwt.2020.26302>
- Peter, K. T., Tian, Z., Wu, C., Lin, P., White, S., Du, B., McIntyre, J. K., Scholz, N. L., & Kolodziej, E. P. (2018). Using High-Resolution Mass Spectrometry to Identify Organic Contaminants Linked to Urban Stormwater Mortality Syndrome in Coho Salmon. *Environment science and technology*, 52(18), 10317–10327. <https://doi.org/https://doi.org/10.1021/acs.est.8b03287>
- Piarc. (2022). *Winter maintenance*. Piarc. <https://tunnelsmanual.piarc.org/en/operation-and-maintenance-maintenance/winter-maintenance>
- Posavec, D. (2018). *Leaching Of Metals From Paint And Rubber Particles* School of Engineering and Science J. <https://vbn.aau.dk/>. https://vbn.aau.dk/ws/files/281189293/Damir_Posavec_Master_s_thesis.pdf
- Prata, J. C., da Costa, J. P., Lopes, I., Duarte, A. C., & Rocha-Santos, T. (2020). Environmental exposure to microplastics: An overview on possible human health effects, . *Science of The Total Environment*, 702(134455,). https://doi.org/ISSN_0048-9697,
- Rai, P. K., Sonne, C., Brown, R. J. C., Younis, S. A., & Kim, K.-H. (2022). Adsorption of environmental contaminants on micro- and nano-scale plastic polymers and the influence of weathering processes on their adsorptive attributes. *Journal of Hazardous Materials*. <https://doi.org/10.1016/j.jhazmat.2021.127903>
- Rauert, C., Charlton, N., Okoffo, E. D., Stanton, R. S., Agua, A. R., Pirrung, M. C., & Thomas, K. V. (2022). Concentrations of Tire Additive Chemicals and Tire Road Wear Particles in an Australian Urban Tributary. *Environmental Science & Technology Letters*, 56(4), 2421–2431 <https://doi.org/https://doi.org/10.1021/acs.est.1c07451>
- Rauert, C., Rødland, E. S., Okoffo, E. D., Reid, M. J., Meland, S., & Thomas, K. V. (2021). Challenges with Quantifying Tire Road Wear Particles: Recognizing the Need for Further Refinement of the ISO Technical Specification. *Environmental Science and Technology Letters (ES&T Letters)*, 8(3), 231–236. <https://doi.org/10.1021/acs.estlett.0c00949>
- Reddy, C. M., & Quinn, J. G. (1997). Environmental Chemistry of Benzothiazoles Derived from Rubber. *Environmental Science & Technology Letters*, 31(10), 2847–2853. <https://doi.org/https://doi.org/10.1021/es970078o>
- Rist, S., Baun, A., & Hartmann, N. B. (2017). Ingestion of micro- and nanoplastics in Daphnia magna - Quantification of body burdens and assessment of feeding rates and reproduction. *environment pollution*, 228. <https://doi.org/10.1016/j.envpol.2017.05.048>
- Roger Roseth, & Søvik, A. K. (2006). *Vann og veg. Binding og nedbrytning av rengjøringsmidler brukt til vask av tunneler og annet vedlikehold av veg*. . Statens Vegvesen. <https://vegvesen.brage.unit.no/vegvesen-xmlui/bitstream/handle/11250/191136/UTB%20rapport%202006-01.pdf?sequence=1&isAllowed=y>
- Rogge, W. F., Hildemann, L. M., Mazurek, M. A., Cass, G. R., & Simoneit, B. R. T. (1993). Sources of fine organic aerosol. 3. Road dust, tire debris, and organometallic brake lining dust: roads as sources

- and sinks. *Environmental Science & Technology Letters*, 27(9), 1892–1904. <https://doi.org/DOI:10.1021/es00046a019>
- Rossbach, A. (2024). As Global Cities Expand Rapidly, People Must Be at the Center of Planning. <https://time.com/7203147/sustainable-urban-development/>
- Rødland, Elisabeth S., Lind, O. C., Reid, M., Heier, L. S., Skogsberg, E., Snilsberg, B., Gryteselv, D., & Meland, S. (2022). Characterization of tire and road wear microplastic particle contamination in a road tunnel: From surface to release. *Journal of Hazardous Materials*, 435(5). <https://doi.org/https://doi.org/10.1016/j.jhazmat.2022.129032>
- Rødland, E., & Lundgaard, M. K. R. (2023). *Dekkgummi og antioksidant fra tunnelvask*.
- Rødland, E. S. (2022). *Microplastic particles from roads and traffic : occurrence and concentrations in the environment* (Publication Number 2022:34) NMBU
- J. nmbu.brage.unit.no. <https://nmbu.brage.unit.no/nmbu-xmlui/handle/11250/3014022>
- Rødland, E. S., Samanipour, S., Rauert, C., Okoffo, E. D., Reid, M. J., Heier, L. S., Lind, O. C., Thomas, K. V., & Meland, S. (2022). A novel method for the quantification of tire and polymer-modified bitumen particles in environmental samples by pyrolysis gas chromatography mass spectroscopy. *Journal of Hazardous Materials*, 423(127092). <https://doi.org/https://www.sciencedirect.com/science/article/pii/S0304389421020604?via%3Dihub>
- Saba, R. G., Uthus, N., & Aurstad, J. (2012). LONG-TERM PERFORMANCE OF ASPHALT SURFACINGS CONTAINING POLYMER MODIFIED BINDERS. <https://www.h-a-d.hr/pubfile.php?id=582> (5th Eurasphalt & Eurobitume Congress)
- Samferdselsdepartementet. (2023-2024). *Meld. St. 14 (2023–2024): Nasjonal transportplan 2025–2036*. Regjeringen.no: Regjeringen Retrieved from <https://www.regjeringen.no/no/dokumenter/meld.-st.-14-20232024/id3030714/?ch=1>
- Schell, T., Martinez-Perez, S., Dafouz, R., Hurley, R., Vighi, M., & Rico, A. (2022). Effects of Polyester Fibers and Car Tire Particles on Freshwater Invertebrates. *Environmental Toxicology and Chemistry*, 41(6). <https://doi.org/10.1002/etc.5337>
- Schlabach, M., van Bavel, B., Bæk, K., Dadkhah, M. E., Eikenes, H., Halse, A. K., Nikiforov, V., Bohlin-Nizzetto, P., Reid, M., Rostkowski, P., Rundberget, J. T., Baz Lomba, J., Kringstad, A., Rødland, E. S., Schmidbauer, N., Harju, M., Beylich, B., & Vogelsang, C. (2020). *Plastic Additives and REACH Compounds* (REPORT SNO.7684-2021). (Screening Programme 2020, Part 1 and 2.; Issue. NIVA. <https://niva.brage.unit.no/niva-xmlui/bitstream/handle/11250/2992346/7684-2021%2bhigh.pdf?sequence=1&isAllowed=y>
- Schmitt-Jansen, M., Lips, S., Schäfer, H., & Rummel, C. (2022). Microplastic: A New Habitat for Biofilm Communities. https://doi.org/https://doi.org/10.1007/978-3-030-39041-9_22
- Seda, J., & Petrusek, A. (2011). Daphnia as a model organism in limnology and aquatic biology: introductory remarks *Journal of Limnology*, 70(2). https://www.researchgate.net/publication/232709444_Daphnia_as_a_model_organism_in_limnology_and_aquatic_biology_Introductory_remarks
- Seitz, F., Lüderwald, S., Rosenfeldt, R. R., Paul, A., & Bundschuh, M. (2015). Aging of TiO₂ Nanoparticles Transiently Increases Their Toxicity to the Pelagic Microcrustacean *Daphnia magna*. *PLOS ONE*. <https://doi.org/10.1371/journal.pone.0126021>
- LicenseCC BY 4.0
- Seiwert, B., Klöckner, P., Wagner, S., & Reemtsma, T. (2020). Source-related smart suspect screening in the aqueous environment: search for tire-derived persistent and mobile trace organic contaminants in surface waters. *Analytical and Bioanalytical Chemistry*, 412, 4909–4919. <https://doi.org/https://doi.org/10.1007/s00216-020-02649-w>
- Sherman, A., Masset, T., Wimmer, L., Maruschka, L. K., Dailey, L. A., Hüffer, T., Breider, F., & Hofmann, T. (2025). The Invisible Footprint of Climbing Shoes: High Exposure to Rubber Additives in Indoor Facilities. *ACS ES&T Air*, 2, 930–942. <https://doi.org/10.1021/acsestair.5c00017>
- Shiny, K. J., Remani, K. N., Nirmala, E., Jalaja, T. K., Sasidharan, & V.K. (2005). Biotreatment of wastewater using aquatic invertebrates, *Daphnia magna* and *Paramecium caudatum*. *Bioresource Technology*, 96. <https://www.sciencedirect.com/science/article/pii/S096085240400032X>

- Skanska. (n.d). *E18 Ekeberg- og Svartdalstunnelen, tunnelrehabilitering*. Skanska.
<https://www.skanska.no/hva-vi-gjor/prosjekter/203374/E18-Ekeberg-og-Svartdalstunnelen%2c-tunnelrehabilitering/>
- Sommer, F., Dietze, V., Baum, A., & Gieré, R. (2018). Tire Abrasion as a Major Source of Microplastics in the Environment. *Aerosol and Air Quality Research*, 18, 2014–2028.
<https://doi.org/10.4209/aaqr.2018.03.0099>
- Sossalla, N. A., Uhl, W., Vistnes, H., Rathnaweera, S. S., Vik, E. A., & Meyn, T. (2025). Tunnel wash water in a cold climate: characteristics, ecotoxicological risk, and effect of sedimentation. *Environmental Science and Pollution Research* 32. <https://doi.org/https://doi.org/10.1007/s11356-024-35773-7>
- Statens Vegvesen. (2010). Tunneler i Oslo og Akershus. In. <https://vegvesen.brage.unit.no/>: Region øst
 Strategi-, veg- og transportavdelingen.
- Statens Vegvesen. (2016). Vegtunneler. In *Håndbok N500*. vegvesen.brage.unit.no: Vegdirektoratet.
- Statens Vegvesen. (2023). Renhold og støvdemping av
 veg, gate og tunnel. In *Erfaringer og «beste praksis» Norway*: Statens vegvesen.
- Statens Vegvesen. (2024a). *Ekeberg tunnelen nordgående*. Statens Vegvesen.
<https://trafikkdata.atlas.vegvesen.no/#/utforsk?datatype=averageDailyYearVolume&display=chart&from=2025-03-18&trpids=90310V625649>
- Statens Vegvesen. (2024b). *Ekeberg tunnelen sørgående*. Statens Vegvesen.
<https://trafikkdata.atlas.vegvesen.no/#/utforsk?datatype=averageDailyYearVolume&display=chart&from=2025-03-18&trpids=62363V625649>
- Statens Vegvesen. (2024c). *Piggdekkandeler i norske byer 2024*. Statens Vegvesen. Retrieved 17.12.2024 from <https://www.vegvesen.no/fag/fokusomrader/nasjonal-transportplan/den-nasjonale-reisevaneundersokelsen/reisevaner-2024/piggdekkandeler-i-norske-byer-2024/#:~:text=P%C3%A5%20nasjonalt%20niv%C3%A5%20er%20andelen,minst%20en%20av%20sine%20biler>
- Statens Vegvesen. (2024d). R610 Standard for drift
 og vedlikehold av
 riksveger. In *RETNINGSLINJE R610*. Norway: Statens vegvesen.
- Stephan Wagner, Philipp Klöckner, & Reemtsma, T. (2022). Aging of tire and road wear particles in terrestrial and freshwater environments – A review on processes, testing, analysis and impact. *chemosphere*, 288, Article 132467.
<https://www.sciencedirect.com/science/article/pii/S0045653521029398?via%3Dihub>
- Straffellini, G., Ciudin, R., Ciotti, A., & Gialanella, S. (2015). Present knowledge and perspectives on the role of copper in brake materials and related environmental issues: A critical assessment. *Environmental Pollution*, 207. <https://doi.org/https://doi.org/10.1016/j.envpol.2015.09.024>
- Sundt, P., Rønnekleiv Hagedal, S., Rem, T., & Schulze, P.-E. (2020). *Norske landbaserte kilder til mikroplast*. Miljødirektoratet. file:///C:/Users/Oleho/Downloads/M1910.pdf
- Suryapratap Ray, & Rahul Vashishth. (2024). From water to plate: Reviewing the bioaccumulation of heavy metals in fish and unraveling human health risks in the food chain, . *Emerging Contaminants*, 10(4). <https://doi.org/https://doi.org/10.1016/j.emcon.2024.100358>.
- Szklarek, S., Górecka, A., & Wojtal-Frankiewicz, A. (2022). The effects of road salt on freshwater ecosystems and solutions for mitigating chloride pollution - A review, . *Science of The Total Environment*, 805(150289,). <https://doi.org/https://doi.org/10.1016/j.scitotenv.2021.150289>.
- Tamis, J. E., Koelmans, A. A., Dröge, R., Kaag, N. H. B. M., Keur, M. C., Tromp, P. C., & Jongbloed, R. H. (2021). Environmental risks of car tire microplastic
 particles and other road runoff pollutants. *Microplastics and Nanoplastics*
<https://doi.org/https://doi.org/10.1186/s43591-021-00008-w>
- Tangudom, P., Thongsang, S., & Sombatsompop, N. (2014). Cure and mechanical properties and abrasive wear behavior of natural rubber, styrene–butadiene rubber and their blends reinforced with silica hybrid fillers, . *Materials & Design*, 53, Pages 856-864,.
<https://doi.org/https://doi.org/10.1016/j.matdes.2013.07.024>.
- Terzakis, S., M.S. Fountoulakis, I. Georgaki, D. Albantakis, I. Sabathianakis, A.D. Karathanasis, N. Kalogerakis, & T. Manios. (2008). Constructed wetlands treating highway runoff in the central

- Mediterranean region, . *Chemosphere*,, Volume 72, Issue 2,, Pages 141-149.
<https://doi.org/https://doi.org/10.1016/j.chemosphere.2008.02.044>.
- Thorpe, A., & Harrison, R. M. (2008). Sources and properties of non-exhaust particulate matter from road traffic: A review, . *Science of The Total Environment*, 400(1-3), 270-282.
<https://doi.org/https://doi.org/10.1016/j.scitotenv.2008.06.007>.
<https://www.sciencedirect.com/science/article/pii/S004896970800658X>)
- Tian, Z., Peter, K. T., Gipe, A. D., Scott, J. A., Hodgson, E., Kolodziej, E. P., & Scholz, N. L. (2021). A ubiquitous tire rubber-derived chemical induces acute mortality in coho salmon. *Science* 371(6525), 185-189. <https://doi.org/https://doi.org/10.1126/science.abd6951>
- Timmers, V. R. J. H., & Achten, P. A. J. (2016). Non-exhaust PM emissions from electric vehicles. *Atmospheric Environment*,, 134, 10-17.
<https://doi.org/https://doi.org/10.1016/j.atmosenv.2016.03.017>
- Tomislav Ivanković, & Hrenović, J. (2010). SURFACTANTS IN THE ENVIRONMENT. [https://doi.org/ DOI: 10.2478/10004-1254-61-2010-1943](https://doi.org/DOI:10.2478/10004-1254-61-2010-1943)
- Toni Klauschies, & Jana Isanta-Navarro. (2022). The joint effects of salt and 6PPD contamination on a freshwater herbivore, . *Science of The Total Environment*,, 829(154675,).
<https://doi.org/https://doi.org/10.1016/j.scitotenv.2022.154675>.
- Trotter, B., Wilde, M. V., Brehm, J., Dafni, E., Aliu, A., Arnold, G. J., Fröhlich, T., & Laforsch, C. (2021). Long-term exposure of *Daphnia magna* to polystyrene microplastic (PS-MP) leads to alterations of the proteome, morphology and life-history. *Sci Total Environ.*, 795.
<https://doi.org/10.1016/j.scitotenv.2021.148822>
- Turner, A., & Rice, L. (2010). Toxicity of tire wear particle leachate to the marine macroalga, *Ulva lactuca*, . *Environmental Pollution*,, 158(12), Pages 3650-3654,.
<https://doi.org/https://doi.org/10.1016/j.envpol.2010.08.001>.
- Union, E. P. a. C. o. t. E. (2013). Directive 2013/39/EU of the European Parliament and of the Council of 12 August 2013 Amending Directives 2000/60/EC and 2008/105/EC as Regards Priority Substances in the Field of Water Policy. <https://eur-lex.europa.eu/legal-content/EN/TXT/PDF/?uri=CELEX:32013L0039>
- Vannportalen. (2022). Miljømål i vannforskriften. <https://www.vannportalen.no/miljomal/miljomal2/>
- Ventura, D., S. Barbagallo, S. Consoli, M. Ferrante, M. Milani, F. Licciardello, & Cirelli, G. L. (2019). On the performance of a pilot hybrid constructed wetland for stormwater recovery in Mediterranean climate. *Water Science and Technology*, 79(6).
<https://doi.org/https://doi.org/10.2166/wst.2019.103>
- Vistnes, H. (2024). *Content and Treatment of Trace Elements and Organic Micropollutants in Tunnel Wash Water* [Norwegian University of Science and Technology]. Norway. <https://ntnuopen.ntnu.no/ntnu-xmloi/handle/11250/3166018>
- Vistnes, H., Sossalla, N. A., Uhl, W., Sundsøy, A. W., Asimakopoulos, A. G., Spahr, S., Escher, B. I., & Meyn, T. (2024). Effect of tunnel wash water treatment processes on trace elements, organic micropollutants, and biological effects. *Journal of Hazardous Materials*, 480(136363).
<https://doi.org/https://doi.org/10.1016/j.jhazmat.2024.136363>.
- Vogelsang, C., Lusher, A. L., Dadkhah, M. E., Sundvor, I., Umar, M., Ranneklev, S. B., Eidsvoll, D., & Meland, S. (2020). *Microplastics in road dust – characteristics, pathways and measures*. Miljødirektoratet.
<https://www.miljodirektoratet.no/globalassets/publikasjoner/m959/m959.pdf>
- Wagner, S., Hüffer T, Klöckner P, Wehrhahn M, Hofmann T, & T., R. (2018). Tire wear particles in the aquatic environment - A review on generation, analysis, occurrence, fate and effects. *Water research*. [https://doi.org/doi: 10.1016/j.watres.2018.03.051](https://doi.org/doi:10.1016/j.watres.2018.03.051).
- Wang, J., Liu, X., Liu, G., Zhang, Z., Wu, H., Cui, B., Bai, J., & Zhang, W. (2019). Size effect of polystyrene microplastics on sorption of phenanthrene and nitrobenzene, . *Ecotoxicology and Environmental Safety*,, 173, Pages 331-338,. <https://doi.org/https://doi.org/10.1016/j.ecoenv.2019.02.037>.
- Wang, Y., Fu, R., Li, X., Zhao, W., Liu, M., & Li, Y. (2023). Potential thyroid hormone disorder risks of tire antioxidants to aquatic food chain organisms after absorbing free radicals in marine and freshwater environments. *Aquatic Toxicology*

260. <https://doi.org/https://doi.org/10.1016/j.aquatox.2023.106587>
- Wik, A., & Dave, G. (2009). Occurrence and effects of tire wear particles in the environment – A critical review and an initial risk assessment, . *Environmental Pollution*,, 157(1), Pages 1-11,. <https://doi.org/https://doi.org/10.1016/j.envpol.2008.09.028>.
- Wikipedia. (2009, 10.01.2025). *Ekeberg tunnelen*. Wikipedia. https://no.wikipedia.org/wiki/Ekeberg_tunnelen
- Williams, R. L., & Cadle, S. H. (1978). Characterization of Tire Emissions Using an Indoor Test Facility. *Rubber Chemistry and Technology*, 51, 7-25. <https://doi.org/DOI:10.5254/1.3535728>
- Woo, S.-H., Jang, H., Mun, S.-H., Lim, Y., & Lee, S. (2022). Effect of treadwear grade on the generation of tire PM emissions in laboratory and real-world driving conditions, . *Science of The Total Environment*, 838. <https://doi.org/https://doi.org/10.1016/j.scitotenv.2022.156548>.
- Wright, S. L., Thompson, R. C., & Galloway, T. S. (2013). The physical impacts of microplastics on marine organisms: A review. *Environmental Pollution*,, 178, Pages 483-492,. <https://doi.org/https://doi.org/10.1016/j.envpol.2013.02.031>.
- Xuan, L., Ju, Z., Skonieczna, M., Zhou, P.-K., & Huang, R. (2023). Nanoparticles-induced potential toxicity on human health: Applications, toxicity mechanisms, and evaluation models. <https://doi.org/https://doi.org/10.1002/mco2.327>
- Yan, W., Wang, Q., Gao, Y., Xu, M., Li, H., Zhou, Y., Liu, C., & Xiao, Y. (2023). Coupling between Increased Amounts of Microplastics and Dissolved Organic Compounds in Water *Water* 15. <https://doi.org/https://doi.org/10.3390/w15234126>
- Yan Xia, Juan-Juan Zhou, Yan-Yan Gong, Zhan-Jun Li, & Eddy Y. Zeng. (2020). Strong influence of surfactants on virgin hydrophobic microplastics adsorbing ionic organic pollutants, . *Environmental Pollution*,, 265(1150261). <https://doi.org/https://doi.org/10.1016/j.envpol.2020.115061>.
- Youn, J., Kim YM, Siddiqui MZ, Watanabe A, Han S, Jeong S, Jung YW, & KJ., J. (2021). Quantification of tire wear particles in road dust from industrial and residential areas in Seoul, Korea. . *Sci Total Environ*. <https://doi.org/https://doi.org/10.1016/j.scitotenv.2021.147177>.
- Yu Wang, Xinao Li, Hao Yang, Yang Wu, Qikun Pu, Wei He, & Li, X. (2024). A review of tire wear particles: Occurrence, adverse effects, and control strategies. *Ecotoxicology and Environmental Safety*, 283. <https://www.sciencedirect.com/science/article/pii/S0147651324008583>
- Zhang, Hai-Yan, Huang, Z., Liu, Y.-H., Hu, L.-X., He, L.-Y., Liu, Y.-S., Zhao, J.-L., & Ying, G.-G. (2023). Occurrence and risks of 23 tire additives and their transformation products in an urban water system *Environment International*, 171. <https://doi.org/https://doi.org/10.1016/j.envint.2022.107715>
- Zhang, J., Peng J, Song C, Ma C, Men Z, Wu J, Wu L, Wang T, Zhang X, Tao S, Gao S, Hopke PK, & H., M. (2020). Vehicular non-exhaust particulate emissions in Chinese megacities: Source profiles, real-world emission factors, and inventories. . *Environmental Pollution*,, 266. <https://doi.org/https://doi.org/10.1016/j.envpol.2020.115268>
- Zhang, M., Yin, H., Tan, J., Wang, X., Yang, Z., Hao, L., Du, T., Niu, Z., & Ge, Y. (2023). A comprehensive review of tyre wear particles: Formation, measurements, properties, and influencing factors, . *Atmospheric Environment*,, 297(119597,). <https://doi.org/https://doi.org/10.1016/j.atmosenv.2023.119597>.
- Aasum, J.-H. (2013). *The effects of detergent (TK601) on the mobility of metals during sedimentation of tunnel wash water from the nordbytunnel at a motorway (E6) in Norway. - A laboratory experiment*. NMBU]. nmbu.brage.no. <https://nmbu.brage.unit.no/nmbu-xmlui/bitstream/handle/11250/189649/Aasum2013.pdf?sequence=1&isAllowed=y>

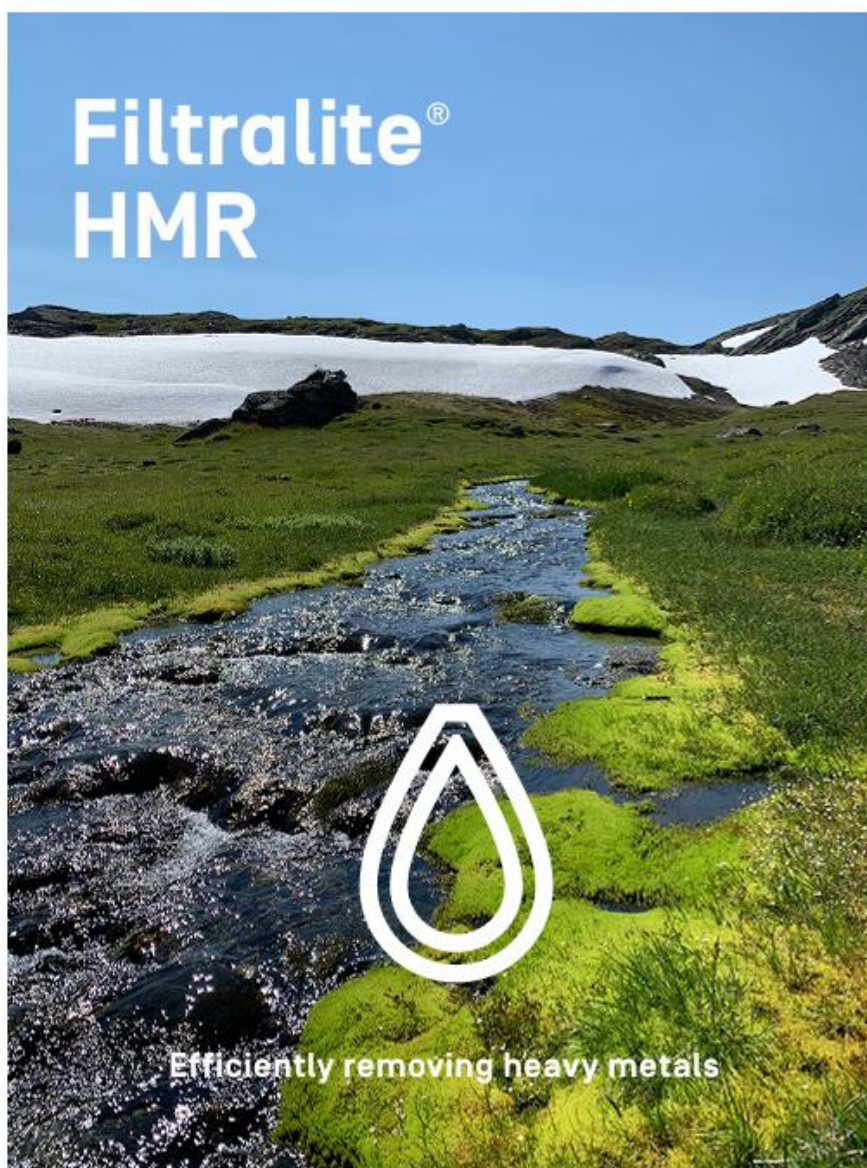
7.0 Appendix

The appendix presents selected datasets relevant to the study. Additional raw data can be made available upon request by contacting the author.

Appendix A: Filtralite® HMR Brochure

Filtralite® HMR - High-Performance Filter Media for Heavy Metal Removal

This brochure presents Filtralite® HMR, a thermally treated clay-based filter media engineered for efficient sorption of heavy metals from water. The document outlines the material composition, filtration performance, regeneration capacity, and comparative advantages.



Our purpose

Pure water is a necessity for human health and for protection of the environment. Heavy metals from drinking water, industry, mining, traffic, tunnels etc. can be purified and removed by sorption by a dedicated filter material.

Product description

Filtralite® HMR is a high quality filter media, manufactured by thermally treating selected clay minerals. Filtralite® HMR, with its extremely large mineral surface area, enables high sorption capacity towards charged particles. The clay consists of alumina silicates forming different clay minerals and is enriched with exchangeable cations in the mineral structure in addition to physio-chemical bonding capacity. Filtralite® HMR is produced in an industrial process to secure stability and reproducibility. The choice of clay mineral composition is unique for Filtralite® HMR and is selected to enhance maximum specific bonding capacity in addition to creating strong mechanical filter grains. This combination of optimized bonding capacity and mechanical strength is necessary to achieve a filter material which can be backwashed and regenerated at the water purification plant.



Why and how?

Heavy metals are found and transported in soil and water or released from industry, roads and cities into the environment. Although many heavy metals are common, most of them become toxic at high concentration. Thermally treated clays can be used for sorption of heavy metals due to their huge surface area and their cationic exchange capacity. Clays are not possible to use as filter material as is. We turn the clay to a practical and useable filter material which allows water to flow through the filter. By thermal treatment of our special clay, the Filtralite® HMR increase both the surface area as well as the volume of clay micropores and mesopores due to loss of water by dehydration and dehydroxylation. The enhanced surface area directly affects the number of adsorptive sites and thereby the sorption capacity. The thermal treatment is also to increase the lamellar interplanar distance of the the clay structure.

This process is called calcination and creates the increase of the surface area, ion exchange capacity and mechanical strong grains. The grains are then crushed and sieved to specific size suited for filtration of water and air. With this we are able to achieve the best of the clay sorption capacity and the filter hydraulic permeability. Our clay also balance pH in contact with water and will secure a neutral or high pH. For many metals an increase of sorption capacity is seen as the pH of the adsorbate solution increases.

Our clay also balance pH in contact with water and will ensure a neutral or high pH. Some effluents may have low pH and for many metals an increase of sorption capacity is seen as the pH of the adsorbate solution increases. The Filtralite® HMR therefore provides a large large surface area for physio-chemical sorption, ion-exchange capacity and is a pH modifier in one product.

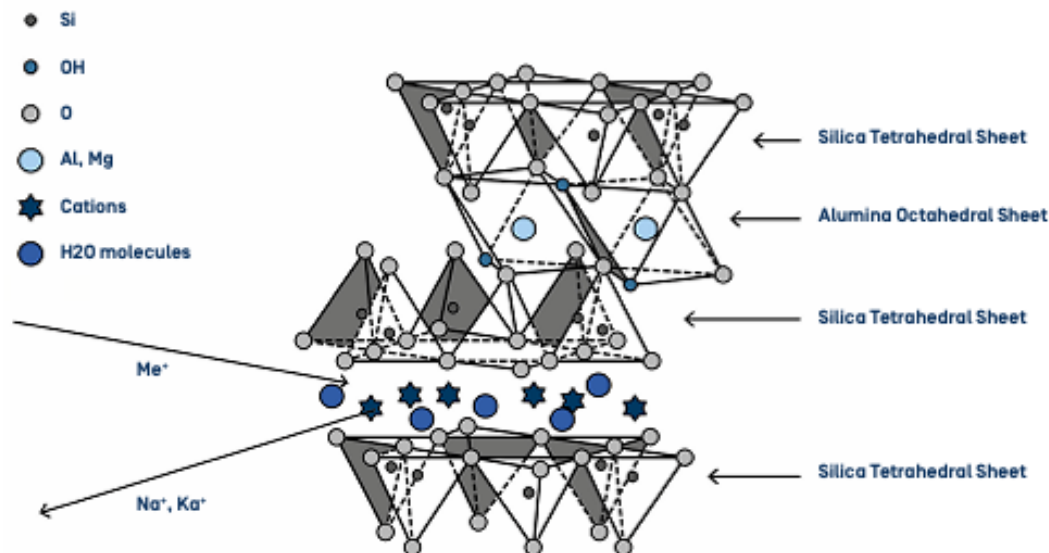


Figure 1. Schematic sketch of Filtralite® HMR. powerful chemical bonds form the alumina octahedral and silica tetrahedral sheets. Cations are held between the sheets by relatively weak electrostatic attraction and are exchangeable with metals.

Filtration capacity

Several laboratory studies, tests and full scale plant operations have resulted in remarkable, reproducible and consistent results.

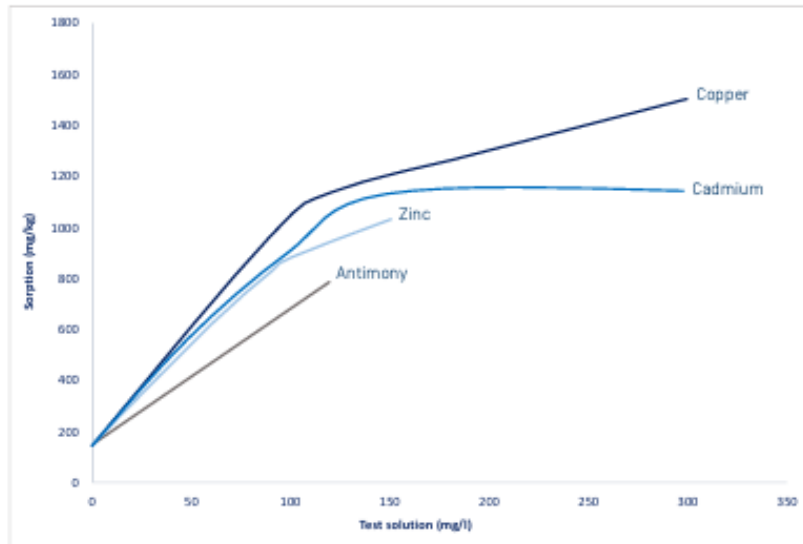
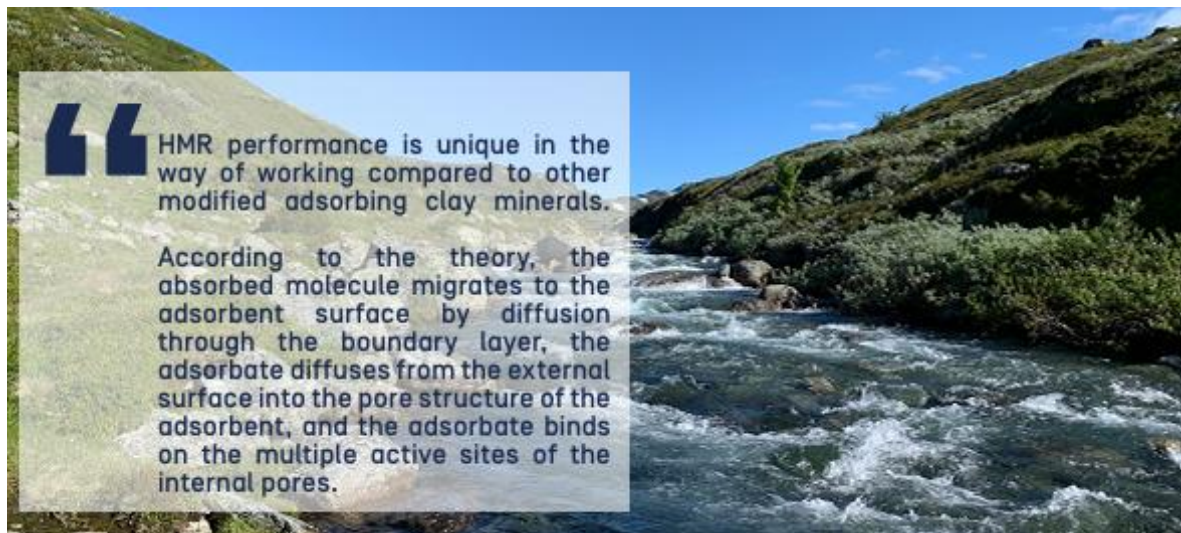


Figure 2. Batch experiments on 4 metals, 3 cations and 1 anion showing that Filtralite® HMR has high sorption capacity towards both cations and anions. Experiments executed at NMBU - Norwegian University of Life Sciences.



Studies comparing Filtralite® HMR and Granulated Activated Carbon (GAC) for different metals both cations and anions demonstrate the potential of removing dissolved metals from other polluted waters.

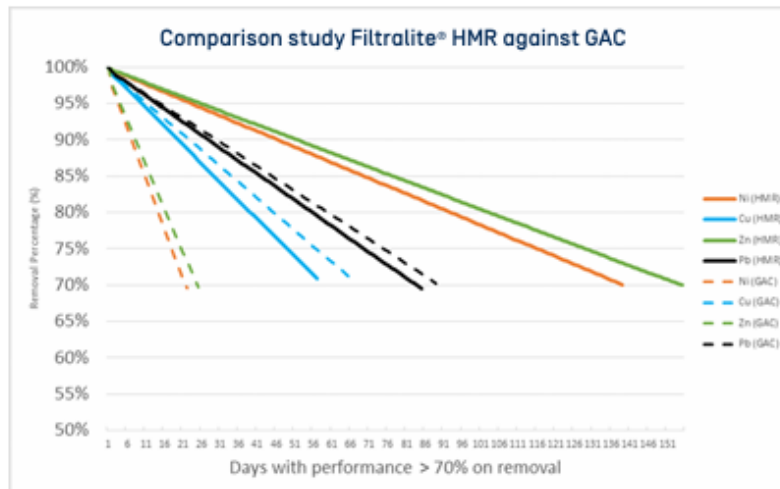


Figure 3. Comparison study at Norwegian University of Science and Technology, Trondheim Norway, of Filtralite® HMR and GAC for sorption of four different heavy metals. 1 ppm of four different metals are added into fresh water, filter retention time of 20 minutes. Results display the time the filter materials exceed 70% removal efficiency.

Isotherm for Filtralite® HMR for 4 metals at >70% removal

HMR	DAYS (>70% REMOVAL)	TOTAL G OF EACH CATION (RETAINED)	ISOTHERM G CATION /KG HMR	PERCENTAGES
Ni	139,3	4,02	12,22	32%
Cu	58,8	1,70	5,16	13%
Zn	154,8	4,46	13,58	35%
Pb	83,6	2,41	7,33	19%
TOTAL ISOTHERM (>70% REMOVAL)			38,30	100%

Isotherm for Granulated Activated Carbon (GAC) for 4 metals at >70% removal

GAC	DAYS (>70% REMOVAL)	TOTAL G OF EACH CATION (RETAINED)	ISOTHERM G CATION /KG HMR	PERCENTAGES
Ni	21,7	0,60	1,90	11%
Cu	68,1	1,96	5,98	33%
Zn	24,8	0,71	2,17	12%
Pb	89,8	2,59	7,88	44%
TOTAL ISOTHERM (>70% REMOVAL)			17,93	100%

Table 1 and 2. Comparison study of Filtralite® HMR and GAC for sorption of four different heavy metals. Into fresh water it is added 1 ppm of 4 different metals combined with filter retention time of 20 minutes. The table display the isotherms for each metal and the total sorption capacity as g cations/kg filter material.

At the specialized water treatment laboratory Ingeobras in Zaragoza we have conducted several experiments for removal of heavy metals from drinking water with excellent results.

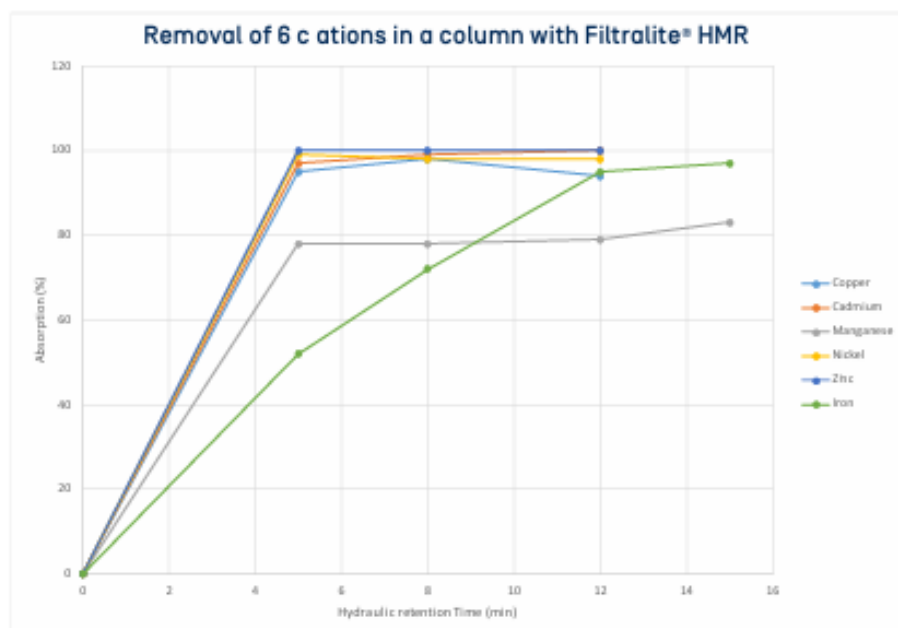


Figure 4. Tests conducted at an external laboratory: 500 ppb of metals in water at pH 7.5 and 15 CO₂.

The same laboratory came to the following maximum retention capacity of Filtralite® HMR for Iron and Zinc:

Maximum retention capacity of Iron is 59,76 g Fe³⁺ / kg Filtralite® HMR.

Maximum retention capacity of Zinc is 17,57 g Zn²⁺ / kg Filtralite® HMR.

Based on the experience from several purification plants and experimental results obtained and on the characteristics of Filtralite® HMR, we can confirm with enough certainty that the material has the capacity to adsorb metals, cations and anions, from the transition periods of the periodic table.

Periodic Table of the Elements

1 H Hydrogen 1.008	2 He Helium 4.003																	18 Ar Argon 39.948	19 K Potassium 39.098	20 Ca Calcium 40.078	21 Sc Scandium 44.956	22 Ti Titanium 47.88	23 V Vanadium 50.942	24 Cr Chromium 52.00	25 Mn Manganese 54.938	26 Fe Iron 55.845	27 Co Cobalt 58.933	28 Ni Nickel 58.693	29 Cu Copper 63.546	30 Zn Zinc 65.38	31 Ga Gallium 69.723	32 Ge Germanium 72.64	33 As Arsenic 74.922	34 Se Selenium 78.96	35 Br Bromine 79.904	36 Kr Krypton 83.80	37 Rb Rubidium 85.468	38 Sr Strontium 87.62	39 Y Yttrium 88.906	40 Zr Zirconium 91.224	41 Nb Niobium 92.906	42 Mo Molybdenum 95.94	43 Tc Technetium 98.00	44 Ru Ruthenium 101.07	45 Rh Rhodium 102.91	46 Pd Palladium 106.36	47 Ag Silver 107.87	48 Cd Cadmium 112.41	49 In Indium 114.82	50 Sn Tin 118.71	51 Sb Antimony 121.76	52 Te Tellurium 127.6	53 I Iodine 126.91	54 Xe Xenon 131.29	55 Cs Cesium 132.91	56 Ba Barium 137.33	57-71 Lanthanides	72 Hf Hafnium 178.49	73 Ta Tantalum 180.95	74 W Tungsten 183.84	75 Re Rhenium 186.21	76 Os Osmium 190.23	77 Ir Iridium 192.22	78 Pt Platinum 195.08	79 Au Gold 196.97	80 Hg Mercury 200.59	81 Tl Thallium 204.38	82 Pb Lead 207.2	83 Bi Bismuth 208.98	84 Po Polonium 209	85 At Astatine 210	86 Rn Radon 222	87 Fr Francium 223	88 Ra Radium 226	89-103 Actinides	104 Rf Rutherfordium 261	105 Db Dubnium 262	106 Sg Seaborgium 266	107 Bh Bohrium 264	108 Hs Hassium 277	109 Mt Meitnerium 268	110 Ds Darmstadtium 271	111 Rg Roentgenium 272	112 Cn Copernicium 285	113 Nh Nihonium 284	114 Fl Flerovium 289	115 Mc Moscovium 288	116 Lv Livermorium 293	117 Ts Tennessine 294	118 Og Oganesson 294	119 Lu Lutetium 174.967	120 Lr Lawrencium 260
-----------------------------	----------------------------	--	--	--	--	--	--	--	--	--	--	--	--	--	--	--	--	-----------------------------	--------------------------------	-------------------------------	--------------------------------	-------------------------------	-------------------------------	-------------------------------	---------------------------------	----------------------------	------------------------------	------------------------------	------------------------------	---------------------------	-------------------------------	--------------------------------	-------------------------------	-------------------------------	-------------------------------	------------------------------	--------------------------------	--------------------------------	------------------------------	---------------------------------	-------------------------------	---------------------------------	---------------------------------	---------------------------------	-------------------------------	---------------------------------	------------------------------	-------------------------------	------------------------------	---------------------------	--------------------------------	--------------------------------	-----------------------------	-----------------------------	------------------------------	------------------------------	----------------------	-------------------------------	--------------------------------	-------------------------------	-------------------------------	------------------------------	-------------------------------	--------------------------------	----------------------------	-------------------------------	--------------------------------	---------------------------	-------------------------------	-----------------------------	-----------------------------	--------------------------	-----------------------------	---------------------------	---------------------	-----------------------------------	-----------------------------	--------------------------------	-----------------------------	-----------------------------	--------------------------------	----------------------------------	---------------------------------	---------------------------------	------------------------------	-------------------------------	-------------------------------	---------------------------------	--------------------------------	-------------------------------	----------------------------------	--------------------------------

Applications

Typical applications are removal of dissolved metals from run-off water from trafficked areas, tunnels drainage water from mining, shooting ranges, agriculture, industry effluents etc.

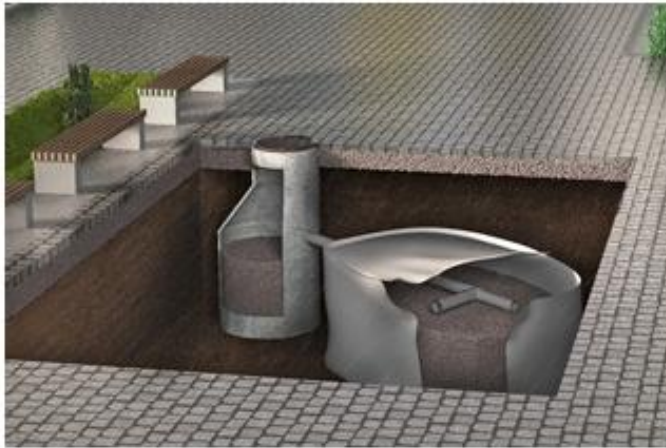


Figure 5. Possible solution with pre filtration to remove organics and a final filter with Filtralite® HMR.



Figure 6. Typical solution with pre filtration to remove organics and a final filter with Filtralite® HMR.



Figure 7. Typical filter solution with Filtralite® HMR.

“

The material strength, unlike conventional modified expanded clay is its enormous available adsorption surface. Under standard conditions (neutral Ph and 15 °C) the isotherm for Fe^{2+} dissolved adsorption is around 59 g Fe^{2+} /kg of HMR following Langmuir model.

How to regenerate Filtralite® HMR

Operational experiences have proven that after backwashing a partial recovery of the isotherm capacity come back. The selection of clay mineral composition and the specific and gentle designed heating process during manufacturing of Filtralite® HMR, generate filter grains which have perfect surface hardness for backwashing. While backwashing the filter, mechanical erosion scratches of some of the surface bonded particles and ions due to constant collision between the filter grains. The mechanical erosion is limited to the surface and do impact the filter grains very little. Dissolved ions which are bound to the filter material surface are removed together with filter dust and polluted particles. Polluted backwash water may be returned to pre-filtration for sedimentation as the heavy metal is now bound in particles. The backwash velocity can be set to 20-100 m/h based on local conditions with limited loss of filter material.

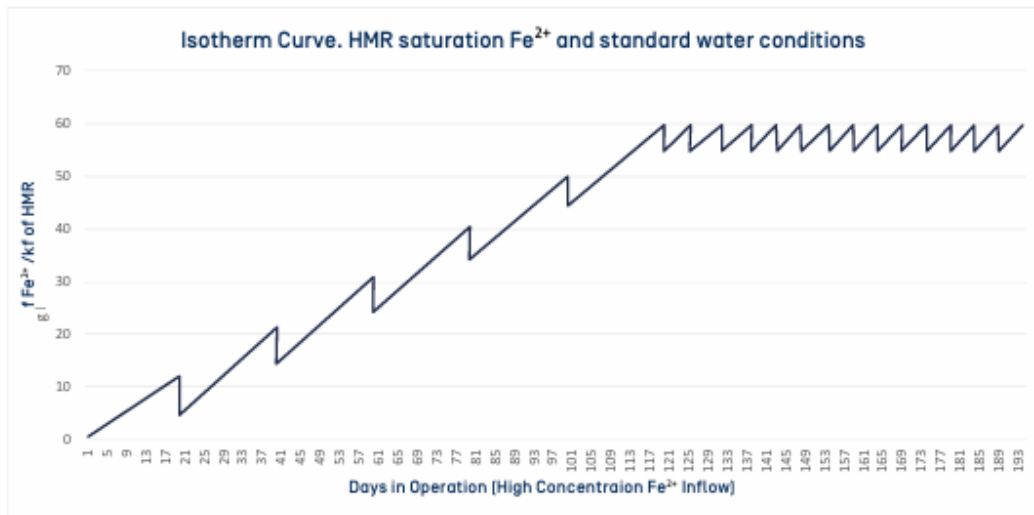
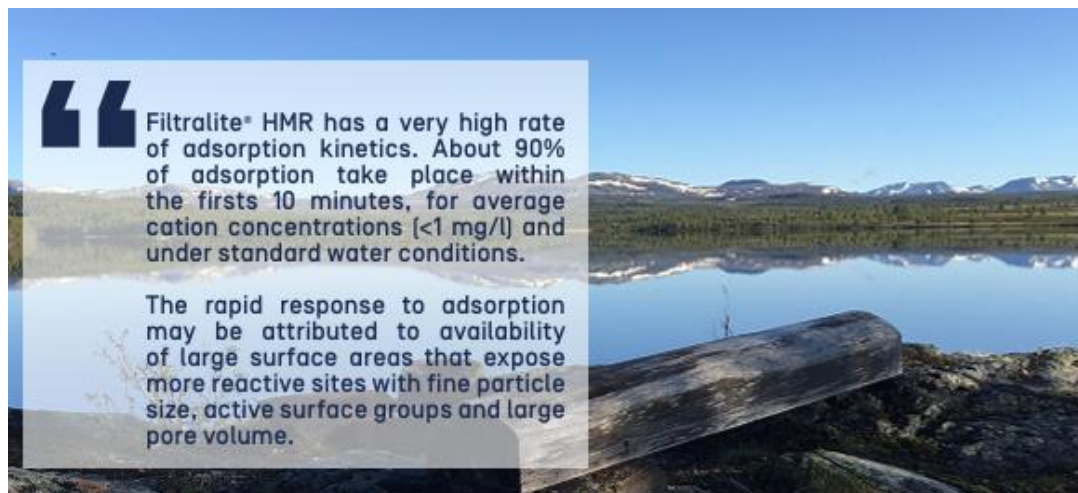


Figure 8. Tests conducted at Ingeobras Laboratory in Zaragoza Spain. Isotherm for sorption of Fe^{2+} and indication of regeneration after each backwash.



This regeneration effect could also be explained by a stochastic and intense movement of the filter material that creates new water flow lines. The water flow goes through new paths thanks to the microporous and mesoporous material structure. In addition to this effect the anions present in the backwashing water remove parts of the adsorbed cations. The cations removed are the ones with the weakest bounds to the Filtralite® HMR surface. This effect creates an extension of the isotherm capacity and has a positive impact on the material lifespan. In order to achieve the effect of replacement of cations by anions from the backwash water, it is necessary to use water with average values of alkalinity and hardness of drinking water.

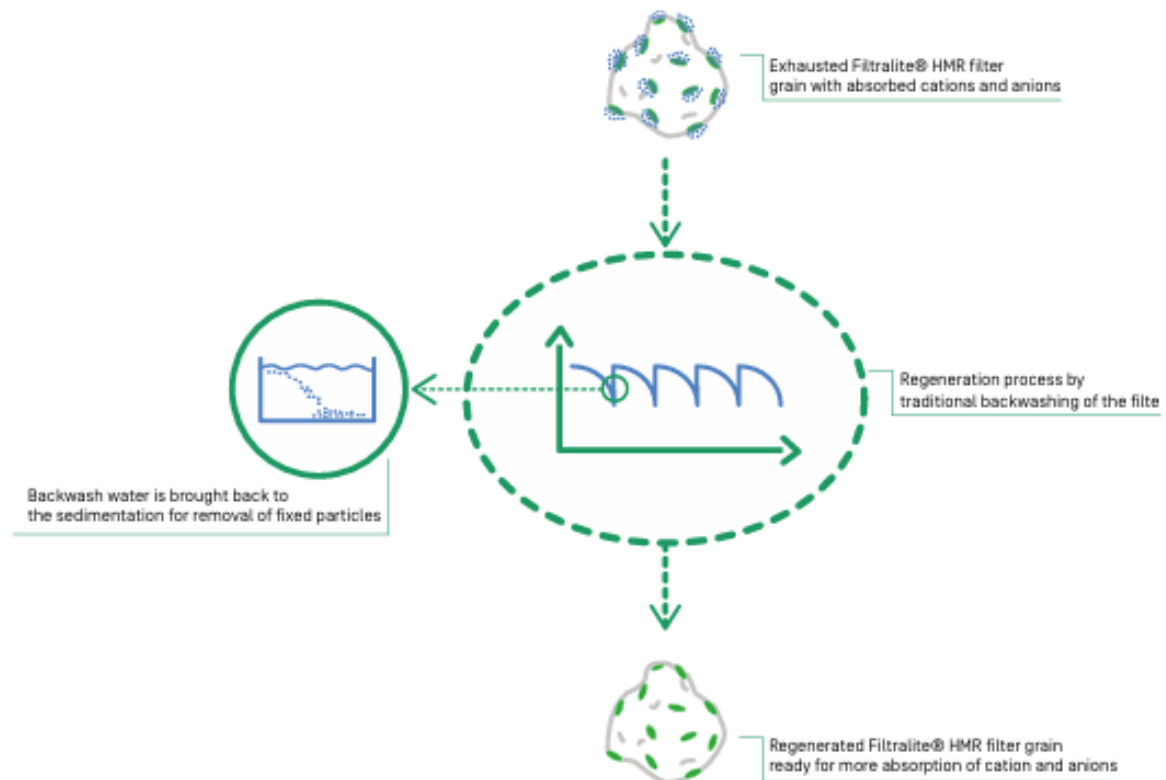


Figure 9. Schematic sketch of regeneration of exhausted Filtralite® HMR filter. During backwashing fixed cations and anions are removed with filter dust for settling in a pre-step like sedimentation. Backwashing with clean water with pH at about 7 has best effect on regeneration.



More about Filtralite®...

While Filtralite® HMR is made by carefully heating a selected clay, other Filtralite® filter media is made by heating clay to around 1200° C, followed by crushing and sieving. Dry particle densities in the range from 500 to 1.600 kg/m³ and aggregate size from 0 to 20 mm can be "tailor-made" for specific applications. In addition to its low density and high porosity, Filtralite® offer high abrasion and impact resistance.

Filtralite® develops and manufactures quality filter media for all water treatment applications:

- **Filtralite® Pure** for drinking water solutions, both for physical filtration and biological treatment.
- **Filtralite® Clean** for wastewater treatment, both for biological process and tertiary filtration.
- **Filtralite® Nature** for onsite water remediation.
- **Filtralite® Air** is a premium filtering product.
- **Filtralite® HMR** for cation and anion sorption.

FILTRALITE®

Contact information:

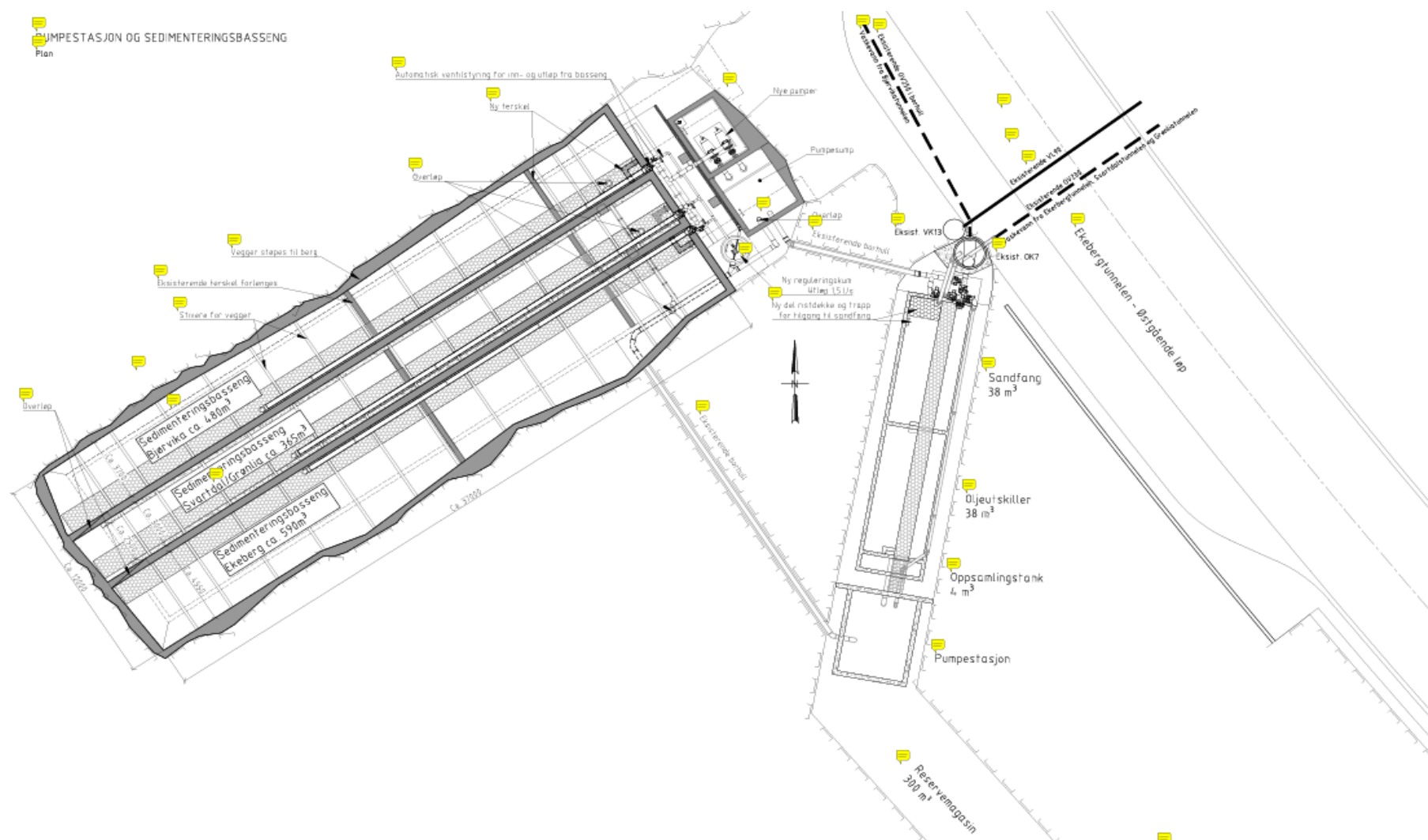
www.filtralite.com

Filtralite® is a Saint Gobain trademark

How to handle used Filtralite® filter media

For return of used material, please contact local Filtralite® organization

PLAN



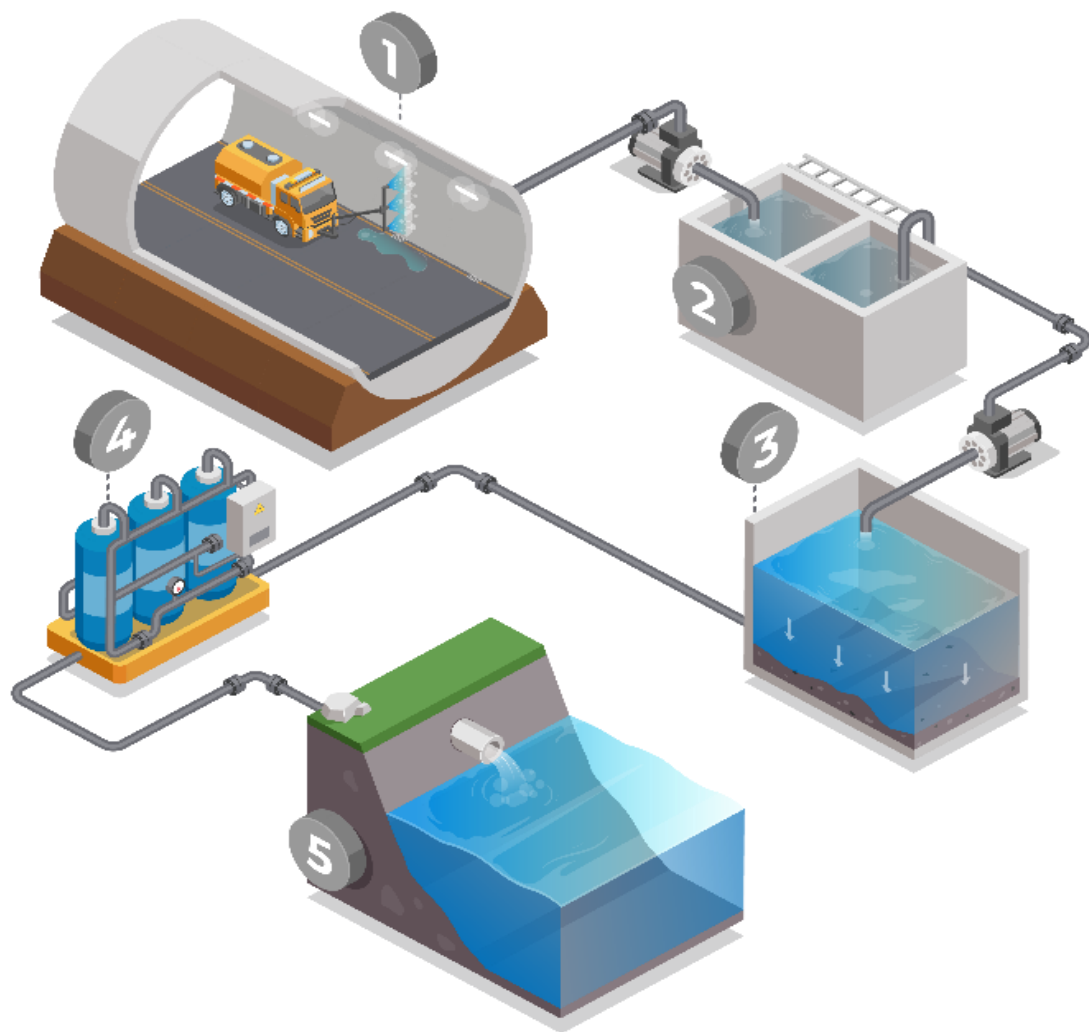


Figure B2: TWW cycle in the Ekeberg tunnel made by Ole Holthusen.

Appendix C: M7 medium

M7 medium (cultivation medium)

The Elendt M7 medium (10x) was prepared in 10-liter cans with distilled water. An air pump supplied air and the medium was kept in the dark. The medium was prepared at least 1 week before use.

Table: C1 M7 Medium stock solution 2

M7 Stock II Solution Recipe				
Chemical	mg/L	mL/0,5L	mL/L	10x (mL/L)
H ₃ BO ₃	57190	0,125	0,25	2,5
MnCl ₂	4584,585	0,125	0,25	2,5
LiCl	6120	0,125	0,25	2,5
RbCl	1420	0,125	0,25	2,5
SrCl ₂ *6H ₂ O	3040	0,125	0,25	2,5
NaBr	320	0,125	0,25	2,5
MoNa ₂ O ₄ *2H ₂ O	1260	0,125	0,25	2,5
CuCl ₂ *2H ₂ O	335	0,125	0,25	2,5
ZnCl ₂	260	0,5	1	10
CoCl ₂ *6H ₂ O	200	0,5	1	10
KI	65	0,5	1	10
Na ₂ SeO ₃	43,8	0,5	1	10
NH ₄ VO ₃	11,5	0,5	1	10
Fe-EDTA solution		2,5	5	50

Table C2: M7 Medium recipe.

M7 Media Recipe			
Stock	mL/L	mL/10L	mL/20L
Stock Solution II (10x)	5	50	100
CaCl ₂ *6H ₂ O	1	10	20
MgSO ₄ *7H ₂ O	0,5	5	10
KCl	0,1	1	2
NaHCO ₃	1	10	20
Na ₂ SiO ₃ *9H ₂ O	0,2	2	4
NaNO ₃	0,1	1	2
KH ₂ PO ₄	0,1	1	2
K ₂ HPO ₄	0,1	1	2
Vitamin Stock	0,01	0,1	0,2

Appendix D: EPA Medium

Table D1: Recipe for moderately hard water (EPA medium)

TABLE 7. PREPARATION OF SYNTHETIC FRESHWATER USING REAGENT GRADE CHEMICALS¹

	Reagent Added (mg/L) ²				Approximate Final Water Quality		
	NaHCO ₃	CaSO ₄ •2H ₂ O	MgSO ₄	KCl	pH ³	Hardness ⁴	Alkalinity ⁴
Very soft	12.0	7.5	7.5	0.5	6.4-6.8	10-13	10-13
Soft	48.0	30.0	30.0	2.0	7.2-7.6	40-48	30-35
Moderately Hard	96.0	60.0	60.0	4.0	7.4-7.8	80-100	57-64
Hard	192.0	120.0	120.0	8.0	7.6-8.0	160-180	110-120
Very hard	384.0	240.0	240.0	16.0	8.0-8.4	280-320	225-245

¹Taken in part from Marking and Dawson (1973).

²Add reagent grade chemicals to deionized water.

³Approximate equilibrium pH after 24 h of aeration.

⁴Expressed as mg CaCO₃/L.

Appendix E: Z8 Medium

Table E1: Recipe for Z8 medium for algae cultivation

Z8 medium (Z8) (Rippka 1988)

Freshwater algae and cyanobacteria

Preparation of stock solutions: [Solution A](#), [B](#), [C](#) and [Trace element](#)

N° solution Stock	Component	Mass (g) for 1 L	Final molar concentration mM
A	NaNO ₃	46.7	5.49
	Ca(NO ₃) ₂ •4H ₂ O	5.9	0.25
	or Ca(NO ₃) ₂	4.1	0.25
	MgSO ₄ •7H ₂ O	2.5	0.10
B	K ₂ HPO ₄	3.1	0.18
	or K ₂ HPO ₄ •3H ₂ O	4.1	0.18
	Na ₂ CO ₃	2.1	0.20

For stock solutions **A** and **B**

- Adjust to 1000 mL with mili-Q water
- Autoclave at 121°C for 15-20 minutes

N° solution Stock	Component	Mass (g) for 100 mL	Final molar concentration mM
C	C1 FeCl ₃ •6H ₂ O	2.80	0.01
	C2 EDTA : Ethylene diamine tetra-acetate xNa ₂ x 2H ₂ O	3.9	0.01

For stock solutions **C**

- Adjust **C1** and **C2** to 100 mL with mili-Q water, for **C2** microwave heating to dissolve
- Add 10 mL of **C1** and 9.5 mL of **C2** adjust to 1000 mL with mili-Q water
- Do not autoclave the **C1** and **C2** solution, keep at 4°C

Stock solution	Component	Mass (g) for 100 mL	Final molar concentration
Trace element Solution	T1 Na ₂ WO ₄ , 2H ₂ O	0,33	0.10 µM
	T2 (NH ₄) ₆ Mo ₇ O ₂₄ , 4H ₂ O	0,88	0.07 µM
	T3 KBr	1,21	1.02 µM
	T4 KI	0,83	0.50 µM
	T5 ZnSO ₄ , 7H ₂ O	2,87	1.00 µM
	T6 Cd (NO ₃) ₂ , 4H ₂ O	1,55	0.50 µM
	T7 Co (NO ₃) ₂ , 6H ₂ O	1,46	0.50 µM
	T8 CuSO ₄ , 5H ₂ O	1,25	0.50 µM
	T9 (NH ₄) ₂ Ni(SO ₄) ₂ , 6H ₂ O	1,98	0.50 µM
	T10 Cr(NO ₃) ₃ , 9H ₂ O	0,41	0.10 µM
	T11 Al ₂ (SO ₄) ₃ K ₂ SO ₄ , 24H ₂ O	4,74	0.50 µM
	T12 V ₂ O ₅	0,089 g for 1L	0.05 µM
	T13 H ₃ BO ₃ MnSO ₄ , 4H ₂ O	31 g for 1L 22,3 g for 1L	0.05 mM 0.01 mM

For stock solutions **Trace element Solution**

- Adjust **T1** to **T11** to 100 mL with mili-Q water
- Adjust **T12** to **T13** to 1000 mL with mili-Q water
- Add 1 mL of **T1** to **T11** and 10 mL of **T12** to **T13** adjust to 1000 mL with mili-Q water
- Autoclave at 121°C for 15-20 minutes

Preparation of Z8 medium with stock solutions:

N° solution Stock	Volume (mL) for 1 L
A	10
B	10
C	10
Trace element solution	1

- Adjust to 1000 mL with mili-Q water
- Optional: pH can be adjusted to 7 with about 0,5mL NaOH (1M) ou HCl (1M)
- Autoclave at 121°C for 15-20 minutes

Notes:

- For solid culture media :
 - prepare 250 mL of Z8 medium with 5 mL of solution A, B and C and 0,5mL of Trace element solution.
 - Prepare 250 mL of mili-Q water with 6 - 7 g/L of agar in a 500 mL bottle
 - Autoclave at 121°C for 15-20 minutes
 - Mix the 2 solutions under laminar flow hood
 - Place the medium in petri dishes and wait 24 hours before use.
- For semi - solid culture media, add 5 g/L of agar

Appendix F: RAMP - Road associated microplastic

Table F1: Mean and SD from SBR+BR, TRWP and TWP in AG and GF fractions

Sample names	size	Treatment	M4 SBR+BR Mean µg/L	M4 SBR+BR SD µg/L	TRWP Mean mg/L	TRWP SD mg/L	TWP Mean mg/L	TWP std mg/L	A G G F	Particles >5µm Particles 0.4- 5µm
Spring	AG	Untreated-1	2578,805196	805,3032102	48,412846	15,1182495	24,20642314	7,5591247		
Spring	AG	Untreated-2	2882,786988	91,81237374	54,119607	1,72362702	27,05980341	0,8618135		
Spring	AG	Untreated-3	3293,215185	330,0629335	61,824724	6,19639129	30,9123622	3,0981956		
Spring	GF	Untreated-1	894,2100422	360,9429712	16,787330	6,77611345	8,393664899	3,3880567		
Spring	GF	Untreated-2	686,6399033	0	12,890540	2	6,445270108	2,1294929		
Spring	GF	Untreated-3	471,5687553	258,3074301	8,852931	4,84929917	4,426465732	3		
Spring	AG	Treated-1	300,3032264	45,3939926	5,637702	0,85219790	2,818850752	2,4246495		
Spring	AG	Treated-2	350,2014997	45,48701259	6,574460	0,85394420	3,287229953	0,3479083		
Spring	AG	Treated-3	415,8906112	176,1365236	7,807665	1,60194482	3,903832724	0,3486212		
Spring	GF	Treated-1	0	0	0,000000	7	0	61		
Spring	GF	Treated-2	0	0	0,000000	0	0	1,3499443		
Spring	GF	Treated-3	279,5702436	53,14806775	5,248474	0,99776797	2,624236846	79		
Spring	AG	Filtered-1	184,42068	13,31470242	3,462196	0,24996174	1,731098196	0,4988839		
						3		87		
								0,1020464		
								54		

	Spring							0,1180770
Spring	AG	Filtered-2	165,216799	22,39846007	3,302545	0,33397238	1,651272692	67
	Spring							0,1924764
Spring	AG	Filtered-3	172,644932	25,11372029	3,241126	0,47146899	1,620562993	09
	Spring							
Spring	GF	Filtered-1	0	0	0,000000	0	0	0
	Spring							
Spring	GF	Filtered-2	0	0	2,754425	0	0	0
	Spring							
Spring	GF	Filtered-3	0	0	0,000000	0	0	0
	Autum	Untreated				4,97740178		2,4887008
Autum	AG	-1	3335,097609	815,7464886	20,349607	1	10,1748037	91
	Autum	Untreated				9,26503272		4,6325163
Autum	AG	-2	7081,70299	1518,446419	43,210092	5	21,60504616	62
	Autum	Untreated						1,5542524
Autum	AG	-3	6158,877841	509,4529422	37,579334	3,10850493	18,78966686	65
	Autum	Untreated				0,14967201		0,0748360
Autum	GF	-1	381,6657743	24,52974941	2,328792	2	1,164396005	06
	Autum	Untreated				0,24353918		0,1217695
Autum	GF	-2	375,2809912	39,91364277	2,289834	7	1,14491714	93
	Autum	Untreated				0,50777993		0,2538899
Autum	GF	-3	429,4027411	83,22006467	2,620066	4	1,310033202	67
	Autum							0,0242833
Autum	AG	Treated-1	213,2782616	7,959593389	1,301350	0,048567	0,650674942	37
	Autum							0,1832070
Autum	AG	Treated-2	345,9726655	60,05161059	2,111005	0,366414	1,055502528	37
	Autum							0,3716999
Autum	AG	Treated-3	422,4635116	121,8358329	2,577726	0,743400	1,288862817	71
	Autum							0,2242721
Autum	GF	Treated-1	222,6255944	0	1,358384	0,000000	0,679192032	63
	Autum							0,3636516
Autum	GF	Treated-2	360,9817707	0	2,202585	0,000000	1,101292702	4

	Autum							0,4771211
Autum	GF	Treated-3	350,8743372	156,3907987	2,140913	0,954242	1,070456677	71
	AutumA					0,08970494		0,0448524
Autum	G	Filtered-1	110,1426548	14,7017455	0,672052	5	0,336026115	73
	AutumA					0,16390564		0,0819528
Autum	G	Filtered-2	102,9114941	26,86249912	0,627930	1	0,313965099	2
	AutumA					0,08355257		0,0417762
Autum	G	Filtered-3	139,1481221	13,69343361	0,849034	6	0,424516759	88
	AutumG							
Autum	F	Filtered-1	0	0	0,000000	0	0	0
	AutumG					0,08468104		0,0423405
Autum	F	Filtered-2	101,3110703	13,87837891	0,618165	8	0,309082484	24
	AutumG							
Autum	F	Filtered-3	83,57837688	0	0,509966	0	0,254983115	0

Appendix G: Tire Derived Chemicals

Table G1 : All tire derived chemicals analyzed in total water and centrifuged water with mean and SD in nanograms/L.

Season	Analysis Type	Samples	6PPD Mean	6PPD SD	6PPD Q Mean	6PPD Q SD	DPPD Mean	DPPD SD	IPPD Mean	IPPD SD	CPPD Mean	CPPD SD	7PPD Mean
Spring	Total Water	Untreated-1	6533,5	591,8	2090,5	72,8	2160,5	154,9	73,0	9,9	51,0	15,6	100,0
Spring	Total Water	Untreated-2	6895,5	337,3	2134,5	205,8	2083,5	78,5	66,5	4,9	36,5	10,6	94,0
Spring	Total Water	Untreated-3	5563,0	475,2	1652,5	70,0	1706,0	73,5	51,0	8,5	25,4	9,3	77,5
Spring	Centrifuged water	Untreated-1	1042,7	2,6	968,6	108,0	433,5	36,0	10,8	1,3	4,5	0,1	59,0
Spring	Centrifuged water	Untreated-2	1126,7	56,9	1094,5	123,8	442,5	33,2	14,3	2,7	4,1	1,4	63,0
Spring	Centrifuged water	Untreated-3	992,4	177,6	992,0	22,4	384,8	32,0	14,2	1,0	4,4	0,2	58,8
Spring	Total Water	Treated-1	787,7	96,6	644,0	78,1	99,7	9,2	6,0	0,6	3,2	0,6	76,5
Spring	Total Water	Treated-2	1135,7	82,2	705,2	55,4	207,7	11,2	17,3	0,7	7,9	0,4	49,0
Spring	Total Water	Treated-3	1246,8	112,0	768,7	55,0	250,6	15,8	18,2	1,7	4,7	2,7	37,5
Spring	Centrifuged water	Treated-1	439,4	28,5	622,2	27,9	40,1	0,5	4,0	0,1	2,5	0,1	53,9
Spring	Centrifuged water	Treated-2	596,4	28,1	862,9	37,1	69,3	3,4	10,1	1,0	3,3	0,1	45,0
Spring	Centrifuged water	Treated-3	561,7	53,8	881,9	122,7	73,2	3,0	9,7	0,8	3,1	0,5	33,3

Sprinkler	Total Water	Filtered-1	659,5	24,7	609,7	13,2	61,2	5,9	6,5	1,0	4,1	0,7	22,1
Sprinkler	Total Water	Filtered-2	737,6	67,3	707,2	60,2	66,4	3,1	7,7	0,1	4,5	0,7	27,2
Sprinkler	Total Water	Filtered-3	699,7	10,3	655,3	66,9	60,9	3,8	7,6	0,0	3,0	1,1	27,2
Sprinkler	Centrifuged water	Filtered-1	350,6	8,6	672,5	65,4	16,4	0,1	3,5	0,7	2,2	0,1	18,0
Sprinkler	Centrifuged water	Filtered-2	414,1	24,8	811,5	35,8	17,5	0,3	4,0	0,2	2,3	0,1	22,8
Sprinkler	Centrifuged water	Filtered-3	408,5	2,9	798,4	15,5	17,4	0,2	3,7	0,4	2,4	0,2	23,8
Autumn	Total Water	Untreated-1	1611,0	243,2	901,8	58,3	222,3	58,3	17,8	10,3	15,0	0,0	15,0
Autumn	Total Water	Untreated-2	2464,8	29,3	1214,0	29,7	451,3	31,5	23,0	2,1	15,0	0,0	15,0
Autumn	Total Water	Untreated-3	2090,5	65,8	1055,0	60,8	370,5	17,0	24,0	10,6	15,0	0,0	15,0
Autumn	Centrifuged water	Untreated-1	144,6	72,8	400,3	433,1	157,6	1,5	1,1	1,3	1,0	0,0	1,0
Autumn	Centrifuged water	Untreated-2	217,9	72,8	689,5	433,1	214,8	1,5	2,5	1,3	1,0	0,0	1,0
Autumn	Centrifuged water	Untreated-3	176,5	2,1	391,8	12,9	250,9	5,8	1,6	0,0	1,0	0,0	1,0
Autumn	Total Water	Treated-1	489,0	15,3	756,1	21,9	121,9	12,6	5,0	0,0	5,0	0,0	5,0
Autumn	Total Water	Treated-2	730,6	38,5	789,9	60,7	187,4	12,4	6,1	1,6	5,0	0,0	5,0
Autumn	Total Water	Treated-3	796,2	69,6	818,0	84,3	220,9	20,8	7,4	3,1	5,0	0,0	5,0
Autumn	Centrifuged water	Treated-1	46,5	13,2	127,1	34,7	66,7	14,1	0,5	0,0	0,5	0,0	0,5

Autu m	Centrifuged water	Treated- 2	65,6	12,8	187,1	45,8	124,9	15,3	0,3	0,3	0,5	0,0	0,5
Autu m	Centrifuged water	Treated- 3	97,5	3,4	249,6	100,3	130,9	2,0	0,6	0,1	0,5	0,0	0,5
Autu m	Total Water	Filtered-1	329,1	16,3	421,8	18,4	29,8	9,6	5,0	0,0	5,0	0,0	5,0
Autu m	Total Water	Filtered-2	323,8	10,7	437,2	24,9	33,3	1,3	5,0	0,0	5,0	0,0	5,0
Autu m	Total Water	Filtered-3	310,0	37,9	420,1	49,9	35,5	8,1	5,0	0,0	5,0	0,0	5,0
Autu m	Centrifuged water	Filtered-1	43,1	4,8	113,3	45,7	16,5	3,3	0,5	0,0	0,5	0,0	0,5
Autu m	Centrifuged water	Filtered-2	45,5	20,2	167,4	96,6	23,4	8,8	0,5	0,0	0,5	0,0	0,5
Autu m	Centrifuged water	Filtered-3	43,3	11,5	163,0	141,7	22,5	2,9	0,5	0,0	0,5	0,0	0,5

Seas on	Analysis Type	Samples	7PPD SD	HMMM Mean	HMMM SD	DPG Mean	DPG SD	TMQ Mean	TMQ SD	MTBT Mean	MTBT SD	PhBT Mean	PhBT SD
Sprin g	Total Water	Untreated -1	21,2	12768,5	265,2	83250,0	6010,4	2292,5	68,6	113,6	43,0	2749,0	209,3
Sprin g	Total Water	Untreated -2	2,8	13588,0	521,8	81000,0	10606,6	2511,0	72,1	99,7	17,8	2723,0	479,4
Sprin g	Total Water	Untreated -3	0,7	12047,0	124,5	69500,0	4949,7	1769,0	367,7	118,5	17,5	2079,5	784,2
Sprin g	Centrifuged water	Untreated -1	7,8	9800,0	495,0	84375,0	6894,3	256,8	13,1	87,7	2,5	160,1	10,0
Sprin g	Centrifuged water	Untreated -2	6,8	10027,5	371,2	98000,0	1767,8	288,9	54,9	97,7	7,2	167,8	9,8
Sprin g	Centrifuged water	Untreated -3	0,6	9895,0	77,8	84500,0	5303,3	297,6	2,3	84,5	2,2	206,4	89,7
Sprin g	Total Water	Treated-1	9,2	10041,8	1167,0	13525,0	1859,7	108,5	22,8	72,9	7,5	313,9	21,4

Sprin													
g	Total Water	Treated-2	2,5	10426,7	567,5	72345,0	4999,2	262,6	18,7	66,1	6,6	314,7	43,4
Sprin													
g	Total Water	Treated-3	2,7	10137,3	601,2	82090,0	6477,1	574,5	6,6	59,3	6,1	312,7	75,4
Sprin													
g	Centrifuged water	Treated-1	2,4	9868,8	279,3	16192,5	1796,1	45,2	5,5	59,6	1,3	33,7	0,9
Sprin													
g	Centrifuged water	Treated-2	1,8	13770,0	852,1	99645,0	6984,4	96,0	2,7	79,6	3,0	42,2	13,3
Sprin													
g	Centrifuged water	Treated-3	3,7	12972,5	1815,5	110395,0	16394,3	301,9	17,7	86,4	5,1	36,3	2,2
Sprin													
g	Total Water	Filtered-1	0,4	9266,8	207,3	21690,0	2050,6	442,0	11,3	127,0	11,3	376,0	6,5
Sprin													
g	Total Water	Filtered-2	1,4	10591,0	737,1	28975,0	2128,4	489,0	39,9	138,3	9,5	427,6	48,6
Sprin													
g	Total Water	Filtered-3	2,5	9906,0	685,9	28630,0	3054,7	453,0	84,0	128,5	8,1	365,9	15,1
Sprin													
g	Centrifuged water	Filtered-1	0,5	9935,6	1096,9	24486,9	2161,1	244,2	9,6	112,5	3,7	40,1	1,1
Sprin													
g	Centrifuged water	Filtered-2	0,8	12585,0	348,3	37647,5	1481,4	255,6	2,1	121,1	2,9	45,5	3,9
Sprin													
g	Centrifuged water	Filtered-3	0,6	12115,6	271,4	39302,5	724,8	250,1	1,9	120,3	1,3	42,0	1,2
Autu		Untreated											
m	Total Water	-1	0,0	603,3	3,2	25025,0	1944,5	74,0	4,9	302,5	10,6	50,0	0,0
Autu		Untreated											
m	Total Water	-2	0,0	544,0	50,9	30850,0	1767,8	162,0	1,4	332,8	7,4	50,0	0,0
Autu		Untreated											
m	Total Water	-3	0,0	481,3	30,8	30025,0	459,6	110,0	7,8	298,5	43,8	50,0	0,0
Autu		Untreated											
m	Centrifuged water	-1	0,0	280,5	50,9	18902,5	7265,5	18,6	15,8	215,4	67,5	5,7	0,6
Autu		Untreated											
m	Centrifuged water	-2	0,0	252,0	50,9	21012,5	7265,5	24,5	15,8	259,6	67,5	6,8	0,6

Autu	Centrifuged	Untreated											
m	water	-3	0,0	201,3	16,6	31175,0	4348,7	16,8	1,0	203,3	0,4	6,7	0,2
Autu													
m	Total Water	Treated-1	0,0	433,8	28,8	18650,0	947,5	494,6	18,1	192,7	0,7	20,0	0,0
Autu													
m	Total Water	Treated-2	0,0	391,3	30,4	24178,0	1326,5	661,3	111,0	159,3	4,4	20,0	0,0
Autu													
m	Total Water	Treated-3	0,0	361,6	5,7	29550,0	4963,9	788,8	111,2	182,2	5,4	20,0	0,0
Autu	Centrifuged												
m	water	Treated-1	0,0	58,3	14,1	1856,3	76,0	18,1	0,3	49,5	7,4	3,1	0,9
Autu	Centrifuged												
m	water	Treated-2	0,0	61,4	38,0	1070,9	117,9	34,3	8,2	75,0	7,8	2,8	0,4
Autu	Centrifuged												
m	water	Treated-3	0,0	74,7	11,2	1958,0	495,7	38,6	1,9	88,5	13,1	3,0	0,5
Autu													
m	Total Water	Filtered-1	0,0	225,7	8,1	4990,0	410,1	296,6	6,2	134,7	4,7	20,0	0,0
Autu													
m	Total Water	Filtered-2	0,0	242,8	2,0	7260,0	56,6	383,0	45,5	149,8	5,1	20,0	0,0
Autu													
m	Total Water	Filtered-3	0,0	225,9	24,5	5920,0	707,1	373,0	69,0	132,6	26,6	20,0	0,0
Autu	Centrifuged												
m	water	Filtered-1	0,0	34,4	12,6	555,0	109,6	21,2	6,9	56,9	23,5	2,5	0,4
Autu	Centrifuged												
m	water	Filtered-2	0,0	39,1	20,7	610,0	42,4	24,9	9,5	75,5	36,4	2,8	0,3
Autu	Centrifuged												
m	water	Filtered-3	0,0	27,4	17,5	547,5	381,8	24,7	16,9	70,6	44,7	2,1	0,1

Appendix H: Metals

Table H1 : All metals analyzed in total water and in 0,45 micrometer filter with mean and SD in mg/l and micrograms/L.

Sea son	Type	Treatme nt stage	Al		V		Cr		Mn		Fe		Co		Ni	
			Mean mg/L	Al SD mg/L	Mean ug/L	V SD ug/L	Mean ug/L	Cr SD ug/L	Mean ug/L	Mn SD ug/L	Mean mg/L	Fe SD mg/L	Mean ug/L	Co SD ug/L	Mean ug/L	Ni SD ug/L
Spri ng	Total	Untreate	13,225	0,5227	32,529	0,7768	43,726	1,3081	341,421	6,1047	14,0547	0,2077	11,766	0,1151	25,580	1,1562
	Water	d-1	21490	20124	32834	1264	2738	33584	1740	18999	3902	96095	60635	20279	2165	0512
Spri ng	Total	Untreate	12,845	0,8012	31,350	2,2972	45,257	2,6669	342,581	11,115	13,9034	0,6349	11,607	0,2447	28,238	3,3955
	Water	d-2	55806	39206	74204	7547	1225	67296	0220	14124	2982	12604	19697	63421	8681	9176
Spri ng	Total	Untreate	13,104	0,6981	31,571	0,9687	50,877	6,7008	346,859	11,367	14,1647	0,6392	11,883	0,4094	38,188	10,355
	Water	d-3	53693	92962	04389	1886	6408	82753	9353	73987	7953	64629	93841	85833	2535	6667
Spri ng	0.45	Untreate	0,0771	0,0355	2,0185	0,0407	9,0480	4,5167	109,426	3,3366	0,11691	0,0373	4,2239	0,0615	26,588	11,636
	µm	d-1	62903	17697	26807	5469	2351	81144	3533	58617	8412	12130	86389	78445	1132	8317
Spri ng	0.45	Untreate	0,0829	0,0204	1,9063	0,0979	28,194	13,073	104,554	3,6338	0,10526	0,0094	4,1037	0,1540	76,237	33,879
	µm	d-2	73785	66652	96367	6837	9941	12090	5066	52043	9436	23395	99419	76131	838	417
Spri ng	0.45	Untreate	0,0716	0,0262	1,8785	0,0503	9,7579	7,6346	104,091	3,0445	0,09286	0,0069	4,0072	0,1266	27,249	20,204
	µm	d-3	04454	78656	70010	9359	696	46190	0351	02028	9172	54463	65281	72580	0029	4573
Spri ng	Total	Treated-	0,7479	0,0244	2,7821	0,0847	2,5585	0,0854	139,165	2,6273	0,88042	0,0327	4,9200	0,0515	7,5416	0,0883
	Water	1	17391	91593	00723	1837	1032	97269	2274	68421	8544	18429	05168	33140	2831	8047
Spri ng	Total	Treated-	1,8157	0,0714	5,2302	0,1702	6,0166	0,8927	158,349	1,8020	1,93323	0,0405	5,7453	0,0531	10,469	1,8442
	Water	2	19619	21000	34405	8110	1283	52318	0131	98189	3526	35360	75400	11220	4627	9667
Spri ng	Total	Treated-	2,5669	0,3216	6,7019	0,7934	7,6907	1,0054	163,622	20,854	2,68537	0,3422	5,6797	0,7212	10,287	1,3311
	Water	3	80327	96038	20189	4793	6031	45214	0703	57963	2425	41662	27458	14515	3761	6998
Spri ng	0.45	Treated-	0,0436	0,0027	1,4908	0,1164	1,0922	0,4156	125,388	5,5011	0,25344	0,0326	4,5161	0,2212	7,1657	1,0372
	µm	1	58623	76651	14699	8574	676	26634	9828	02196	8737	45118	88669	31512	4533	3328
Spri ng	0.45	Treated-	0,0832	0,0791	1,7903	0,1321	0,9451	0,0282	137,467	10,658	0,63357	0,0529	4,7375	0,3285	7,4329	0,5338
	µm	2	62029	23054	39067	4273	8751	45800	9769	81659	0399	34198	92835	48780	957	3183

Spri	0.45	Treated-	0,0394	0,0004	1,8914	0,0523	1,0127	0,0910	146,293	3,2207	0,79156	0,0136	4,9368	0,1481	8,1877	0,1017
ng	µm	3	67504	64400	64510	8748	921	54252	7283	20597	5792	48611	49199	42801	6317	3091
Spri	Total	Filtered-	1,2737	0,0200	7,6509	0,1957	3,7640	0,0788	423,151	9,4626	1,17160	0,0226	6,1026	0,1384	12,048	0,2909
ng	Water	1	66374	90315	54224	3173	1021	10247	4428	54285	9544	38351	46324	49618	7863	8199
Spri	Total	Filtered-	1,2851	0,0996	7,3970	0,0537	4,3641	0,6706	414,313	5,3132	1,20278	0,0237	6,1470	0,0476	12,695	1,4213
ng	Water	2	07865	00253	23577	3110	991	87513	2653	69709	9655	14802	48335	09972	3086	743
Spri	Total	Filtered-	1,2747	0,0228	6,8827	0,0920	3,8872	0,1060	396,974	4,4316	1,18510	0,0221	5,9980	0,0612	11,514	0,0705
ng	Water	3	69432	20152	55069	7057	2927	22228	6622	52961	0008	60822	13910	00945	5066	8079
Spri	0.45	Filtered-	0,0471	0,0074	5,0521	0,3001	0,9020	0,0959	390,126	20,554	0,26239	0,0168	5,2873	0,3132	10,403	0,6096
ng	µm	1	06560	84705	69655	8092	2664	22130	1207	74856	1626	52584	60307	39212	181	0594
Spri	0.45	Filtered-	0,0423	0,0019	5,3024	0,1254	0,9613	0,0103	404,264	3,1712	0,27167	0,0016	5,5047	0,0208	10,700	0,0207
ng	µm	2	93929	31154	42971	9893	9154	95044	9798	33691	2479	76341	74896	33111	4861	6241
Spri	0.45	Filtered-	0,0539	0,0202	4,4962	0,1429	0,9798	0,0976	375,327	1,0311	0,28731	0,0031	5,3336	0,0233	9,8998	0,0808
ng	µm	3	22722	51202	38368	3278	719	07563	9705	04911	604	88633	75805	05952	7652	757
Aut	Total	Untreate	2,4879	0,3780	7,4141	0,5804	14,464	2,4388	307,947	8,1395	6,01954	0,3269	4,4657	0,7807	16,284	3,1004
um	Water	d-1	00434	1502	25737	3348	3893	96878	9089	03136	1168	32962	6899	07275	9157	9555
Aut	Total	Untreate	6,4198	0,7720	18,225	0,9260	31,768	1,7014	359,367	8,0068	11,0892	0,3668	5,9478	0,1702	20,071	0,9411
um	Water	d-2	19783	30779	06922	2598	4072	94188	1701	05471	538	07119	0151	49394	5688	9373
Aut	Total	Untreate	6,1290	0,3470	18,746	0,6450	32,504	1,5358	356,371	15,908	11,1542	0,6988	5,5373	0,3955	18,631	1,2938
um	Water	d-3	64193	43582	25019	7407	9961	24709	0745	96299	6287	98853	18483	0675	1019	4503
Aut	0.45	Untreate	0,0312	0,0017	1,2442	0,1010	1,0640	0,1806	232,984	21,556	0,90310	0,0633	1,9312	0,2070	7,3605	2,1005
um	µm	d-1	08869	65943	61088	0224	4743	86676	6819	16608	6077	44754	9826	58446	9076	9377
Aut	0.45	Untreate	0,0314	0,0014	1,4124	0,0534	1,0470	0,1051	216,583	9,4261	0,77199	0,0180	2,0166	0,0751	6,2392	0,2213
um	µm	d-2	29687	81446	49254	9734	3424	72956	6649	46274	9119	07405	86653	18973	7697	8403
Aut	0.45	Untreate	0,0445	0,0208	1,4434	0,1228	1,2924	0,0973	206,067	15,234	0,83840	0,1158	2,6925	1,1917	6,4627	0,2280
um	µm	d-3	93191	08582	40503	6094	8406	53706	3429	17408	2158	51377	30963	20699	934	059
Aut	Total	Treated-	0,2577	0,0035	2,2057	0,0476	2,0640	0,2387	142,148	0,7179	0,89086	0,0079	2,7098	0,0417	7,5416	0,3646
um	Water	1	79759	98429	33458	5527	4219	68691	0014	35833	8151	79599	52932	43023	0216	8229
Aut	Total	Treated-	1,2167	0,0085	4,5263	0,0848	6,1916	0,1390	171,794	7,9261	2,20611	0,1077	3,3342	0,1362	9,3057	0,2043
um	Water	2	29128	86582	97872	1874	178	62615	2331	54584	5434	26237	65742	25404	6445	345

Aut	Total	Treated-	1,3807	0,1112	5,0982	0,3314	7,9146	1,6366	182,262	12,620	2,40944	0,1482	3,5469	0,1737	10,222	0,4898
um	Water	3	92221	87399	1675	293	1156	91551	2672	6928	4827	73503	93569	47341	0006	2269
Aut	0.45	Treated-	0,0303	0,0042	1,6624	0,1367	1,0674	0,1355	152,674	16,905	0,84255	0,0585	2,7303	0,3091	7,2980	0,8144
um	µm	1	04018	15933	3312	3016	0573	36994	058	05469	0098	23212	96148	83518	2669	7104
Aut	0.45	Treated-	0,0342	0,0015	1,7349	0,0905	1,3783	0,0994	160,720	9,2782	1,12266	0,0425	2,8047	0,1372	9,3057	0,4567
um	µm	2	9606	26274	59636	439	7593	51062	0883	05334	9606	22803	5469	79317	6445	4819
Aut	0.45	Treated-	0,0375	0,0045	1,7510	0,0542	1,3463	0,1017	167,708	6,8273	1,15966	0,0317	2,8074	0,1425	7,5996	0,4014
um	µm	3	95876	04761	12509	3141	695	4894	0298	78903	2193	69458	0117	25807	6633	7796
Aut	Total	Filtered-	0,3296	0,0230	6,7710	0,0766	2,1137	0,1078	378,119	2,9785	0,66710	0,0104	3,2118	0,0539	11,403	0,2412
um	Water	1	52336	22856	27432	4528	3765	9551	5794	87364	1872	26844	7308	62826	7398	2587
Aut	Total	Filtered-	0,2935	0,0182	5,8736	0,2543	2,3162	0,1224	402,625	14,692	0,73613	0,0266	3,1142	0,1000	11,002	0,5221
um	Water	2	23406	79669	60938	3604	2064	0896	696	24882	1473	32256	14667	58825	4111	9138
Aut	Total	Filtered-	0,2971	0,0151	5,0693	0,1319	2,2265	0,1114	384,038	5,6550	0,79633	0,0247	2,9622	0,0626	9,8269	0,2910
um	Water	3	73984	16045	17653	8356	4491	98969	379	42694	115	91279	33684	07514	0738	4719
Aut	0.45	Filtered-	0,0287	0,0051	5,5947	0,1200	1,1156	0,1386	369,797	5,6059	0,30421	0,0118	2,7358	0,0513	9,7244	0,1942
um	µm	1	41795	46634	89391	1738	443	8319	1535	5187	2256	28934	51266	73301	2202	215
Aut	0.45	Filtered-	0,1397	0,0805	4,9335	0,4810	1,3873	0,2412	381,666	22,996	0,43170	0,0568	2,8555	0,2953	9,6026	0,8385
um	µm	2	95999	18687	66606	2204	4861	37363	9501	42448	7211	88877	26221	08228	8788	0859
Aut	0.45	Filtered-	0,0598	0,0085	4,4568	0,1444	1,4952	0,2840	361,988	23,210	0,42214	0,0104	2,6448	0,2233	10,132	0,5140
um	µm	3	79228	77804	01566	3469	6399	01522	8568	21778	2651	54880	83776	20736	1824	882

Se as on	Treatm ent stage	Cu Mean ug/L	Cu SD ug/L	Zn Mean ug/L	Zn SD ug/L	As Mean ug/L	As SD ug/L	Mo Mean ug/L	Mo SD ug/L	Cd Mean ug/L	Cd SD ug/L	Sn Mean ug/L	Sn SD ug/L	Sb Mean ug/L	Sb SD ug/L	W Mean ug/L	W SD ug/L	Pb Mean ug/L	Pb SD ug/L
	Total				24,9	2,794	0,08		0,57		0,04	8,463			2,90		4,81		0,12
Spr ing	Water r Untreat ed-1	133,3 49794	2,58 5533	644,2 22308	3491 13	7082 1	6721 83	15,74 17183	3938 85	0,138 93363	8817 09	3043 2	2,48 4699	5,323 5998	8815 06	5,718 41433	8770 72	9,286 09246	3079 88
	Total		3,70		21,4	2,771	0,13		0,42		0,01		0,66		2,43		4,00		0,29
Spr ing	Water r Untreat ed-2	134,7 20734	7165 97	636,9 28909	5860 3	3257 6	9230 37	16,80 62129	5824 72	0,112 74766	0284 49	11,40 79	3463 83	8,929 93865	3999 42	11,42 15764	4089 12	9,257 77915	8971 31
	Total		4,54		21,9	2,773	0,08		1,89		0,04	9,683	1,60		2,29		3,88		0,39
Spr ing	Water r Untreat ed-3	135,5 26518	1411 23	639,2 89224	6931 53	8640 1	6090 85	18,48 71379	3389 38	0,129 3403	3279 04	5187 8	7272 72	6,655 89312	9891 02	8,509 97127	3221 12	9,242 34503	0764 06
			0,94		1,42	0,874	0,02		1,57		0,00	0,203	0,09		0,06		0,23		0,24
Spr ing	0.45 µm Untreat ed-1	22,07 1601	0503 17	241,0 62018	6522 45	5650 6	5647 09	15,14 27396	3512 08	0,016 37143	8908 63	2175 6	4668 21	4,154 15227	3066 15	9,234 79856	8406 17	0,293 67434	5443 48
			1,05		6,92	0,829	0,04		5,03		0,01	0,549			0,13		0,37		0,57
Spr ing	0.45 µm Untreat ed-2	20,92 02961	5760 91	231,9 56181	8796 86	8910 4	6211 01	22,41 47907	0088 22	0,031 58927	1852 15	5505 7	0,25 1627	3,891 89438	1429 63	9,271 89197	9636 05	1,139 58658	9844 31
			0,82		6,72	0,827	0,02		3,21		0,00	0,240	0,15		0,10		0,29		0,56
Spr ing	0.45 µm Untreat ed-3	20,22 18642	9566 99	224,2 09138	7611 1	1683 6	5408 59	14,89 34578	1218 07	0,015 468	7760 39	5244 2	6224 06	3,954 23573	6509 06	8,723 5399	7198 5	0,495 447	8240 45
	Total		0,51		8,60	0,984	0,01		0,24		0,00	0,765	0,01		0,02		0,10		0,01
Spr ing	Water r Treated -1	41,00 53195	1567 51	406,3 36902	0316 21	5719 1	5644 98	15,30 89437	3860 91	0,026 88289	0577 46	8597 6	8376 23	3,834 81779	9032 67	9,337 59066	7612 3	0,870 62075	9971 02
	Total		0,18		2,21	1,159	0,01		0,39		0,00	2,068	0,07		0,05		0,05		0,00
Spr ing	Water r Treated -2	55,37 71395	4219 12	475,4 32521	7577 26	9873 7	9448 49	14,61 67169	6796 24	0,036 30919	2430 68	6714 8	3039 97	4,069 9148	1415 56	10,06 26873	4942 13	1,724 91696	7571 87
	Total		6,82		69,1	1,121	0,14		1,88		0,00	3,063	0,41		0,70		1,32		0,28
Spr ing	Water r Treated -3	60,46 62915	6069 45	538,3 50708	5800 2	8521 9	1268 03	13,87 04267	2842 31	0,037 73702	4679 33	0657 4	4651 67	4,548 557	4799 2	9,843 31926	1588 27	2,152 77507	4023 6

				1,45		12,9	0,882	0,03		0,83		0,00	0,218	0,01		0,04		0,52		0,03
Spr	0.45	Treated	18,69	9229	347,9	4691	7464	9132	15,17	7868	0,015	2657	9220	5938	3,119	1181	8,926	2489	0,180	7480
ing	µm	-1	24742	48	70109	13	1	54	84794	99	68017	44	9	79	58456	22	40352	82	27853	45
				0,33		13,1		0,07		0,84		0,00	0,447	0,04		0,13		0,61		0,02
Spr	0.45	Treated	6,284	6859	174,6	8164	0,923	2949	13,71	6200	0,003	2099	1594	3980	0,940	7992	9,008	6959	0,209	1593
ing	µm	-2	67633	3	78232	29	0388	06	26166	16	14731	01	8	48	97576	45	12292	08	59687	11
				0,59		7,16	0,861	0,02		0,13		0,00	0,357	0,02		0,11		0,20		0,01
Spr	0.45	Treated	5,968	9082	65,43	1888	1956	4945	14,39	4816	0,000	0133	7306	4470	0,876	3985	9,409	3748	0,229	5956
ing	µm	-3	78132	9	19581	6	2	52	25312	19	98996	66	3	18	00516	65	0088	54	18266	35
	Total			1,06		12,8	2,289	0,08		0,36		0,00	1,544	0,03		0,02		0,18		0,12
Spr	Water	Filtered	38,53	5806	543,8	5891	7808	5045	15,58	5365	0,026	0908	1866	7617	3,405	9032	9,652	8301	1,445	6705
ing	r	-1	10712	35	3848	68	5	63	30421	95	76322	3	2	72	26429	67	85629	83	73203	55
	Total			0,29		4,87	2,096	0,03		0,39		0,00		0,01		0,05		0,12		0,03
Spr	Water	Filtered	39,74	4282	554,8	6826	5114	1092	15,83	5727	0,027	1173	1,569	8710	3,460	9930	9,890	0880	1,446	8807
ing	r	-2	23809	81	90962	61	9	77	83936	47	98794	66	7243	12	63893	58	38218	15	74538	23
	Total					9,61	1,887	0,01		0,25		0,00	1,577	0,06		0,11		0,12		0,01
Spr	Water	Filtered	39,32	0,67	529,6	1471	7838	5970	15,22	5480	0,037	4921	6133	4056	3,439	9535	9,675	8315	1,358	8881
ing	r	-3	20092	0429	70231	08	8	18	2321	76	73702	19	6	08	05147	48	69114	74	47175	11
				0,52		13,5		0,07		0,78	-	0,00	0,207	0,03		0,08		0,47		0,02
Spr	0.45	Filtered	4,333	1194	148,5	9160	1,684	7026	14,76	9471	0,000	1879	9881	0701	0,944	1603	9,056	2996	0,173	9757
ing	µm	-1	17076	32	59635	05	2022	1	75201	54	1073	21	6	02	08098	84	69817	97	31714	15
				0,04		3,05	1,722	0,03		0,11	-	0,00	0,217	0,02		0,03		0,11		0,01
Spr	0.45	Filtered	3,912	8719	143,7	5959	0718	1282	15,21	0206	0,000	0258	9170	0311	0,980	9867	9,257	8700	0,158	7838
ing	µm	-2	16461	37	27372	14	8	62	95941	13	1158	29	6	12	12271	63	20016	04	71098	46
				0,10		1,96	1,530	0,03		0,22		0,00	0,214	0,00		0,01		0,33		0,00
Spr	0.45	Filtered	3,967	9453	124,7	0568	2671	3784	14,62	1802	0,001	0718	6100	7778	0,777	9455	9,149	1023	0,149	7750
ing	µm	-3	24808	11	94011	39	7	23	60132	78	79281	85	2	45	16232	44	54552	16	13738	17

	Total			1,87		11,2	1,197	0,04		0,89		0,00	8,268	0,77		0,80		0,15		0,18
Aut	Water	Untreated-1	46,58	0709	381,4	4616	1291	2677	21,77	8455	0,054	6701	9323	1623	14,19	5041	4,960	3983	4,468	2530
um	r		97762	47	1098	95	2	27	65504	77	96884	74	9	18	85408	47	47743	05	67511	17
	Total			2,26		12,3	1,852	0,02		0,48		0,00	16,67	1,21		2,35		0,33		0,29
Aut	Water	Untreated-2	80,81	4266	610,1	3268	5167	5235	23,85	6248	0,086	8473	7614	6447	21,26	0871	6,384	1395	7,979	7146
um	r		96104	45	98278	54	9	03	01266	29	0248	7	3	79	60694	22	4437	08	88139	67
	Total			4,99		41,3	1,814	0,06		1,59		0,00	12,43	4,05		5,74		1,86		0,45
Aut	Water	Untreated-3	78,40	0278	610,3	4436	1762	3403	23,90	2304	0,083	6759	6041	4091	13,19	6406	4,152	4740	7,545	8497
um	r		52601	27	20674	09	9	23	35484	02	9608	47	1	55	40404	14	43963	59	98473	84
				0,61		16,2	0,535	0,03		1,88		0,00	0,170	0,01		0,31		0,30		0,02
Aut	0.45	Untreated-1	8,701	6771	212,9	7134	4720	9473	20,06	2438	0,012	2508	7045	5929	3,395	1661	2,606	9706	0,390	6789
um	µm		76111	77	6742	46	5	93	57768	53	99634	94	4	41	83922	58	21709	55	33601	75
				0,23		6,56	0,575	0,04		0,54		0,00				0,15		0,07		0,01
Aut	0.45	Untreated-2	10,76	0943	231,0	7759	2592	2177	20,38	5388	0,014	2633	0,180	0,01	3,418	3357	2,626	4096	0,347	1389
um	µm		83149	32	86421	25	5	32	84167	65	80129	28	3512	2088	22427	17	66408	03	3474	8
				6,50		15,5	0,554	0,05		1,74		0,00	0,275	0,13		0,25		0,27		0,06
Aut	0.45	Untreated-3	11,70	0440	237,0	7291	1215	4645	20,82	0871	0,017	2713	5304	6358	3,472	8862	2,630	8389	0,484	3928
um	µm		61227	52	60693	86	3	55	5687	85	90724	33	3	53	54017	89	88346	23	22662	34
	Total			0,11		0,73	0,878	0,00		0,22		0,00		0,03		0,11		0,05		0,02
Aut	Water	Treated-1	25,63	4070	458,2	1869	8804	3607	19,01	9255	0,030	2980	0,754	3295	3,533	6530	2,782	5747	0,777	2949
um	r		67247	76	80409	39	7	51	89118	35	65802	61	2959	03	43017	7	68484	03	07444	94
	Total			2,01		26,9	2,150	2,06		0,68		0,00	3,083	0,06		0,28		0,20		0,07
Aut	Water	Treated-2	41,62	9610	612,0	2088	2227	1755	18,74	3767	0,039	4234	5731	4088	5,598	8953	3,420	0900	1,929	5041
um	r		81339	89	18388	31	5	85	5376	2	04555	7	6	04	02295	51	1677	49	59555	55
	Total			2,48		63,2	1,058	0,05		1,60		0,00	3,700	0,22		0,52		0,27		0,14
Aut	Water	Treated-3	43,39	2513	649,0	2049	5546	2019	21,30	6048	0,017	3896	4556	7676	6,516	3244	3,843	5872	2,136	3273
um	r		07105	19	11589	9	1	41	12525	91	90724	26	3	06	47715	3	41891	29	8561	65
				0,57		15,0	0,625	0,05		1,90		0,00	0,286	0,02		0,12		0,12		0,01
Aut	0.45	Treated-1	4,990	0513	122,5	2861	4426	6970	18,88	4064	0,008	3159	0462	3055	1,226	5803	2,895	7945	0,189	9037
um	µm		26106	14	62589	58	2	91	57822	79	43643	65	8	5	49359	04	63347	33	34874	28
				0,23		4,59	0,326	0,02		1,22		0,00	0,349	0,06		0,05		0,17		0,01
Aut	0.45	Treated-2	3,959	4071	66,79	0679	9798	7509	18,32	5697	0,039	0874	7861	4088	0,863	4256	2,888	0982	0,194	2932
um	µm		00119	49	42735	04	7	32	22254	93	04555	51	8	04	97692	4	35876	25	41143	11

				0,12		2,73	0,303	0,00		0,94		0,00	0,320	0,22		0,03		0,07		0,02
Aut	0.45	Treated	3,762	1754	66,88	3022	7416	5696	18,41	7195	0,005	1140	1031	7676	0,885	3745	3,128	1840	0,209	0932
um	µm	-3	80797	34	04207	64	5	14	08102	17	4938	85	2	06	07577	43	79741	68	46602	67
	Total			0,16		4,36	1,535	0,02		0,38		0,00	0,852	0,03		0,16		0,06		0,03
Aut	Wate	Filtered	15,72	5018	592,7	0251	6158	5334	20,33	4584	0,036	5031	3965	9479	5,006	0264	4,868	9075	1,028	4964
um	r	-1	95918	15	37277	28	7	84	95511	24	96823	11	6	36	93008	73	00418	29	67567	43
	Total			0,61		22,2	1,351	0,05		0,68		0,00	0,988	0,05		0,19		0,07		0,05
Aut	Wate	Filtered	16,79	8934	631,3	1899	1341	5361	23,30	3767	0,025	4081	1603	6261	4,680	9881	5,064	1705	1,121	0523
um	r	-2	14906	69	09822	27	2	93	49768	2	31554	63	9	69	42373	4	23932	9	52034	19
	Total			0,52		12,2	1,230	0,02		0,57		0,00	1,045	0,03		0,08		0,08		0,04
Aut	Wate	Filtered	17,64	8296	614,2	6264	8312	5218	20,90	7212	0,021	1525	6322	1438	4,375	2680	4,824	2814	1,152	8275
um	r	-3	35187	21	87863	38	8	62	27386	25	91666	98	2	45	4646	63	05116	88	20202	64
				0,07		4,29	1,468	0,69		0,37		0,00	0,135	0,00		0,09		0,08		0,02
Aut	0.45	Filtered	2,403	1889	264,0	1152	5054	8749	18,57	6729	0,005	1176	8526	4443	2,820	4103	4,492	2814	0,180	1220
um	µm	-1	60926	03	08515	39	8	98	83458	22	31944	91	8	13	9436	28	27683	88	38713	6
				0,63		10,3	1,129	0,19		3,43		0,00	0,244	0,02		1,15		0,62		0,02
Aut	0.45	Filtered	4,465	3523	228,4	1139	8640	3198	19,84	9666	0,007	2601	7843	6772	4,243	1901	4,967	0360	0,263	4868
um	µm	-2	36667	14	37247	34	8	84	05868	17	06583	39	4	26	39423	33	15888	34	85191	87
				1,03		3,45	1,152	0,09		1,06		0,00	0,186	0,03		0,63		0,17		0,04
Aut	0.45	Filtered	6,330	6440	203,9	5475	4434	0365	22,05	1270	0,008	3577	1424	6453	5,782	8153	4,571	1115	0,253	0811
um	µm	-3	49025	35	58431	19	7	88	08269	9	59555	32	1	57	6393	49	35246	77	53245	22

Appendix I: Anion

Table I1 : Concentrations Anions analysed mg/L.

Sample number	F- mg/L	Cl- mg/L	SO4 mg/L	NO3 mg/L	PO4 mg/L
RM1 ion 96	0,114	76,179	81,672	11,709	n.a.
RM2 Sangamon 03	0,203	16,955	17,873	50,757	n.a.
QC3060	0,985	163,805	85,127	50,155	3,754
Instrument blank 1	n.a.	0,056	n.a.	n.a.	n.a.
Instrument blank 2	n.a.	n.a.	n.a.	0,205	n.a.
Instrument blank 3	n.a.	0,078	n.a.	0,207	n.a.
B1-1	n.a.	885,214	55,000	24,972	n.a.
B1-2	0,258	938,313	56,659	25,361	n.a.
B1-3	n.a.	930,119	56,367	25,655	n.a.
D1-1	1,195	999,783	58,620	50,241	n.a.
D1-2	1,272	867,931	54,807	46,689	n.a.
D1-3	1,274	996,660	58,488	50,115	n.a.
M1-1	0,256	880,841	54,509	23,200	n.a.
M1-2	0,307	996,860	58,097	23,665	n.a.
M1-3	0,313	883,369	54,658	23,172	n.a.

Appendix J: Tox Parameters

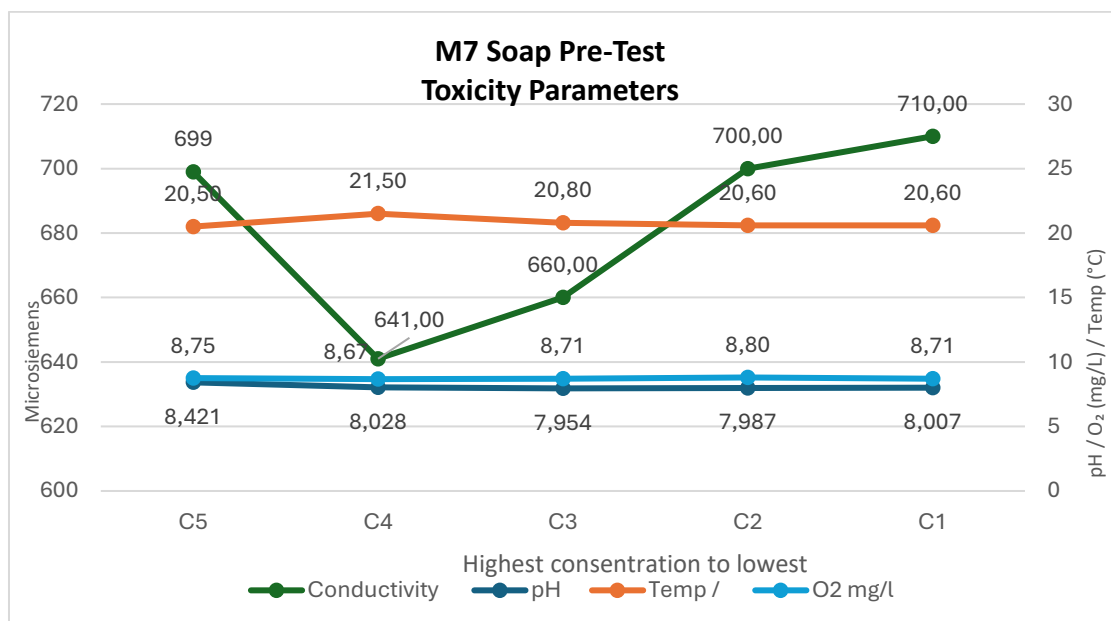


Figure J1: Tox parameters for TWW detergent experiment

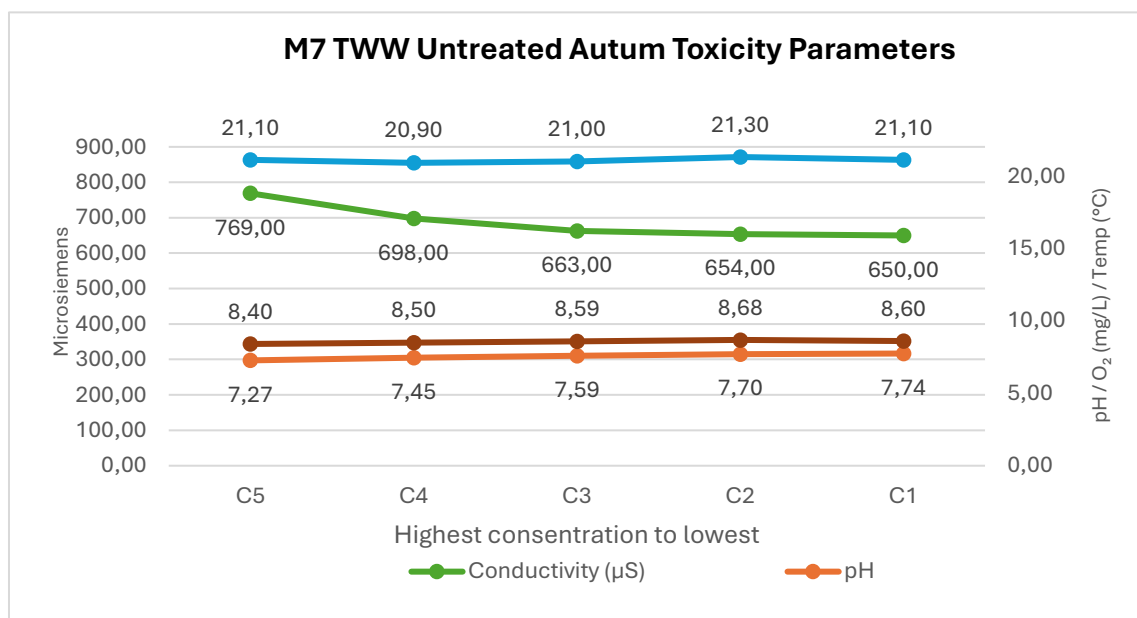


Figure J2: Tox parameters for TWW Autum untreated M7 water

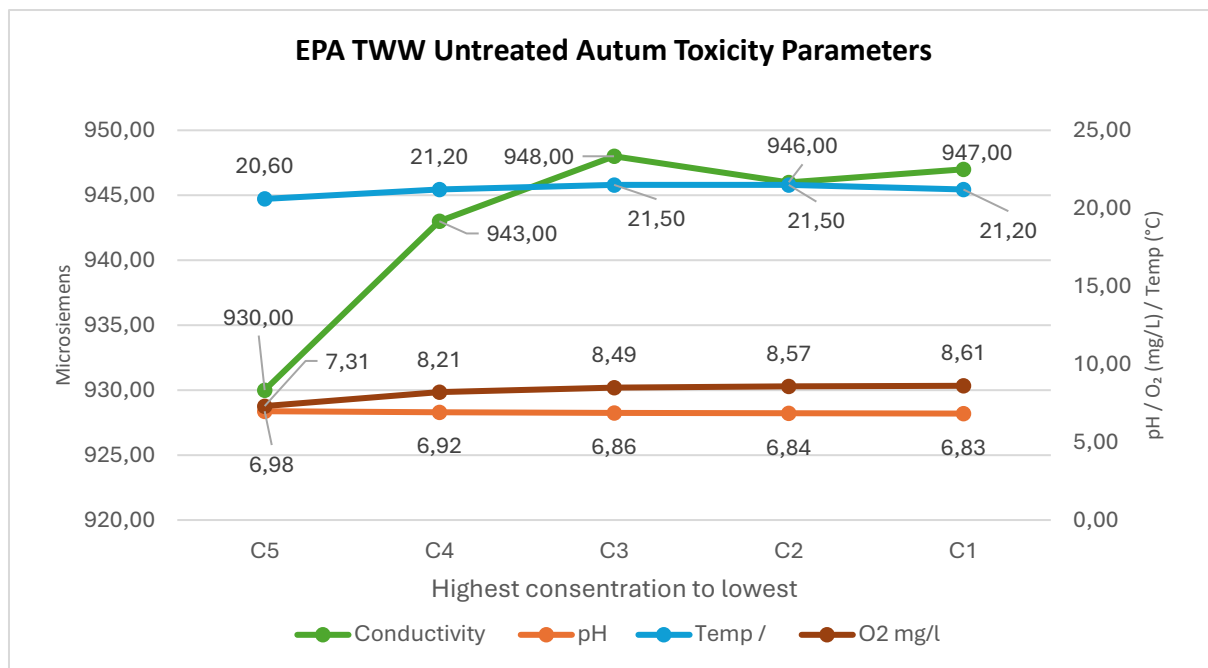


Figure J3: Tox parameters for TWW Autum untreated EPA water

Appendix K: Tox Survival chart

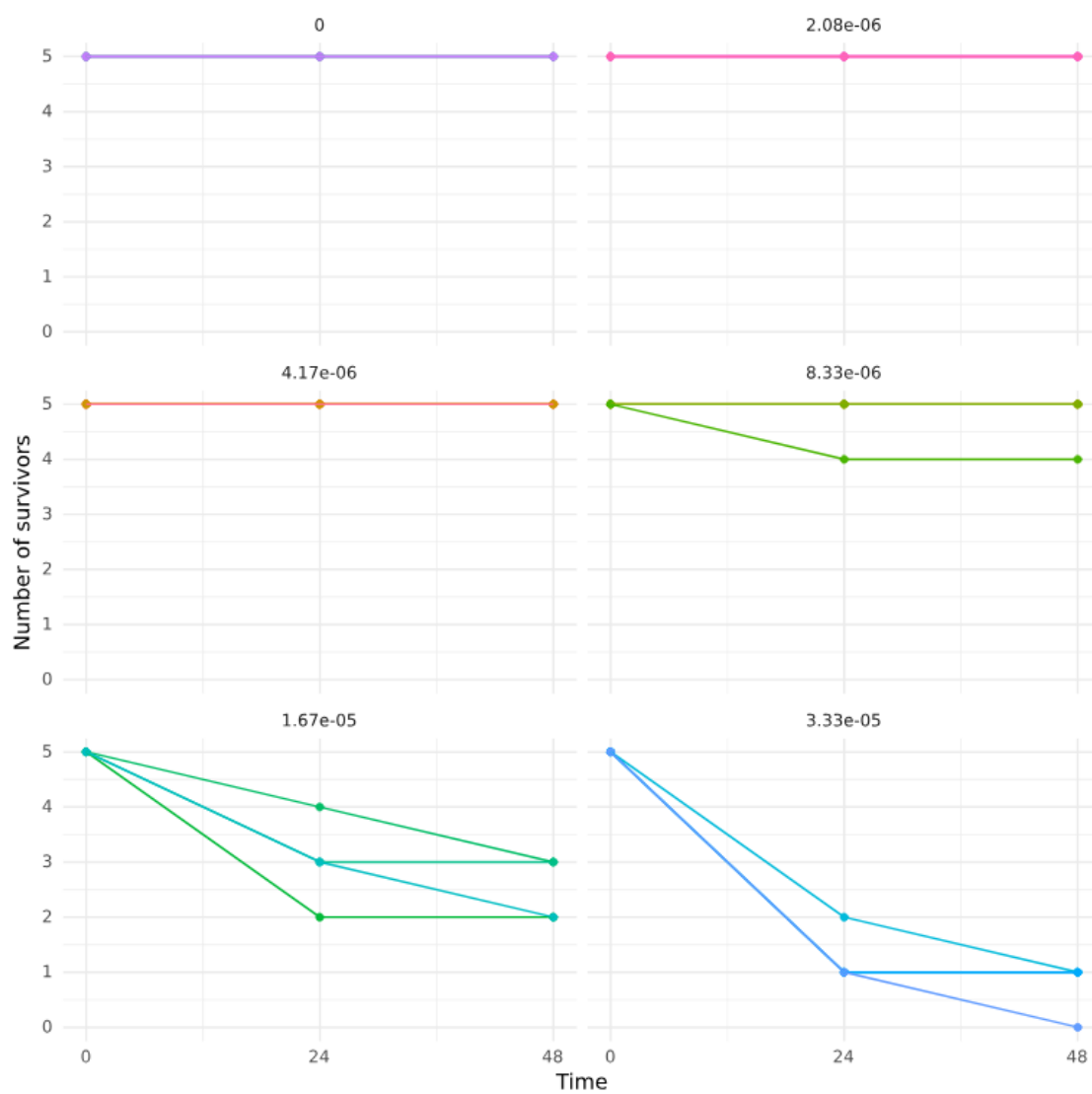


Figure K1: Tox parameters for TWW Detergent

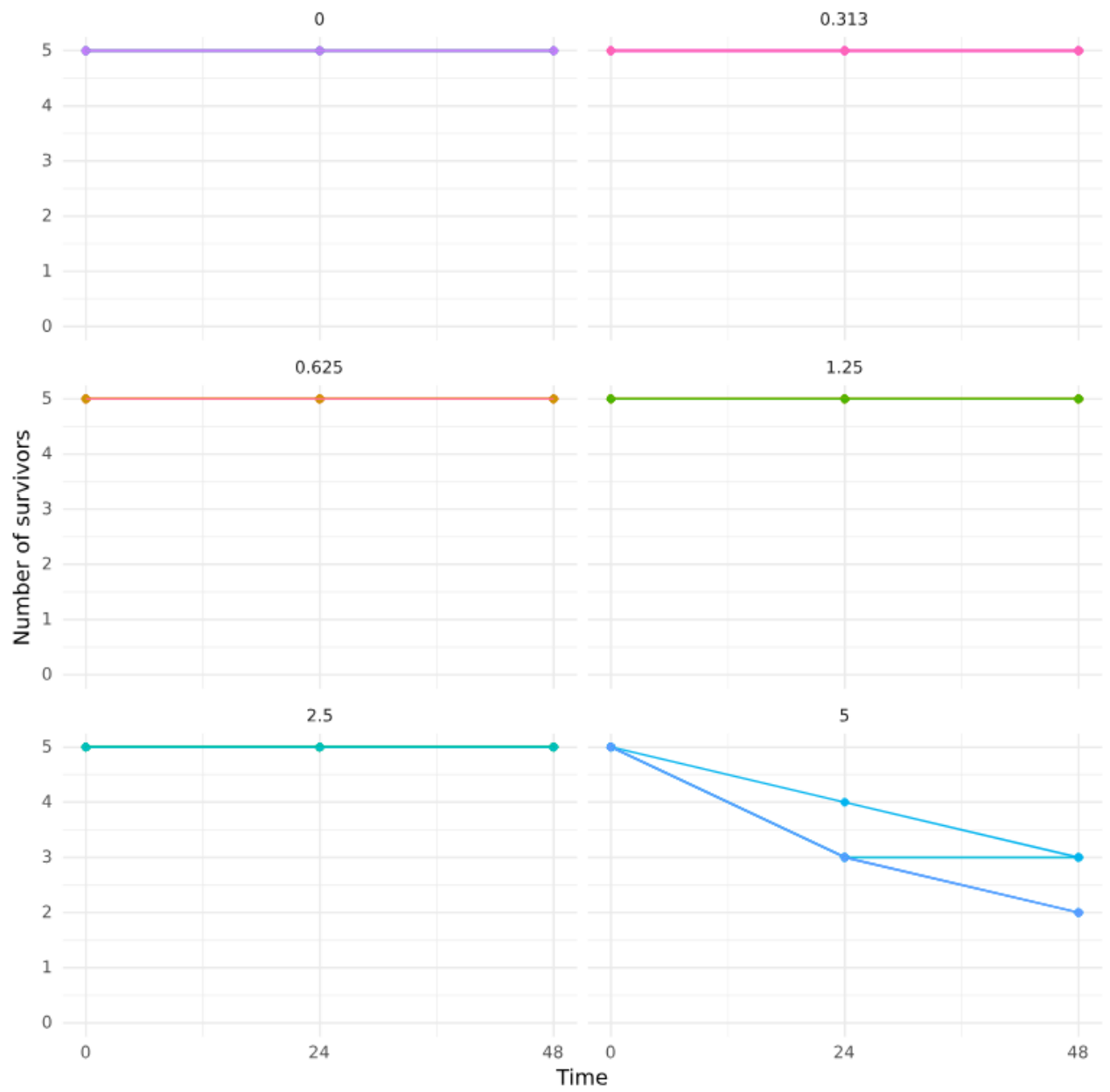


Figure K2: Tox parameters for TWW Untreated M7

Appendix L: TWW Detergen composition.



I henhold til forordning (EF) nr. 1907/2006(REACH), vedlegg II med endringer, Forordning (EU)2020/878

SIKKERHETSDATABLAD

Mac 213 Bio

AVSNITT 1: IDENTIFIKASJON AV STOFFET/STOFFBLANDINGEN OG AV SELSKAPET/FORETAKET

1.1. Produktidentifikator

▼ Handelsnavn

Mac 213 Bio

Unik Formular Identifikasjon (UFI)

P7QG-CWSC-78CC-QA1Q

1.2. Relevante identifiserte bruksområder for stoffet eller stoffblandingen og bruk som frarådes

Aktuelle identifiserte anvendelser for stoffet eller blandingen

Rengjøringsmiddel

Bare for yrkesbrukere.

Ikke tilrådde anvendelser

Ingen kjente

1.3. Opplysninger om leverandøren av sikkerhetsdatabladet

Selskapsopplysninger

MacSerien Produktion AB

Mossvägen 3

177 42 Järfälla

Sweden, SE

+46 08-584 304 80

Kontaktperson

Macserien Norge AS

Trollåsveien 36

1414 TROLLÅSEN

Norge

Telefon +4741307272

AVSNITT 3: SAMMENSETNING / OPPLYSNINGER OM BESTANDDELER

3.1. Stoffer

Ikke relevant. Dette produktet er en stoffblanding.

3.2. Stoffblandinger

Produkt/bestanddel	Identifikatorer	% w/w	Klassifisering	Anm.
ISODECANOL ETHOXYLATE	CAS-nr.: 26183-52-8 EF-nr.: 500-046-6 REACH: Indeksnr.:	5-10%	Acute Tox. 4, H302 Eye Dam. 1, H318	
Glutamic acid, N, N-diacetic acid, tetrasodium salt, 47% aqueous	CAS-nr.: 51981-21-6 EF-nr.: 257-573-7 REACH: 01-2119493601-38-0000 Indeksnr.:	1-3%	Met. Corr. 1, H290	
propane-1,2-diol	CAS-nr.: 57-55-6 EF-nr.: 200-338-0 REACH: Indeksnr.:	<1%		
natriumhydroksid kaustisk soda natronlut	CAS-nr.: 1310-73-2 EF-nr.: 215-185-5 REACH: Indeksnr.: 011-002-00-6	<1%	Met. Corr. 1, H290 Skin Corr. 1A, H314 Skin Corr. 1B, H314 (SCL: 2,00 %) Skin Irrit. 2, H315 (SCL: 0,50 %) Eye Irrit. 2, H319 (SCL: 0,50 %)	
POLY L-ASPARTIC ACID SODIUM SALT	CAS-nr.: 181828-06-8 EF-nr.:	<1%		

I henhold til forordning (EF) nr. 1907/2006(REACH), vedlegg II med endringer, Forordning (EU)2020/878

	REACH: Indeksnr.:		
kaliumhydroksid kalilut	CAS-nr.: 1310-58-3	<1%	Met. Corr. 1, H290
	EF-nr.: 215-181-3		Acute Tox. 4, H302
	REACH:		Skin Corr. 1A, H314
	Indeksnr.: 019-002-00-8		Skin Corr. 1B, H314 (SCL: 2,00 %)

Se avsnitt 16 for de fullstendige H-setningene det vises til ovenfor. Administrative norm(er) er, hvis tilgjengelig, oppført i avsnitt 8.

Figure L: Detergent composition



Norges miljø- og biovitenskapelige universitet
Noregs miljø- og biovitenskapelege universitet
Norwegian University of Life Sciences

Postboks 5003
NO-1432 Ås
Norway